

DRAINAGE AND RECLAMATION OF SALT-AFFECTED SOILS

CENTRALE LANDBOUWCATALOGUS



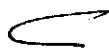
0000 0086 7438

BIBLIOTHEEK
VIR
LANDEBOWWETENSCHAPPELIJK
WAGENINGEN

Promotoren: dr. ir. W. H. VAN DER MOLEN, hoogleraar in de agrohydrologie
dr. ir. P. BURINGH, hoogleraar in de tropische bodemkunde

hm 0201

730²



J. MARTINEZ BELTRAN

**DRAINAGE AND RECLAMATION OF
SALT-AFFECTED SOILS IN THE
BARDENAS AREA, SPAIN**

PROEFSCHRIFT

TER VERKRIJGING VAN DE GRAAD
VAN DOCTOR IN DE LANDBOUWWETENSCHAPPEN,
OP GEZAG VAN DE RECTOR MAGNIFICUS
DR. H. C. VAN DER PLAS,
HOGLERAAR IN DE ORGANISCHE SCHEIKUNDE
IN HET OPENBAAR TE VERDEDIGEN
OP VRIJDAG 27 OKTOBER 1978
DES NAMIDDAGS TE VIER UUR IN DE AULA
VAN DE LANDBOUWHOGESCHOOL TE WAGENINGEN

INTERNATIONAL INSTITUTE FOR LAND RECLAMATION AND IMPROVEMENT/ILRI
P.O. BOX 45, 6700 AA WAGENINGEN, THE NETHERLANDS, 1978

1274

This thesis is also published as **ILRI Publication no. 24**

© **International Institute for Land Reclamation and Improvement/ILRI, Wageningen, 1978**

Printed in The Netherlands

PROPOSITIONS

I

The use of trickle irrigation can prevent the decrease in the acreage of irrigated areas in the Canary Islands.

II

Since primary soil salinity is closely connected with geomorphology, the physiographic approach is suitable for reconnaissance surveys -if one of their objectives is to map saline soils.

III

The option of integration of Spain in the EEC appears to be the best among the possible ones of joining other socio-economic areas, and the option is favourable for Spanish agriculture in overall terms.

F. Botella. 1977. Situación actual, problemática y consecuencias de la adhesión de España a la EEC. Revista de estudios agrosociales no. 100.

IV

In the saline soils of the irrigated areas of the Ebro basin, sugar-beet appears to be a more suitable reclamation crop than rice.

V

Crop rotations should be considered not only in terms of their economic return, but also in terms of the suitability of crops in connection with soil and water qualities and their effect on the salt balance.

Recommendation of an expert consultation on prognosis of salinity and alkalinity. FAO. Soils Bulletin no. 31. Rome. 1975.

VI

The successful long-term use of any irrigation water depends more on rainfall, leaching, irrigation water management, salt tolerance of crops, and soil management practices than upon water quality itself.

M. Fireman. 1960. Quality of water for irrigation. University of California Extension Service. Davis.

VII

The leaching efficiency coefficient depends not only on the irrigation method and soil conditions but also on the subsurface drainage system.

VIII

It is more rewarding to invest in the preservation of the present land resources under cultivation than to shift to new areas and draw on the reserve of land resources.

Recommendation of an expert consultation on secondary salinization. FAO. Rome. December 1977.

IX

The use of waste water for irrigation purposes appears to be advisable in areas where water resources are scarce and where climate allows the growth of early crops.

X

The increasing industrial expansion of a developing country has an indirect effect on its agrarian reform.

Proefschrift J. MARTINEZ BELTRAN

Drainage and Reclamation of Salt Effected Soils in the Bardenas Area, Spain.

Wageningen, 27 oktober 1978

ACKNOWLEDGEMENTS

At the beginning of this book I would like to express my gratitude to everyone who made this publication possible.

I am most grateful to Prof. W. H. VAN DER MOLEN and Prof. P. BURINGH for their supervision, advice and discussions both in the field and in the University Departments.

I am greatly indebted to Dr. J. W. VAN HOORN for encouraging me to start with this thesis and for his contributions during the research work.

My sincere appreciation to Dr. N. A. DE RIDDER for his many valuable suggestions on the text and for his work as head of ILRI editorial committee.

I am most grateful to Ing. A. MARTINEZ BORQUE, former Director of the Instituto Nacional de Colonización, for his suggestion on the possibilities of reclaiming the saline soils of the Ebro irrigated areas, and for his constant support and encouragement.

I express my gratitude to Ing. T. VILLANUEVA ECHEVARRIA, Director of the Instituto de Reforma y Desarrollo Agrario, for his interest in the reclamation of the soils affected by salinity and for giving me the privilege of working in the experimental fields of the Bardenas area.

I am also indebted to Dr. J. BARDAJI CANDO, Head of the Soils Department of IRYDA, for his advice, especially on the geomorphology of the area, and for his valuable comments on the manuscript. Thanks are due to Mr G. GARCIA CRESPO and Mr. G. MORALES MURCIA for their collaboration in the field work of the reconnaissance survey, and to the staff of the soil laboratories of IRYDA in Madrid and Sevilla.

Special acknowledgement is due to Mr. A. P. WARDLE for his continuous advice and whose knowledge of the soil conditions of the Bardenas area was of great value. He also read the manuscript and corrected the English text.

The author is most grateful to Mr. U. CONDE BARREALES, whose accurate daily observations at the Alera experimental field made it possible to obtain the results presented in this book. The time spent by him in the field was a continuous lesson in practical agriculture. Thanks are also due to Mr. H. MARIN for his meteorological observations at the station of the Oliva Abbey.

The drawings were made by Mr. C. RUIZ whose work was most worthwhile. I am particularly grateful to Miss M. HERNANDO ANTON for her splendid work in typing the draft and to Dr. J. STRANSKY (ILRI) for typing the definitive text and for his work on the lay-out.

My sincere gratitude to Mrs M. F. L. WIERSMA-ROCHE for her comments on, and corrections in, the English text.

I wish to express my gratitude to Ir F. E. SCHULZE, Director of the International Institute for Land Reclamation and Improvement, and to the editorial committee for publishing the text in the ILRI series.

Finally, I wish to express my debt to my wife and children for the leisure time I spent, not with them, but in research work, and whose patience and generosity made this publication possible.

To my parents

Contents

1.	INTRODUCTION	1
2.	GENERAL CHARACTERISTICS OF THE AREA	3
2.1	Geology	3
2.2	Geomorphology	8
2.2.1	Drainage basins	8
2.2.2	Catchment area fringes	9
2.2.3	Main geomorphological processes	10
2.2.4	Major physiographic units	12
2.3	Climate	18
2.3.1	Temperature	19
2.3.2	Precipitation	20
2.3.3	Relative humidity	24
2.3.4	Wind	25
2.3.5	Evapotranspiration	25
2.4	Natural vegetation	27
2.5	Present land use	30
2.5.1	Irrigated farming	30
2.5.2	Dry farming	31
3.	HYDROLOGY	32
3.1	The irrigation and drainage systems	32
3.1.1	The irrigation scheme	32
3.1.2	The main drainage system	35
3.2	The groundwater table and drainage conditions	35
3.2.1	Rough mountainous land	38
3.2.2	Aragón alluvial valley	38
3.2.3	Rough eroded plain	39
3.2.4	Alluvial fans	40
3.2.5	Alluvial plain	40
3.2.6	Gypsum ridges and valleys	41
3.2.7	Mesas	41
3.2.8	Eroded mesas	42
3.2.9	Riguel alluvial plain	42
3.2.10	"Badlands", alluvial valleys and fans	43

4. SOILS AND SOIL CONDITIONS

45

- 4.1 General characteristics 45
 - 4.1.1 Soil-forming processes 45
 - 4.1.2 Parent materials 45
 - 4.1.3 Topography 46
 - 4.1.4 Land and water management 47
 - 4.2 Mapping units 47
 - 4.2.1 Mesas 52
 - 4.2.2 Fluvio-colluvial valleys, slightly saline-alkali phase 54
 - 4.2.3 Piedmont slopes, slightly saline-alkali 56
 - 4.2.4 Riguel river plain 57
 - 4.2.5 High and middle Aragón terraces 59
 - 4.2.6 Low Aragón terrace 62
 - 4.2.7 Gypsum valleys 64
 - 4.2.8 Stony ridges 64
 - 4.2.9 Colluvial slopes 66
 - 4.2.10 Fluvio-colluvial valleys, imperfectly drained and saline-alkali phase 67
 - 4.2.11 Alluvial plains, imperfectly drained and saline-alkali phase 70
 - 4.2.12 Alluvial valleys, saline-alkali phase 71
 - 4.2.13 Alluvial fans, saline-alkali phase 74
 - 4.2.14 Alluvial fans, slightly saline phase 75
 - 4.2.15 Other minor mapping units 77
- Soil profiles 1 to 17 78-111

5. SOIL SALINITY

112

- 5.1 Origin and localization of the salts 112
- 5.2 Types of salts and their distribution in the soil profile 114
- 5.3 Salinity in the soil associations 115
- 5.4 Local crop tolerance to salinity and alkalinity 125
- 5.5 Soil salinity and land reclamation 129

6. DRAINAGE AND RECLAMATION EXPERIMENTAL FIELDS

132

- 6.1 Objectives of the field experiments 132
- 6.2 Selection criteria 133
- 6.3 Detailed soil survey 134
 - 6.3.1 Outline of the survey 134
 - 6.3.2 Hydrological soil properties 135
 - 6.3.3 Initial salinity 142

7.	EXPERIMENTAL FIELD DESIGN	148
7.1	Design of the drainage system	148
7.1.1	Alera experimental field	148
7.1.2	Valareña experimental field	162
7.2	Design of the irrigation system	168
7.2.1	Alera experimental field	168
7.2.2	Valareña experimental field	170
7.3	Soil improvement	170
7.4	Field observation network	170
7.5	Field observation programme	176
8.	DERIVATION OF AGRO-HYDROLOGICAL FACTORS	177
8.1	Groundwater flow conditions	177
8.1.1	Alera experimental field	177
8.1.2	Valareña experimental field	181
8.2	Drainage equations	183
8.2.1	Steady flow	183
8.2.2	Unsteady flow	184
8.3	Determination of the drainable pore space	190
8.4	Determination of the hydraulic conductivity	193
8.4.1	Unsteady flow: Boussinesq equation	193
8.4.2	Steady flow: Hooghoudt equation	202
8.4.3	Hydraulic conductivity of the less pervious layer	203
8.4.4	Comparison of the results obtained	205
8.5	Determination of the entrance resistance	207
8.5.1	Direct method of determining the W_e -value	208
8.5.2	Indirect method of determining the W_e -value	214

9.	DESALINIZATION PROCESS	220
9.1	Stages of the process	220
9.2	Water balance of the initial leaching phase	221
9.3	Theoretical leaching approach	229
9.3.1	Series of reservoirs	229
9.3.2	Numerical method	234
9.4	Actual desalinization process	235
9.5	Determination of the leaching efficiency coefficient	244
9.6	Prediction of the initial leaching requirements	252
9.7	Leaching requirement during the cropping stage	254
10.	SUBSURFACE DRAINAGE SYSTEM	258
10.1	Drainage criteria for unsteady-state conditions	258
10.1.1	Relation between crop yields and water table depth	259
10.1.2	Relation between water table depth and mobility of agricultural machinery	267
10.1.3	Rainfall distribution and water table rise	269
10.1.4	Relation between percolation losses from irrigation and water table rise	270
10.1.5	Assessment of drainage criteria for unsteady-state conditions	271
10.2	Drain spacing	273
10.3	Drainage criteria for steady-state conditions	274
10.4	Drain spacings required for different combinations of drainage and filter materials	276
10.4.1	Steady flow	276
10.4.2	Unsteady flow	278
	LIST OF SYMBOLS	282
	LITERATURE	285
	SUMMARY	289
	RESUMEN	299
	SAMENVATTING	311
	CURRICULUM VITAE	322

1. Introduction

The Ebro basin is situated in north-eastern Spain and forms a geographic unit that is bounded to the north by the Pyrenees, to the east by the Catalan Coastal Mountains, and to the south-west by the Spanish Plateau. It covers about 85 500 km².

The basin is drained by the Ebro river and its tributaries, which rise in the Pyrenees and the Iberian Mountains.

The region is the driest part of northern Spain because it is surrounded by high mountain ridges which isolate it from any Atlantic and Mediterranean influences. If water is available, however, the climate permits irrigated agriculture, the main crops being maize, lucerne, and fruit trees.

The oldest irrigation schemes consist of canals diverted from the Ebro river. Construction of the Canal de Tauste on the left bank commenced in 1252 and the system of the Canal Imperial de Aragón, which irrigates the right bank downstream of Tudela, was finished in 1786.

Early in the 20th century new irrigation plans were made to use the surface water resources from the Pyrenees for agriculture. The Canal de Aragón y Cataluña and the Canal de Urgel were first constructed and some years later the Bardenas-Alto Aragón irrigation scheme was designed.

This irrigation scheme consists of a series of reservoirs which will regulate the flow of the three main tributaries of the Ebro river along its middle reach, i.e. Aragón, Gállego and Cinca, and three main irrigation canals. Although parts of these canals had previously been constructed,

it was only after the Civil War that the Instituto Nacional de Colonización began the full transformation of the areas under irrigation command. When the scheme is finally completed, about 276 000 hectares will be irrigated.

The first part of the Bardenas area forms part of the Bardenas-Alto Aragón irrigation scheme. This area covers approximately 57 000 hectares. It is irrigated with water from Bardenas canal, which receives its supplies from the Yesa reservoir in the Aragón river.

Within the area under command of the Bardenas canal, soil units affected by salinity occur. To study the possibilities of reclaiming the land for irrigated agriculture, the Soils Department of the Instituto Nacional de Reforma y Desarrollo Agrario conducted a reconnaissance survey in the area between 1972 and 1974. During the survey the saline soils and those with a risk of secondary salinization were mapped and a study was made of the causes of soil salinization.

One of the conclusions of the soil survey was that a field experiment should be conducted to study the technical and economic aspects of draining and leaching these saline soils. In 1974, therefore, following a detailed hydro-pedological survey, two drainage and desalinization experimental fields were selected. In these pilot fields the drainage system, the leaching process, and the land and water management required to prevent resalinization were studied from 1974 to 1978.

2. General characteristics of the area

2.1 Geology

The Bardenas area forms part of the Ebro basin, which is bounded to the north by the Pyrenees, to the east by the Catalan Coastal Mountains, and to the south-west by the Spanish Plateau (Fig.2.1).

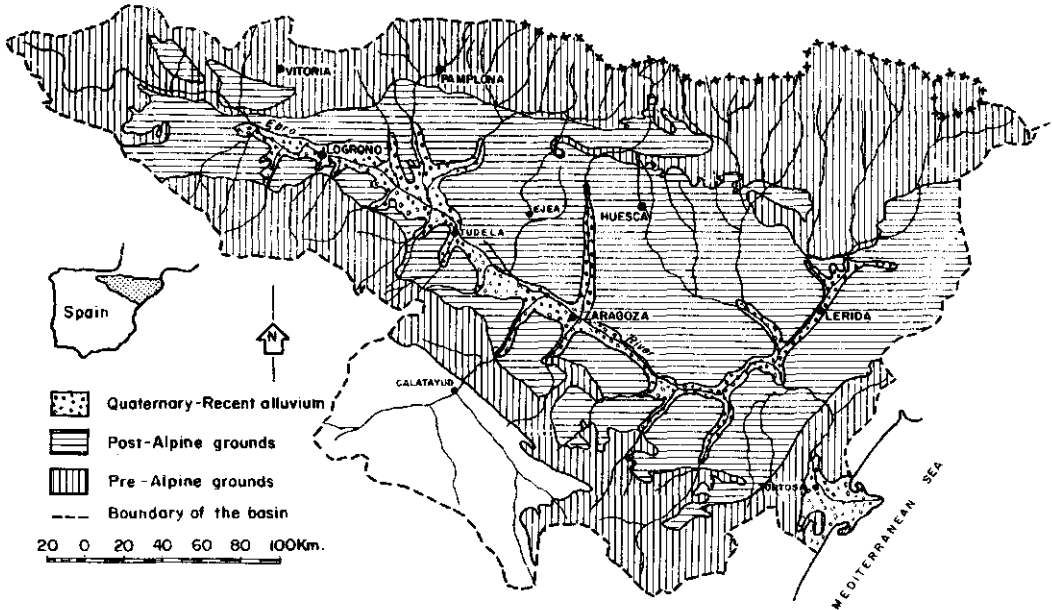


Fig.2.1: Simplified geology of the Ebro basin (from the Geological Map of Spain 1 : 1 000 000).

The origin of the salinity that affects some of the soils in the area is related to the geological processes involved in the formation of the Ebro basin.

During the Secondary Era the present Ebro basin was a sea arm between the Mediterranean and the Atlantic. In that period transgressions with marine deposition and regressions with continental deposition alternated.

When the Cenozoic period started, Alpine folding affected the basin structure. During the first folding phase both the Pyrenees and the Catalan Coastal Mountains emerged, the Iberian Plateau arose, and the former sea arm was closed and became a great Oligocene lake of brackish water.

During the Tertiary Era dry and wet periods alternated. Fine sediments were deposited in a brackish environment during periods of high evaporation and evaporites were locally formed. Meanwhile during wet periods coarser sediments were deposited near the borders of the basin.

During the late-Pliocene/early Pleistocene a system of ancient water courses carried coarse sediments from the basin border into the area. This coarse alluvium was deposited on the finer lacustrine sediments. Mesas of coarse mixed alluvium were formed (Fig.2.2).

Finally the present Ebro River was formed after a breakthrough of the Catalan Mountains. As a result the former Oligocene lake was drained.

During the Quaternary the base level was considerably lowered. The Ebro river and its main tributaries thus incised and formed alluvial valleys in the Tertiary sediments.

In the Bardenas area the lacustrine sediments comprise mudstones with interbedded layers of siltstones (Fig.2.3). In the south fine limestone layers overlie the mudstones and in the west gypsum strata are interbedded in the mudstone layers (Fig.2.4).



Fig. 2.2: Coarse mixed alluvium (mesa).

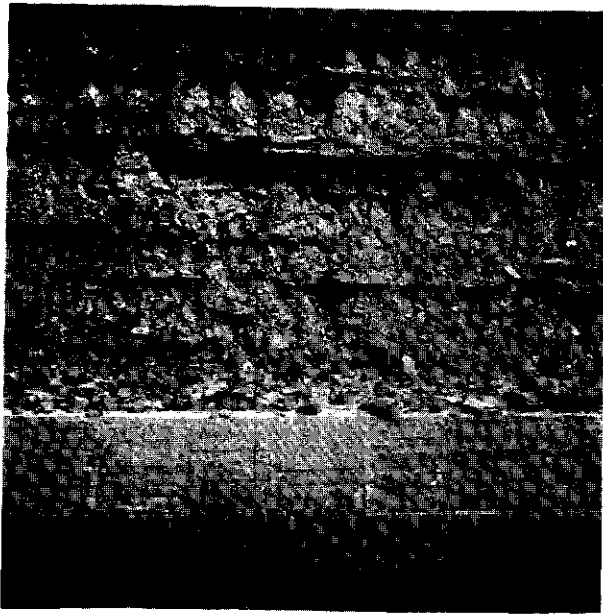


Fig. 2.3: Mudstones with interbedded layers of siltstones (Bardenas canal).

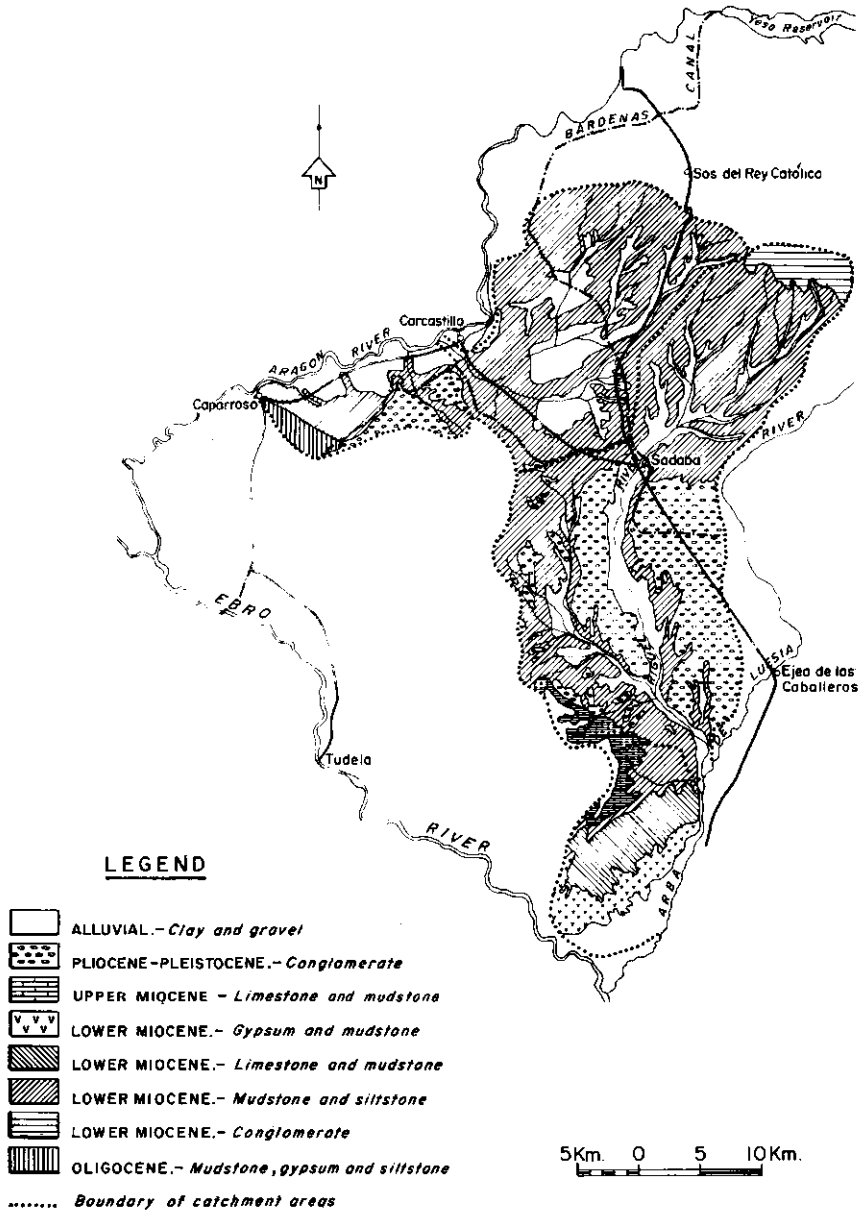


Fig.2.4: Geology of the Bardenas area (simplified from the Geological Map of Spain 1 : 200 000).

Where the sediments contain thick layers of gypsum, folding has occurred due to diapiric processes by which the more plastic evaporites were deformed under the weight of the overlying strata (Fig.2.5).

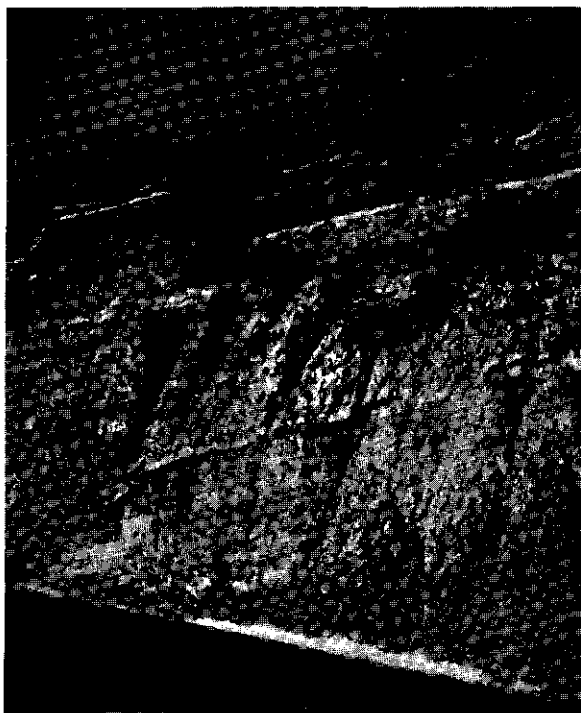


Fig.2.5: Folded gypsum strata interbedded in saline mudstones (road Zaragoza - Pamplona).

Two points are important in regard to soil formation. The first is that the siltstones consist of silt and clay-sized particles cemented by calcium carbonate. The second is that both mudstones and siltstones contain soluble salts because they were formed in a brackish environment. This means that the soil parent materials derived from these rocks are fine-textured with a high content of clay and silt, and a low content of fine sand. They are also saline. Other soil parent materials derived from coarser

sediments, e.g. the mesas and the river terraces, have a coarser texture and are relatively free of salts.

2.2 Geomorphology

During the Quaternary period the main landscape forming process was erosion, followed by transport and local deposition of material. The predominance of erosion, together with a gradual lowering of the base level, has resulted in the oldest Miocene-Oligocene formations occupying the highest points in the landscape, thus forming the uplands of a dissected plain. At a lower level are the mesas, which consist of partially eroded lacustrine sediments covered by younger deposits of coarse gravel. Subsequent erosion has removed large parts of the mesas and has cut deeply into the underlying lacustrine formations.

Most of the eroded sediments were removed from the area, but local sedimentation also occurred. In this semi-arid area both sediments and salts moved together and were even deposited together. The highest salt concentrations are therefore found in the lowest parts of the alluvial formations where the alluvium was derived from the eroded mudstones and siltstones.

To understand the origin of the salinity and its distribution and intensity, one must carefully analyse the main physiographic units and the processes involved in the landscape formation. Once a relationship is established between soil salinity and the physiographic units, one has a sound basis on which to map the saline soils.

2.2.1 Drainage basins

Within the project area two catchment areas can be distinguished (Fig.2.4). The northern part drains towards the Aragón river, which is deeply incised into the Miocene-Oligocene sediments in the north. The river changes its course westwards at Carcastillo and below this point has formed a broad alluvial valley.

The southern part of the area is drained by the Riguel river, which comes from the north-east and flows through the area from north to south. The Riguel debouches into the Arba de Luesia river at the southern end of the area.

Both the Aragón and the Arba are tributaries of the Ebro. The first flows into the Ebro near Milagro 70 km upstream from Gallur, where the Arba joins the Ebro.

This means that the base levels of the two valleys differ by an altitude of some 70 m. This has important consequences for the geomorphology of the area, the Riguel basin being far more deeply eroded and more dissected than the Aragón valley.

2.2.2 Catchment area fringes

a) The Aragón basin. Though the whole northern part of the project area drains towards the Aragón river, only a section of the north-western part does so directly. The rest of the basin is virtually isolated because it is almost surrounded by Miocene-Oligocene uplands.

The eastern border of the basin is the mesa de Larrate which, apart from the uplands, is the highest feature of the northern area. To the south some residual relief forms the interfluvium between the Aragón and the Riguel basins. The Castiliscar stream has cut the eastern mesa into two parts and through this gap the basin drains towards the Aragón.

The north-western end of the area is bounded to the south by a high mesa, while to the west the watershed runs along an Oligocene mudstone and gypsum formation.

b) The Riguel and Arba basin. Uplands of Miocene sediments form the western fringe of the Riguel catchment area. These sediments consist of mudstones and siltstones, while in the south higher Miocene

limestone occurs. The river has cut up an ancient Quaternary mesa and has formed an alluvial valley in between. The interfluvium between the Riguel and the Arba catchment areas runs along the eastern edge of the mesa. Only a very small part of the studied area drains directly into the Arba.

2.2.3 Main geomorphological processes

The evolution of the present landscape is the result of erosion working upon the Miocene-Oligocene sediments and the ancient Quaternary mesas, plus deposition of sediments transported by streams. Thus erosion followed by transport and deposition under semi-arid climatic conditions is the main process involved.

In the northern basin a former rough Miocene plain of mudstones and siltstones was eroded during the Quaternary. As a result some residual relief remains wherever a hard siltstone layer has protected softer mudstone underneath. Denudation and transport of coarse materials from eastern uplands during the early Quaternary formed local colluvium that was afterwards eroded again. Of this coarse alluvium, stony ridges remain as residual relief.

Further erosion-deposition processes have formed narrow fluvio-colluvial valleys, which run westwards between the residual relief. Major streams coming from the surrounding uplands have formed alluvial fans. These fans have not developed their characteristic triangular shape because their deposition has been restricted by the presence of many residual hills.

Near Alera several fluvio-colluvial valleys merge into a flat alluvial plain which is surrounded by higher residual hills. As the plain outlet is rather narrow, both the lowest part of the fluvio-colluvial valleys and the alluvial plain itself are poorly drained.

Between the residual hills and the alluvial formations, eroded slopes mixed with local colluvium prevail.

In the north-western part of the project area the main geomorphological process has been the deposition of mixed alluvium by the Aragón river during the Quaternary inter-glacial periods and erosion during the glacial epochs. Sedimentation still continues and so mixed alluvial land is being formed in the present flood plain. The result of these processes is the formation of a broad alluvial valley in which three levels of fluvial terraces can be distinguished.

Between the fluvial terraces and the higher conglomerate mesa, a piedmont slope occurs which is now being eroded.

In the north-western end of the area, erosion working upon the tilted Oligocene gypsum sediments has resulted in parallel gypsum-ridges and associated valleys.

In the Riguel basin erosion was deeper and has worked upon the Miocene sediments and upon the remaining mesas as well. Between the mesas and the Riguel alluvial valley a piedmont slope occurs. Erosion is now working upon the soft mudstone of the slope and upon the harder conglomerate of the mesa escarpment. The result is the formation of eroded slopes and narrow erosion valleys which are cutting the mesa edges. Due to this process some isolated mesas remain as residual hills.

In the western part of the area soft mudstones and some parts of the remaining old colluvial ridges have been eroded. Denudation of nearby Miocene uplands and further transport and deposition of fine saline alluvium by streams have formed narrow alluvial valleys and fans.

The weathered mudstones and siltstones still contain salts. The alluvium derived from these Miocene-Oligocene sediments also contains soluble salts as in this semi-arid climate no desalinization occurred during its transport. This alluvium is even more salty than the weathered mudstones themselves, and the further it has been transported the higher is its salt content.

On the other hand, the ancient alluvium of coarse fragments covering the Pliocene-Pleistocene mesas and the mixed alluvium deposited by the

Aragón and Riguel rivers are non-saline because their denudation areas are outside the Miocene-Oligocene saline sediments. Moreover these formations have a higher permeability and during rainy periods have lost any salts initially present.

2.2.4 Major physiographic units

Within the whole project area the major physiographic units were defined (Fig.2.6). Each of these is subdivided into minor components indicated on the physiographic soil map (Chap.4). The relative position and the relationship between the different physiographic units are illustrated in schematic cross sections (Figs. 2.7 through 2.12).

Of the units described 1-6 are confined to the Aragón drainage basin and therefore only occur in the northern part of the area. Unit 7 is common to both, whereas units 8-10 are only found in the Riguel-Arba basin.

1. Rough mountainous land. This is formed by the dissected Miocene-Oligocene uplands surrounding the area. It appears inside the area only near the northern border.

2. Aragón alluvial valley. This comprises three fluvial terraces and a recent flood plain of mixed alluvial land (Fig.2.7). The different terraces are separated by terrace escarpments. Medium and high terraces consist of coarse alluvium and the lower terrace of alluvial sands. All terraces are covered by medium textured sediments no thicker than 1 m. The thickness of the alluvium above the mudstone is more than 3 m in all terraces. The lower terrace is about 325 m above mean sea level, the medium terrace about 360 m, and the higher terrace about 370 m.

3. Rough eroded plain. This unit has a highly irregular surface consisting of the residual relief of a Miocene plain which was eroded during the Quaternary (Fig.2.8). It comprises minor physiographic units as residual stony ridges and siltstone outcrops, eroded slopes with local colluvium, and intervening fluvio-colluvial valleys. In these valleys

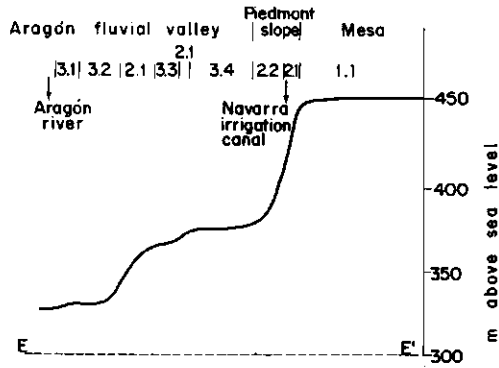


Fig.2.7: Schematic cross-section of the Aragón alluvial valley.

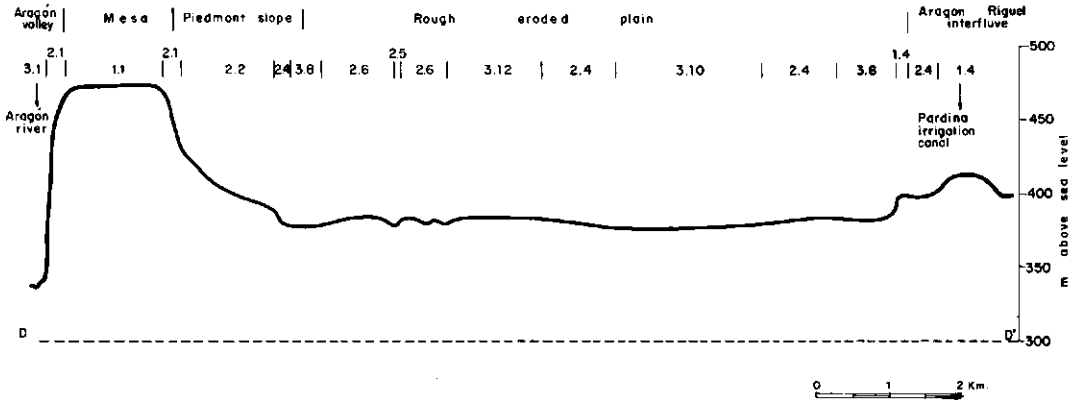


Fig.2.8: Schematic cross-section of the rough eroded plain.

5. Alluvial plain. Several fluvio-colluvial valleys coalesce to form a poorly drained alluvial plain. This was formerly a seasonally swampy area composed of relatively recent alluvium which has now been drained by improving and deepening the natural outlets.

6. Gypsum ridges and valleys. In the north-western end of the project area a distinct unit is formed by long parallel gypsum ridges and narrow valleys (Fig.2.9). They are the consequences of the erosion of the tilted gypsiferous sediments of the area. The ridges form steep escarpments facing south.

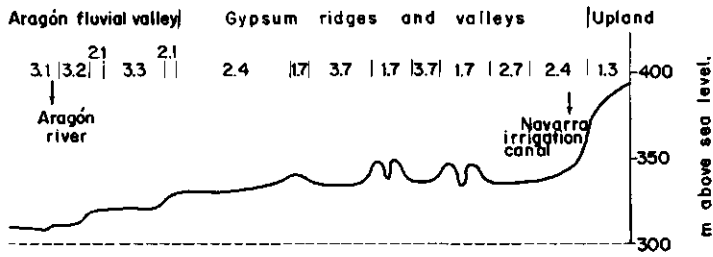


Fig.2.9: Schematic cross-section of the gypsum ridges and valleys.

7. Mesas. With the exception of the rough mountainous land the mesas, locally named "sasos", form the highest physiographic unit of the project area. This unit is very extensive within the area and occurs in both drainage basins.

These mesas are high old alluvial plains formed in late-Pliocene/early-Pleistocene by deposition of coarse alluvium transported by water courses flowing down from the Pyrenees in times of heavy rainfall (Figs. 2.10 and 2.11).

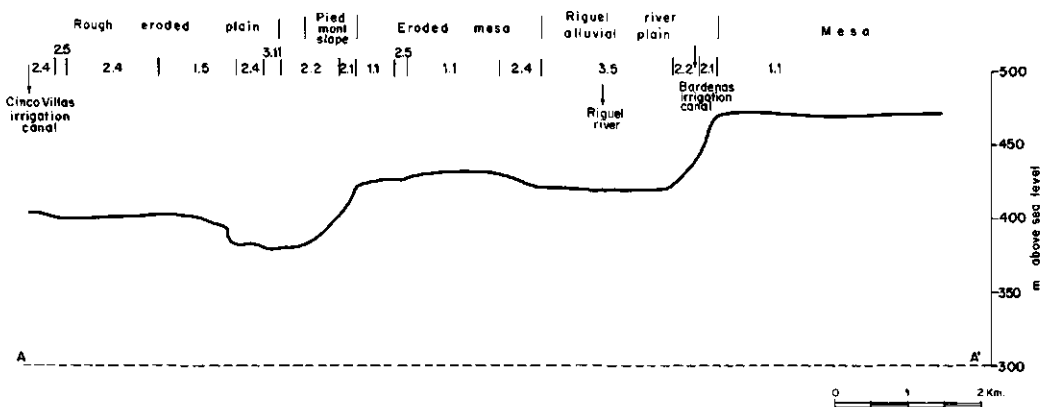


Fig.2.10: Schematic cross-section of the studied area showing the Riguel river alluvial plain and two levels of mesas.

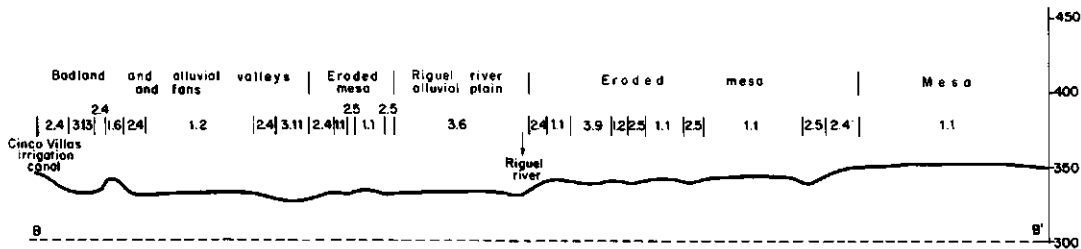


Fig. 2.11: Schematic cross-section of the studied area at a lower level than that of Fig. 2.10.

The mean altitude of the mesas is 450 m above sea level, though eroded mesas occur in lower positions. They are characterized by moderately shallow red soils overlying calcified well-rounded coarse alluvium which in turn overlies the Miocene mudstone.

The mesas are flat and their slope is generally less than 1 per cent but always in north-south direction.

8. Eroded mesas. Together with the gradual lowering of the base level of the Riguel river the mesa edges have been deeply incised by temporary streams (Figs. 2.10 and 2.11). Once the harder conglomerate has been removed erosion working upon the softer mudstone becomes more intensive. As a result of this process the mesa edges are severely eroded and only small isolated remnants of the major unit remain.

A transition between the mesas and the lower alluvial land is formed by piedmont slopes, which consist of a mixture of local colluvium from the higher ground and Miocene mudstone.

9. Riguel alluvial plain. Between the two eroded parts of the ancient uniform mesa the Riguel river has laid down its own deposits forming a broad alluvial plain (Figs. 2.10 and 2.11). This alluvium is more than 3 m thick and consists of fine sediments which overlie the Miocene mudstone. These sediments are derived from outside the mudstone area and are consequently free of salts.

At the moment the Riguel is entrenched in its own sediments and a narrow levee of sandy loam soils can be distinguished.

10. Badlands, alluvial valleys, and fans. This unit is found between the western mudstone and siltstone uplands and the western edge of the eroded mesa (Fig.2.11). All temporary streams that transport the eroded material from the uplands drain towards a permanent stream which joins the Riguel in the south of the area. This Valareña stream runs close to the mesa edge.

This major unit comprises the residual relief which remains as evidence of the erosion of the mudstones and old colluvial ridges composed of angular cobbles. The unit also comprises narrow alluvial valleys and in the south of the area alluvial fans whose lower parts reach the Riguel and Arba valleys (Fig.2.12).

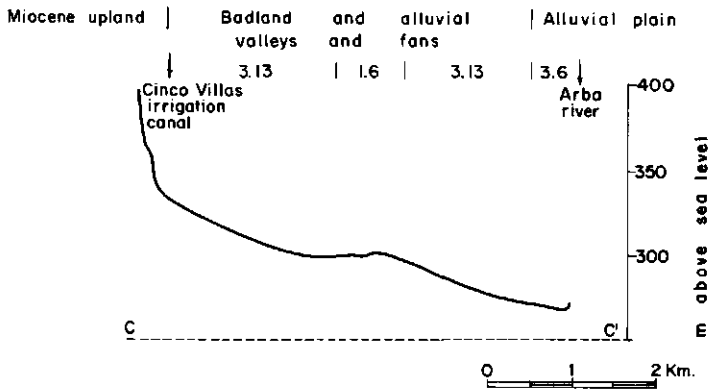


Fig.2.12: Schematic cross-section of the southern piedmont unit.

The result of erosion and alluvial deposition is a "Badland" of residual stony ridges and eroded slopes with intervening valleys and fans.

The alluvium of valleys and fans is quite similar and consists of very fine saline material, very finely stratified, which locally overlies a coarse alluvium of rounded gravel which in turn overlies the Miocene impervious mudstone.

As the main object of the reconnaissance survey was to map and investigate the salt-affected soils and as there is a close relationship between soil salinity and physiographic units, these units form the main soil landscapes and broad soil associations. Every major unit comprises minor physiographic units whose soils have a well-defined level of salinity.

The main physiographic soil units may therefore be regarded as the basis for the highest level of soil classification for salinity mapping. The physiographic soil map is in fact a soil association map which shows the distribution of the units over the project area.

2.3 Climate

The Ebro basin is the driest part of northern Spain because it is surrounded by high mountain ridges which isolate the region from any Atlantic and Mediterranean influences. The centre of aridity is sited around Zaragoza (Fig.2.13).

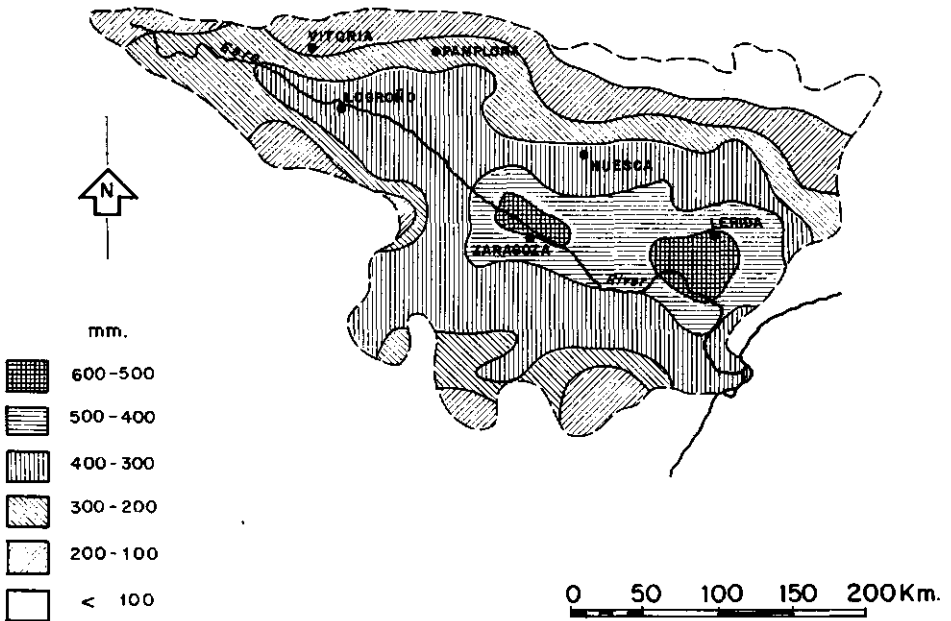


Fig.2.13: Mean annual precipitation deficit in the Ebro basin (from Thornthwaite water balance). From F.Elias and R.Gimenez Ortiz, Madrid 1965).

By the Köppen classification the climate of the Bardenas area is temperate with hot summers and evenly distributed rainfall (Cfa). By the Thornthwaite classification the climate is semi-arid with a slight excess of water in winter only in the north of the area (DB'₂).

From north to south the climate becomes drier. There is a marked seasonal temperature variation with hot summers and cold winters. Evapotranspiration exceeds total precipitation; the latter is extremely variable and is not concentrated in distinct rainy seasons, although summer and winter are slightly drier than autumn and spring. Wind velocity is high mainly in winter and spring, and both cold and warm dry winds are common.

Climatological data have been collected from two observation stations, one in the north (La Oliva) and one in the south (Gallur). The data are compiled in Table 2.1.

2.3.1 Temperature

Figure 2.14 shows a great variation of mean temperature over the year. The average values range between 5 °C in winter and 23 °C in summer and there is 1 °C mean temperature difference from north to south. In summer day temperatures will sometimes reach 40 °C and in winter minimum temperatures as low as - 7 °C have been recorded.

The frost-free period is about 165 days and the growing season for irrigated summer crops starts in early April and finishes in late October. It is therefore long enough for maize but too short for rice. Night frosts in early spring and frequent strong winds make fruit-tree cultivation difficult in most parts of the area.

TABLE 2.1 Climatological data from Bardenas area observation stations
(kindly provided by the National Meteorological Service)

Sta.	No. of years	J	F	M	A	M	J	J	A	S	O	N	D	Year
Mean temperature in °C														
1	36	4.3	5.8	9.4	12.2	15.3	19.6	22.5	22.1	19.1	14.3	8.5	5.3	13
2	18	5.5	6.9	10.6	13.0	17.4	21.1	22.7	23.2	20.3	14.8	9.4	6.6	14
Extreme maximum temperature in °C														
1	36	15.7	17.5	22.6	25.6	31.0	35.8	38.5	37.6	33.6	26.9	20.0	15.2	38.5
2	18	15.5	17.2	22.8	25.2	30.4	34.7	36.7	35.2	31.7	25.3	19.3	15.3	36.7
Mean maximum temperature in °C														
1	36	8.9	11.0	15.5	18.5	22.2	27.0	30.7	30.0	26.3	20.4	13.6	9.3	19.5
2	18	9.0	11.3	16.0	18.5	23.7	27.6	28.7	29.4	25.8	19.6	13.4	9.8	19.4
Mean minimum temperature in °C														
1	36	-0.4	0.5	3.2	5.9	8.4	12.1	14.2	14.1	11.9	8.1	3.3	1.2	6.9
2	18	1.9	2.5	5.2	7.4	11.1	14.5	16.6	16.9	14.8	9.9	5.4	3.3	9.1
Extreme minimum temperature in °C														
1	36	-7.0	-5.8	-2.8	-0.5	2.3	6.7	9.4	8.9	5.8	1.3	-3.2	-5.2	-7.0
2	18	-3.3	-3.5	0.6	2.1	5.5	9.7	12.0	12.1	9.7	3.9	1.4	2.9	-3.5
Mean relative humidity in percentage														
3	56	75	68	62	59	58	57	53	56	63	69	74	78	-
Mean precipitation in mm														
1	39	35	28	33	44	52	45	22	30	46	44	51	45	475
2	18	23	20	25	23	33	47	17	15	45	41	30	31	350
Mean number of days with precipitation of 0.1 mm or more														
1	39	7	7	8	8	8	7	4	4	6	7	9	10	85
2	18	6	6	7	7	8	6	4	4	6	6	8	8	76
Mean number of days with snow on the ground														
1	39	1.1	0.9	0.2	-	-	-	-	-	-	-	0.1	0.5	2.8
2	18	0.9	0.7	0.3	-	-	-	-	-	-	-	0.1	1.0	3.0
Wind speed in m.sec ⁻¹														
3	56	4.2	4.5	4.5	4.8	4.3	4.5	4.3	4.0	3.8	3.6	3.8	4.1	-
Mean sunshine duration in hours per day														
3	56	4.4	5.9	6.4	7.7	9.0	10.4	11.7	10.5	7.9	6.2	5.3	4.1	-

NOTE:
 Station 1: La Oliva 41°22' - 1°27' W 342 m
 Station 2: Gallur 41°52' - 1°19' W 267 m
 Station 3: Zaragosa 41°39' - 53' W 237 m

2.3.2 Precipitation

Annual total precipitation decreases southwards towards the centre of the Ebro basin. Mean values vary between 475 mm in the northern area and 350 mm at the southern border.

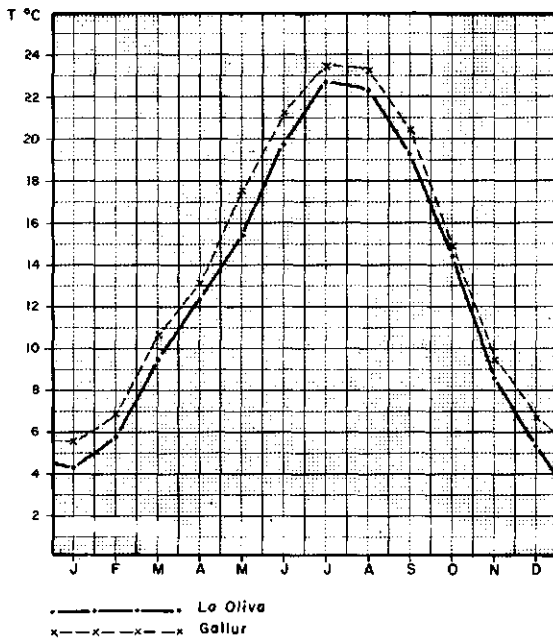


Fig.2.14: Mean temperatures in °C.

Total rainfall and its distribution differ from year to year, but continuous periods of heavy rainfall are uncommon. The total amount is well distributed over the year and there is no seasonal concentration of precipitation. Both factors have their influence on the salt regime of the soils.

For drainage design purposes a maximum rainfall analysis was made. Depth duration frequency diagrams were drawn, using the Gumbel probability distribution (Figs.2.15 and 2.16). From the data of mean precipitation (Table 2.1) and Figs. 2.15 and 2.16, it could be concluded that in areas of lower total yearly precipitation heavy rainfall intensity is higher. The graphs show that periods of continued heavy rainfall are uncommon and there is hardly any difference between the amount of precipitation expected in 3 and 6 consecutive days.

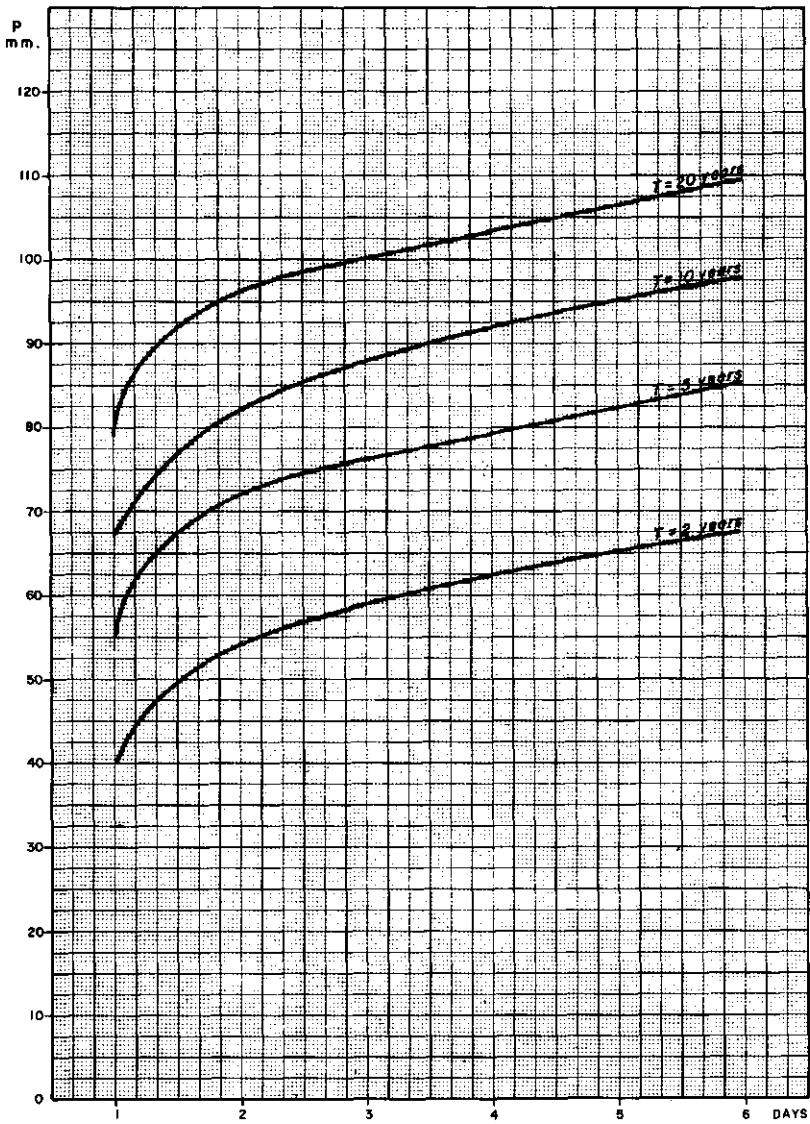


Fig. 2.15: Depth-duration-frequency relation (La Oliva - northern Bardenas).

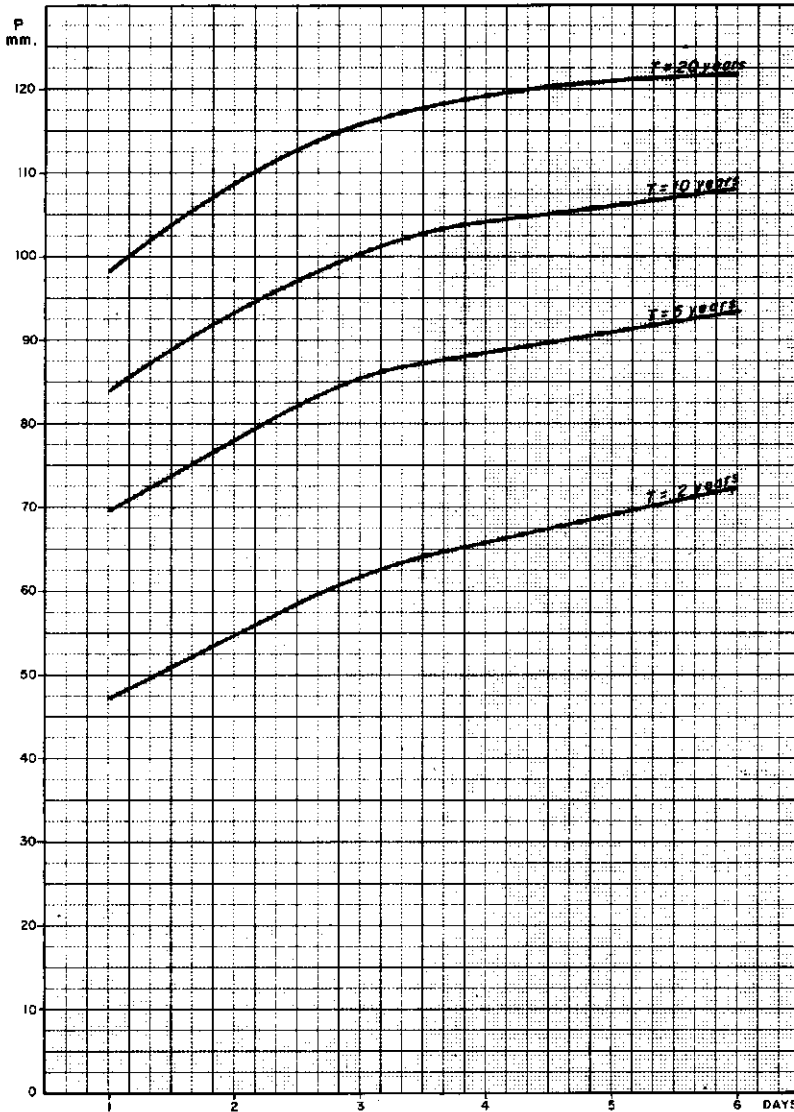


Fig.2.16: Depth-duration-frequency relation (Ejea - southern Bardenas).

In the northern area the maximum 3-day rainfall with a 5-year return period would be 76 mm. The corresponding amount in southern Bardenas is 85 mm. Taking into account only the irrigation season 68.5 and 75 mm respectively are the amounts to be expected in 3 days for a return period of 5 years (Fig.2.17).

TABLE 2.2 Potential evapotranspiration data

Sta.	No. of years	J	F	M	A	M	J	J	A	S	O	N	D	Year
Mean potential evapotranspiration in mm (Thornthwaite method)														
1	36	9.8	14.8	32.6	51.8	73.2	110.3	136.2	125.2	89.5	53.2	22.6	11.8	731.0
2	18	10.1	15.3	38.2	52.4	91.2	122.1	145.8	131.7	94.2	53.7	24.6	13.8	793.1
3	56	12.4	17.4	37.1	53.4	86.5	121.3	145.0	135.5	93.6	54.6	24.6	14.3	795.7
Mean potential evapotranspiration in mm (Penman method)														
3	56	20.5	32.6	71.5	97.5	143.4	170.6	194.6	164.8	95.0	54.3	22.4	15.1	1082.3
Mean potential evapotranspiration in mm (Turc method)														
3	56	23.8	36.9	64.5	91.0	120.4	146.9	164.2	143.2	100.8	65.0	37.7	23.6	1018.0

NOTE:
 Station 1 La Oliva 45°32' - 1°37' W 342 m
 Station 2 Gallur 41°52' - 1°19' W 257 m
 Station 3 Zaragoza 41°39' - 53' W 237 m

The variation of mean daily potential evapotranspiration (E-Thornthwaite) is shown in Fig.2.19. There is a good agreement between the average E-values (Thornthwaite) for the south of the area and Zaragoza meteorological station.

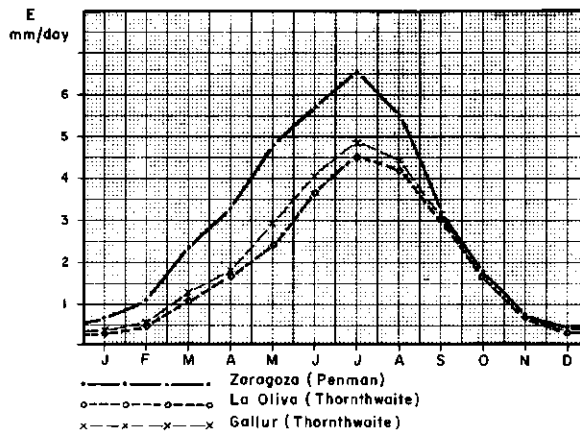


Fig. 2.19: Mean daily potential evapotranspiration.

Comparing the E-values derived by the Thornthwaite method with those of the Penman method (Zaragoza) a good agreement is observed during autumn (September - December), but for the rest of the year Penman values are greater. This is explained by the absence of wind in autumn.

The actual consumptive use of irrigated crops has not been calculated but in the irrigation season the total deficit of precipitation ranges between 580 and 700 mm. The peak E-values of 6 and 6.5 mm day⁻¹ occur in July.

2.4 Natural vegetation

A great part of the area is under crops, so that natural vegetation is restricted to residual and eroded soils not used for agriculture and to salt-affected soils.

The natural vegetation cover is of mediterranean semi-arid type and can be broadly grouped into the following plant associations:

1. In the northern area on the edges and escarpments of mesas roughly above the 400 m contour line, there is a sparse forest of *Pinus halepensis* with bushes of *Quercus coccifera* and *Pistacia* (Fig.2.20).



Fig.2.20: Sparse forest of *Pinus halepensis*.

2. Below that altitude on residual salt-free soils there is a plant association of bushes of *Juniperus*, *Thymus vulgaris*, *Rosmarinus officinalis* and *Genista*.

3. Halophytes grow on the saline soils of alluvial valleys and fans. Dominant species are *Suaeda brevifolia*, *Plantago crassifolia* and *Hordeum murinum* (Fig.2.21). On the borders of fields and along the roads bushes of *Atriplex halimus*, *Salsola vermiculata*, and *Artemisia herba-alba* grow where salt concentration is not too high. In fluvio-colluvial valleys and plains, where drainage conditions are so poor that a very saline groundwater table is close to the soil surface, *Arthrocnemum glaucum* and *Suaeda* are found. Near water courses of saline areas there are isolated trees of *Tamarix africana*.



Fig.2.21: Halophytes on a saline soil.

4. In patches of slight salinity in the northern alluvial plain there is a transitional subhalophyte association in which *Lygeum spartum* is the dominant species (Fig.2.22).

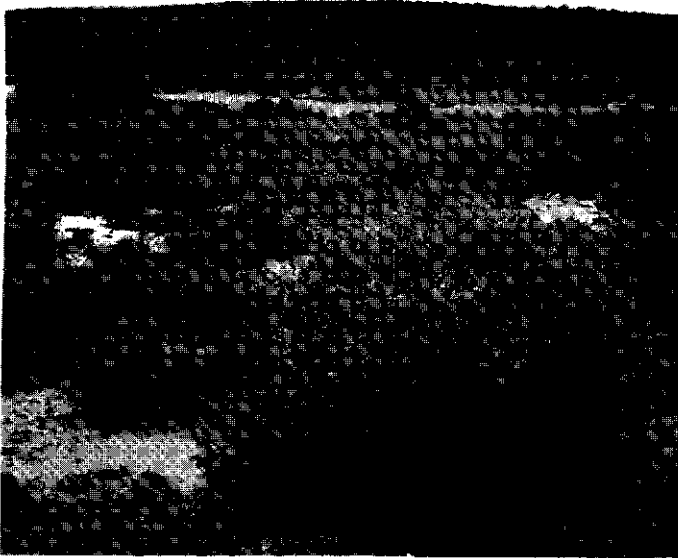


Fig.2.22: Subhalophyte association with *Lygeum spartum*.

Along main water courses and roads new plantations of *Populus* have been established and round new villages *Pinus halepensis* is grown in public parks.

Plant associations of the Ebro Basin were investigated by Braun-Blanquet and O.de Bolós (1957).

2.5 Present land use

2.5.1 Irrigated farming

Irrigated farming is influenced by soil conditions. Salt-free soils of mesas and alluvial valleys are under full irrigation, the main crops being maize, lucerne, sugar beet, and some horticultural crops. Crop rotations include winter cereals, mainly barley and wheat, which are irrigated in spring. Soybean is a new crop which is being introduced in the area.

Seed-beds are prepared by ploughing late in winter, heavy soils requiring further harrowing and rolling. Summer crops are sown in April and early May. Harvesting starts in late October, with the harvest of beet continuing until January.

Lucerne stays on the field for four or five years, depending on the effective depth of soil. Sowing time varies from late summer to spring. Sowing in autumn involves a risk of damage by early autumn frosts. On the other hand in clayey soils dry spring winds can form surface crusts which may hamper germination.

In the piedmont and colluvial slopes where salinity levels are low, winter cereals are grown. In spring one or two irrigations are applied depending on weather conditions. Because land levelling exposes deeper saline and less pervious layers, most parts of the slopes are unlevelled. For cereals spring irrigation is done by gravity flow which means an uneven water distribution. When slopes are irrigated by sprinkler irrigation, lucerne is included in the crop rotation.

Cropping pattern and intensity on the saline soils of alluvial valleys and fans depends on their salinity level. Crops include barley, sugar beet, and lucerne, although lucerne is only grown on successfully leached soils. Severely salt-affected soils are not cultivated.

Average yields per hectare obtained on some soil units are listed in Table 2.3.

TABLE 2.3 Average yields (kg/ha) for different soil units

Crops	Soils of the mesas	Alluvial soils		Soils of the slopes
		non saline	slightly saline	slightly saline
Maize	8 000	7 000	-	-
Lucerne	40 000	55 000	30 000	-
Sugar beet	30 000	40 000	30 000	-
Wheat	3 500	4 500	3 500	2 000
Barley	3 500	4 000	3 500	3 000

Farm operations are completely mechanized, except for sugar beet grown on small areas, where much manual work is required in the singling and harvesting stages. The rise in labour costs is the main reason for not increasing sugar-beet acreages.

Farmers use mineral fertilizers on a large scale but as animal husbandry is uncommon in the area manure applications are limited.

Grain and fodder are sold and sent outside the area. In the villages, farmers keep some milking cows and pigs for their own use.

Rural industries are mainly confined to maize-grain drying and to lucerne drying, but some vegetable processing and canning has commenced.

The size of newly established holdings was about 8 hectares at the start of the settlement (1955). Nowadays, new farms average 20 hectares of irrigated land. In addition, the settlers receive some non-irrigated arable land.

2.5.2 Dry farming

On the higher lands not under command of irrigation barley is grown. Seed-bed preparation starts in early autumn. The most common date of sowing is late October, but depends very much on the rainfall distribution. New wheat varieties less sensitive to spring frosts are now being introduced in the area and sowing time is delayed until January. Harvesting starts late in June for barley and in July for wheat.

Residual soil areas unfit for cultivation are used as rough pasture for sheep.

and sub-lateral canals are listed in Table 3.2.

TABLE 3.2 Secondary canals of Bardenas-I area
(From F.de los Rios, 1966.)

Canal	Total length (km)	Flow m ³ /sec	Origin
Pardina	7	29	Bardenas
Navarra	36	8.7	Pardina
Cinco Villas	51	17.8	Pardina
Cascajos	23	7.8	Bardenas
Saso	11	7.5	Bardenas

At present the Bardenas canal debouches into the Arba river, but the aqueduct of Biota over the Arba has now been completed and the second part of the canal is under construction. When it is completed, it will irrigate the second part of the Bardenas area (approximately 30 000 hectares more).

Quality of the irrigation water

The Bardenas canal water is of good quality for irrigation as its electrical conductivity (EC_1) varies from 250 to 750 micromhos/cm.

The small amount of leaching water needed to maintain a low salinity level in the irrigated soils is met by the normal application losses associated with surface irrigation.

There is no marked annual variation in the salt content of the irrigation water, though salinity increases slightly towards the end of the irrigation season. Table 3.3 gives the mean composition of the irrigation water in 1972/73.

TABLE 3.3 Bardenas canal irrigation water analysis

	Winter	Spring	Summer	Autumn
Total salt content meq/l	6.8	6.5	6.9	7.5
Cl ⁻ meq/l	0.5	0.3	0.5	1.4
CO ₃ ⁼ meq/l	0.1	0.1	0.2	0.1
CO ₃ H ⁻ meq/l	2.2	2.9	2.4	1.6
SO ₄ ⁼ meq/l	0.3	0.2	0.4	0.8
Ca ⁺⁺ + Mg ⁺⁺ meq/l	3.0	3.2	2.9	2.2
Na ⁺ meq/l	0.7	0.2	0.4	1.4
K ⁺ meq/l	-	-	-	0.1
Ca ⁺⁺ meq/l	2.8	2.4	2.3	1.5
Boron meq/l	-	-	-	-
EC-25°C micromhos/cm	280	305	295	345
pH	7.8	7.5	7.7	7.7
SAR	0.6	0.2	0.3	1.3
RSC meq/l	0	0	0	0
Classification	C ₂ -S ₁			

The sodium adsorption ratio of the irrigation water is in the lowest range (S₁), and the residual sodium carbonate (RSC) value is zero, so that there is no danger of alkalinization.

3.1.2 The main drainage system

The area studied can be divided into five hydrological units, each drained by a main water course (Fig.3.2).

Unit A drains toward the Castiliscar stream, which joins the Aragón river at Carcastillo. The unit receives water from rainfall, irrigation, and run-off from the surrounding uplands. Former intermittent streams have been deepened and are now used as main drains.

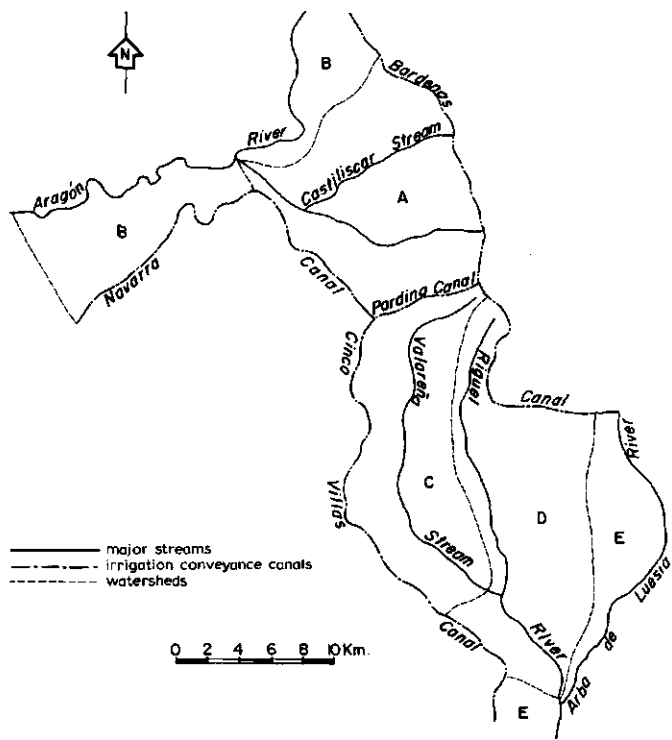


Fig.3.2: Schematic map of the main irrigation and drainage systems.

Unit B drains directly toward the Aragón river. Ephemeral water courses flowing through the Aragón alluvial valley are used as main drains.

Unit C, apart from receiving rainfall and irrigation water, also receives seepage water from the adjacent western uplands. Intermittent streams flowing down join the Valareña stream, which receives supplies from the adjacent mesa as well. The Valareña debouches into the Riguel river in the south of the area.

Unit D drains toward the Riguel river, which receives water from irrigation and rainfall on the Riguel alluvial plain and from part of the two adjacent mesas. Water courses in the erosion valleys of the mesas have been deepened and are now used as main drains.

Unit E drains directly toward the Arba river and comprises the eastern edge of the eastern mesa and the southern part of the studied area.

Generally the salinity of the water in the main drains is low. In fact in 1974/75 the EC of the Aragón water at the north-western end of the area was never higher than 0.4 mmhos/cm. In the same period the Arba water at the south of the area had a variable salinity between 0.9 and 4.5 mmhos/cm. The latter value is more representative of the salinity of the drainage water, as the Bardenas canal tail escape flows into the Arba river.

The value of 4.5 mmhos/cm was found when the canal ran dry (February). Likewise the salinity of both the Castiliscar stream and the Riguel varied between 2 and 5 mmhos/cm.

As the salinity of the groundwater is very high in some geomorphological units (see Tab.3.4), the low EC-values in the main drains indicated that the saline soils were being leached at a very slow rate. The greater part of the area's drainage water comes from the tail escapes of the irrigation system, from non-saline groundwater, and from run-off. Very little is derived from the saline areas, which are not cultivated and therefore not irrigated.

3.2 The groundwater table and drainage conditions

The depth and hydraulic gradient of the groundwater table and the salinity of the water depend on the situation of each geomorphological unit and its relation to adjacent units.

The drainage conditions in each unit depend on the depth of the least permeable layer, the hydraulic conductivity of the permeable layer and its drainable pore space, and the recharge of water received. The recharge may be supplied by rainfall, by net percolation from irrigation, or by seepage from surrounding high-lying areas.

In the project area some units of a characteristic hydrology can be defined in relation to the major geomorphological units.

3.2.1 Rough mountainous land

In the uplands that surround the irrigated area, the effective rainfall is very low because the unweathered mudstone and siltstone are impervious and so prevent infiltration. Most of the rainfall becomes surface run-off, which causes erosion of the soft sediments. Ephemeral streams catch this run-off and transport the water into adjacent low-lying areas.

3.2.2 Aragón alluvial valley

No water table has been detected in the upper 3 m of the fluvial terraces of the Aragón valley. The whole unit drains freely toward the Aragón river.

The transmissivity of the coarse alluvium ($k > 2$ m/day) is so high that no drainage problems have been created by the irrigation of the area. The impervious layer is formed by the underlying mudstone, which is always deeper than 3 m.

There is local seepage from the terrace escarpments but no deep seepage from higher to lower terraces because the underlying mudstone is impervious.

Although no groundwater samples were taken, its salinity is assumed to be very low because it is recharged only by rainfall and by irrigation percolation losses.

3.2.3 Rough eroded plain

In this major geomorphological unit, drainage conditions and water table depths differ in each minor unit.

The fluvio-colluvial valleys receive water from rainfall, irrigation, and seepage from the surrounding residual hills and slopes. The depth of the impervious layer varies between 1 and 2 m and the transmissivity of the permeable layer is low ($K = 0.2$ to 0.5 m/day, $D = 1$ to 2 m). The hydraulic gradient is low as the slope of the unit is less than 1 per cent. The lower-lying valleys thus have a shallow groundwater table and poor drainage conditions.

In the eroded and colluvial slopes there is no indication of a water table within 2 or 3 m of the surface. At present, however, the eroded plain is not under full irrigation, the slopes being only locally irrigated in spring. Any increase in water use could cause the groundwater tables in the lower valleys to rise. If that were to happen, a cut-off drainage system would be sufficient to control the lateral seepage, as the pervious layer in the valleys is restricted to the mixed alluvium-colluvium and the impervious layer is not deeper than 2 m.

The salinity of the phreatic water of the fluvio-colluvial valleys is very high, sometimes reaching EC-values of about 50 mmhos/cm (Table 3.4).

As the lower areas do not drain freely toward the main drains, a sub-surface drainage system is necessary to allow the soils to be leached and to prevent a rise of the saline water table.

TABLE 3.4 Characteristic groundwater analysis

		G e o m o r p h o l o g i c a l u n i t s						
		Mesas	Piedmont slopes	Riguel alluv. plain	Erosion valleys	Fluvio-colluvial valleys	Saline alluvial valleys	Saline alluvial fans
Cl ⁻	meq/l	2.8	11.7	23.9	38.5	348.0	342.2	894.4
CO ₃ ⁼	meq/l	0.4	0.1	0.3	0.4	0.6	-	-
CO ₃ H ⁻	meq/l	3.9	8.7	3.9	4.3	3.0	11.9	2.4
SO ₄ ⁼	meq/l	4.6	7.5	14.3	24.2	133.1	55.0	79.7
Ca ⁺⁺ + Mg ⁺⁺	meq/l	5.8	9.5	20.0	11.8	102.2	107.0	228.6
Na ⁺	meq/l	6.6	19.5	23.3	56.8	380.0	304.1	751.1
K ⁺	meq/l	-	-	0.1	0.1	0.1	-	0.1
Ca ⁺⁺	meq/l	4.5	5.6	10.9	4.9	36.0	51.1	72.8
Boron	meq/l	-	-	-	-	-	-	-
EC-25°C	mmhos/cm	1.2	2.7	4.2	6.4	48.0	32.8	62.9
pH		7.9	7.6	7.5	8.0	7.7	7.2	7.8
SAR		3.9	8.9	7.4	23.4	53.2	41.6	70.2
RSC	meq/l	-	-	-	-	-	-	-
Classification		C ₃ -S ₁	C ₄ -S ₃	C ₄ -S ₃	C ₄ -S ₄	C ₅ -S ₄	C ₅ -S ₄	C ₅ -S ₄

3.2.4 Alluvial fans

In this unit with the present low intensity of irrigation, there is no indication of a groundwater table within 3 m of the surface. Deep borings showed water levels between 5 and 6 m.

3.2.5 Alluvial plain

Drainage conditions and water table depths in this unit are similar to those of the fluvio-colluvial valleys. The hydraulic gradient is even lower than that in the valleys as the slope is smaller.

A deepening of the drainage outlet and an initial drainage system of open ditches have allowed some control of the water table with the

present low rate of irrigation. When the area is more intensively irrigated a more efficient drainage system will be required.

3.2.6 Gypsum ridges and valleys

The gypsum valleys receive water from the adjacent parallel ridges and from the higher lands to the east. They are also recharged by leakage water from the tail escape of the Navarra canal. As the area is not intensively irrigated losses of irrigation water are negligible.

At present there is a drainage system which consists of a main open drain running along the valley and several lateral ditches. The system is sufficient to control the water table which in the lowest parts of the valleys is still more than 1 m below the surface. When the area is under full irrigation the present drainage system will need to be improved.

3.2.7 Mesas

The mesas receive water only from rainfall and irrigation as they are at the highest level of the irrigated area and are cut off from the higher surrounding uplands. The permeable layer of coarse alluvium bears a perched water table above the underlying mudstone which acts as an impervious layer. The transmissivity of the coarse alluvium is high enough ($K > 2$ m/day, $D = 1$ to 3 m) to provide adequate natural drainage. The unit drains freely toward the mesa edges and finally to the main drains of the erosion valleys.

For this reason there is no permanent phreatic aquifer but an ephemeral perched water table. Its depth varies locally depending on the water management. There is also a seasonal variation due to the unit being under full irrigation. The water table is at its lowest in the non-irrigation season, but even during the irrigation season it is never high enough to affect crop growth.

As the water table is recharged only by rainfall and irrigation, its salinity is low ($EC < 2$ mmhos/cm). Diffusion of salts from the underlying saline mudstone, where it exists, is almost negligible.

3.2.8 Eroded mesas

In small depressions of the mesas where the coarse alluvium is shallow, and in the erosion valleys of the mesas where the alluvium has been removed, permanent water tables can exist, if they are fed by lateral seepage from the higher mesas.

Where an open drain leading from such depressions through the erosion valley has been constructed, the local drainage problem has generally been solved.

In the depressions the salinity of the water may rise to EC-values of about 9 mmhos/cm.

There is no deep seepage from the mesas to the low-lying alluvial valleys because the mudstone underlying the coarse alluvium is totally impervious. In the mesa escarpments, however, there is lateral water flow which creates local surface seepage. Cut-off drainage ditches intercepting this local seepage prevent the waterlogging of lower lands.

In the piedmont slopes between the mesas and the valleys, the impervious layer is formed by the mudstone or siltstone underlying the local colluvium. This impervious layer tends to prevent deep percolation, thus creating surface run-off in the upper shallow part of the slope and shallow interflow through the lower part.

If the natural gradient of the impervious layer has not been disturbed by land levelling, the slope drains freely towards the lower unit. Piedmont slopes therefore do not have a permanently high water table and ephemeral levels are extremely variable, although generally deeper than 2 m.

The salinity of the water varies between 2 and 8 mmhos/cm.

3.2.9 Riguel alluvial plain

The permeable alluvium ($K = 0.3$ to 0.5 m/day) extends deeper than 3 m. For this reason natural drainage is generally sufficient to prevent waterlogging and salinization.

The whole unit drains freely into the Riguel river. The water table depth is therefore determined by the water level in the river and locally by the water management of individual farmers.

The salinity of the water ranges between 1 and 5 mmhos/cm (Table 3.4). In the lower part of the plain, where seepage from the higher units recharges the water table, the salinity of the water increases up to 10 mmhos/cm due to a high sodium chloride content.

3.2.10 'Badlands', alluvial valleys and fans

The residual ridges and eroded slopes have shallow impervious sub-horizons which prevent infiltration. Thus most of the rainfall is removed as surface run-off and recharges the lower-lying alluvial valleys and fans.

The soils of the alluvial formations have surface horizons whose hydraulic conductivity varies from low to moderate ($K = 0.1$ to 0.5 m/day). Very fine stratification frequently occurs in the subsurface layers.

Where it exists, hydraulic conductivity for vertical flow (percolation rate almost zero) differs from lateral permeability ($K = 0.2$ m/day). Occasionally the sub-surface layers are compact and impervious. Below these impervious layers a gravel and coarse sand alluvium often occurs, which in turn is underlain by totally impervious mudstone.

Rainfall or irrigation water remains on the soil surface until it evaporates and sometimes a temporary perched water table is formed near the soil surface. In this way surface run-off is common even in levelled soils, thus creating a severe erosion problem.

The deeper coarse alluvium (between 3 and 5 m) is always saturated with water and forms a confined aquifer between the impervious mudstone and the confining stratified or compact layers.

Though a specific geohydrological survey of the confined aquifers was not made, they seem discontinuous because the gravel layers have a variable thickness and were not found in some deep bores.

In addition to the recharge from rainfall and irrigation, further water is supplied by leakage from the Cinco Villas canal and from uncontrolled seepage from higher irrigated areas.

The salinity levels of both the perched and confined water are both high and variable (EC = 10 to 75 mmhos/cm). High electrical conductivity values are caused by high sodium chloride contents (Table 3.4).

With the exception of some low-lying areas, there is no indication of a true groundwater table within several metres of the surface. It was therefore useless to attempt to draw an isohypses map of a phreatic aquifer.

4. Soils and soil conditions

4.1 General characteristics

4.1.1 Soil-forming processes

Most soils of the Bardenas area show no distinct characteristics of soil development. Except in the ancient alluvium of the mesas, soil-forming processes have had little time to act upon the very recent parent materials of alluvial and colluvial origin. Moreover, the climate being characterized by a marked aridity, an excess of water rarely occurs owing to the low amount of precipitation and its even distribution. Therefore, except for the soils of the mesas, there is little soil profile development. The soils of the mesas, formed over a much longer period, have diagnostic cambic and calcic, or petrocalcic horizons. The other soils, apart from an ochric epipedon, show the beginnings of argillic, calcic, gypsic and even salic horizons but only in a very incipient stage.

Two soil-forming factors are relevant in understanding the origin and extent of the salt-affected soils of the area. These factors are parent material and the relative position of each soil association within the landscape.

4.1.2 Parent materials

Parent materials can be grouped into three classes. First is the ancient coarse alluvium of the mesas, which consists of well-rounded stones, gravel, and coarse sand. Above this layer a reddish loamy generally stoneless layer occurs. Both the coarse and the reddish layers are rich in calcium carbonate and are salt-free.

Second are the parent materials of alluvial origin brought by the two main water courses flowing through the area - the Aragón and Riguel rivers - whose catchment areas are respectively outside and just at the edge of the Miocene-Oligocene sedimentation basin. The parent materials of the Aragón valley soils are salt-free coarse alluvium in the medium and higher terraces and loamy sands in the lower terrace. In the Riguel valley a fine alluvium is found, which consists of clay loam and is salt-free in the upper part of the valley. Both clay content and salinity increase towards the lower end of the valley. A narrow sandy levee not sufficiently wide to be represented on the map can be distinguished.

The third class of parent materials are those derived from the saline mudstone and siltstone, which are characterized by a very high percentage of silt. In the alluvial valleys and fans a fine alluvium has been deposited and in the lower parts of the slopes a fine colluvium. Both occur mixed in the fluvio-colluvial valleys. In the upper part of the piedmont slopes the parent material is mainly weathered mudstone. As these rocks are widespread throughout the area, soil texture varies within a narrow range, silt loam and loam being the most common textures. Salinity, though always present in these parent materials, is highly variable. In general the amounts of salts are highest in the low-lying alluvial formations (Chaps.2 and 3).

High calcium carbonate content (>40%) is a common property of the soils. In non-saline soils pH varies between 7.5 and 8. In soils with higher sodium content higher pH-values are common (8 to 8.5).

4.1.3 Topography

The soils of the mesas, fluvial terraces, and alluvial valleys and plains are flat. The eroded plain has an undulating topography with gentle slopes and flat low-lying fluvio-colluvial valleys. Stony ridges and mesa escarpments have a pronounced slope.

Topography has had a marked effect on the redistribution of salinity. The colluvial and piedmont slopes have lost salts which have accumulated in the lower flat areas (Chap.3).

4.1.4 Land and water management

Where the soils of the slopes have been levelled, the original soil profile has been truncated. Sometimes less pervious and more saline layers, previously deep, form the present surface soil. The flat soils of the mesas and alluvial valleys required only a slight smoothing of the land and the present soil represents only a slight re-arrangement of the original profile.

Irrigation has also played a role in the redistribution of salts. The percolation losses inherent in surface irrigation have leached the salts from the more permeable soils and carried them to other soils, particularly to soils deficient in natural drainage.

4.2 Mapping units

During the reconnaissance survey which formed the basis upon which the soil map was prepared, the physiographic approach was applied. The objective of the reconnaissance survey was to delineate the saline and potentially saline areas for their subsequent reclamation under irrigation. The mapping units are therefore based on those conditions that were relevant to the specific practical agricultural purpose of the survey, namely the salinity hazard and the land reclamation possibilities.

The mapping units thus represent landscape units based on the geomorphological features of land forms, slope, elevation and relative situation, parent materials, and drainage conditions. As has been described in the preceding chapters, all these features contribute to soil salinity.

The soil map prepared in this way is shown in Figs.4.1 and 4.2. The main mapping unit is a landscape or geomorphological unit. Some subdivisions were made on the basis of soil salinity level and drainage conditions. Erosion hazard also had to be added because it is a condition that radically affects the land suitability for irrigation.

Each mapping unit is equivalent to a broad soil association but with a similar salinity range and similar drainage conditions.

Some miscellaneous land types are also included. They indicate land with little or no soils, which serve no purpose for irrigated agriculture, and whose soil conditions were therefore not studied.

To standardize the various investigations and to ease correlation with soils of other areas, representative soil profiles were morphometrically classified. Descriptions of soil profiles are in conformity with the Soil Survey Manual (1951). Most of the soil analyses were done in line with those of Agric. Handbook No.60 of the USDA (1955). Soil classification was based on Soil Taxonomy, Agric. Handbook No.936, USDA (1975).

Four main zones, each of them related to a drainage basin, can be distinguished on the soil map (Chap.3).

The northern "Rough Eroded Plain" has a complicated soil pattern (cross-section in Fig.2.8). It comprises residual siltstone outcrops in the highest position and saline alluvial soils in the low-lying fluvio-colluvial valleys and plains. The transition between the two mapping units is formed by soils of eroded slopes in the upper part of the hills and soils of colluvial slopes in the middle and lower parts of the slope.

The north-western part of the area is dominated by the "Aragón Alluvial Valley" (see cross-section in Fig.2.7) where soils of fluvial terraces are found. In the south this zone is bordered by a high mesa situated outside the irrigation scheme. Between the alluvial soils of the valley and the higher soils of the mesa, transitional soils occur on piedmont slopes.

The same soil pattern dominates the south-eastern zone of the area as well (Fig.2.10). The soils of the mesas occupy the highest position and the soils of the Riguel alluvial plain the lowest. The soils of the piedmont slopes form a transition between the two.

The south-western major zone of "Piedmont slopes" has a highly irregular

soil pattern (Fig.2.12). It is composed of residual soils of the stony ridges and miscellaneous land in the highest position, and saline alluvial soils in the low-lying alluvial valleys and fans. Eroded slopes are situated between the residual soils and the depositional ones.

The mapping units and their main features for irrigated agriculture are described in the following paragraphs.

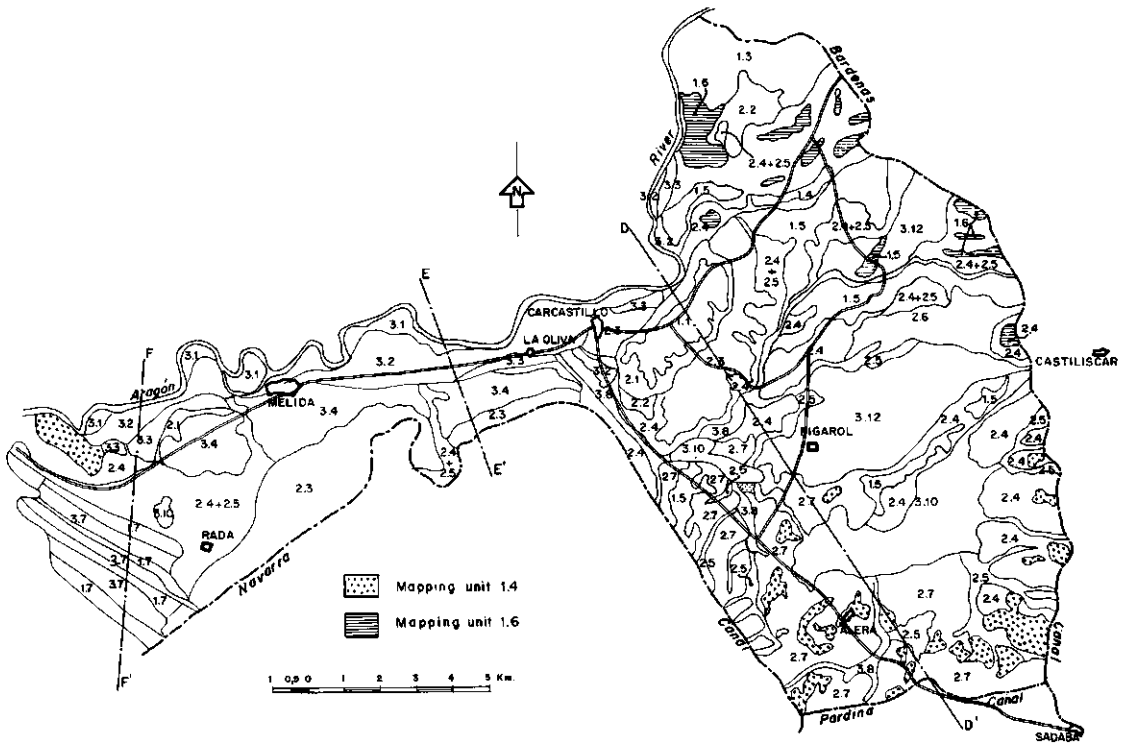


Fig.4.1: Physiographic soil map of the Bardenas area. Sheet I - Aragón basin. (Base map drawn from aerial photographs on an approximate scale of 1 : 31 000).

For legend, see p.50.

4.2.1 Mesas

Mesa soils (Mapping Unit 1.1) are the more developed soils of the area because the ancient coarse alluvium from which they derived had infiltration and percolation rates high enough to allow an illuviation of calcium carbonate and even clay during former periods of wetter weather. Calcic (Profile 2) and petrocalcic (Profile 1) horizons were thus formed.

Part of the original surface soil has been removed by erosion so that the soils are shallow with a limited rooting depth. On lower-level mesas however, a deep reddish fine soil overlies the semi-consolidated alluvium. In some small depressions the coarse alluvium is not found and the soils lie immediately on the impervious mudstone.

This mapping unit is a broad soil association in which effective depth of cultivable soil and soil texture vary (Fig.4.3).



Fig.4.3: Landscape of a soil of the mesas.

As the purpose of the survey was to map saline areas and as this soil association is in general free of salinity, phases of slightly different soils were not defined, except in an isolated phase (1.2) for remnants of eroded mesas which are out of the irrigation command.

The general soil properties of the mesa soils are:

a) Depth above the petrocalcic horizon varies between 30 and 80 cm. Root proliferation is well developed in the surface soil and even the petrocalcic horizon is occasionally penetrated.

b) Textures vary from sandy loam to silt loam, although soils may become more sandy with depth.

c) In the shallowest soils the degree of stoniness is high, but in general the surface soil is free of stones and gravel.

d) Structure is weakly to moderately developed although the surface soil generally has a strong crumb structure.

e) Infiltration and percolation rates are more than adequate to allow water to pass through the soil profile. The transmissivity value is sufficient to permit adequate drainage (Chap.3). Total moisture-holding capacity varies with the soil textures and effective depths of soil.

f) Salinity is uncommon but slight salinization can occur in depressions where the coarse alluvium is only shallow over underlying impervious mudstone (Chap.5).

g) There is a rapid increase in calcium carbonate content with depth, being highest in the calcic and petrocalcic horizons.

h) Soil colour above the calcic and petrocalcic horizons is normally 7.5 YR 4/4.

Where the soils of the mesas are moderately deep (Fig.4.4), prosperous irrigated agriculture has been established. Maize, lucerne, sugar-beet, barley, and tomato are the main crops.

Effective depth of cultivable soil and moisture-holding capacity are the main soil features on which land suitability for irrigation depends.

Their general properties are:

- a) Depth is generally greater than 2 m, but root proliferation is limited to 50 cm.
- b) Textures vary down the profile and signs of stratification are evident, as could be expected in young alluvial soils. The surface textures are mainly clay loam. Stones are rare.
- c) Structure development is weak and often non-existent, particularly in the subsoil.
- d) Soil moisture-holding capacity is the highest of all the soils of the studied area. Infiltration and percolation rates, though low, are sufficient to allow surface irrigation. In general no water table is found in the upper 3 m (Chap.3).
- e) The surface soil is free of salts but below 2 m soil salinity increases to an overall value slightly higher than 4 mmhos.

Profile 5 represents a characteristic soil of the middle valley. The clay content increases in the lower part of the plain (Profile 7). The narrow natural levee of the river consists of very recent sandy soils (Profile 6, Fig.4.7).

In the lower valley soil salinity varies in accordance with the amount of leaching achieved under normal irrigation. It has been separated as a general saline phase, however, because its overall degree of salinization is higher than in the upper and middle valley (Mapping unit 3.6). A halophyte vegetation, which does not occur in the non-saline phase (Fig.4.8), is found in this unit.

With the present drainage system of open ditches desalinization is possible as the percolation rate is sufficient to allow leaching (Chap.5).

Together with the deeper non-saline soils of the mesas, the non-saline soils of the Riguel river plain are the best soils in the area. They are under irrigated agriculture, the main crops being lucerne, wheat, and barley.

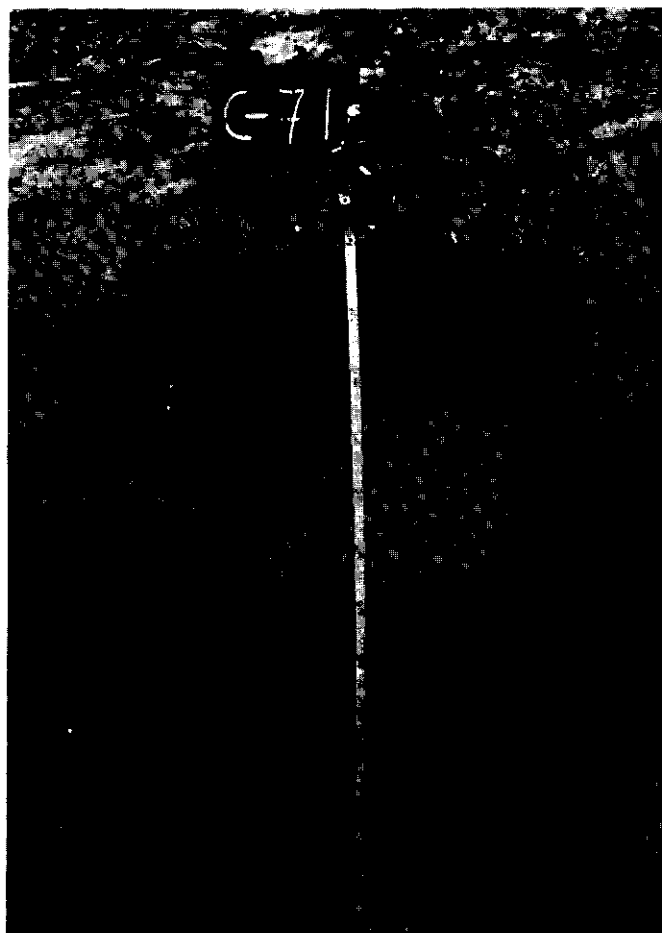


Fig.4.7: Profile 6.

4.2.5 High and middle Aragón terraces

On both the high and middle Aragón terraces (Mapping Units 3.3 and 3.4) similar soils are found. They derive from a similar parent material which consists of a coarse alluvium deposited by the Aragón river (Fig.4.9). Above this coarse substratum a finer layer occurs (Profile 8).



Fig.4.8: Profile 7.



Fig.4.9: Coarse alluvium of the middle Aragón river terrace.

These loamy alluvial soils show a moderate profile development. Structures are better developed than in the soils of the lower terrace and overall there is slightly more clay present. Incipient clay skins are frequent in the subsurface horizon. Calcium is present as mycelia but is insufficient to allow a calcic horizon to be diagnosed. The underlying coarse layer contains such high levels of calcium carbonate that it is impossible to state which is depositional and which is intrinsic.

In general the profile development of these soils (Fig.4.10) is less intense than that of the soils of the mesas which are the oldest soils of the area.

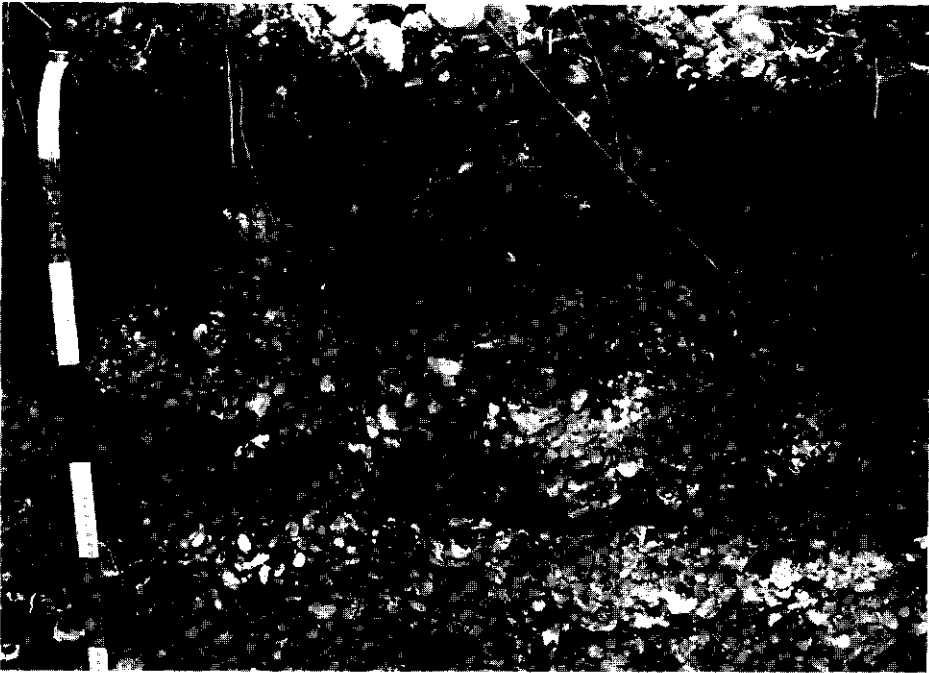


Fig.4.10: Profile of a soil of the highest Aragón river terrace.

Their general properties are:

a) A minimum of 50 cm depth of cultivable soil, limited by a continuous layer of semi-cemented rounded stones. The possibility of root proliferation into this substratum is only slight.

b) The most common texture of the surface soil is loam, with a slight increase of clay content in the subsurface horizon. Surface stoniness is frequent and the coarse fragment percentage increases with depth.

c) There is good structure development in the cultivated surface soil. Below 25 to 30 cm structure is weakly blocky down to the conglomerate substratum.

d) Internal drainage is extremely good and no water table is found. The infiltration rate is high, and the moisture-holding capacity moderately low because of the lack of deep fine-textured soil.

e) As the parent material is non-saline and drainage conditions are excellent, the soils are free of salinity.

The main restrictions for irrigated agriculture are depth of cultivable soil and surface stoniness, which prevent the cultivation of sugar beet and lucerne. Cereal crops, maize, and soya bean are cultivated successfully, but need frequent small irrigation applications.

4.2.6 Low Aragón terrace

The soils of the low Aragón terrace (Mapping Unit 3.2) represent only a small part of the total area. They are deep sandy loam alluvial soils with no profile development (Fig.4.11). Stratification is evident at moderate depth, with gravel and coarse sand layers interbedded between the sandy loam layers (Profile 9).

The general properties are:

a) Depth of cultivable soil, though variable, is greater than 50 cm. It is limited by the cobbles and gravel layers which appear at varying depths. The coarse alluvium is completely loose, as might be expected with an immature soil.

b) Textures vary from loam to sandy loam. Surface stoniness is rare.

c) Structure is almost non-existent, though slight structure development appears in the cultivated surface soil.

Soils are excessively drained and no water tables were found in the studied profiles. The main restrictions for irrigation are the high infiltration rate and the low moisture-holding capacity. Percolation losses under surface irrigation are therefore high.

The soils are non-saline and a permanent irrigated agriculture is maintained, maize being the most common crop.

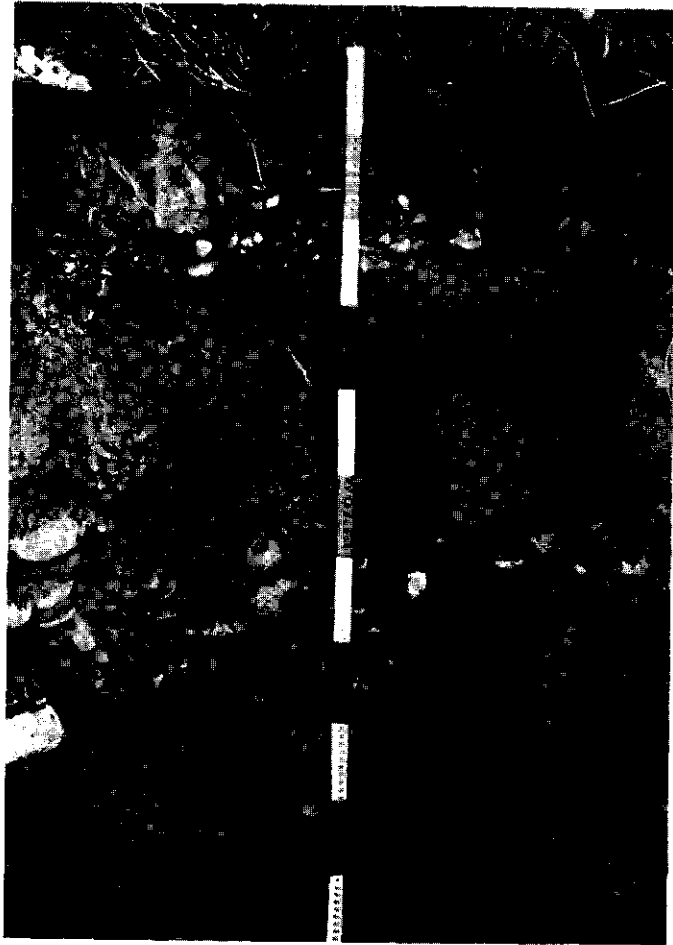


Fig.4.11: Profile 10.

Land use for irrigated agriculture depends mainly on the effective depth of cultivable soil and the relative size of non-eroded areas.

4.2.9 Colluvial slopes

The soils of the colluvial slopes (Mapping Unit 2.7) are brown soils with only an incipient profile development. They derive from a mixture of colluvium and material from the underlying Miocene-Oligocene sediments.

The only profile development is a cambic horizon underlying an ochric epipedon, and the movement of calcium carbonate and soluble salts down the profile. The underlying substratum is generally siltstone, often interbedded with mudstone. Both are saline sediments with very low permeability (Profile 12).

The general properties are:

a) Average depth of cultivable soil is variable but always more than 50 cm above the slowly permeable substrata. Depth over decomposing mudstone and siltstone is variable depending on slope and situation, but where erosive forces are less the depth can be more than 2 m.

b) Textures vary from sandy loam to silty clay loam. The decomposition of the siltstone produces fine structureless sandy loam textures and the mudstone silty clay loam textures with partial structure development. There is very little gravel.

c) Soil structure is not well developed. It is moderately fine granular in the surface soil and subangular blocky in the subsoil. The underlying substrata are structureless.

d) Soil salinity is variable. Some of the studied profiles were free of salt and in others salt content increased in the deeper layers. Nevertheless there is an overall slight salinity in the unit.

Though most of these soils are under irrigation command, dry farming is practised. As deeper layers are less pervious and more saline than the

surface soil, land levelling is not a suitable practice and irrigation should be by sprinkler.

A moderate excess of irrigation water over the consumptive use requirement should be sufficient to leach the salt to deeper layers. Only small amounts of leaching water should be applied as otherwise saline water would seep to adjacent low-lying areas and an interceptor drainage system would be required to cut off the flow.

An eroded phase (Mapping Unit 4.2) has been separated where erosion processes predominate over the colluvial ones.

4.2.10 Fluvio-colluvial valleys, imperfectly drained and saline-alkali phase

These soils (Mapping Unit 3.8) are light yellowish brown alluvial-colluvial soils formed in the bottoms of flat valleys scoured out in the Miocene-Oligocene sediments. They have developed from a mixed parent material of fine alluvium from the erosion valleys (2.5), fine colluvium from the surrounding slopes and hills, and locally decomposed sediments (Fig.4.13). They show a moderate profile development (Profile 13).

The soils are saturated with water because they suffer from impeded drainage and are situated in areas receiving seepage from the surrounding slopes and hills. They are saline and many are alkali as well, but because of their immaturity no true salic or natric horizon has developed sufficiently to become diagnostic. There is a downward movement of calcium carbonate, and gypsum crystals have accumulated at an average depth of 1 m.

The general properties are:

- a) Average effective soil depth is 75 cm. Deeper layers are too compact for root proliferation.
- b) Their textures are finer than other surrounding soils and are generally silty clay loam, but clay layers are occasionally found. In the

subsoil very fine sandy layers sometimes occur as a result of the weathering of underlying siltstone.

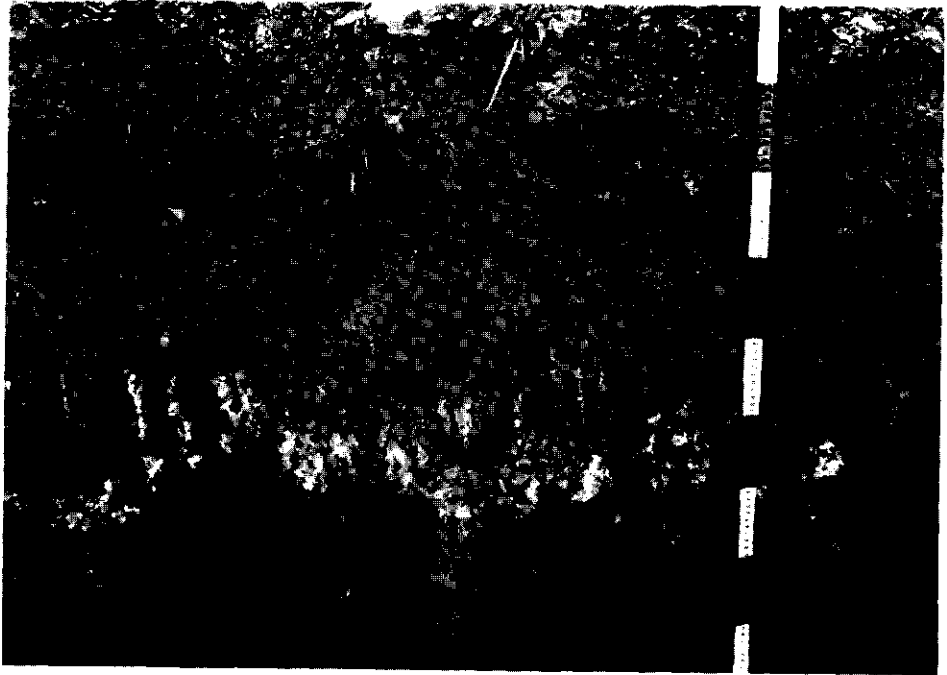


Fig.4.13: Profile 14.

c) Structure is moderately good. In the surface soil, structure is crumbly and in the subsurface blocky and prismatic. Below 75 cm there is no structure development. There are indications of clay movement down the profile and clay and silt skins on prism sides and pores are evident (Fig.4.14). Lime mycelia and gypsum crystals are also common.

d) Salinity is severe because the valleys receive constant saline seepage from higher levels (Chap.3). The salt content is variable in the surface soil but increases with depth where it is very high (Chap.5).

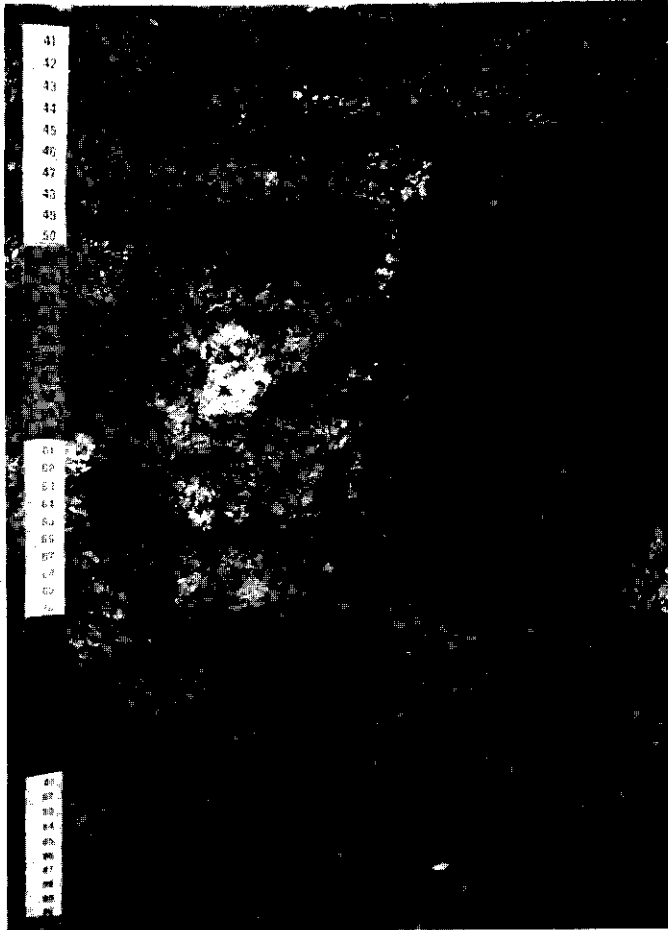


Fig.4.14: Detail of profile 14.

As these soils are severely saline, few of them are cultivated and only halophytic vegetation is found. The fact that the salt content increases with depth means that infiltration and percolation are probably adequate for leaching. Thus, if the drainage system were improved and the amount of leaching water increased by irrigation, these soils could most likely be reclaimed.

4.2.11 Alluvial plains, imperfectly drained and saline-alkali phase

As the alluvial plains (Mapping Unit 3.10) have formed in the flat areas where fluvio-colluvial valleys coalesce, their soils are very similar to those of the fluvio-colluvial valleys. The upper 1.5 m is saturated with water for some period of the year. The characteristics associated with water-logging are insufficient to allow any diagnostic horizons other than a cambic horizon to be defined. These soils are saline and sodic but again their immaturity means that no true salic or natric horizon has developed sufficiently to become diagnostic.

The general properties are:

- a) Effective depth of cultivable soil is rarely more than 75 cm and root proliferation is mainly restricted to the upper 40 cm.
- b) Their textures are finer than the soils of the surrounding slopes, varying generally from silt loam to clay, with silty clay loam as the most frequent texture.
- c) Structure is moderately good with indications of clay movement down the profile. Lime mycelia and salt crystals with occasional gypsum are common.
- d) These soils have been almost completely drained with an open drainage system. Below 1 m, however, olive mottling, with the particular shininess associated with gleying, is found.

Profile 14 is an extreme example of the salinity and alkalinity. Otherwise it is very typical as it is situated in one of the very few areas in the central swampy zone which has not yet been cultivated.

Some areas of these soils have never been cultivated or at least not for many years. The drained areas are under irrigation, with sugar beet and barley as the most common crops. There is an overall high level of salinity. For the reclamation of these soils, the same considerations are valid as for the reclamation of the saline soils of the fluvio-colluvial valleys.

4.2.12 Alluvial valleys, saline-alkali phase

These young soils (Mapping Unit 3.11) show only an ochric epipedon. Below the levelled surface soil, they are highly stratified.

The lack of profile development in these yellowish brown alluvial soils is partly due to their characteristic lamellae sedimentation pattern which impedes the percolation of water. The infiltration rate is very low, being almost negligible if the soil is unploughed. Consequently rain water does not percolate to deeper layers and almost the total amount of rainfall becomes surface runoff or remains on the surface until it evaporates. There is no profile development and even salt movement is very slight in the layers below the surface.

Profile 15 is a representative soil of this mapping unit, the general properties of which are:

a) Depth of cultivable soil is equal to the depth of soil affected by the levelling and subsoiling operations, namely about 50 cm. In the studied soil profiles of non-cultivated land, no root proliferation was detected in the stratified substratum. In fact when the roots of the halophytes reach the stratified layers, they grow in a horizontal direction.

b) Texture varies between silt loam and silty clay loam but occasionally very fine sandy loam layers are found. The soils are free of gravel, at least in the upper 1.5 m.

c) The surface soil shows a weak structure development of the sub-angular blocky type. If the soils remain uncultivated the upper 3 to 5 cm shows a very fine platy structure with a high salt concentration. Salt puffs are common on the surface. A strong very fine or fine stratification is observed in the subsurface layers (Fig.4.15). At greater depth a gravel and coarse sand layer saturated with water is generally present (Chap.3).

These soils have a poor structure stability and their erosion hazard is therefore high, even in flat levelled land.



Fig.4.15 A: Soil profile of a saline soil of an alluvial valley.

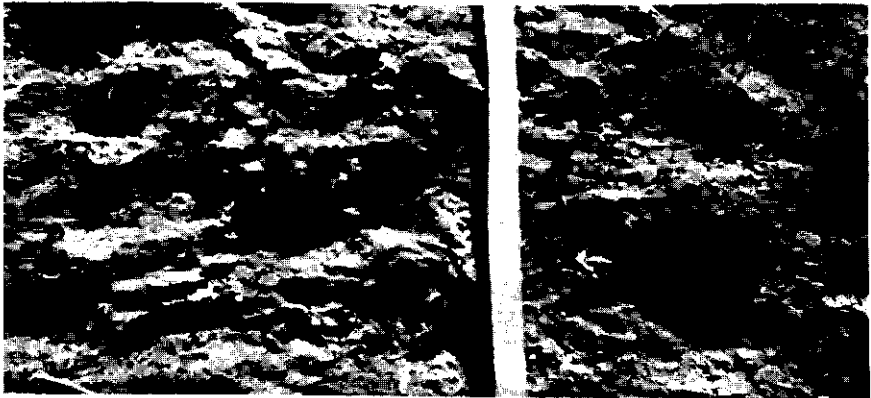


Fig.4.15 B: Stratified layer of a soil of the saline alluvial valley.

d) Pores are common between the lamellae but are vesicular and discontinuous. Hydraulic conductivity measured by the inversed auger hole method varied within a restricted low range.

e) The soils are severely affected by salinity and are to a similar degree sodic (Chap.5).

Of all the soils in the area, these soils are the most unfavorable for irrigated agriculture (Fig.4.16). Their high salinity severely restricts crop growth and their lack of internal drainage makes water management difficult.

An artificial drainage system combined with deep subsoiling is required to reclaim these soils. If their infiltration and percolation rates were to be increased with soil management, the surface soil could become non-saline. Their intrinsic fertility, however, is so poor that an intense fertilization programme would be needed to enable permanent agriculture under irrigation.

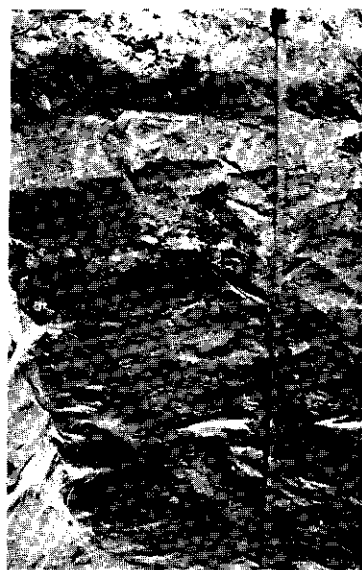


Fig.4.16: Landscape of a soil of the saline alluvial valleys.

Fig.4.17: Profile 18.

Secondly, there are no stratified layers in the soil profile and consequently the percolation rate is higher;

Thirdly, these soils have had more time to lose any intrinsic salinity of the soil parent material.

Profile development is obvious only in a slight downward movement of calcium carbonate and no diagnostic horizons other than an ochric epipedon are found (Profile 17).

The general soil conditions are as follows:

a) Although a truly impenetrable layer occurs below 1 m, the effective depth of cultivable soil is no more than 50 cm because the subsurface horizons are so compact.

b) Textures vary between clay loam and silty clay loam and there is no surface stoniness.

c) Only a weak structure development in the form of fine subangular blocks can be seen.

d) As these soils have a shallow impervious layer and the permeability of the surface soil is moderately low, natural drainage is moderate. Overall there is a slight level of salinity though some of the soils included are non-saline (Profile 17).

As the salt content of these soils is lower than that of the soils of the southern alluvial fans, their suitability for irrigated agriculture is higher. At present, however, they are not under full irrigation.

An eroded phase (2.6) has been separated from this unit where the erosion hazard is so high as to prevent irrigated agriculture.

4.2.15 Other minor mapping units

Some minor mapping units with no agricultural significance have been separated on the soil map. These units are not capable of maintaining permanent irrigated agriculture and are generally situated out of the irrigation command. Their land use possibilities are dry farming in some instances and more usually sheep grazing.

Such mapping units are the rough mountainous land at the northern border of the studied area (1.3), the siltstone outcrops in the rough eroded plain (1.4; Fig.4.19), the gypsum ridges at the north-western end of the area (1.7), and the escarpments of the fluvial terraces and mesas (2.1).

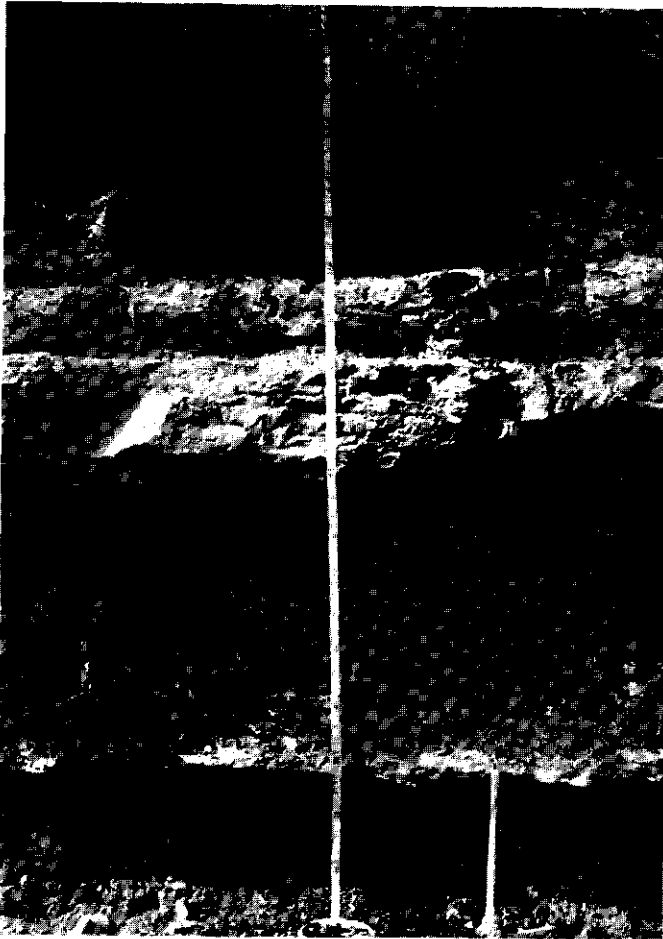


Fig.4.19: Residual soil above a siltstone layer.

P R O F I L E

2

PHYSIOGRAPHIC POSITION: Mesa (mapping unit 1.1)

LOCATION: Pinsoro

DATE: May 24, 1972

LAND USE: irrigated crops; sugar beet and maize

PARENT MATERIAL: red old alluvium

TOPOGRAPHY: nearly level

DRAINAGE: well-drained

SALINITY: free

DIAGNOSTIC HORIZONS: ochric epipedon; cambic horizon and calcic horizon

CLASSIFICATION: Calcixerollic Xerochrept

0 - 20 cm very dark brown (7.5 YR 4/4) sandy clay; moderate fine crumb structure; friable (moist); common pores; common very fine roots; clear and wavy boundary

20 - 45 cm very dark brown (7.5 YR 4/4) sandy clay; weak coarse subangular blocky structure; firm (moist); common white lime concretions; some very fine roots; clear and wavy boundary

45 - 80 cm dark brown (7.5 YR 4/4) and strong brown (7.5 YR 5/6) sandy clay; moderate coarse subangular blocky structure; friable (moist); white lime concretions; gradual smooth boundary

80 - 110 cm dark yellowish brown (10 YR 4/4) clay loam; weak coarse subangular structure; friable (moist); lime concretions

110 - 150 cm brownish yellow (10 YR 6/6) silt loam; structureless; friable (moist); many lime concretions; rootless

PROFILE 2

ANALYTICAL DATA

Depth cm	Size class and particle diameter (mm)						Carbonate as CaCO ₃ <2 mm %	Organic matter %	pH	
	Total			S a n d					H ₂ O	KCl
	Sand	Silt	Clay	Medium coarse	Fine- very fine	Coarse fragments >2				
	2-0.05	0.05-0.002	<0.002	2-0.25	0.25-0.05	%	%	%		
0 - 20	46.0	15.5	38.5	4.1	41.9	14.0	30.3	1.8	7.6	6.9
20 - 45	49.5	13.5	37.0	3.9	45.6	10.0	30.2	1.8	7.6	6.9
45 - 80	50.0	13.0	37.0	3.6	46.4	16.0	42.8	0.7	7.6	6.9
80 - 110	43.5	18.0	38.5	6.9	36.6	18.0	54.4	0.4	7.8	7.0
110 - 150	12.0	63.5	24.5	0.1	11.9	-	64.3	0.3	7.9	7.1

P R O F I L E

3

PHYSIOGRAPHIC POSITION: alluvial-colluvial valley (mesa/within)
(mapping unit 3.9)

LOCATION: El Bayo

DATE: March 14, 1974

LAND USE: dry farming (barley)

PARENT MATERIAL: mixed local alluvium

TOPOGRAPHY: nearly level

DRAINAGE: well-drained

SALINITY: slight in deeper horizons

DIAGNOSTIC HORIZONS: ochric epipedon

CLASSIFICATION: Typic Xerofluvent

0 - 30 cm brown (10 YR 5/3) sandy clay loam; moderate fine granular structure; friable (moist); abundant fine roots

30 - 65 cm yellowish brown (10 YR 5/4) clay loam; weak subangular medium blocky structure; firm (moist) few roots

65 - 100 cm brown (10 YR 4/3) silty clay; weak subangular blocky structure; firm (moist); very incipient clay illuviation

100 - 150 cm brown (10 YR 5/3) clay loam; structureless

PROFILE 3

ANALYTICAL DATA

Depth cm	Size class and particle diameter (mm)						Carbonate as CaCO ₃	Organic matter
	Total			Sand		Coarse fragments >2	<2 mm	%
	Sand	Silt	Clay	Medium coarse	Fine- very fine			
	2-0.05	0.05-0.002	<0.002	2-0.25	0.25-0.05	%	%	%
0 - 30	49.0	27.0	24.0	8.2	40.8		41.5	1.0
30 - 65	43.5	27.0	29.5	1.0	42.5		37.5	0.9
65 - 100	16.5	42.0	41.5	0.6	15.9		35.2	1.4
100-150	23.0	41.0	36.0	0.9	22.1		41.5	0.7

Depth cm	Extractable bases			Exchange- able so- dium %	pH		Chlori- des %	Water extract from saturated paste			
	Ca + Mg	Na	K		H ₂ O	KCl		Ca + Mg	Na	Sodium ad- sorption ratio	Electrical conductivity mmhos/cm
	meq/100 g							meq/l			
0 - 30	7.2	0.8	0.2	9.8	8.2	7.4	0.007	9.0	0.8	0.4	0.6
30 - 65	7.5	1.9	0.2	19.8	8.2	7.4	0.016	10.0	14.6	6.5	2.3
65 - 100	13.6	2.8	0.2	16.9	8.0	7.2	0.046	18.0	15.6	5.2	3.7
100-150	11.1	2.2	0.1	16.4	8.0	7.3	0.069	22.0	20.1	6.1	4.2

P R O F I L E

4

P R O F I L E

8

PHYSIOGRAPHIC POSITION: Middle Aragón river deposition
terrace (mapping unit 3.3)

LOCATION: Monasterio de la Oliva

DATE: June 26, 1975

LAND USE: irrigated barley

PARENT MATERIAL: coarse alluvium

TOPOGRAPHY: nearly level

DRAINAGE: extremely good

SALINITY: free

DIAGNOSTIC HORIZONS: ochric epipedon, cambic and calcic
horizon

CLASSIFICATION: Calcixerollic Xerochrept

0 - 25 cm yellowish red (5 YR 4/6) sandy clay loam; very common rounded stones over 5 cm; moderate fine crumbly structure; friable (moist); hard (dry); common fine roots; clear smooth boundary

25 - 40 cm yellowish red (5 YR 4/6) sandy clay loam; very common rounded stones; moderate very fine subangular blocky structure; firm (moist); very hard (dry); few roots; abrupt and undulate boundary

40 - 55 cm continuous layer of semi-cemented rounded stones over 5 cm

PROFILE 8

ANALYTICAL DATA

Depth cm	Size class and particle diameter (mm)						Carbonate as CaCO ₃ <2 mm %	Organic matter %
	Total			Sand		Coarse fragments >2 %		
	Sand 2-0.05	Silt 0.05-0.002	Clay <0.002	Coarse & Medium 2-0.25	Fine Very fine 0.25-0.05			
0 - 25	52.0	20.5	27.5	12.7	39.3	34.1	1.8	
25 - 55	46.5	21.5	32.0	9.4	37.1	30.3	1.4	

Depth cm	pH		Chlor- ides %	Water extract from saturated paste			
	H ₂ O	KCl		Ca + Mg meq/l	Na	Sodium adsorption ratio	Electrical conductivity mmhos/cm
0 - 25	7.7	7.1	0.006	14.0	1.0	0.4	1.2
25 - 55	7.8	7.0	0.002	8.0	0.8	0.1	0.6

P R O F I L E

9

PHYSIOGRAPHIC POSITION: Low Aragón river terrace
(mapping unit 3.2)

LOCATION: Rada

DATE: August 29, 1976

LAND USE: maize

PARENT MATERIAL: mixed alluvium

TOPOGRAPHY: nearly level

DRAINAGE: excessively drained, groundwater
table +2.50 m

SALINITY: free

DIAGNOSTIC HORIZONS: ochric epipedon

CLASSIFICATION: Typic Xerofluvent

0 - 25 cm pale brown (10 YR 6/3) loam with gravel; weak granular structure; friable (moist); abundant roots; clear smooth boundary

25 - 50 cm pale brown (10 YR 6/3) loam; structureless; friable (moist); abundant pores and roots; abrupt and smooth boundary

50 - 70 cm layer of cobbles and gravel; abrupt and undulate boundary

70 - 85 cm brown (10 YR 5/3) fine sandy loam; very friable (moist); abrupt and smooth boundary

85 - 150 cm layer of cobbles, gravel and coarse sand

150 - 250 cm brown (10 YR 4/3) fine sandy loam

PROFILE 9

ANALYTICAL DATA

Depth cm	Size class and particle diameter (mm)								Carbonate as CaCO ₃ <2 mm %	Organic matter %
	Total			S a n d				Coarse fragments >2 % soil		
	Sand	Silt	Clay	Coarse Very coarse 2-0.5	Medium 0.5-0.25	Fine 0.25-1	Very fine 0.1-0.05			
0 - 25	41.2	44.9	13.9	7.3	6.7	16.3	10.9	50	37.4	3.2
25 - 50	41.0	43.5	15.5	0.6	3.1	27.8	9.5	-	38.7	1.4
70 - 85	61.4	27.7	10.9	1.1	14.1	26.8	19.4	-	42.0	1.4
150-250	51.3	37.8	10.9	1.6	13.5	18.5	15.7	-	39.4	0.8

Depth cm	Extractable bases				Exchange- able so- dium %	Water extract from 1:1 paste										
	Ca + Mg		Na	K		Ca + Mg		Ca	Na	K	HCO ₃	Cl	SO ₄	pH	Sodium adsorption ratio	Electr. conduct. umhos/cm
	meq/100 g					meq/l										
0 - 25	7.1	0.2	2.2	2.1	4.7	4.3	1.1	3.4	5.7	0.008	0.3	8.5	0.7	0.8		
25 - 50	3.6	0.2	2.2	3.3	4.5	4.3	2.2	4.4	2.8	0.014	2.2	8.4	1.5	1.1		
70 - 85	4.0	0.3	0.2	6.7	6.5	4.1	4.9	0.1	1.1	0.055	3.2	7.9	1.4	2.9		
150-250	5.8	0.2	0.1	3.3	5.8	4.1	1.5	-	1.3	0.010	-	8.2	0.9	0.7		

P R O F I L E

13

PHYSIOGRAPHIC POSITION: alluvial-colluvial valley
(mapping unit 3.8)

LOCATION: Alera pilot field-control area

DATE: August 28, 1976

LAND USE: saline vegetation (suaeda etc.)

PARENT MATERIAL: saline-alkali local on decomposed
mudstone and sandstone

TOPOGRAPHY: nearly level

DRAINAGE: imperfectly drained, very slow runoff,
groundwater table at 1.40 m

SALINITY: high salinity and alkalinity content,
increasing with depth

DIAGNOSTIC HORIZONS: ochric epipedon, natric horizon

CLASSIFICATION: Aquic, Glossic Natrargid

0 - 15 cm pale yellow (2.5 Y 7/3) silty clay; light olive brown (2.5 Y 5/3) when moist; moderate medium crumb structure; adherent (wet); slightly firm (moist); slightly hard (dry); many fine pores; many horizontal medium roots; cracks in 35 cm; clear wavy boundary

15 - 35 cm light yellowish brown (2.5 Y 6/3) silty clay, dark gray brown (2.5 Y 4/2) when moist; strong coarse subangular blocky structure; adherent (wet), very firm (moist); many fine and medium horizontal roots; frequent root pores; salt efflorescences; clear and wavy boundary

35 - 70 cm pale yellow (2.5 Y 8/3) silty clay loam; dark gray brown (2.5 Y 4/2) when moist, with very dark gray brown (2.5 Y 5/3) tongues; moderate coarse prismatic structure; clay and silt skins on prism sides and pores; many fine continuous pores; frequent fine and medium roots; salt efflorescences; clear and wavy boundary

70 - 200 cm light yellowish brown (2.5 Y 6/4) when moist silt loam; structureless; medium gypsum crystals at 85-100 cm; very firm (moist); very fine pores decreasing with depth; compact; at 1.4 m saturated with saline water

> 200 cm very pale brown (10 YR 7/4) and white (5 Y 8/2) silty clay loam; structureless; poreless and extremely compact; very hard (dry); impervious

PROFILE 13

ANALYTICAL DATA

Depth cm	Size class and particle diameter (mm)								Carbonate as CaCO ₃ <2 mm %	Organic matter %
	Total			Sand				Coarse fragments >2 % soil		
	Sand 2-0.05	Silt 0.05-0.002	Clay <0.002	Coarse Very coarse 2-0.5	Medium 0.5-0.25	Fine 0.25-1	Very fine 0.1-0.05			
0 - 15	2.2	51.1	46.7	0.3	0.2	0.8	0.9	-	20.8	2.5
15 - 35	1.6	46.3	52.1	0.1	0.2	0.4	0.9	-	19.1	2.5
35 - 70	1.8	68.0	30.2	0.3	0.1	0.3	1.1	-	34.1	1.4
70 -200	2.1	73.7	24.2	0.1	0.1	0.3	1.6	-	43.5	0.6

Depth cm	Extractable bases				Exchange- able so- dium %	Water extract from 1:1 paste									
	Ca + Mg		Na	K		Ca + Mg	Ca	Na	K	HCO ₃	Cl	SO ₄	pH H ₂ O	Sodium adsorption ratio	Electr. conduct. umhos/cm
	meq/100 g			meq/l											
0 - 15	12.0		0.8		51.2	37.3	119.8	0.1	1.9	0.46	23.0	8.1	23.7	14.8	
15 - 35	15.7		0.9		42.8	30.2	146.4	-	2.3	0.47	55.2	8.0	31.7	16.3	
35 - 70	14.9		0.5		81.3	25.9	210.0	-	1.2	0.71	91.1	7.8	32.9	23.2	
70 -200	9.5		0.1		91.8	22.0	313.7	-	0.8	1.18	71.9	7.6	46.3	34.4	

P R O F I L E

16

PHYSIOGRAPHIC POSITION: alluvial fan
(mapping unit 3.13)

LOCATION: Sabinar

DATE: July 12, 1972

LAND USE: barley (poor)

PARENT MATERIAL: saline fine alluvium

TOPOGRAPHY: smooth 1 per cent slope

DRAINAGE: groundwater table +1.5 m;
slow hydraulic conductivity

SALINITY: high

DIAGNOSTIC HORIZONS: ochric epipedon

CLASSIFICATION: Salorthidic Xerorthent

0 - 45 cm light yellowish brown (10 YR 6/4) when moist, very pale brown (10 YR 7/3) silty clay loam; weak coarse subangular blocky structure; saline efflorescences; smooth and abrupt boundary

45 - 85 cm very pale brown (10 YR 7/4) silty loam, light yellowish brown (10 YR 6/4) when moist; moderate fine platy structure; hard (dry); whitish efflorescences; abrupt and smooth boundary

85 - 150 cm very pale brown (10 YR 7/4) loam, light yellowish brown (10 YR 6/4), when moist; strong very fine platy structure; friable (moist)

PROFILE 16

ANALYTICAL DATA

Depth	Size class and particle diameter (mm)						Carbonate as CaCO ₃	Organic matter
	Total			S a n d		Coarse fragments >2		
	Sand	Silt	Clay	Coarse Medium	Fine Very fine		<2 mm	%
cm	2-0.05	0.05-0.002	<0.002	2-0.25	0.25-0.05	%	%	%
0 - 45	12.5	56.0	31.5	-	12.5		38.5	0.8
45 - 80	28.5	51.0	20.5	-	28.5		44.0	0.3
80 -150	30.5	49.0	20.5	-	30.5		44.7	0.4

Depth	pH		Chlorides	Water extract from saturated paste			
	H ₂ O	KCl		Ca + Mg	Na	Sodium adsorption ratio	Electrical conductivity
	cm	%		meq/l		ratio	mmhos/cm
0 - 45	7.9	7.6	1.352	22.8	257.0	24.1	49.4
45 - 80	8.2	7.8	0.358	80.0	141.0	22.3	21.0
80 -150	8.5	8.0	0.554	10.2	205.7	28.8	31.1

5. Soil salinity

5.1 Origin and localization of the salts

The primary origin of the salinity that affects some soil associations of the studied area is the intrinsic salt content of the Oligocene-Miocene mudstone and siltstone from which most of the soil parent materials derived (Chap.4). These Oligocene-Miocene sediments were deposited under brackish lacustrine conditions (Chap.2).

Erosion of these saline geological formations and their further transport and sedimentation under even more saline conditions (salt concentration increases with the evaporation of water during the transport and sedimentation processes) have formed alluvium and mixed alluvium-colluvium with an even higher salt content than the original Tertiary sediments.

Although the salinity of the soils has a primary origin, there has been some redistribution of the salts and a secondary salinization process has taken place which has changed the original salinity status.

In previous climatic periods when a net percolation of water occurred, i.e. when rainfall exceeded evapotranspiration, the upper soil horizons were leached and the salts accumulated at some depth. The leaching rate depended on the water-transmitting properties of the soils, the more permeable horizons losing their salts more readily.

This natural leaching process no longer takes place under present climatic conditions where evapotranspiration exceeds effective rainfall for the greater part of the year, except for a short period during the rainy season. The introduction of irrigation, however, has changed the water and salt

balances in the irrigated soils, and again net percolation of water and leaching of salts is occurring.

The relative position of the physiographic units and their mutual interrelation in regard to water flow have played a leading part in the redistribution of salts (Chap.3). The salts lost from the upper lands have accumulated in the lower lands. The transport processes are lateral seepage and to a lesser extent surface runoff.

These processes are still continuing. The higher physiographic units, however, still contain large amounts of salts. Although this may not always be evident at the soil surface.

In the lowlands that lack natural drainage or where drainage is impeded, the groundwater is fed by lateral seepage and the groundwater table remains near the soil surface. This has produced secondary salinization due to capillary rise of the saline groundwater.

The more severely salt-affected soils are therefore either in water receiving areas with impeded drainage or in those physiographic units where the soil parent material has intrinsic salinity and where water-transmitting properties are so low as to impede leaching.

As might be expected, these saline areas are low-lying in relation to their surroundings. An exception is formed by the recently formed alluvial soils of the Aragón and Riguel valleys, which, despite their low position, are non-saline because their soil parent material was free of salinity. They have satisfactory water-transmitting properties, a low water table, and apart from the lower end of the Riguel alluvial plain there is no saline seepage to affect them.

In summary, the source of salts is the intrinsic salinity of some soil parent materials in combination with a further movement of salts and secondary salinization in water-receiving areas lacking natural drainage. Under irrigated conditions the mobilization and redistribution of salts continues and salinity increases.

5.2 Types of salts and their distribution in the soil profile

The saline soils of the area are characterized mainly by the presence of sodium chloride. From the analysis of groundwater samples (Chap.3) the composition of the salts of each soil association could be derived.

The soils of the fluvio-colluvial valleys and alluvial plains of the Castiliscar basin, contain considerable amounts of magnesium sulphate associated with calcium sulphate; some sodium sulphate is also present.

The soils of the saline-alluvial valleys and fans of the south-western piedmont major unit contain not only sodium chloride, but also calcium and magnesium chlorides which predominate over the sulphates.

In the areas associated with the gypsum formations, calcium sulphate occurs as a major constituent in conjunction with sodium chloride.

In non-saline soils ($EC_e < 4$ mmhos/cm) the calcium plus magnesium content is in excess of sodium. At higher salinity levels the sodium ion content increases at a greater rate than calcium and magnesium.

As sodium chloride is the most soluble salt, it is leached in periods of heavy rainfall and low evapotranspiration and during the irrigation season. Under arid conditions sodium chloride accumulates in the soil surface owing to an upward movement of soil moisture containing dissolved salts.

The main movement of this cycle takes place in the upper horizons of the soil profile because the saline soils of the area generally have a low hydraulic conductivity in the unsaturated zone below 50 cm and are almost impervious below one metre.

Saline soil layers deeper than one metre - and even shallower in soils with stratified subsoils impervious for vertical flow - are not affected by

the present soil moisture cycle. Where deep percolation water flows laterally through such layers, however, the seepage water is highly saline. Although such movements may be extremely slow, their long-lasting effect partly accounts for the high degree of salinity of these layers.

In the non-saline soils calcium and magnesium are present throughout the soil profile. In the more developed soils carbonates tend to accumulate in the subsurface horizons. Their common presence combined with a slight amount of sodium chloride gives a background salinity level for all soil associations. This is rarely less than 1 mmho/cm, expressed in terms of electrical conductivity of the saturated paste (EC_p).

The sodium adsorption ratio (SAR) increases in conjunction with the rise of EC, and a similar trend holds for exchangeable sodium percentage (ESP). However, the ratios between EC and ESP and between SAR and ESP may vary considerably. Non-saline alkali soils have not been found and pH-values greater than 8.5 are uncommon.

5.3 Salinity in the soil associations

The soils of the mesas (1.1) are in general non-saline (Fig.5.1). The parent material from which they derived was salt free and their natural drainage prevents any secondary salinization. In small depressions, however, where the coarse alluvium has been removed and a perched water table fed by lateral seepage overlies the impervious mudstone, salinization can occur, although in such cases EC-values are only slightly higher than 4 mmhos/cm.

In the soils of the narrow fluvio-colluvial valleys (3.9) formed by the water courses flowing from the erosion valleys of the mesas, a shallow water table can be present at places where drainage is impeded. Moderate secondary salinization then takes place due to lateral seepage from the adjacent high-lying mesas whose transmissivity is high.

¹ From a large collection of data, a few have been selected as examples of the salinization problem of each mapping unit.

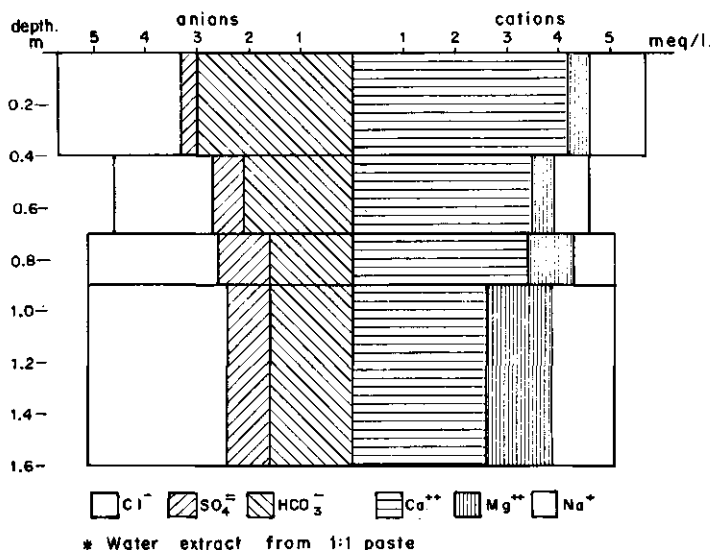


Fig.5.1. Composition of salts in a mesa soil.

Table 5.1 shows the salinity distribution throughout the soil profile. A slight increase of the chlorides can be distinguished in the surface horizon probably due to the effect of evaporation. In addition, the salinity increases in the deeper layers above the mudstone with its intrinsic salinity.

TABLE 5.1 Distribution of the salinity in a soil of a fluvio-colluvial valley, slightly saline phase

Soil depth cm	Chlorides %	EC _e mmhos/cm	pH
0 - 50	0.052	6.1	8.2
50 - 100	0.053	4.5	8.5
100 - 150	0.040	3.5	8.5
150 - 200	0.033	4.3	8.4
200 - 250	0.052	5.1	8.5
250 - 300	0.072	7.4	8.5

NOTE: Groundwater table at 0.3 m, EC_w=6.6 mmhos/cm

The soils of the stony ridges (1.5) are salt-free. Natural drainage is adequate and salts, even though initially present in the coarse colluvium, have been leached by rainwater. Even in irrigated soils no salinity is observed.

The soils of the piedmont slopes (2.3) and colluvial slopes (2.7) are generally slightly saline, though non-saline or moderately saline patches could be included in the mapping units. Leaching occurs in these soils but they also receive salts from higher levels. Thus their actual salinity status depends on their relative topographical position: they can be net losers or net receivers of salts. They are generally somewhat saline at depth (Fig.5.2) and can therefore be regarded as internal solonchaks.

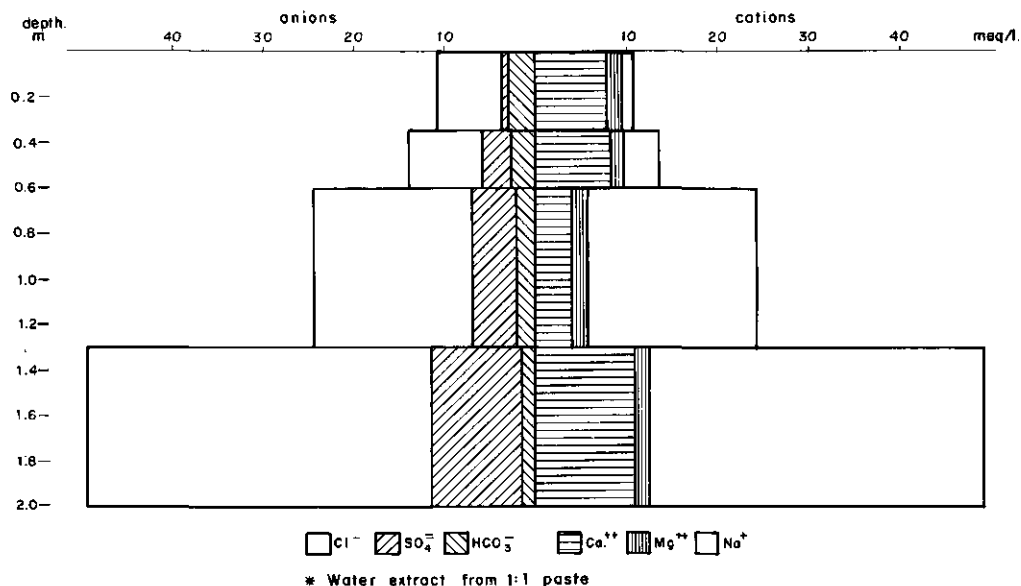


Fig.5.2. Composition of salts in a soil of the colluvial slopes.

The soils of the upper and middle alluvial plain of the Riguel river (3.5) are not salt affected, except at depths of two or more metres where a slight salinity can be observed. Table 5.2 shows the increase in the salt content with depth. An explanation of this could be that the

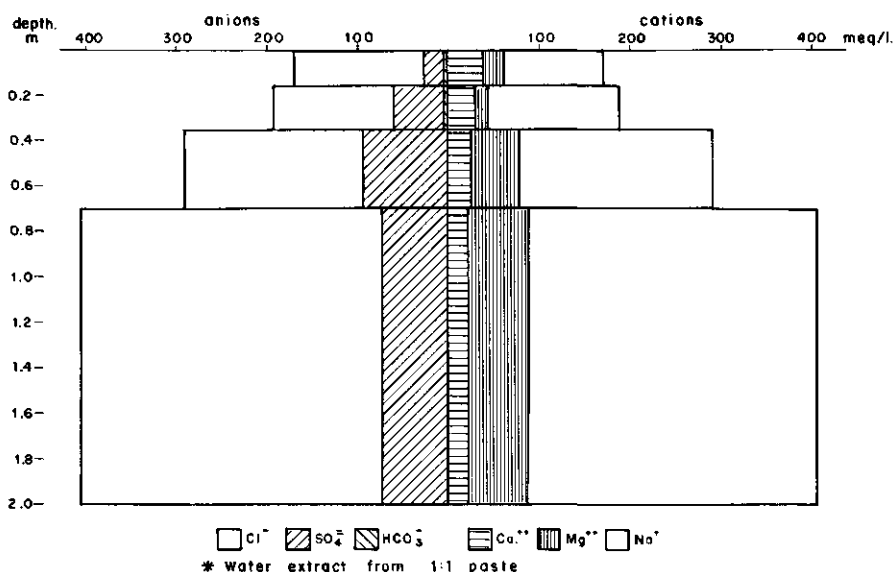


Fig.5.4. Composition of salts in a soil of the fluvio-colluvial valley, saline-alkali phase.

The differences in surface structure development give different possibilities for natural leaching. In fact, the extremely saline patches observed correspond with soils that are more compact than those in adjacent less saline patches. It is not possible to map with accuracy areas of high or low salinity because variations can occur over very short distances (see Chap.6).

Figure 5.4 shows an increase of the most soluble salts with depth, mainly sodium chloride and some magnesium sulphate. In non-cultivated soils, however, high concentrations of salts can occur in the surface soil, which may be covered by a thin layer of salt efflorescence or by a salt crust. Their presence is due to the fluctuating water table which is a constant supplier of salts, in combination with high evapotranspiration rates which occur even in the cold season because of the dryness, intensity, and frequency of wind.

In the subsurface layer a secondary accumulation of calcium sulphate is found (Fig.5.4). At depths between 80 and 120 cm a horizon with gypsum crystals ("punta de lanza") is observed (Fig.5.5). It coincides with the zone in which the water table fluctuates.

The mobility of the soluble and even less soluble salts through the surface soil and the existence of soil structure or stratification development in the upper 80 cm are useful indications of the possibilities of reclaiming these soils by leaching and artificial drainage.



Fig.5.5: Accumulation of gypsum crystals (Profile 14).

Sodification in most soils is no problem because although sodium ions are present in the clay complex, they are easily exchanged by calcium, which is present in large quantities. Even in irrigated soils with simple drainage facilities, no true alkali soils were found but only saline-alkali soils. This indicates that the leaching of soluble salts is invariably followed by a corresponding decrease in exchangeable sodium. In fact, the less saline soils are rarely sodic and pH-values are rarely greater than 8.5.

Consequently, with higher leaching amounts supplied by the irrigation system, and an improvement in the drainage system a decrease in harmful salts could be expected. The exchangeable sodium on the exchange complex may well be replaced by calcium ions.

Most of the soils of the alluvial valleys (3.11) and alluvial fans (3.13) of the south-western piedmont unit are severely affected by salinity. Table 5.3 shows an overall increase of the total salt content from the upper to the lower valleys.

TABLE 5.3 Electrical conductivity values ($EC_e \times 10^3$), chlorides in % and pH of three soil sites in the Valareña alluvial valley

Upper valley				Middle valley				Lower valley			
depth cm	Cl ⁻ %	EC _e mmhos/cm	pH H ₂ O	depth cm	Cl ⁻ %	EC _e mmhos/cm	pH H ₂ O	depth cm	Cl ⁻ %	EC _e mmhos/cm	pH H ₂ O
0 - 3	0.690	30.7	7.9	0 - 30	0.325	13.7	8.1	0 - 40	0.077	-	8.3
3 - 20	0.325	14.8	8.2	30 - 40	0.225	12.5	8.3	40 - 75	0.460	25.2	8.3
20 - 30	0.275	13.6	8.1	40 - 60	0.325	18.3	8.1	75 - 85	0.165	12.8	8.5
30 - 50	0.157	11.3	8.3	60 - 70	0.425	19.7	8.2	85 - 115	0.390	24.5	8.5
50 - 60	0.230	14.5	8.2	70 - 90	0.382	17.3	8.3	115 - 150	0.245	12.8	8.5
60 - 65	0.140	11.0	8.4	90 - 150	0.410	21.3	8.1				
65 - 80	0.312	17.2	8.2								
80 - 130	0.242	15.3	8.1								
130 - 150	0.142	10.1	8.2								

The salts are rather uniformly distributed in the soil profile (Table 5.3) because the water movement is mainly restricted to the upper 50 cm, particularly where stratified layers occur.

During dry periods, however, the surface of these soils is covered with a salt crust (Table 5.3; 0-3 cm depth) which is dissolved again when rain falls. When the soil surface dries again a very thin crust of platy structure is formed which breaks out in hexagonal polyhedrons (Fig.5.6). These soils thus have an uneven surface in which small salt-enriched puffs (EC_e up to 68 mmhos/cm) can be found (Fig.5.7).

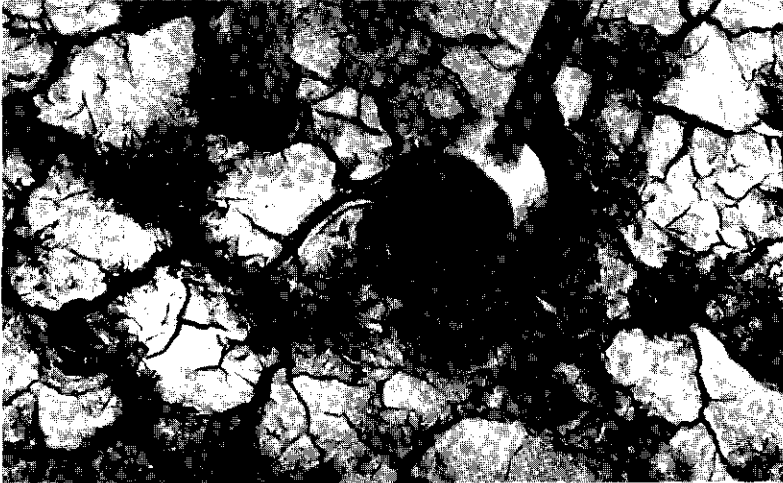
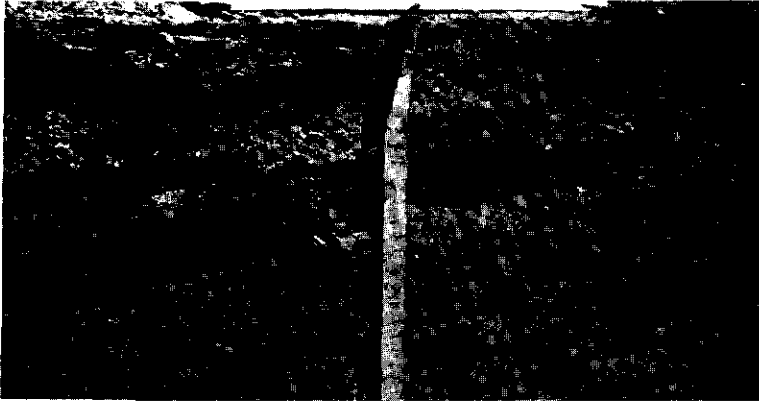


Fig.5.6 a,b: Surface crust of a saline soil.

The salts usually present are sodium chloride and, in appreciable quantities, sulphates and chlorides of calcium and magnesium. On the soil surface, patches of darker hygroscopic salt efflorescences can be distinguished from the light-coloured crust of sodium chloride (Fig.5.8).

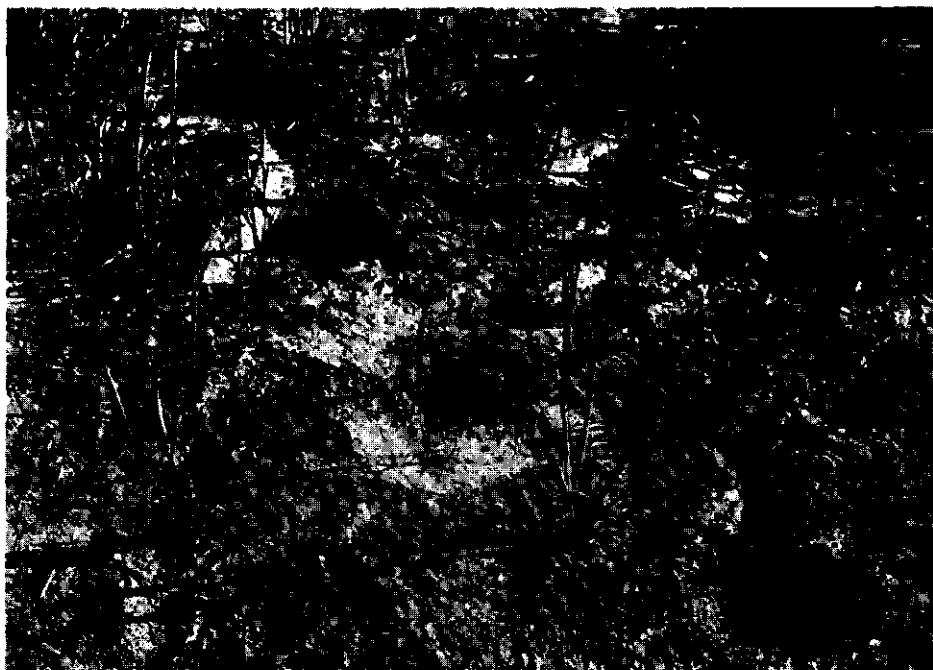


Fig.5.7: Salty puffs in a soil of a saline alluvial valley.



Fig.5.8: Darker patches of hygroscopic salt efflorescences.

Where the water-transmitting properties of the unsaturated zone allow rain water to pass through the soil, there has been a downward movement of soluble salts. In such cases the surface soil is slightly saline and internal solonchaks may occur (Table 5.4).

TABLE 5.4 Distribution of the salt content in a soil of the saline alluvial fans

Depth cm	Cl ⁻ %	EC mmhos/cm	pH
0-50	0.122	7.7	8.3
50-100	0.244	12.8	8.1
100-150	0.468	21.0	8.1
150-200	0.536	22.2	8.0
200-250	1.088	40.9	8.0
250-300	1.052	38.5	8.0

NOTE: Water table at 1.25 m, $EC_w = 60$ mmhos/cm

The possibilities of reclaiming these alluvial soils by leaching with irrigation water and providing an artificial drainage system are highly variable, depending as they do absolutely on the water-transmitting properties of the soil. Soil with compact and platy or stratified layers would be the most difficult to reclaim because water passage through the soil profile is impeded. The data of Table 5.4, however, indicate favourable leaching in the upper one metre and thus give a more optimistic picture.

5.4 Local crop tolerance to salinity and alkalinity

Several crop tolerance tests were conducted on the saline soils of the area to compare their results with the generally accepted values for the tolerance of field crops to salinity and alkalinity.

- 2) *Soils slightly affected by salinity ($EC_e = 4$ to 8 mmhos/cm) in the rootzone but with increasing salinity at depth.*

Comprising this class are the soils of the colluvial (2.7) and piedmont slopes (2.3).

- 3) *Soils highly affected by salinity ($EC_e > 15$ mmhos/cm)*

This class includes the soils of the saline alluvial valleys (3.11) and fans (3.13) of the south-western major physiographic unit and the soils of the fluvio-colluvial valleys (3.8), gypsum valleys (3.7), and alluvial plain (3.10) of the northern drainage basin.



Fig.5.12: Present salt accumulation in a soil with impeded drainage.

The soils classified under 1) can be reclaimed simply by maintaining the present drainage system, which consists of open ditches and interceptor drains laid in the contact between the slope and the low-lying valley, and by applying full irrigation. The percolation losses normal with basin irrigation are sufficient to leach the salts deposited by secondary salinization in the rootzone. Where moderate salinity ($EC_e = 8$ to 15 mmhos/cm) affects some soil patches, sugar beet is a suitable reclamation crop because of its relatively high tolerance level and its high water requirements.

In the soils of the slopes, classified under 2), severe problems arise when the land is levelled for basin irrigation. Deep saline and less pervious layers are exposed and the original natural drainage deteriorates. A second problem is that, after irrigation, saline water seeps from the slopes to adjacent low-lying areas and increases the original salinity of the flat alluvial soils.

Irrigation of the slopes should be by sprinkler since this does not require the land to be levelled. The soil profile is thus not truncated and the natural drainage remains unchanged. Moreover, better water management is possible due to better control of the amounts of water applied. In this way salts can be leached to deeper layers and the seepage of saline water reduced. The only drainage system required is an interceptor drain between the slope and the valley. As the impervious layer in the valley soils is shallow, an open ditch 1.5 to 2.5 m deep will suffice to catch the seepage flow.

The alluvial soils classified under 3), which lack natural drainage and are highly saline, will require a much more rigorous reclamation. Before they can be used for the full production of irrigated crops, they must be provided with a drainage system and be subjected to initial leaching.

The Alera experimental field represents the poorly drained soils of the saline fluvio-colluvial valleys (3.8) and the alluvial plains (3.10) of the northern drainage basin. These soils have an intrinsic salinity because the mixed alluvium-colluvium derives from the denudation of the saline Tertiary mudstones. They have also been subjected to secondary salinization owing to the presence of a shallow saline groundwater table. Soil profile 13 (Chap.4) is situated in this experimental field.

The Valareña experimental field represents the saline soils of the alluvial valleys (3.11) and fans (3.13) of the south-western area. Here, soil salinity has a primary origin only; the alluvium was derived from erosion of the saline mudstone and was deposited in a stratified fashion in a brackish fluvial environment. Soil profile 15 (Chap.4) is situated in this experimental field.

The Alera experimental field was initially 7.5 ha but one year later it was increased to 10 ha; in the extension new drainage materials of corrugated PVC pipe pre-wrapped with cocos and esparto fibers were used.

The Valareña experimental field was originally 11 ha but was increased by a further 9 ha to enable the study of a new drainage system designed in accordance with groundwater flow conditions observed over a period of 2 years on the original drainage system.

6.3 Detailed soil survey

6.3.1 Outline of the survey

In each of the experimental fields representing the two types of saline soils a detailed soil survey was made. The objectives of this survey were to test the homogeneity of soil conditions and to determine the soil hydrological properties, the initial salt content, and its variability.

Soil observations were made by means of bore-holes reaching the less pervious layer (about 2 m deep). The observation points were distributed on

a grid system, the average density of the network being 6 sites/ha in the Alera field and 4 sites/ha in the Valareña field, where soil salinity of the surface soil was more uniform.

The soil survey included descriptions of a representative soil profile for each unit and four deep bore holes reaching the underlying Tertiary mudstone (from 3 to 5 m deep). In the Alera field the soil samples taken with the drilling machine below the groundwater table were completely disturbed, so three extra deep bore holes were made by hand. The deep soil samples were analysed to determine the salt content of deep layers. Piezometer tubes were installed at different depths.

The hydraulic conductivity of the soils of the Alera field could be measured by the auger-hole method, because the groundwater table was only about 1 m deep. At the Valareña field, where the inverse auger hole method (Porchet) was used, the groundwater table was between 2.5 m and 3 m.

The infiltration rate was measured by the double ring method. The moisture-holding capacity was estimated from pF-curves derived from soil core samples.

6.3.2 Hydrological soil properties

Only those soil properties affecting land drainage and leaching are considered in this section. The general characteristics of the soils can be found in the descriptions of the mapping units (Chap.4).

Alera experimental field

The Alera experimental field is representative of the fluvio-colluvial valleys (Profile 13, the soil is an Aquic Glossic Natragid). The soils are fine-textured, from silty clay to silty clay loam, though silty loam layers with a high content of very fine sand produced by the weathering of siltstone occur interbedded between finer layers.

Porosity decreases gradually with depth with a consequent increase in soil compactness and a decrease in hydraulic conductivity (Table 6.1).

Below an average depth of 1.5 m the soil layers become less pervious, though they seem to be saturated with water. At a depth variable from 3 to 4 m a mottled Tertiary mudstone is found. The texture of this mudstone is similar to that of the overlying soil layers, but it is extremely compact and impervious.

When the detailed survey was made the depth of the groundwater table varied from 1.0 to 1.2 m. The measured K-values thus refer to the soil layer between those depths and the bottom of the auger holes (1.5 m). Later, when the drainage system was installed and the initial leaching process had started, the hydraulic conductivity values of the surface soil layers were measured during periods of high water table.

TABLE 6.1 Hydraulic conductivity values obtained by the auger-hole method (Alera experimental field)

Depth (m)	Texture	Structure	Consistency (moist)	K (m/day)
0-0.50	silty clay	moderate blocky	moderately firm	0.6
0.50-0.75	silty clay loam	weak blocky	firm	0.3-0.4
0.75-1.00	silty clay loam	structureless; gypsum crystals	firm	0.2
1.00-1.50	silty loam (very fine sand)	structureless	friable	0.1-0.2

K-values measured by the inversed auger hole method in the surface soil were approximately zero.

The hydraulic conductivity of undisturbed soil cores determined in the laboratory (Table 6.2) revealed that the soil has an anisotropic permeability, the vertical percolation rate being much greater than the horizontal hydraulic conductivity. The downward decrease of hydraulic conductivity was reaffirmed, the layer below 1.5 m being almost impervious, even for vertical flow. Where the surface soil had been subsoiled, however, a relative increase was evident.

TABLE 6.2 Hydraulic conductivity values from laboratory determinations in undisturbed soil cores (Alera experimental field)

Depth (m)	Horizontal-K (m/day)	Vertical-K (m/day)	Remarks
0-0.50	0.004	0.97	-
0-0.30	0.040	0.69	subsoiled surface layer
0.50-0.85	0.010	0.73	-
0.85-1.00	0.040	0.28	-
0.85-1.00	-	2.50	gypsum crystal layer
> 1.50	0.001	0.02	compact subsoil

The absolute K-values determined for horizontal hydraulic conductivity were much lower than those obtained by the auger hole method.

The infiltration rate was initially estimated in a ploughed soil which was later left uncultivated. The measured values varied from 15 to 20 mm/day.

For the initial drainage design the Tertiary mudstone was considered the impervious barrier, at an average depth of 3.5 m. With a drain depth of 1.5 m and assuming a hydraulic conductivity of 0.1 m/day for the layer between 1.5 and 3.5 m, the mean transmissivity value below drain level would be $0.2 \text{ m}^2/\text{day}$.

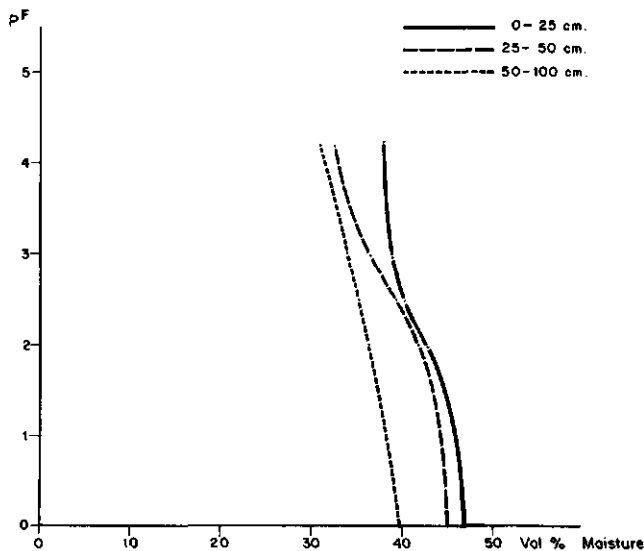


Fig.6.1: pF-curves of the soils of the Alera experimental field.

From pF-curves (Fig.6.1),the drainable pore space (μ) and the available moisture content between field capacity and wilting point could be derived.

The moisture content under saturated conditions ($pF = -\infty$) could be assumed approximately equal to the moisture content 1 cm above the ground-water table under equilibrium conditions ($pF = 0$), because in soils where macropores are absent the pF-curve is almost vertical for pF-values close to zero. If under equilibrium conditions the moisture content 100 cm above the groundwater table ($pF \approx 2$) corresponds with field capacity,the drainable pore space can be estimated from the difference between the moisture content by volume at $pF = 2$ and $pF = 0$.

According to this assumption the estimated drainable pore space of the upper 1 m averages 3.7 per cent. The estimated average available moisture content (between $pF=2.0$ and $pF=4.2$) in the upper 0.5 m is 7 per cent.

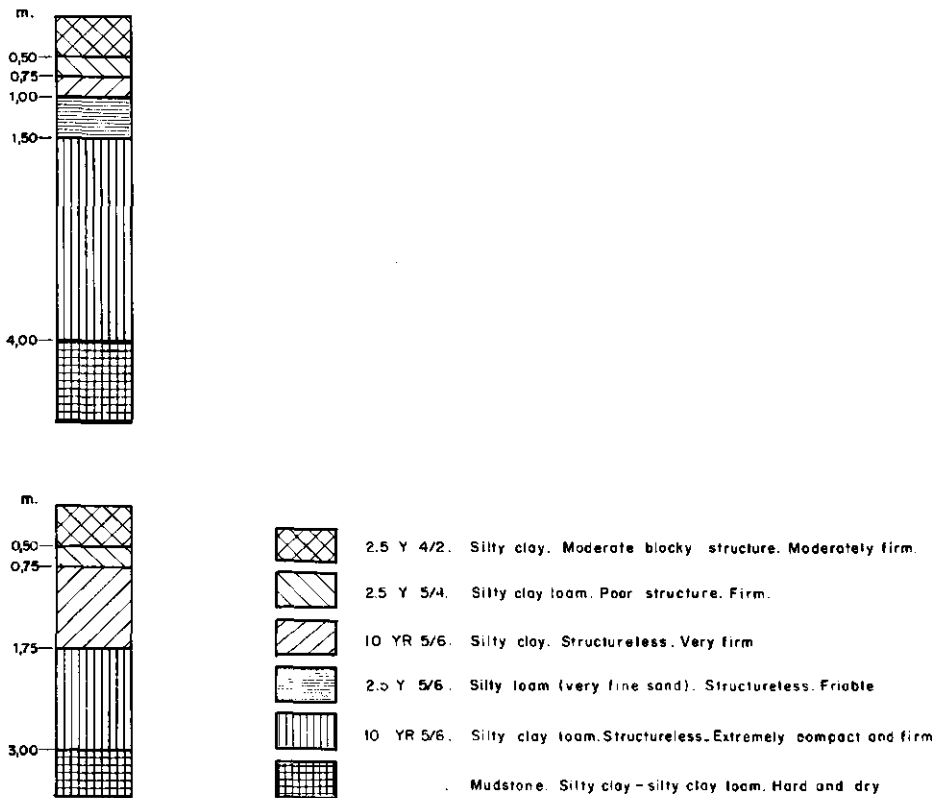


Fig.6.2: Schematic soil profiles. Alera experimental field.

The variation of soil conditions can be observed in Fig.6.2 where a schematic description of two characteristic soil profiles is shown, and in Table 6.3 where the corresponding particle size distribution data are listed.

TABLE 6.3 Textural analysis of soil profiles of Fig.6.2

Deep bore hole - basin 1

Depth m	gravel			s a n d			silt	clay
	>2 mm	2-1	1-0.5	0.5-0.25	0.25-0.125	0.125-0.05	0.05-0.002	<0.002 mm
0-0.50	-	-	-	0.20	0.46	1.24	55.91	42.15
0.50-0.75	-	-	0.31 ¹	0.36 ¹	0.31 ¹	0.67	50.85	47.47
0.75-1.00	-	1.12 ¹	2.24 ¹	2.13 ¹	1.76 ¹	2.66	52.10	37.95
1.00-1.50	-	-	-	0.52	3.78	15.30	56.06	24.27
1.50-2.50	-	-	-	2.05	4.26	4.77	54.80	34.00
2.50-4.00	-	-	-	0.66	3.50	5.89	46.11	43.82
4.00-5.00	-	-	-	1.08	3.90	9.87	46.50	38.63

Deep bore hole - basin 2

Depth m	gravel			s a n d			silt	clay
	>2 mm	2-1	1-0.5	0.5-0.25	0.25-0.125	0.125-0.05	0.05-0.002	<0.002 mm
0-0.50	-	-	-	0.50	0.35	1.41	51.51	46.20
0.50-0.75	-	-	-	-	-	0.73	69.73	29.53
0.75-1.75	-	-	-	0.70 ¹	0.35 ¹	0.35 ¹	52.92	45.66
1.75-2.25	-	-	-	-	-	0.99	66.92	32.07
2.25-3.00	-	-	-	-	-	5.18	52.25	42.55
>3.00	-	-	-	-	-	1.56	50.91	47.52

¹ gypsum crystals

Valareña experimental field

The Valareña experimental field is situated in a saline alluvial valley (3.11). The soils are fine-textured in the upper 2.5 m, the texture varying from silty clay to silty clay loam. Below 2.5 m on average, the very fine sand content increases and a silty loam texture is found.

These fine sediments overlie a gravel and coarse sand layer which has a variable thickness of 1 to 1.5 m. In the experimental unit the gravel layer is continuous and its upper limit is at a depth of 3 to 3.5 m. When the detailed soil survey was made (June 1974) the gravel layer was saturated with very saline water (Chap.4, Profile 15; the soil is a Salic Stratic Xerofluvent).

This aquifer lies above a red and grey mudstone whose depth varies from 4 to at least 5 m. The texture of the mudstone is silty clay and, in spite of underlying a saturated zone, is apparently dry. For this reason it can be considered the impervious barrier.

The upper soil layers show a marked very fine stratification. The hydraulic conductivity is therefore anisotropic, the horizontal hydraulic conductivity being higher than the percolation rate.

The hydraulic conductivity was measured by the inverse auger hole method because the water table was deep. An average K-value of 0.2 m/day was obtained from 12 measurements made in a soil layer situated between 1.0 and 1.5 m (future drain level). In the surface soil where the stratification had been disturbed by land levelling and further by subsoiling and where there was some halophytes root proliferation, a mean K-value of 0.5 m/day was obtained.

Later, during the initial leaching process, attempts were made to determine the hydraulic conductivity by the auger hole method. No results could be obtained, however, as no true water table occurred in the stratified layers.

Assuming a constant K-value of 0.2 m/day in the layers above the gravel layer, the transmissivity below drain level would be $0.4 \text{ m}^2/\text{day}$. No direct hydraulic conductivity measurements were made in the gravel layer, but its

transmissivity is assumed to be higher than $1 \text{ m}^2/\text{day}$.

The infiltration rate as determined by the double ring method averaged 10 mm/day in the unploughed surface soil.

In Fig.6.3 a schematic soil profile is shown, the textural analysis of which is given in Table 6.4.

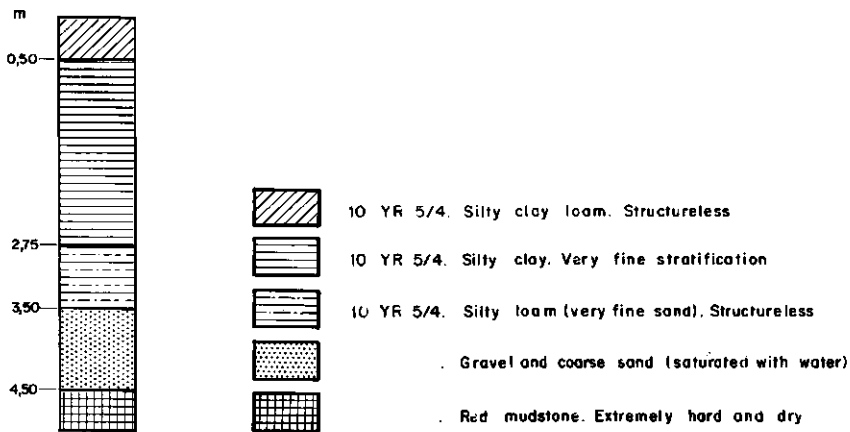


Fig.6.3: Schematic soil profile. Valareña experimental field.

TABLE 6.4 Particle size distribution of soil profile of Fig.6.3

Depth m	coarse fragm. >2 mm	s a n d					silt 0.05-0.002	clay <0.002 mm
		2-1	1-0.5	0.5-0.25	0.25-0.125	0.125-0.05		
0-0.50	-	-	0.06	-	0.12	1.02	70.30	28.47
0.50-1.00	-	-	0.06	-	0.06	0.32	58.10	41.43
1.00-1.50	-	-	0.11	0.05	0.16	0.62	62.98	36.15
1.50-2.00	-	-	0.12	0.06	0.06	0.48	54.48	44.78
2.00-2.75	-	-	0.30	0.10	0.10	0.45	52.73	46.29
2.75-3.25	-	-	0.10	0.10	2.37	10.84	55.58	30.97
3.25-3.50	-	-	3.72	1.18	3.88	11.59	55.86	23.73

6.3.3 Initial salinity

Alera experimental field

Soil salinity increases with depth, being highest in the less pervious layers (> 1.5 m), where the electrical conductivity (EC_e) varied from 20 to 35 mmhos/cm (Table 6.5).

In the surface soil the variation was greater, with slightly saline soil patches ($EC_e \approx 4$ mmhos/cm) close to very saline soils ($EC_e > 30$ mmhos/cm)

Though soil samples were taken on a grid system and the observation density was 4 sites/ha, it was not possible to produce a map with different intervals of soil salinity because variation was so great over short distances.

TABLE 6.5 Salinity of the soil layers of Fig.6.2 (February 1976)

Depth m	$CO_3^{=}$ %	Saturation moisture content %	Organic matter %	pH		Cl^- %	Ca^{++} & Mg^+ meq/l	Na^+ meq/l	SAR	ESP	EC_e mmhos/cm
				H ₂ O	KCl						
0-0.50	25.8	62.5	3.2	7.8	7.2	0.06	17.7	50.0	16.8	19	6.1 ¹
0.50-0.75	35.5	68.0	1.4	7.7	7.2	0.13	48.4	100.4	20.4	22	12.4 ¹
0.75-1.00	36.2	61.0	0.9	7.6	7.3	0.12	43.3	100.4	21.6	24	12.4
1.00-1.50	41.5	40.5	0.8	7.8	7.3	0.12	29.0	106.8	28.0	29	13.0
1.50-2.50	38.3	51.0	0.9	7.9	7.5	0.27	55.6	161.5	30.6	31	19.8
2.50-4.00	36.5	58.4	0.9	7.8	7.3	0.54	82.3	243.0	37.9	35	28.9
4.00-5.00	35.4	52.0	1.2	7.7	7.0	0.55	96.3	267.0	38.5	35	32.7
0-0.50	23.1	64.0	3.2	8.0	7.1	0.017	13.4	19.9	7.7	10	2.9 ¹
0.50-0.75	44.2	49.0	0.7	7.7	7.2	0.028	13.7	30.7	11.7	14	4.0 ¹
0.75-1.75	30.3	75.0	0.7	8.0	7.2	0.170	45.9	110.0	23.0	25	12.4
1.75-2.25	39.1	54.0	0.9	8.0	7.8	0.340	47.8	187.0	38.3	35	22.8
2.25-3.00	35.2	64.0	1.0	7.9	7.4	0.380	64.0	175.0	30.9	31	22.3
>3.00	30.1	70.0	1.1	7.8	7.4	0.470	54.8	193.0	36.9	35	23.6

¹ Layers leached with irrigation water

The salinity levels were reflected in the sodium adsorption ratio and under equilibrium conditions the soils must be assumed to be saline-alkali. Gypsum crystals were evident in the fluctuation zone of the water table.

At the start of leaching the salinity of the groundwater was high. Though the salt content varied slightly, from the evidence of water sample analysis (Table 6.6) it could be observed that highly soluble salts, NaCl, MgSO₄ and Na₂SO₄ were the most commonly occurring. The groundwater appeared to be saturated with CaSO₄.2 H₂O (40 meq/l). Where the total salt content was very high (Drain No.20), some CaCl₂ and MgCl₂ occurred (Fig.6.4).

The gypsum content was not determined because of the particular difficulty of such an analysis in these saline soils. However, a high gypsum content was assumed because of the occurrence of gypsum crystals in the fluctuation zone of the groundwater table (0.85 to 1 m) and because the groundwater was saturated with CaSO₄.2 H₂O. Thus it seemed likely that the soluble salts could be leached without gypsum applications.

TABLE 6.6 Groundwater initial salinity. Alera experimental unit

Drain No.	EC mmhos/cm	Salt g/l	m e q / l							pH	SAR
			Cl ⁻	SO ₄ ⁼⁼	HCO ₃ ⁻	Ca ⁺⁺	Mg ⁺⁺	K ⁺	Na ⁺		
1	60	37.5	470	145.8	3.8	36.0	56.0	0.1	535	7.3	78.9
3	48	29.6	365	116.6	3.7	31.6	40.6	0.1	425	7.8	70.7
7	46	29.6	350	131.6	3.6	46.8	50.2	0.0	400	7.6	57.4
8	50	32.1	435	104.1	3.7	46.8	57.0	0.1	430	7.6	59.7
15	43	26.6	315	116.6	4.6	43.4	44.6	0.0	360	7.7	54.3
18	46	29.4	425	73.3	3.0	44.4	54.8	0.0	400	7.4	56.8
20	85	59.7	950	81.2	3.4	68.0	139.0	0.1	822	7.3	80.8

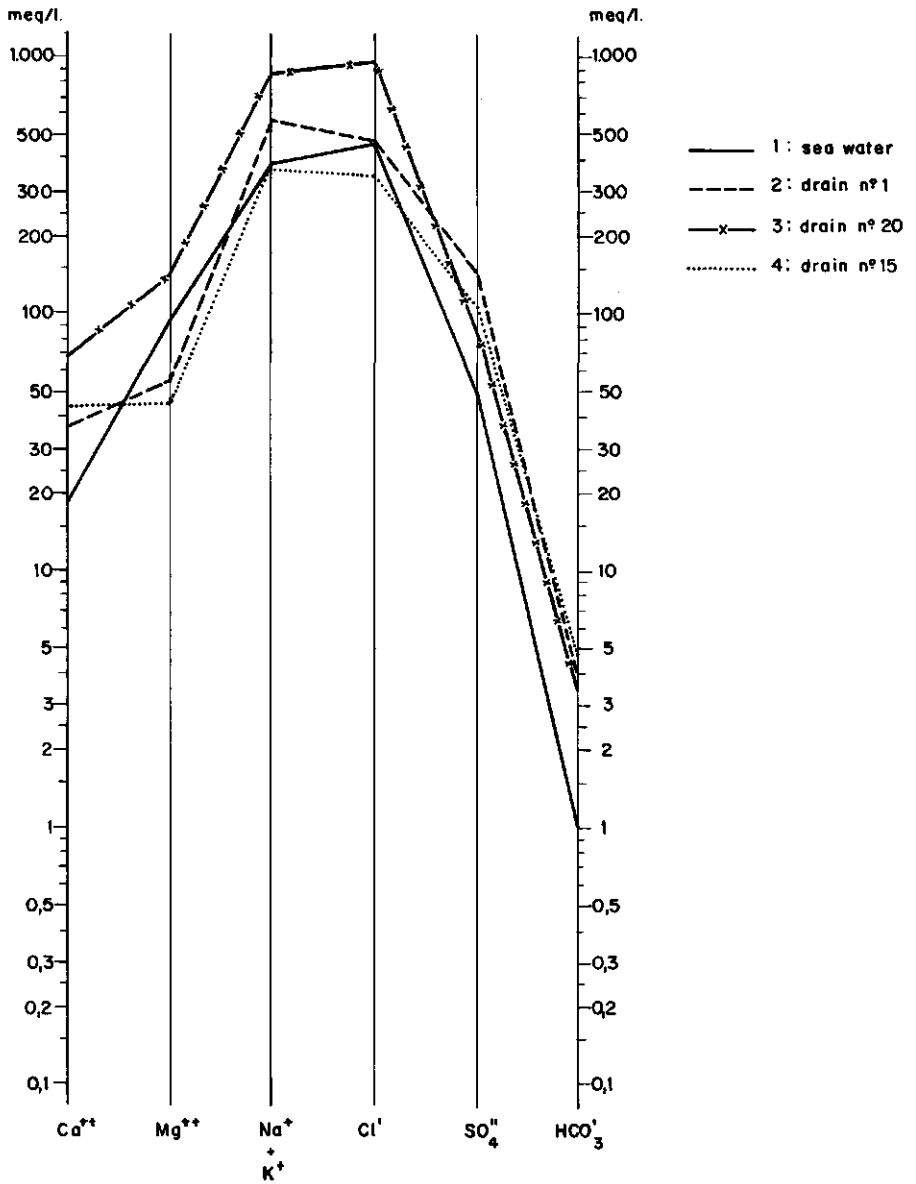


Fig.6.4: Schoeller diagram for groundwater. Alera experimental field (December 1974).

Valareña experimental field

Soil salinity affecting these alluvial soils was more uniformly distributed than in the soils of Alera. There was a slight increase in the salt content of the surface layers when evapotranspiration was high, but the salinity of the deeper stratified silty clay layers was more homogeneous (Table 6.7). The surface crust of uncultivated surface soil (<5 cm) had a high salt concentration ($EC_e \approx 70$ mmhos/cm) and a pseudostructure with saline puffs.

TABLE 6.7 Salinity of soil layers of Fig.6.3 (June 1976).
(Water extract from saturated paste.)

Depth m	$CO_3^{=}$ %	Saturation moisture content %	Organic matter %	pH		Cl^- %	Ca^{++} & Mg^+ meq/l	Na^+ meq/l	SAR	ESP	EC_e mmhos/cm
				H_2O	KCl						
0-0.50	43.2	57.5	3.3	7.5	7.3	1.09	243.3	307.0	27.8	29	49.0
0.50-1.00	39.4	65.0	1.6	7.6	7.4	1.08	190.5	325.0	33.3	32	43.7
1.00-1.50	41.8	62.5	1.5	7.6	7.5	1.07	183.8	355.0	37.0	35	46.3
1.50-2.00	37.1	65.0	1.5	7.8	7.6	0.95	164.3	325.0	35.8	34	40.4
2.00-2.75	35.0	72.5	1.3	7.8	7.6	0.82	144.3	275.0	32.4	31	33.5
2.75-3.25	42.5	47.5	1.0	7.8	7.5	0.66	191.8	307.0	31.3	31	39.3
3.25-3.50	44.0	44.5	1.3	7.8	7.5	0.62	163.0	307.0	34.0	33	40.0

Though salinity did not vary over such short distances as in the Alera unit, the filled in part of the levelled terrace close to the collector drain was less saline than the excavated part. This indicated that where the very fine stratification is altered by levelling operations and further by subsoiling, water passes more easily, and leaching is enhanced.

The sodium adsorption ratio increased with salinity, making the saline soil alkali as well.

The groundwater which saturated the gravel layer above the impervious mudstone was very saline, but there was a great difference in the total salt content of two water samples taken at two different sites.

The composition of the salts was similar to that of the groundwater of the Alera field, NaCl and $MgSO_4$ being the most common (Table 6.8 and Fig.6.5).

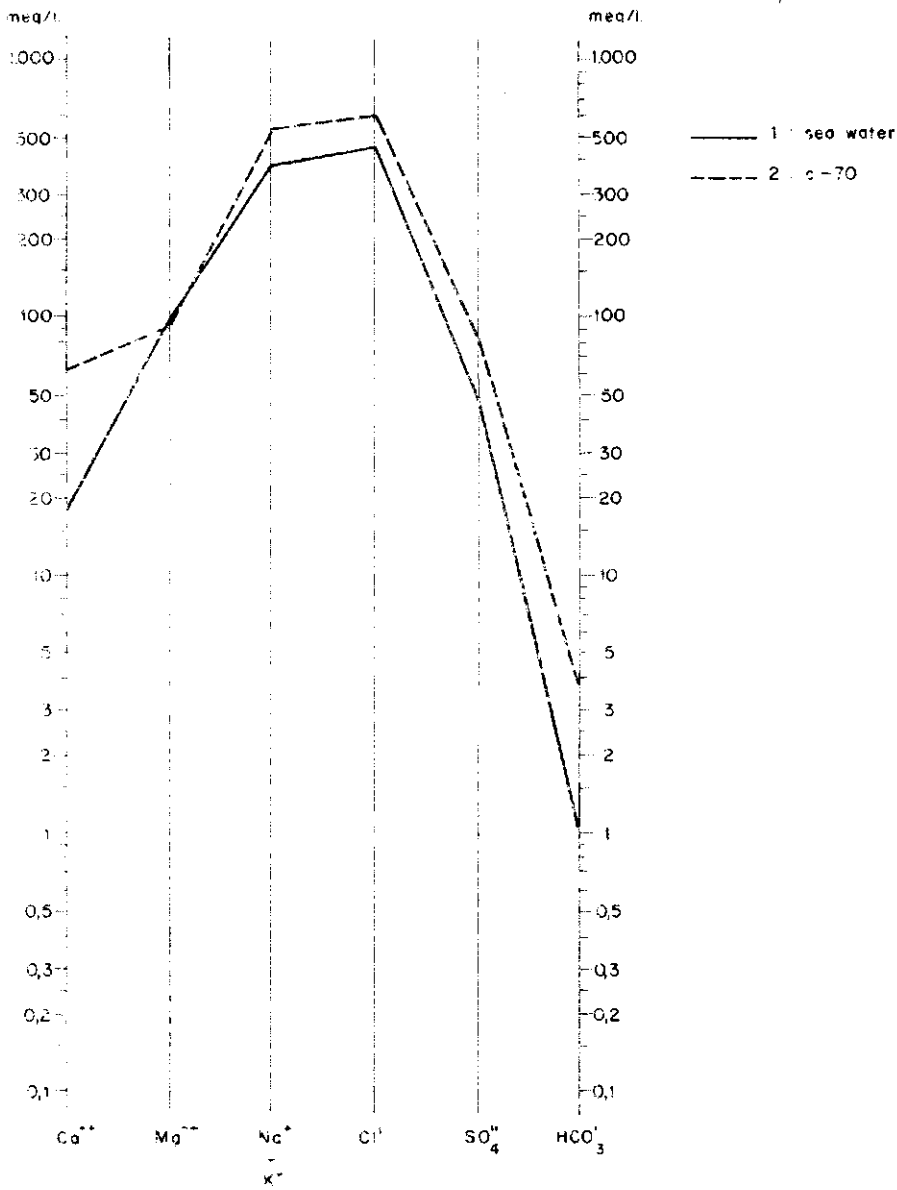


Fig. 2.5: Schöeller diagram for groundwater. Talareña experimental field (June 1974).

As some dispersion was observed in the surface soil crust, a gypsum application seemed a reasonable method of preventing alkalization during leaching.

TABLE 6.8 Salt composition of the groundwater.
Valarena experimental unit

No.	EC mmhos/cm	Salt g/l	Cl ⁻	SO ₄ ²⁻	HCO ₃ ⁻	m e q / l				pH	SAR
						Ca ⁺⁺	Mg ⁺⁺	K ⁺	Na ⁺		
C-70	66	39.1	585	80.4	3.8	62.6	89	0.1	520	7.5	59.8
C-59	28.5	18.7	262	45.2	7.2	25.2	20	0.0	271	7.4	57.0

7. Experimental field design

7.1 Design of the drainage system

The theoretical calculation of the drainage system was based upon the most commonly used drainage equations for steady and unsteady-state conditions. To these equations, simplified and assumed drainage criteria and the hydrological soil properties measured by conventional methods were applied.

7.1.1 Alera experimental field

Hydrological soil conditions

A drainable soil profile with the average hydrological soil properties determined in Section 6.3.2 was considered (Fig.7.1).

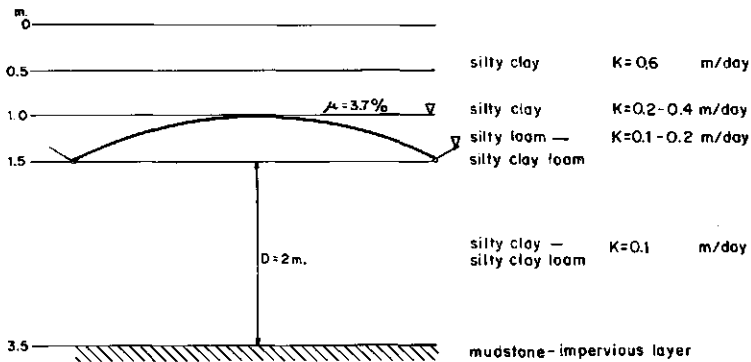


Fig.7.1: Drainable soil profile. Alera experimental field.

Although the hydraulic conductivity decreases gradually with depth, the boundary between the layers with $K = 0.1$ m/day and $K = 0.2$ m/day was considered to be at a depth of 1.5 m. In calculating the drain spacing this boundary was chosen as the average drain depth.

Drainage criteria

Different drainage criteria were formulated for steady and unsteady-state conditions, giving separate consideration to the irrigation season and the winter period when no irrigation takes place.

For the design of the drainage system the initial leaching period without crops was not taken into account, but only the control of the saline groundwater table once the rootzone (the upper 1 m soil) is free of salts.

Drainage criteria for the irrigation season

The irrigation water losses percolating through the unsaturated zone cause a recharge of the groundwater. The rise of the groundwater table depends on the amount of percolation water and the drainable pore space (μ).

The drainage system had to prevent a gradual rise of the water table during the irrigation season. The field application losses could be estimated from irrigation experience in the area. In the peak irrigation period applications of 80 mm every 12 days are common. Since the land is levelled, surface losses are negligible. If the field application efficiency is $e_a = 0.7$, the percolation losses are:

$$s = 0.3 \times \frac{80 \text{ mm}}{12 \text{ days}} = \frac{24 \text{ mm}}{12 \text{ days}} = 2 \text{ mm/day}$$

These losses could be expressed in steady-state conditions as a constant recharge. The drain discharge rate should then be 2 mm/day, with the water table remaining at a depth of 1 m ($h = 0.5$ m and $s = 2$ mm/day).

Instead of steady-state equations, however, it is more logical to apply unsteady-state equations, since percolation losses cause a sudden rise of the water table followed by a gradual fall. With $\mu = 3.7\%$ (see 6.3.2), the initial rise of the water table should be:

$$\Delta h = \frac{24 \text{ mm}}{0.037} = 0.65 \text{ m}$$

Thus a drawdown of 0.65 m is required in a period of 12 days. To obtain a water table that is comparable with the steady-state water table at a depth of 1 m ($h = 0.5 \text{ m}$), the following values were assumed as criteria for unsteady-state flow ($h_0 = 0.825$, $h_t = 0.175$, $t = 12 \text{ days}$):

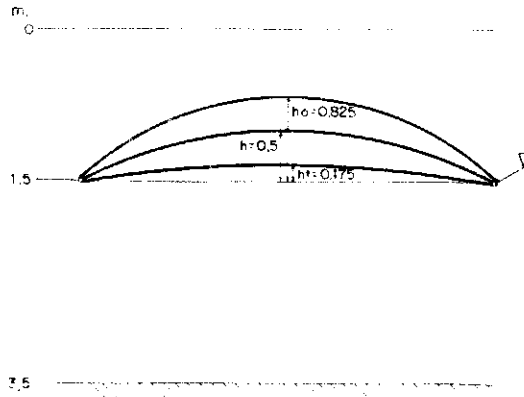


Fig.7.2: Drainage criteria for the irrigation season. Alera experimental field.

From the depth-duration-frequency relation derived with the Gumbel probability distribution (Chap.2) a rainfall of 68.5 mm can be expected over 3 consecutive days during the irrigation season for a return period of 5 years. This amount of rainfall is less than an irrigation application. For this reason the formulated criteria remain valid, if the possibility of heavy rainfall after an irrigation application is neglected.

Although the salinity of the irrigation water is low ($EC_1 = 0.3 \text{ mmhos/cm}$) the leaching requirements during the irrigation season could be calculated

using the salt equilibrium equation (van der Molen and van Hoorn, 1973):

$$R^* = (E - P) \frac{EC_i}{f(2 EC_e - EC_i)} \quad (1)$$

where

- R^* = leaching requirements (mm)
- E = amount of evapotranspiration (mm)
- P = effective amount of precipitation (mm)
- EC_i = mean electrical conductivity of the irrigation water (mmhos/cm)
- f = leaching efficiency coefficient with respect to percolation
- EC_e = maximum value of the electrical conductivity of the soil saturation extract (mmhos/cm)

The precipitation deficit was calculated from the evapotranspiration data. The latter were calculated with the Thornthwaite and Blaney-Criddle methods and in accordance with the Penman method, using meteorological data from Zaragoza (Chap.2). The total amount of precipitation was regarded as effective rainfall because no surface runoff is expected on flat levelled land.

If we assume values of $f = 0.5$ and $EC_e = 2$ mmhos/cm, the leaching requirements calculated by means of Eq.(1) are 122 mm, the corresponding theoretical net irrigation requirements being 873 mm. Annual irrigation applications of 1000 mm are common in the area, so if the field application efficiency is 0.7, normal percolation losses are approximately 300 mm and are thus in excess of the leaching requirements.

The drainage criteria adopted for steady-state conditions are similar to the drainage requirements applied in some irrigation projects in arid and semi-arid zones, for instance those reported from the Medjerda Valley in Tunisia ($s = 2$ mm/day, water table depth = 1 m) and the Habra Valley in Algeria ($s = 2$ mm/day, depth = 0.8 m), as well as those recommended for the Bardenas area by Mr. Wardle and Dr Ede (personal communication).

Drainage criteria for the winter season

During winter, when there is no irrigation, the groundwater is recharged by rainfall and possible seepage from the adjacent slopes.

Maximum rainfalls derived from the depth-duration-frequency curves (Chap.2) were 76 mm over 3 consecutive days and 85 mm over 6 consecutive days for a 5 year return period.

Assuming that the unsaturated zone has a moisture content near field capacity, a percolation of 40 mm would be sufficient to cause the water table to rise to the surface, even though initially the water table was deeper than 1 m.

The drainage system must therefore be capable of obtaining a water table drawdown of 30 cm in 3 days while at the same time maintaining a constant discharge rate equal to the recharge intensity. This recharge can be approximately equal to the basic infiltration rate (about 15 mm/day). In extreme conditions waterlogging occurs for 3 days, with a drainage discharge of 45 mm.

In the hydrogeological survey no measurable seepage was noted, which is not surprising in view of the low transmissivity of the soils of the slopes. The steady-state summer drainage criteria ($s = 2$ mm/day, $h = 0.5$ m) could therefore meet any possible seepage requirement.

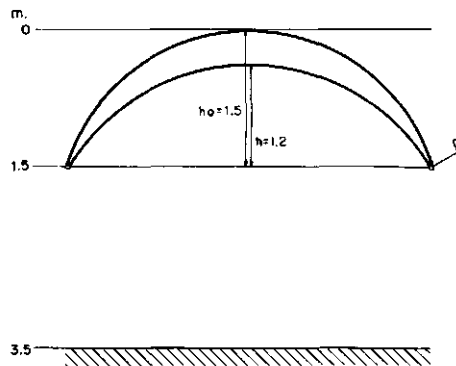


Fig.7.3: Drainage criteria for the winter season. Alera experimental field.

The winter drainage criteria could thus be formulated as follows:
 $s = 15 \text{ mm/day}$, $h = 1.5 \text{ m}$ for steady-state conditions and $h_o = 1.5 \text{ m}$, $h_t = 1.2 \text{ m}$, $t = 3 \text{ days}$ for unsteady-state conditions (Fig.7.3).

The drainage criteria are summarized in Table 7.1.

TABLE 7.1 Drainage criteria.
 Alera experimental field

Season	Water flow conditions	h (m)	s (mm/day)	h_o (m)	h_t (m)	t (days)
Irrigation	steady state	0.5	2	-	-	-
	unsteady state	-	-	0.825	0.175	12
Winter	steady state	1.5	15	-	-	-
	unsteady state	-	-	1.50	1.2	3

Drain spacing

The Hooghoudt theory was used to calculate the drain spacing for steady-state conditions. Though the hydraulic conductivity decreases gradually with depth, the drain level was considered to be at the boundary between two layers with different hydraulic conductivities.

For the flow region above the drain level an average hydraulic conductivity was adopted.

Applying the formulated drainage criteria (Table 7.1) and the measured hydrological factors (Chap.6) to the Hooghoudt Equation (2) the drain spacings of Table 7.2 were obtained.

$$L^2 = \frac{8 K_b dh + 4 K_a h^2}{s} \quad (2)$$

where

- L = drain spacing (m)
- s = discharge rate (m/day)
- K_a = hydraulic conductivity of the layer above drain level (m/day)
- K_b = hydraulic conductivity of the layer below drain level (m/day)
- d = equivalent depth of aquifer below drain level (m)
- h = hydraulic head above the drain level midway between drains (m)

TABLE 7.2 Drain spacing, obtained with Eq.(2).
Alera experimental field

Drainage criteria		Hydrological factors			Drain spacing ¹		
h	s	K_a	K_b	D	L_o	c_o	L
(m)	(m/day)	(m/day)	(m/day)	(m)	(m)	(m)	(m)
0.5	0.002	0.2	0.1	2	22.4	5.5	16.9
1.5	0.015	0.4	0.1	2	20.0	5.5	14.5

¹ van Peere (1978): $L = L_o - c$, $c = D \ln \frac{D}{u}$, $u = \pi r_o$, $r_o = 0.04$ m

It was not easy to select an equation to calculate the drain spacing for unsteady-state conditions. The Glover-Dumm equation was not applicable because the region of flow above drain level is more important than the region below ($d = 1.1$ m, $K_d = 0.11$ m²/day). Besides, neither the thickness of the aquifer nor the hydraulic conductivity in the drainable soil profile is constant.

The Boussinesq equation seemed a better fit if the water flow below drain level was not taken into account and if the hydraulic conductivity for the region of flow above drain level was considered constant. This equation then reads:

$$L^2 = \frac{4.46 K h_o h_t t}{\mu(h_o - h_t)} \quad (3)$$

where

- h_o = hydraulic head above drain level after an instantaneous recharge (m)

- h_t = hydraulic head above drain level midway between drains at any time t (m)
 t = time (days)
 μ = drainable pore space

TABLE 7.3 Drain spacing obtained with Eq.3. Alera experimental field

Drainage criteria		Hydrological factors			Drain spacing
h_o (m)	h_t (m)	t (days)	K (m/day)	μ	L (m)
0.825	0.175	12	0.4	0.037	11.3
1.50	1.2	3	0.4	0.037	29.5

From the calculated drain spacings of Tables 7.2 and 7.3 it could be concluded that a drain spacing of between 15 and 20 m was suitable. The spacing finally selected for testing in the Alera field was 20 m for an average drain depth of 1.5 m (Fig.7.4). Part of the undrained control area is shown in Fig.7.5.

Drainage and filter materials

Smooth clay pipes and corrugated PVC pipes, 8 cm in diameter, were used as field drains.

The hydraulic design of the smooth clay pipes was made with the Wesseling equation (Eq.4), and that of the corrugated pipes with the Manning equation (Eq.5)

$$Q_L = s B L = 89 d^{2.712} i^{-0.572} \quad (4)$$

$$Q_L = s B L = 38 d^{2.667} i^{-0.5} \quad (5)$$

where

$$Q_L = \text{discharge rate (m}^3\text{/day)}$$

$$s = \text{discharge rate per unit surface area (m/day)}$$



Fig.7.4. Partial view of the Alera experimental field.

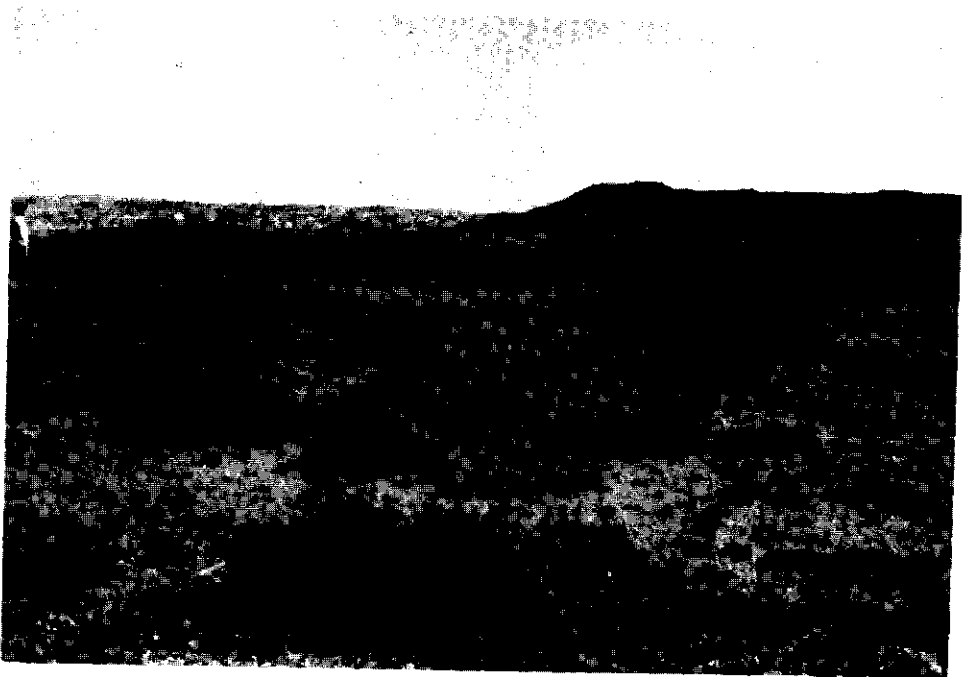


Fig.7.5. Undrained control area. Alera experimental field.

- $B \times L =$ drainable area (m^2)
 $B =$ drain length (m)
 $d =$ drain internal diameter (m)
 $i =$ hydraulic gradient = drain slope

If the maximum specific discharge is 15 mm/day and the drainable area 5 200 m^2 ($L = 20$ m, $B = 260$ m), an internal drain diameter of 8 cm and a drain slope of 0.1% is sufficient for both the clay and PVC pipes. For the first installation, no 8 cm PVC pipes were available and 5 cm pipes were used. For the comparative study of the entrance resistance of drainage and filter materials, the following combinations were selected (Fig.7.6):

- Drain Group 1: clay pipes ($d = 80$ mm, length 40 cm)
 Drain Group 2: clay pipes as group 1 with a gravel cover (gravel $\phi = 2 - 20$ mm, 25 l/m, Fig.7.7)
 Drain Group 3: corrugated PVC pipes ($d = 50$ mm) with a gravel cover as group 2
 Drain Group 4: corrugated PVC pipes ($d = 50$ mm)
 Drain Group 5: corrugated PVC pipes ($d = 50$ mm) with barley straw cover
 Drain Group 6: pre-enveloped corrugated PVC pipes ($d = 50$ mm) with esparto fibre (Fig.7.8)
 Drain Group 7: pre-enveloped corrugated PVC pipes ($d = 50$ mm) with cocos fibre
 Drain Group 8: as drain group 2.

Collector drain and main drain

The simple drainage system consists of (Fig.7.6):

- a) Field laterals installed at a 20 m spacing.
- b) Two open collector drains which collect water from the field laterals (D-IX-0 for drains 1 to 15 and D-IX-3-2 for drains 16 to 26, Fig.7.9)
- c) Main drain which is an existing open ditch (C-XVIII, Fig.7.10)
- d) The existing open collector D-IX-3 which is used as an interceptor drain
- e) A new open ditch was designed to collect the surface drainage of basins 1 to 5 (Fig.7.11).

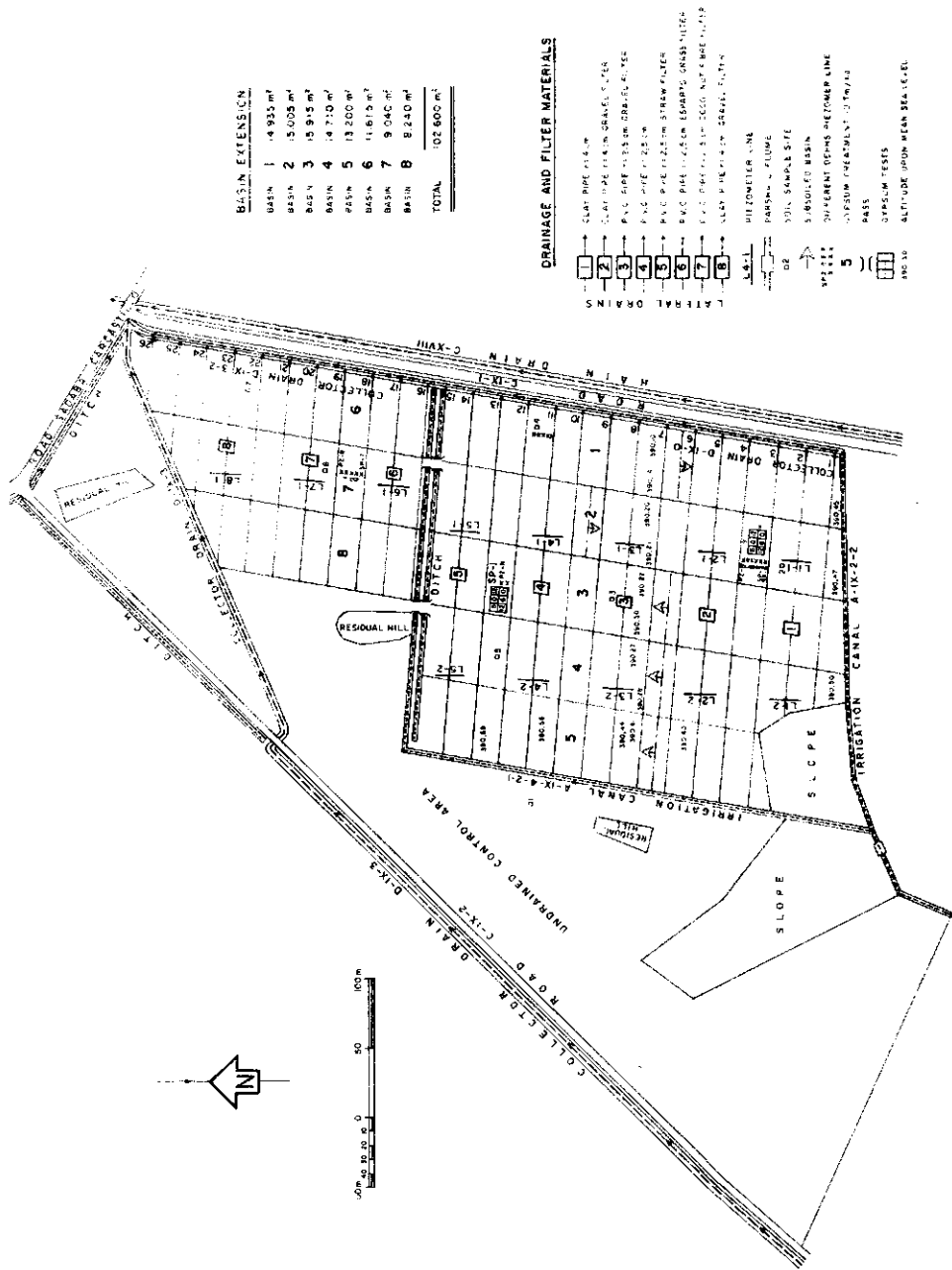


Fig.7.6: Layout of Alera experimental field.



Fig.7.7: Installation of clay drains.

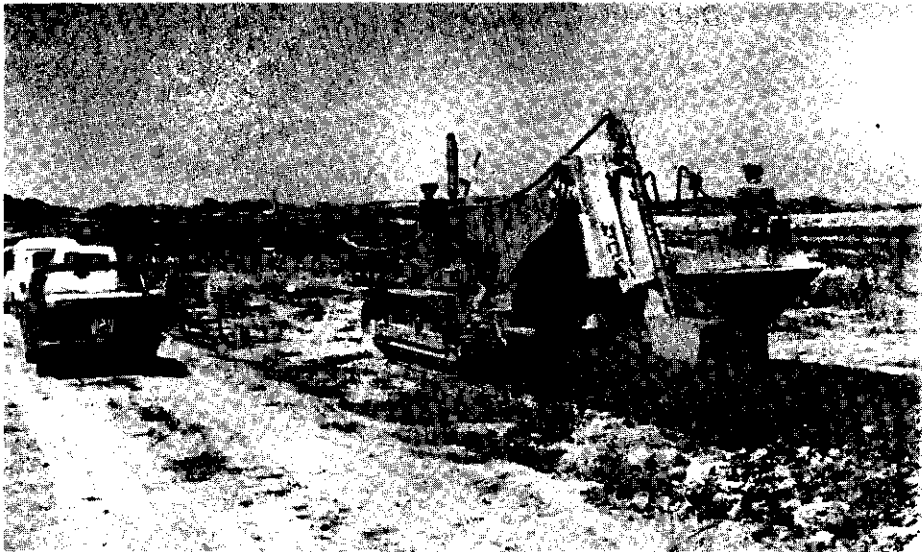


Fig.7.8: Installation of plastic pipes pre-enveloped with esparto fibre.



Fig.7.9: Field drain outlets to collector drain. Alera experimental field.



Fig.7.10: Main drain of the Alera field.

The main drain has a trapezoidal cross-section with a bank slope of 1:1 and an average depth of 2 m. The bank is severely eroded and is partly covered by halophytes (*Suaeda* and *Atriplex*). The salinity of the drainage water is such that it prevents the growth of aquatic weeds so that water is free flowing.

The collector drains debouch into the main drain through concrete culverts built below the road C-IX-1 (Fig.7.12).

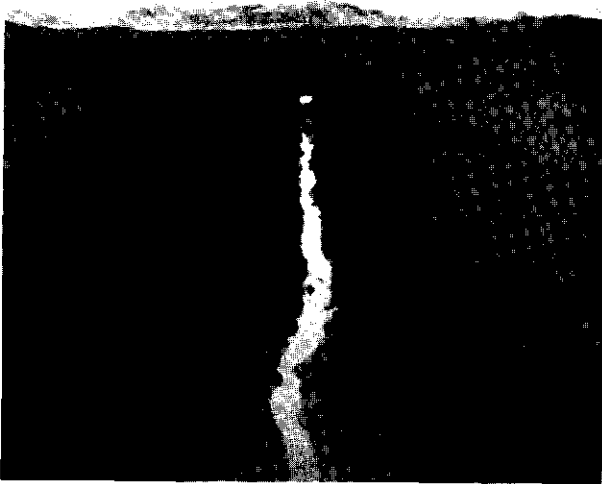


Fig.7.11: Open ditch to collect surface drainage. Alera field.



Fig.7.12: Concrete culvert below road.

The hydraulic design of the open collector ditches was calculated with the Manning equation (Eq.6):

$$Q = K_M AR^{2/3} S^{1/2} \quad (6)$$

where

- Q = design discharge (m^3/s)
- K_M = Manning coefficient ($m^{1/3}/s$)
- A = wetted area (m^2)
- R = hydraulic radius (m)
- S = hydraulic gradient

The design discharge could be calculated because the maximum specific discharge ($s = 15$ mm/day) and the maximum drainable area (7.8 ha) were known. The discharge rate thus obtained was 13.5 l/s ($q = 1.74$ l/s/ha).

If the lateral outlets are at a depth of 1.6 m and the safety margin to the water level in the ditch is 0.2 m, the water in the ditch has to be at a depth of at least 1.8 m.

Assuming a Manning coefficient of $40 \text{ m}^{1/3}/\text{s}$ and a hydraulic gradient of 0.05 per cent (to correspond with the slope of the land), the following section factor was obtained for the design discharge:

$$AR^{2/3} = 0.015 \text{ m}^{8/3}$$

A trapezoidal cross-section with a bank slope of 1:1, a bottom width $b = 0.4$ m, and a water depth in the ditch $y = 0.2$ m, has a section factor of $0.03 \text{ m}^{8/3}$, which is twice the required value.

The flow velocity would be $v = Q/A = 0.1$ m/s, which is less than the maximum permissible velocity in a silty clay soil ($v = 0.7$ m/s).

An open-ditch collector-drain thus has the following characteristics: a trapezoidal cross-section (4.4 m^2), a bank slope of 1:1, bottom width $b = 0.4$ m, depth 2 m, and slope 0.05%.

7.1.2 Valareña experimental field

Hydrological soil conditions

The average hydraulic conductivity of the stratified silty clay layers was $K = 0.2$ m/day (inverse auger hole method). The hydraulic conductivity of the deep gravel layer was not measured, but was assumed to be at least 1 m/day.

Some laboratory measurements were made on undisturbed soil cores and showed lower K-values than those obtained in the field.

The drainable pore space was estimated by a rule-of-thumb developed by van Beers (1962). When the hydraulic conductivity has been determined and the K-value is expressed in cm/day, the root of the K-value is approximately equal to the drainable pore space (in %). It was thus found that $\mu = 4.5\%$.

An average drainable soil profile with the average soil hydrological properties is as shown in Fig. 7.13.

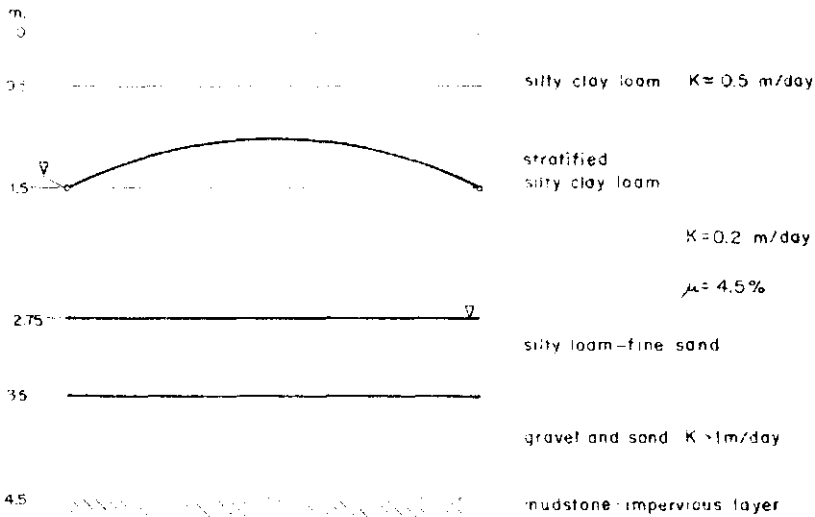


Fig. 7.13: Drainable soil profile. Valareña experimental field.

The boundary between the saturated gravel layer and the underlying reddish dry mudstone was regarded as the impervious barrier.

The design drain depth was chosen at 1.5 m because the nearer it was to the pervious gravel layer the better for drain installation.

Drainage criteria

The steady-state drainage criteria formulated for the Alera field were also applied here. Unsteady-state drainage criteria were not formulated because of the difficulty of applying unsteady-state equations in a stratified soil.

Drainage criteria for the irrigation season

Although the intensity of heavy rainfall increases from north to south, the maximum rainfall to be expected over 3 consecutive days is 75 mm for a 5 year return period (Chap.2). This amount of water is comparable to an irrigation application, so the drainage criteria ($s = 2$ mm/day, $h = 0.5$ m) are valid.

As at the Alera field, the leaching requirements are less than the percolation losses.

Drainage criteria for the winter season

In winter the water table can rise to the soil surface because 85 mm and 93 mm of rainfall are expected respectively over 3 and 6 consecutive days in a 5 year return period (from depth-duration-frequency curves, Chap. 2). The discharge rate under steady-state conditions must therefore be equal to the basic infiltration rate ($s = 10$ mm/day) for a hydraulic head $h = 1.5$ m.

The drainage criteria for steady-state conditions are summarized in Table 7.4.

TABLE 7.4 Drainage criteria.
Valareña experimental field

Season	Water flow conditions	h (m)	s (mm/day)
irrigation	steady state	0.5	2
winter	steady state	1.5	10

Drain spacing

The drain spacing for steady-state flow was calculated with the Ernst formula because of the variability of the hydraulic conductivity due to stratification and also because the design drain level does not coincide with the boundary between the layers of different hydraulic conductivity.

Applying the drainage criteria and the hydrological factors to the Ernst equation (Eq.7), the drain spacings of Table 7.5 were obtained. They refer to summer and winter conditions, respectively.

$$h = s \frac{D_v}{K_1} + s \frac{L^2}{8 (K_1 D_1 + K_2 D_2)} + sL W_{rad} \quad (7)$$

where

- h = total hydraulic head midway between drains (m)
- s = drain discharge rate per unit surface area (m/day)
- L = drain spacing (m)
- K_1 = hydraulic conductivity of the upper less pervious layer (m/day)
- K_2 = hydraulic conductivity of the more pervious layer (m/day)
- D_v = thickness of layer over which vertical flow is considered (m)
- D_1 = average thickness below the water table of the upper layer with hydraulic conductivity K_1 (m)
- D_2 = thickness of the lower layer with hydraulic conductivity K_2 (m)
- W_{rad} = radial resistance (days/m)

The radial resistance could be calculated with Eq.(8) because the design drain level is above the more pervious layer and because $K_2/K_1 < 20$:

$$K_1 W_{rad} = K_1 W^1 + \frac{1}{\pi} \ln \frac{\pi a}{4u} \quad (8)$$

where

- a = geometry factor (m)
- u = wet perimeter (m)

By means of the Ernst nomograph for determining the radial resistance, which is derived by numerical calculation, a W_{rad} -value of 5.5 days/m was obtained.

TABLE 7.5 Drain spacing obtained with Eq.(7).
Valareña experimental field

Season	Drainage criteria		Hydrological factors					Drain spacing
	h (m)	s (m/day)	K_1 (m/day)	K_2	D_1 (m)	D_2 (m)	D_v (m)	L (m)
summer	0.5	0.002	0.2	1.0	1.25	1.75	0.5	33.0
winter	1.5	0.010	0.2	1.0	1.25	1.75	1.5	21.0

As the winter conditions are more restrictive, a drain spacing $L = 20$ m with drain level at 1.5 m was adopted.

Drainage and filter materials

Except for the pre-enveloped PVC pipes with esparto and cocos fibre, the same drainage and filter materials as used at Alera field were installed at Valareña (Fig.7.14).

Pipes 8 cm in diameter and a drain slope of 0.1% were selected because, although the design discharge rate is less than that of Alera, the drainable area is similar.

Collector drain and main drain

The open ditch D-XX-8 collects the water flowing from the field drains and debouches into the Valareña stream, which is the main drain of the irrigation sector.

The depth of the collector drain (> 2 m) is sufficient to allow a safety margin (> 30 m) between the lateral outlets and the water level in the ditch.

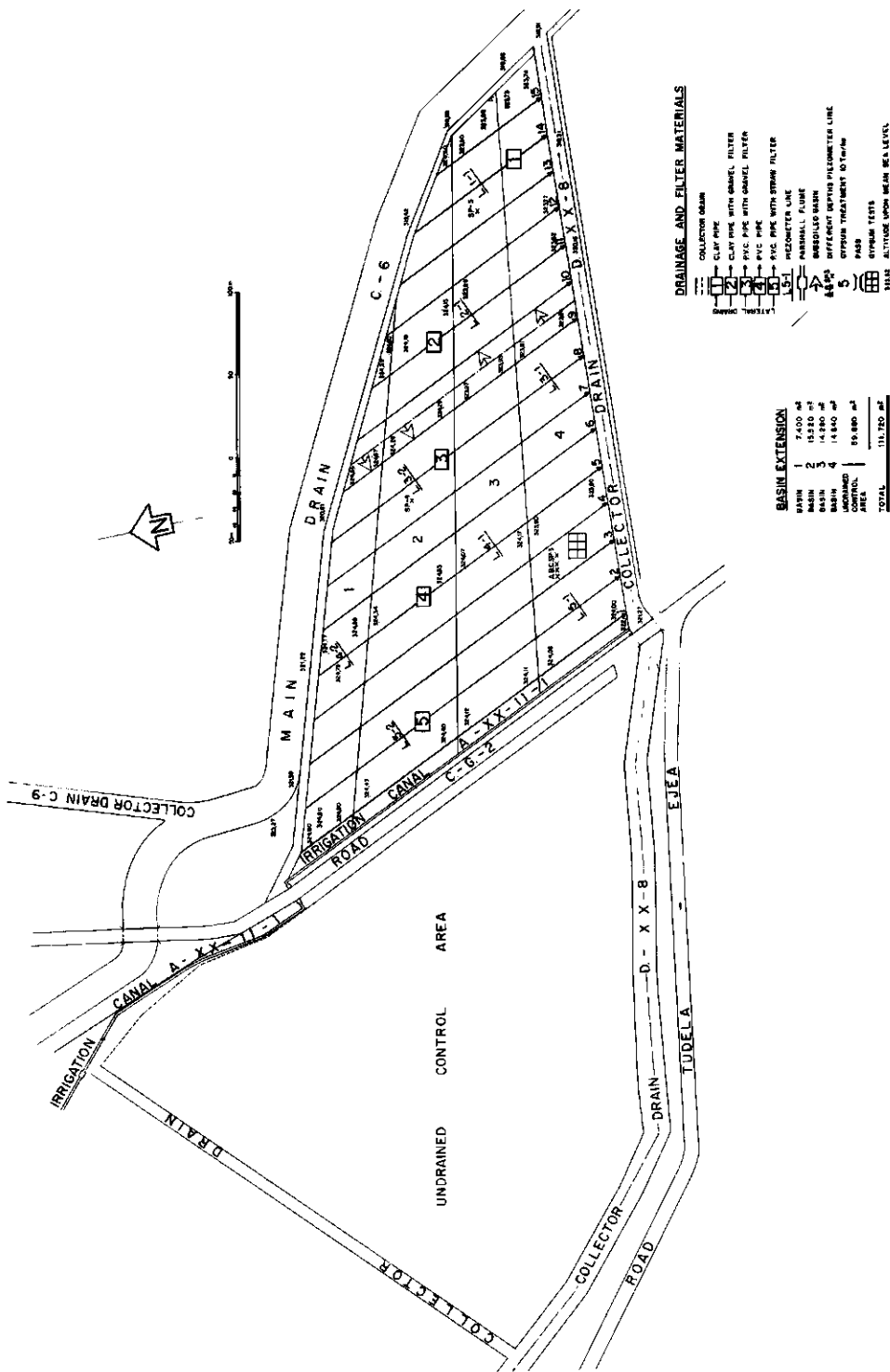


Fig. 7.14: Layout of Valareña experimental field.

7.2 Design of the irrigation system

Since the Bardenas area was planned to be irrigated by gravity flow, the same irrigation method was used in the design of the two experimental fields, though sprinkler irrigation would have offered some advantages due to better control of irrigation applications.

The method chosen for the initial leaching process was intermittent basin irrigation. Once the desalinization process had been completed, barley and wheat could be irrigated by basin flooding, maize and sugar beet by furrow irrigation, and lucerne by borderstrip irrigation.

7.2.1 Alera experimental field

The irrigation system consists of an existing rectangular concrete irrigation canal, A-IX-4-2. Its total height is 0.40 m and its bed width 0.50 m. The discharge capacity of the canal is 50 l/s. It has four outlets for basins 1 to 4 and ends in a tail escape into the main drain (Fig.7.6).

A new irrigation canal was designed to irrigate basins 5 to 8 (Fig.7.15). This canal, A-IX-4-2-1, was calculated with the Manning equation (Eq.9):

$$Q = K_M A R^{2/3} S^{1/2} \quad (9)$$

where

- Q = discharge (m^3/s)
- K_M = Manning coefficient ($m^{1/3}/s$)
- A = cross sectional area (m^2)
- R = hydraulic mean depth (= area/wetted perimeter, m)
- S = bed slope
- $AR^{2/3}$ = section factor ($m^{8/3}$)

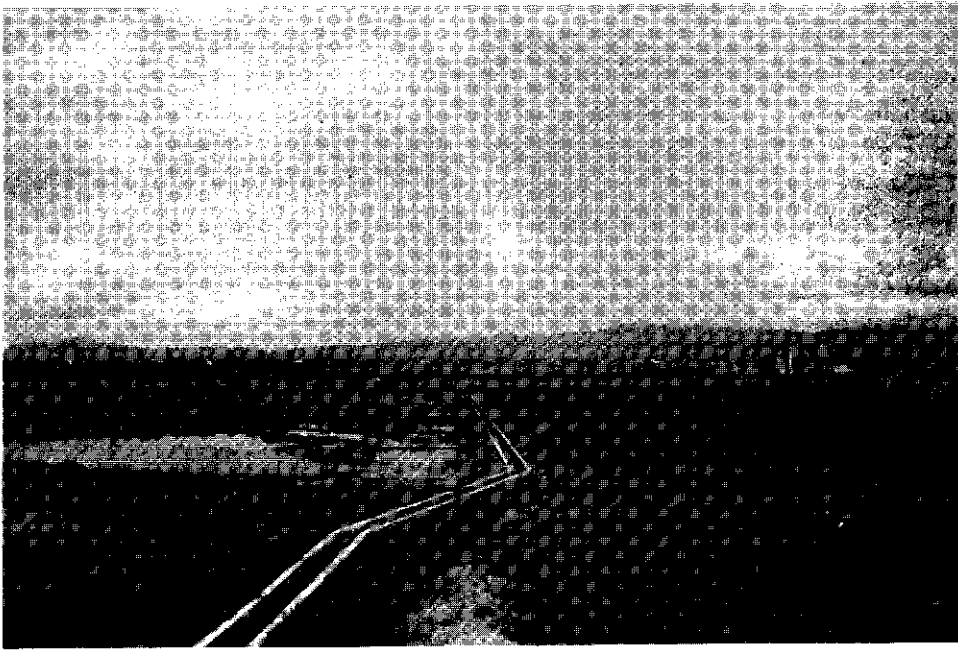


Fig.7.15: Irrigation canal. Alera experimental field.

If for a rectangular concrete canal a coefficient $K_M = 66.7 \text{ m}^{1/3}/\text{s}$ is assumed and the design bed slope is 0.1%, a section factor $AR^{2/3} = 0.024 \text{ m}^{8/3}$ will be sufficient for a discharge capacity $Q = 50 \text{ l/s}$. A rectangular canal with a bed width of 0.5 m and a design water height of 0.25 m has a section factor of $0.03 \text{ m}^{8/3}$, which is greater than required. With a freeboard of 0.15 m, a canal bank equal to 0.4 m is adequate.

This irrigation canal debouches into the collector drain, D-IX-3-2, through a concrete tail escape to a stilling basin at the level of the ditch bed.

The distributary canal outlets have a metal weir with a concrete bed protection downstream of the bed.

For the initial leaching, the land was graded with an almost zero slope. The largest irrigation basins cover an area of 1.5 ha (length = 300 m, width = 50 m. Two transversal checks divide the basins into three smaller ones 0.5 ha) for better water distribution.

In addition, an observation well was installed midway between two drains (10 m) to determine the fluctuation of the watertable and to check the piezometer readings of the tubes placed at that site.

Three extra piezometer lines were installed with tubes at different depths to determine the hydraulic heads of any aquifers affecting the drainage system (Fig.7.18).



Fig.7.17: Piezometer tube on a clay drain.

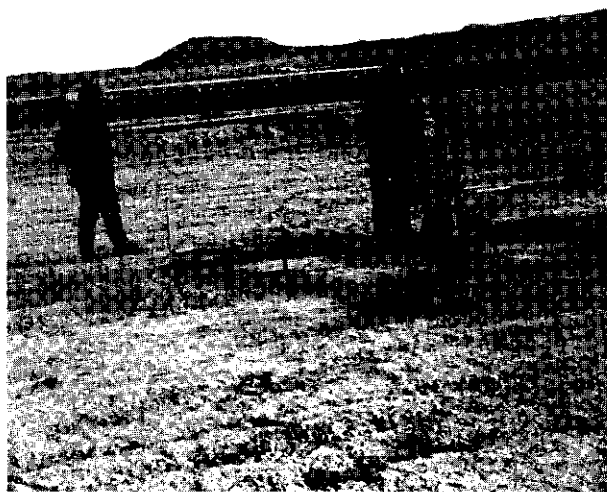


Fig.7.18: Installation of a piezometer line with tubes placed at different depths.

At the Alera field the inlets of these piezometers were at the following depths: 1.5 m (drain level), 2.5 m (less pervious layer), 3.5 m (on the impervious layer)), and 5 m (below the impervious layer).

At the Valareña field the inlet depths were: 1.5 m (drain level), 2.5 m (fine stratified layer), 3.5 m (gravel layer), and 5 m (below the impervious layer).

The piezometers are iron tubes with an internal diameter of 3 cm; their lower 10 cm is perforated (Fig.7.19).

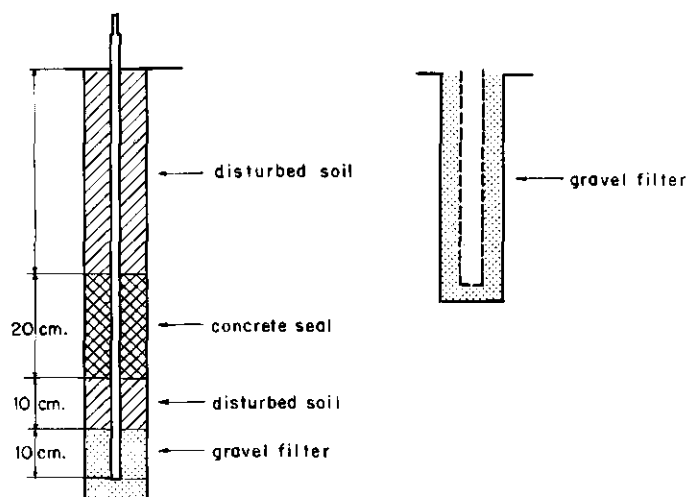


Fig.7.19: Sketch of piezometer and observation well.

Drain discharge

Discharges were measured by hand readings with a 5 l bucket in periods of high discharge and with a 1 l bucket when discharges were lower.

Irrigation flow measurement

The irrigation flow was measured with a metal Parshall flume placed in the irrigation canal (Fig.7.20). The maximum free-flow capacity of the flume was 80 l/s; it had a throat section $W = 15$ cm and a total height $E = 45$ cm.



Fig.7.20: Parshall flume for irrigation flow measurement.

Soil sample analysis

Once the initial salinity status of the surface soil was known, 7 sites with different salt content were selected at Alera and 11 at Valareña to determine the variation of the soil salinity during the leaching process.

At each site soil samples were taken in the following manner. In a square 9 m^2 in extent 9 auger holes were made. For the upper 25 cm, a soil sample was taken by mixing the soil of all the 9 holes. For the 25-50 cm and 50-100 cm layers, soil samples were taken by mixing the soil of 5 holes; 5 holes were considered sufficient because the variation of salinity was less in the deeper layers than in the surface soil.

Of the selected soil samples the salt content of the saturated paste was periodically determined in terms of electric conductivity (EC_e), percentage of chlorides, Na^+ , Ca^{++} , and Mg^{++} contents, and pH.

Afterwards the field salinity was monitored with soil resistance measurements (EC-probe and four-electrode equipment set up in the Wenner arrangement).

Gypsum treatments

To find out whether gypsum improved the surface soil structure and consequently increased the infiltration rate, gypsum tests were conducted on small plots (12 m^2) where amounts of 5 and 10 t/ha were applied.

Meteorological station

Daily data on rainfall, temperature, and evaporation were collected at the Oliva Abbey meteorological station. As this station is 10 km from the Alera experimental field a rainfall gauge was installed at Alera to obtain the local rainfall figures.

At Valareña daily data on rainfall and temperature were collected at the station located there.

Unfortunately it was not possible to obtain an anemometer, hygrometer, and solarimeter in time to allow the calculation of evapotranspiration by the Penman method.

7.5 Field observation programme

Daily readings were made of piezometric levels, drain discharges, and meteorological data. As drain systems with a length of 250 m have two piezometer lines, each line was read every second day.

To observe the rate of groundwater rise during irrigation applications and the reaction of the drainage system to an instantaneous recharge, the piezometer lines and drain discharges were measured two or three times a day in such periods.

In addition, the infiltration rate during irrigation applications was measured with simple rings placed at several points in each basin and in the gypsum test areas.

During the initial leaching process soil samples were taken after each intermittent leaching phase, just before the next irrigation was due and when the soil was sufficiently dry to allow good mixing. Once the leaching process had been completed the soil sampling was done seasonally.

8. Derivation of agro-hydrological factors

8.1 Groundwater flow conditions

The conditions under which the groundwater flows towards the drains were determined by daily measurements of the water table and of the drain discharge. Since these conditions differed in the two experimental fields, they were analysed separately.

8.1.1 Alera experimental field

The groundwater flow was studied in the clay tile drains with gravel cover (Drain Groups 2 and 8). These drains produced the clearest data because they had the lowest entrance resistance and consequently gave the best drainage performance.

Hydrographs of drain discharge (s in mm/day) and hydraulic head midway between drains (h in m) were drawn for several separate periods. From this fairly extensive material a selection has been made to illustrate groundwater flow conditions. Figure 8.1 refers to Drain Group 2 in January-February 1975 during which a leaching application and rainfall recharged the groundwater. Figure 8.2 refers to the same drain group in July-August 1975. The analysis was repeated for another part of the field (Drain Group 8) in January-March 1976, when the groundwater was recharged by heavy rainfall after a leaching application (Fig. 8.3).

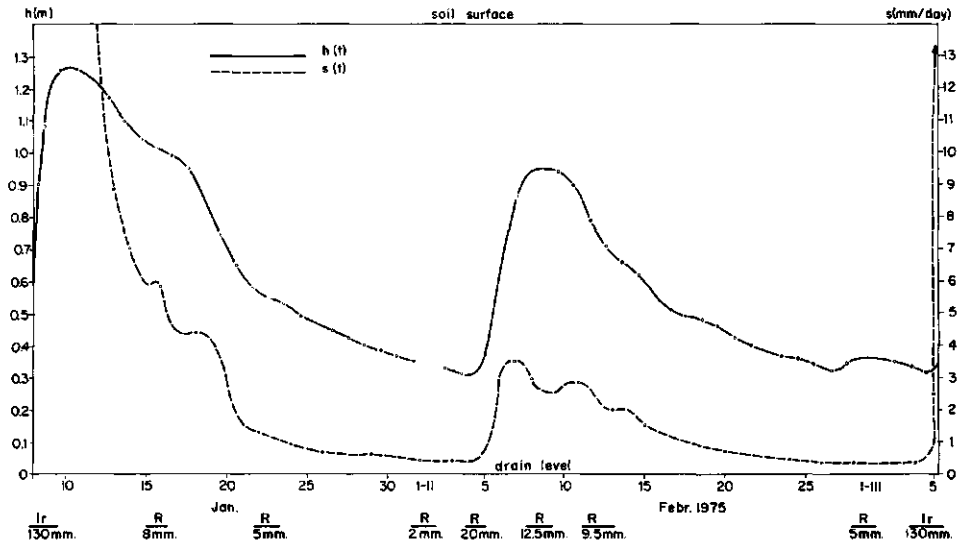


Fig. 8.1: $h(t)$ and $s(t)$ hydrographs after a leaching application and subsequent rainfall in winter (Drain Group 2, clay/gravel, January-February 1975. Alera experimental field).

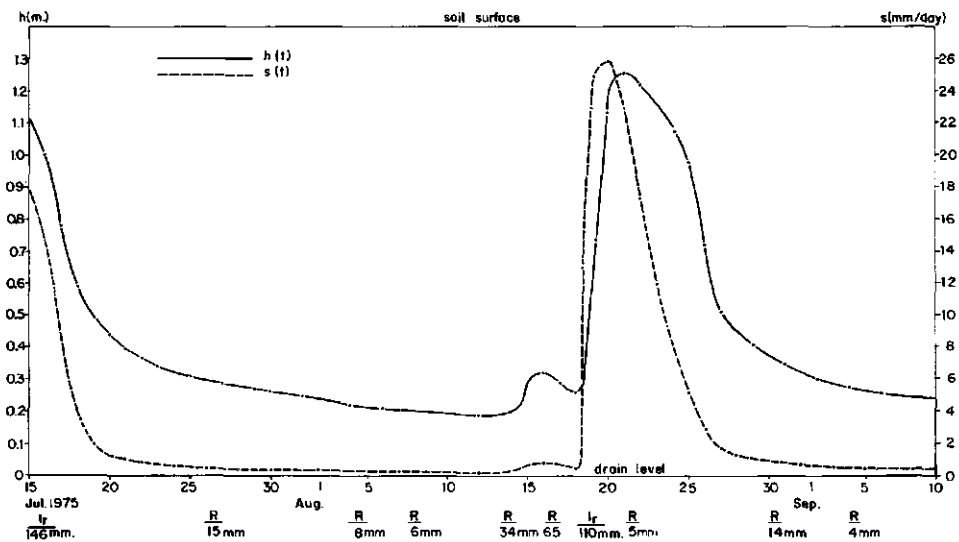


Fig. 8.2: $h(t)$ and $s(t)$ hydrographs after a leaching application in summer (Drain Group 2, clay/gravel, July-August 1975. Alera experimental field).

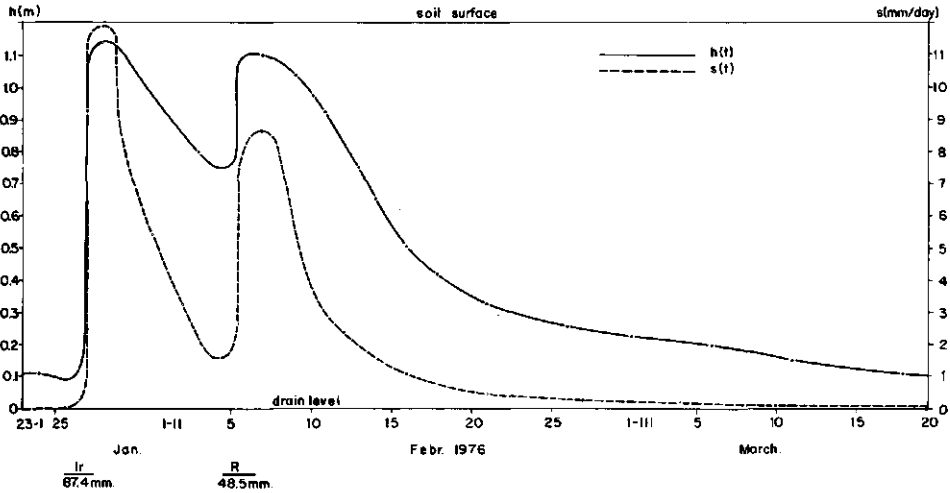


Fig. 8.3: $h(t)$ and $s(t)$ hydrographs after a leaching application in winter, followed by rainfall (Drain Group 8, clay/gravel, January-March 1976. Alera experimental field).

The hydrographs demonstrate that unsteady groundwater flow prevailed.

In periods without recharge, the water table remained slightly above drain level ($h = 0.1$ to 0.2 m). When recharge occurred after leaching or heavy rainfall, it caused an instantaneous rise of the water table. After leaching applications of 100 to 150 mm, the water table rose to within 10 cm of the soil surface ($h = 1.1$ to 1.3 m) and remained there for 1 or 2 days as long as the recharge equalled or exceeded the drain discharge. After the recharge ceased, the water table gradually fell, and at the end of tail recession conditions resembled steady flow. In reality, however, the flow was unsteady since both drain discharge and hydraulic head continued to decrease with time.

A similar pattern appears in the discharge hydrographs. Immediately after an instantaneous rise of the water table, the drain discharge changed from about 0.1 or 0.2 mm/day at conditions approximate to steady-state flow to about 25 mm/day. As long as infiltration continued, this heavy discharge

would last (usually for 3 or 4 days), after which it decreased gradually until it reached its minimum rate at the end of tail recession.

After the initial leaching period had ended, the fluctuation of the water table and the discharge were studied under normal irrigation in summer. Figure 8.4 shows the hydraulic head and discharge hydrographs for August-September 1976. The amounts of irrigation water varied from 85 to 100 mm and were applied at an average interval of 14 days. Percolation losses from 30 to 35 mm are normal with surface irrigation, which means a field application efficiency e_a of 0.7 (see Chap.9). These water losses caused the water table to rise to about 50 cm below the soil surface, at which time the discharge was about 15 mm/day, decreasing to 0.5 mm/day at the end of tail recession.

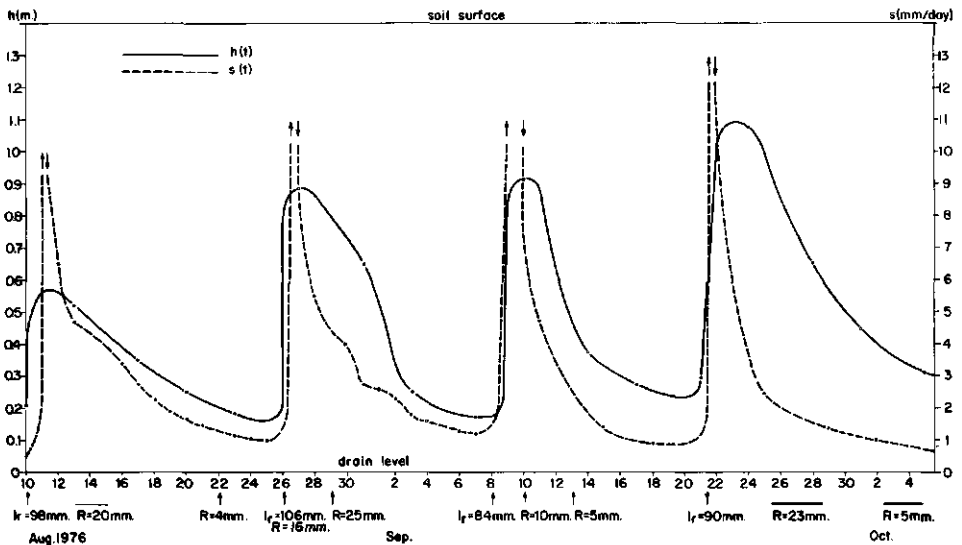


Fig. 8.4: $h(t)$ and $s(t)$ hydrographs during the irrigation of sugar beet (Drain Group 2, clay/gravel, August-September 1976. Alera experimental field).

Table 8.1 summarizes water table depths, hydraulic heads, and discharges during the initial desalinization process and subsequent irrigation seasons. This table is based on a greater amount of data than shown in Figs. 8.1 to 8.4 and covers the whole observation period.

TABLE 8.1 Water table depth, hydraulic head, and discharge. Alera experimental field

Process	Water table depth		Unsteady state				Steady state		
	initial	final	h_o	h_t	t	s	h	s	
	m	m	m	m	days	mm/day	m	mm/day	
Initial leaching	0.1	0.3	1.3	1.1	3	25 ¹	7 ²	-	-
	0.3	0.5	1.1	0.9	2-4	8	4	-	-
	0.5	0.7	0.9	0.7	1-2	6	3	-	-
	0.7	1.0	0.7	0.4	3-9	3	0.5	-	-
	1.0	1.1	0.4	0.3	6	0.5	0.2	0.3	0.4
Irrigation of sugar beet	1.1	1.2	0.3	0.2	6	<0.2	-	0.2	0.2
	0.5	0.7	0.9	0.7	2	15	4	-	-
	0.7	1.0	0.7	0.4	2	4	2	-	-
	1.0	1.2	0.4	0.2	8	2	0.8	-	-

¹ initial ² final

8.1.2 Valareña experimental field

At Valareña the actual flow pattern differed from the assumptions made in the theoretical design of the drainage system (Chap.7). In reality, the water flows toward the drains horizontally over a shallow impervious layer (Fig.8.5).

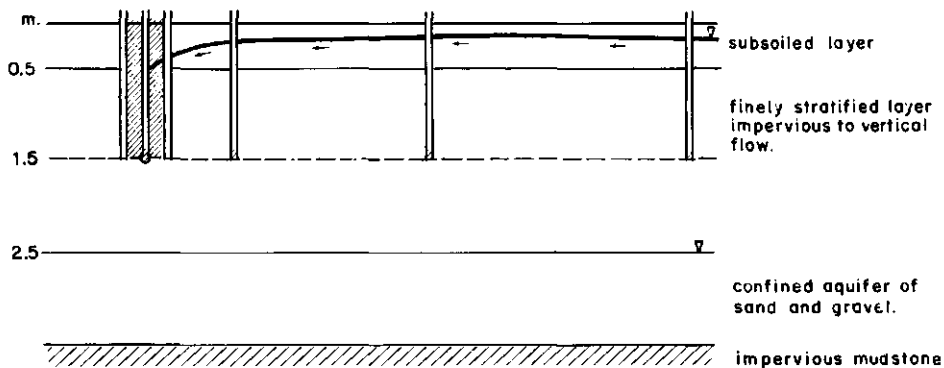


Fig.8.5: Groundwater flow conditions at Valareña experimental field.

The hydraulic conductivity of the stratified silty clay layers is anisotropic. Measured by the inversed auger hole method (Chap.6), their hydraulic conductivity for vertical flow is much lower than that for horizontal flow. This was confirmed in laboratory measurements with undisturbed soil cores. Water movement through the finely stratified layers can thus be neglected and the abundant soil pores observed in the soil survey are obviously discontinuous.

As the impervious stratified barrier is at a depth of 50 cm, the water flows directly into the drain trench through the upper soil layer where the stratification has been broken up by subsoiling and levelling operations. The pervious soil profile is therefore restricted to the upper 50 cm. This restriction causes part of the irrigation water to flow horizontally over the soil surface toward the open collector drains.

Obviously, there is no deep percolation of water. In fact, the piezometers rarely showed any recharge of the groundwater. Most of them remained dry during the entire leaching process. Others indicated low water levels (from 1.2 to 1.4 m below soil surface) which presumably owe their existence to some leakage of surface water through the concrete seal. Minor fluctuations of the water level were observed in a few piezometers.

The actual hydrological conditions are thus those of a shallow ephemeral perched water table which is never in contact with the deeper gravel and sand aquifer which, in its turn, is confined by the overlying stratified layers.

The drain discharge reflected similar conditions, with water flowing through the drains only during irrigations. Afterwards the discharge decreased rapidly and within 4 or 5 days the drains were dry. Another indication that the irrigation water flowed directly into the drains was the low salt concentration of the drainage water.

8.2 Drainage equations

8.2.1 Steady flow

Although, in reality, steady flow did not occur at the Alera experimental field, the fluctuation of the water table and the variation of the drain discharge were so small at the end of tail recession (Table 8.1 and Figs. 8.1 to 8.3) that in these short periods steady flow can be assumed.

The hydraulic conductivity decreases with depth (Chap.6) but a constant K-value can be assumed at small heads ($h = 0.2$ to 0.3 m).

Under these conditions the Hooghoudt theory (1940) can be used. The discharge is then given by the following equation:

$$s = \frac{8 K_b d}{L^2} h + \frac{4 K_a}{L^2} h^2 \quad (1)$$

where

- s = discharge per unit area (m/day)
- L = drain spacing (m)
- K_a = hydraulic conductivity above drain level (m/day)
- K_b = hydraulic conductivity below drain level (m/day)
- d = equivalent thickness of aquifer below drain level (m)
- h = hydraulic head midway between two drains (m)

From the discharge and hydraulic head hydrographs of the Alera field a discharge-head relation was obtained (Fig. 8.6). This curve is parabolic, which shows that the discharge-head relation is not linear but quadratic and means that the term h^2 of Eq.(1) is more important than the term h. Consequently, the greater part of the water flows above drain level, which

indicates that the drains were placed above or near the impervious layer ($4 K_a \gg 8 K_b d$).

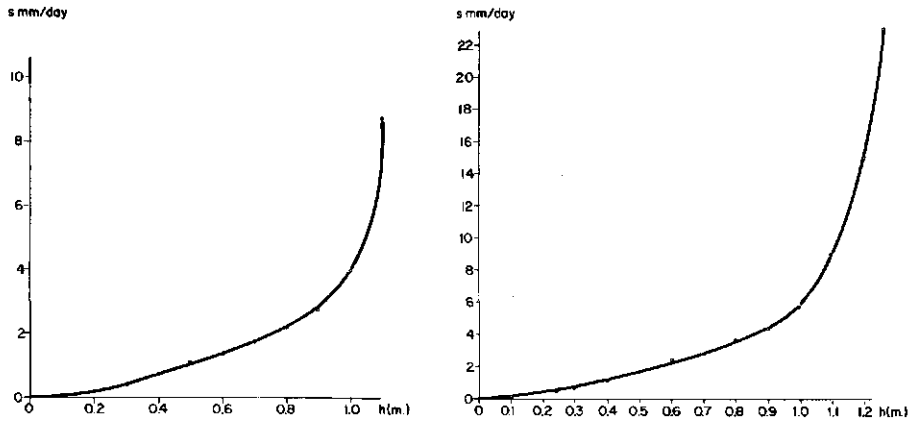


Fig. 8.6: *s-h* relation (Drain Group 8 clay/gravel, February-March 1976 and Drain Group 2, clay/gravel, August-September 1975. Alera experimental field).

8.2.2 Unsteady flow

Alera experimental field

The theory of Kraijenhoff van de Leur (1958), being based on a gradual rise of the water table due to a steady recharge until steady-state conditions are reached, could not be used because the water table rose instantaneously.

The theory of Glover-Dumm (1954) seemed more appropriate because it describes the fall of the water table after an instantaneous rise due to recharge from heavy rainfall or percolation losses of irrigation water in an aquifer of almost constant thickness (D).

The Glover-Dumm equation for the hydraulic head midway between two

drains in relation to drain level reads:

$$h(L/2, t) = \frac{4 h_o}{\pi} \sum_{1,3,5,\dots}^{\infty} (-1)^{\frac{n-1}{2}} \frac{1}{n} e^{-n^2 t/j} \quad (2)$$

where j is the reservoir coefficient (days)

$$j = \frac{\mu L^2}{\pi^2 K D} \quad (3)$$

where

- KD = transmissivity of the aquifer (m^2/day)
- μ = drainable pore space
- t = time (days)
- h = hydraulic head midway between two drains as a function of t (m)
- h_o = hydraulic head of the initial horizontal water table (m)

During tail recession, the second and following terms of Eq.(2) can be neglected as their values are comparatively small. Equation (2) then reduces to:

$$h = \frac{4 h_o}{\pi} e^{-t/j} = 1.27 h_o e^{-t/j} \quad (4)$$

In a later publication, Dumm (1960) assumed that the initial water table is shaped like a fourth-degree parabola. If so, Eq.(4) changes to:

$$h = \frac{192}{\pi^5} h_o (\pi^2 - 8) e^{-t/j} = 1.17 h_o e^{-t/j} \quad (5)$$

The general equation for the discharge per unit area is:

$$s = \frac{8 K D h_o}{L^2} \sum_{1,3,5,\dots}^{\infty} e^{-n^2 t/j} \quad (6)$$

which can be simplified if terms of higher order are neglected:

$$s = \frac{8 KD h_o}{L^2} e^{-t/j} \quad (7)$$

During tail recession the hydraulic head and discharge for times t_1 and t_2 are

$$h_1 = 1.17 h_o e^{-t_1/j}, \quad h_2 = 1.17 h_o e^{-t_2/j}$$

$$s_1 = \frac{8 KD h_o}{L^2} e^{-t_1/h}, \quad s_2 = \frac{8 KD h_o}{L^2} e^{-t_2/j}$$

or

$$h_2 = h_1 e^{-(t_2 - t_1)/j} \quad (8a)$$

$$s_2 = s_1 e^{-(t_2 - t_1)/j} \quad (8b)$$

From Eq. (8) the reservoir coefficient can be expressed as:

$$\frac{1}{j} = 2.3 \frac{\log h_1 - \log h_2}{t_2 - t_1} = 2.3 \frac{\log s_1 - \log s_2}{t_2 - t_1} \quad (9)$$

If the discharge and hydraulic head hydrographs are drawn on semi-logarithmic paper, two straight parallel lines must be obtained, making an angle α with the horizontal axis with

$$\tan \alpha = \frac{\log h_1 - \log h_2}{t_2 - t_1} = \frac{\log s_1 - \log s_2}{t_2 - t_1}$$

and the reservoir coefficient

$$j = \frac{1}{2.3 \tan \alpha}$$

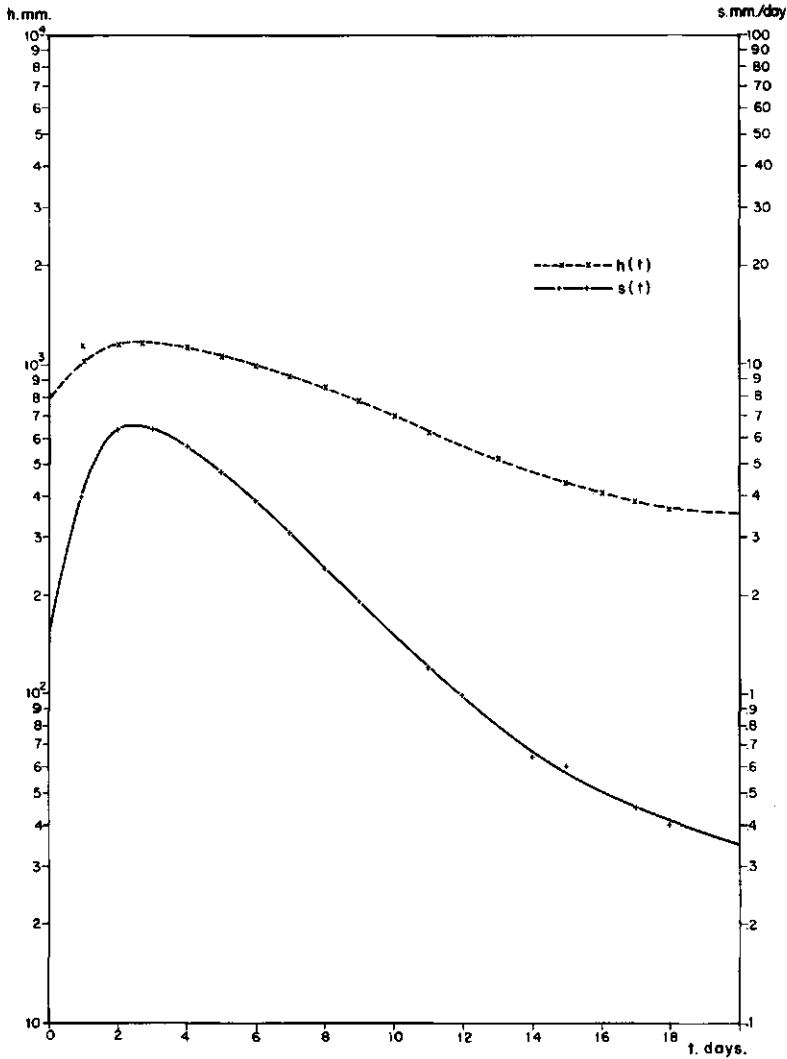


Fig. 8.7: $h(t)$ and $s(t)$ hydrographs showing the inadequacy of Glover-Dumm theory for the Alera groundwater flow conditions.

Figure 8.7 shows a plot of the hydraulic head and discharge of Fig. 8.3 on semi-logarithmic paper. The lines obtained during tail recession are not parallel. This means that the flow above drain level is much greater than that below and that the thickness of the drainable profile (D) is far from constant. It also means that the conditions for which the Glover-Dumm equation were derived are not fulfilled.

The Boussinesq equation could then be applied to solve the drainage problem.

To analyse the groundwater flow conditions during the winter period

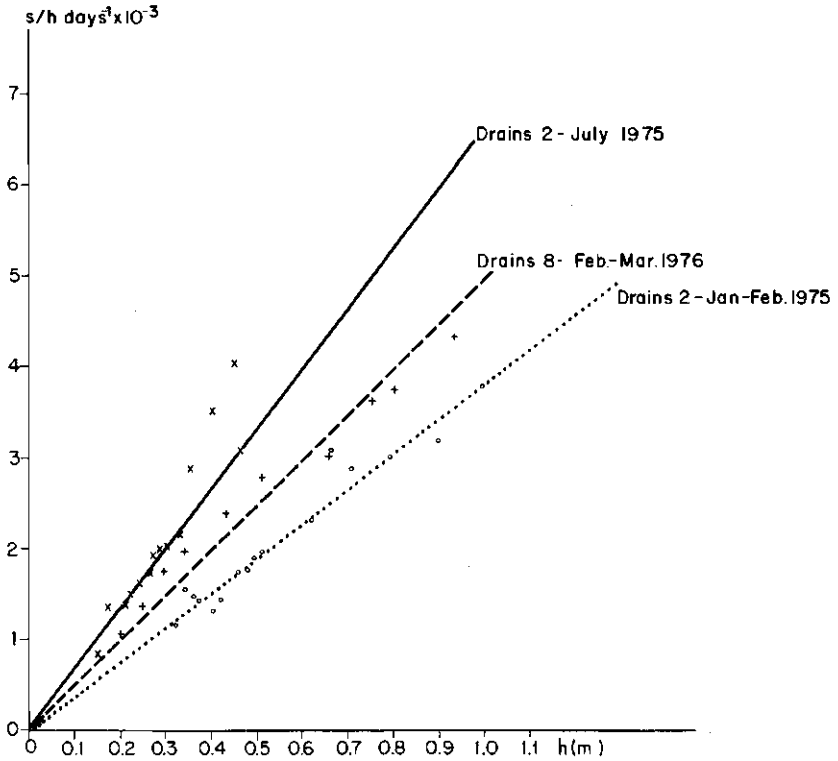


Fig. 8.11: Calculation of the K-values from the $s/h-h$ relation (Boussinesq equation).

By the method of linear regression, using discharge rates and hydraulic heads observed in the clay tile drains with gravel cover (Drain Groups 2 and 8), the straight lines $s/h = f(h)$ were calculated (Fig. 8.11). From these straight lines, K-values were obtained (Table 8.3).

In general the values agreed reasonably well and enabled a mean hydraulic conductivity of 0.6 m/day to be derived.

Table 8.3 shows that the calculated K-value (0.76 m/day) is higher than the average value when the water table is deeper than 0.80 m. The explanation for this may be that if h is small, the flow below drain level could be relatively important. If so, the calculated hydraulic conductivity above drain level will be higher than the actual value.

TABLE 8.3 K-values derived from the s/h-h relation, according to Eq.(15)

Period	No. of drain group	Drawdown of water table	Drain depth	Correlation coefficient	tan α	K m/day
	(clay/gravel)	m	m	s/h-h		
Jan.-Febr. '75	2	0.50 - 1.10	1.4	0.96	3.78×10^{-3}	0.44
July '75	2	0.90 - 1.20	1.4	0.96	6.40×10^{-3}	0.74
August '76	2	0.50 - 1.20	1.4	0.97	7.59×10^{-3}	0.88
Jan.-Febr. '77	2	0.80 - 1.20	1.4	0.97	6.70×10^{-3}	0.77
February '76	8	0.30 - 1.10	1.2	0.96	4.05×10^{-3}	0.47
July - Aug. '76	8	0.10 - 1.10	1.2	0.91	8.67×10^{-3}	1.00
Jan.-Febr. '77	8	0.60 - 1.10	1.2	0.97	3.81×10^{-3}	0.44
June - July '77	8	0.50 - 1.00	1.2	0.94	4.80×10^{-3}	0.55

The hydraulic conductivity of the surface layer (0-50 cm) is higher than the average value because a higher value is calculated when a shallow water table occurs. The hydraulic conductivity of the surface layer can vary from 1 to 1.5 m/day. This reflects the better development of structure in the surface layers.

Second method

Equation (10) expresses the hydraulic head midway between two drains (h_t) as a function of time (t). With this equation theoretical h_t -curves can be calculated for several K-values. By comparing the theoretical curves with the tail recession curve obtained from the piezometer readings, the actual hydraulic conductivity value can be found.

Several hydraulic head hydrographs were drawn for periods in which the initial hydraulic heads midway between drains (h_0) differed. The actual curve was compared with theoretical curves derived for several hydraulic conductivity values. Figure 8.12 shows the fall of the water table in Drain Group 2 during January-February 1975; Fig.8.13 shows that in Drain Group 8 during February-March 1976.

The average K-value determined during three consecutive winters (0.6 m/day) did not agree with that obtained for the summer periods (1.1 m/day). The first value agrees well with the average value (0.6 m/day) obtained from Table 8.3.

The higher K-values in summer may be explained by capillary rise in the intervals between water applications. This causes the water table to fall more rapidly and as a consequence the calculated hydraulic conductivity appears to be higher than it actually is (Figs.8.15 and 8.16).

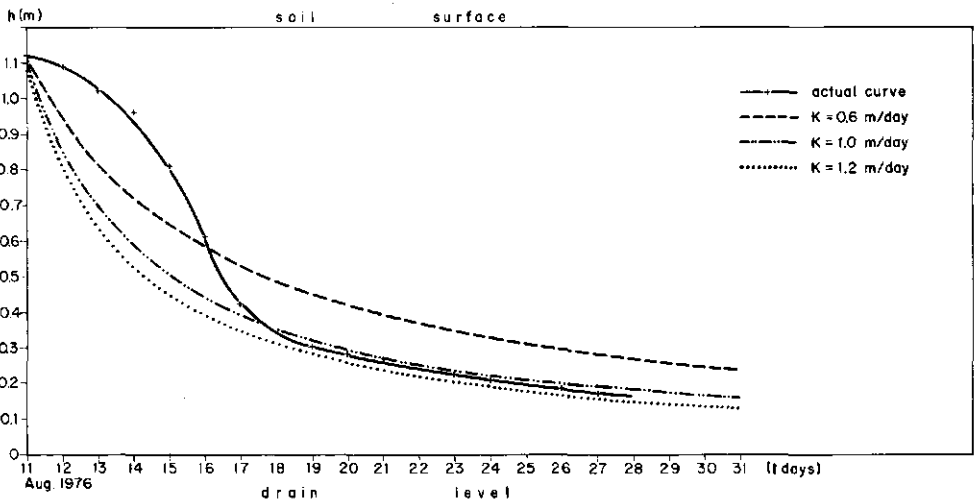


Fig. 8.15: Calculation of the K-values with the $h(t)$ function (Boussinesq equation) in a period of high evapotranspiration (Drain Group 8, clay/gravel, August 1976).

The use of this (second) method for calculating the hydraulic conductivity is limited to periods of low evapotranspiration. Moreover, the drainable pore space must be fairly constant, because otherwise discontinuities appear in the hydraulic head hydrograph when the falling water table passes through a layer of different porosity (Fig.8.17).

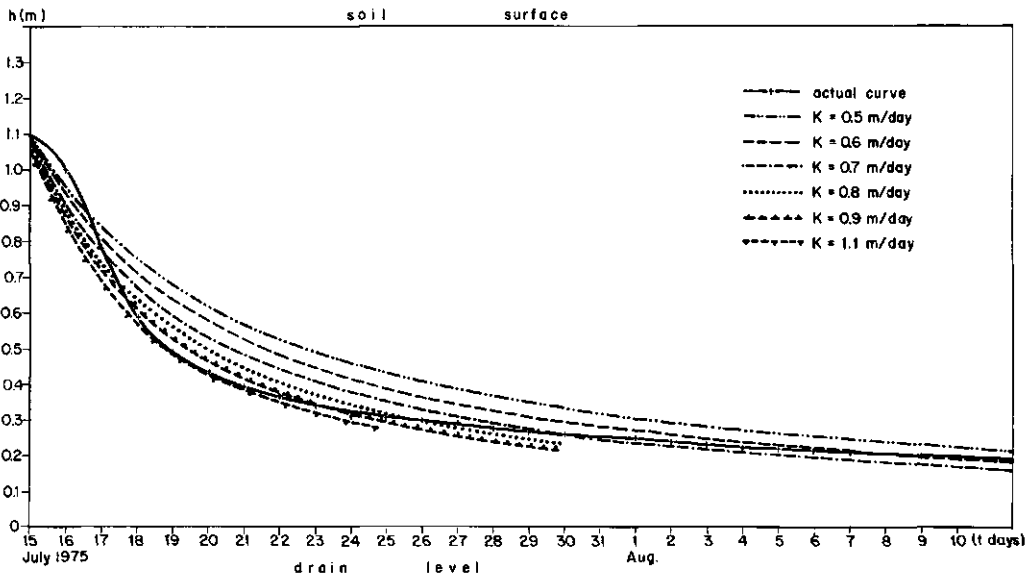


Fig. 8.16: Calculation of the K -values with the $h(t)$ function (Boussinesq equation) in a period of high evapotranspiration (Drain Group 2, clay/gravel, July-August 1975).

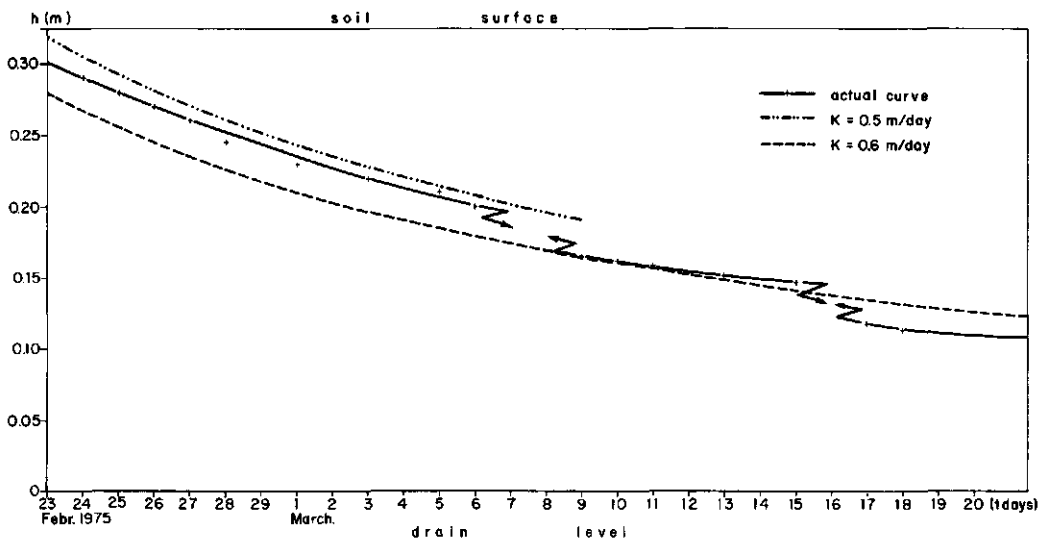


Fig. 8.17: Influence of the μ -value on the calculation of the K -values with the $h(t)$ function (Boussinesq equation).

Third method

The discharge hydrograph was compared with theoretical discharge curves calculated from Eq.(11) for various hydraulic conductivity values.

From the h_t -hydrographs the corresponding theoretical s_t -hydrographs were derived. For the same K -value of 0.6 m/day obtained from the hydraulic head hydrograph (Fig.8.13) and for a depth between 0.9 m and 1.2 m (Fig.8.18), the actual discharge curve of Drain Group 8 (clay/gravel) fits well with the theoretical one. Above 0.9 m the actual discharge is higher than the calculated value. This is because the shape of the water table differs from that assumed by Boussinesq until after the upper part of the saturated soil beside the drain trench is drained (Fig.8.14). Below a depth of 1.2 m the discharge curve is discontinuous at the end of tail recession, probably due to a difference between the drainable pore space of the silty loam layer and the value used in the calculations (Fig.8.19).

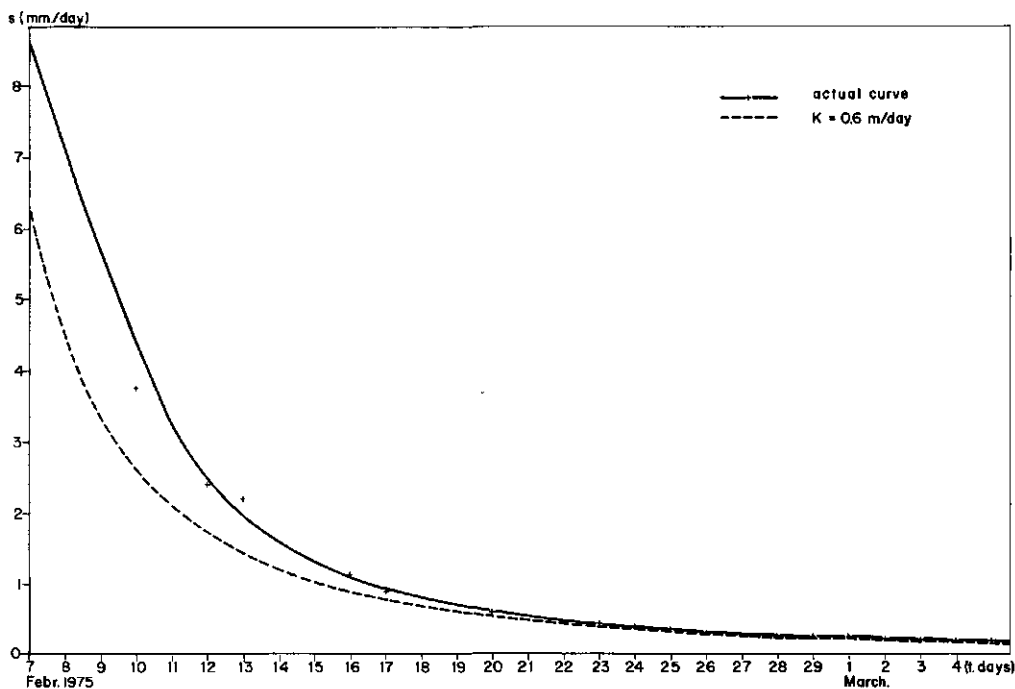


Fig.8.18: Calculation of the K -values from the $s(t)$ hydrograph (Boussinesq equation).

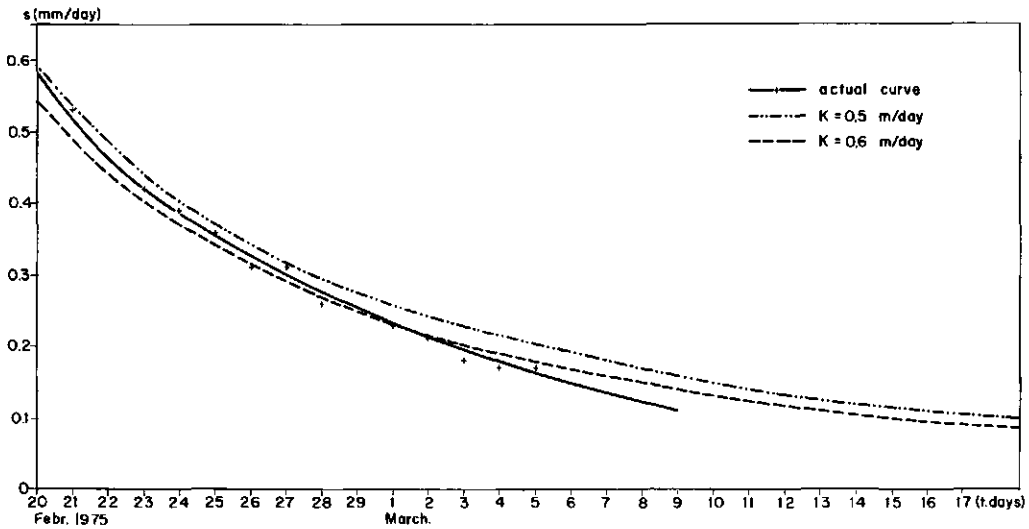


Fig.8.19: Influence of the μ -value on the calculation of the K-values from the $s(t)$ hydrographs (Boussinesq equation).

For Drain Group 2 (clay/gravel) the actual discharge curve is parallel to, but higher than, the theoretical one calculated for the K-value of 0.33 m/day obtained from the h_t -function (Fig.8.12). The difference of 0.15 mm/day (Fig.8.20) is probably due to seepage.

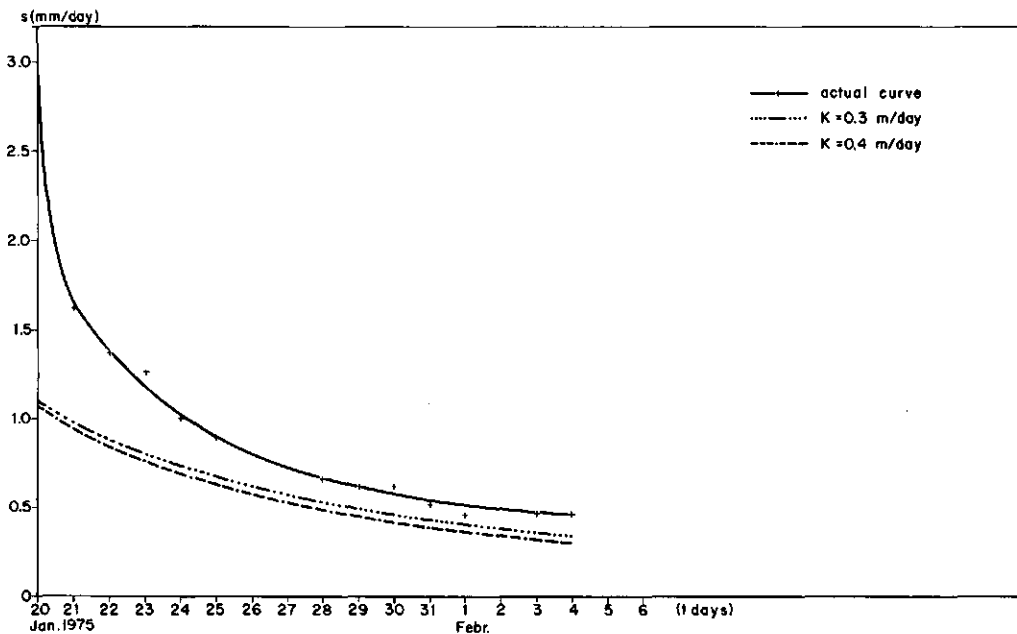


Fig.8.20: $s(t)$ hydrograph showing the existence of a local, low amount of seepage (Drain Group 2, clay/gravel, January-February 1975).

8.4.2 Steady flow: Hooghoudt equation

As explained in Section 1.1, steady flow does not, in reality, occur. At the end of tail recession, however, because of a small amount of seepage, the flow of some drains (Group 2) approximates steady flow.

In such periods, i.e. when the fluctuation of the groundwater table is small and the discharge is almost constant, the Hooghoudt equation can be used to derive the hydraulic conductivity.

As the thickness of the aquifer below drain level can be neglected, the Hooghoudt equation (1) can be simplified to

$$s = \frac{4 Kh^2}{L^2} \quad (16)$$

This equation is similar to the Boussinesq expression for the discharge (Eq. 11). Solving Eq.(16) for K yields:

$$K = \frac{s L^2}{4 h^2}$$

To determine the K-values during the desalinization process, several periods with almost steady-state conditions were selected. The results are given in Table 8.5 and can be compared with those determined with Eq.(11).

TABLE 8.5 K-values derived according to Eq.(16)

Period	No. of drain group	Depth of the layer m	h	s	K
			m	mm/day	m/day
3-4 Febr. '78	2 clay/gravel	1.10-1.40	0.33	0.37	0.35
7-8 July '75	2 clay/gravel	1.15-1.40	0.26	0.27	0.40
20-22 Jan. '76	2 clay/gravel	1.25-1.40	0.17	0.32	1.14 ¹
27-29 Febr. '76	2 clay/gravel	1.25-1.40	0.15	0.25	1.19 ¹
22-23 Aug. '76	2 clay/gravel	1.25-1.40	0.15	0.19	0.84 ¹

¹ Some contribution of flow below drain level

The analysis with the Hooghoudt equation confirms the results obtained with the equations for unsteady flow.

If the drains are not located exactly on the impervious layer but somewhat above it, the influence of the flow below drain level will show up in apparently higher K-values for the layer above drain depth. The higher the h-value used in the calculation, the lower the influence of flow below drain level and consequently the smaller the error.

8.4.3 Hydraulic conductivity of the less pervious layer

At the end of tail recession the piezometers placed at a depth of 3.5 m showed a higher water level than those placed at drain depth. This difference was observed in the three piezometer lines installed at the Alera field.

There is no clear explanation for this difference because below drain level the soil is uniformly compact silty clay down to the impervious mudstone and no pervious layers were detected. However, as a low discharge was observed at the end of tail recession, the hydraulic gradient must have caused an upward flow.

Various periods could therefore be selected in which the vertical hydraulic conductivity of the less pervious layer below drain level could be determined. Darcy's law can be applied to vertical flow:

$$v_z = K' \frac{\Delta h}{D'} = \frac{\Delta h}{c} \quad (17)$$

where

v_z = flow rate = discharge per unit area (m/day)

K' = hydraulic conductivity for vertical flow (m/day)

- Δh = hydraulic head difference between the 3.5 m deep layer and drain level (m)
- D' = thickness of the layer between 1.5 m and 3.5 m (m)
- c = D'/K' hydraulic resistance of the less pervious layer (days)

Table 8.6 shows the results obtained. The average K' -value of the less pervious layer is about 0.002 m/day, which is at least 10 times smaller than that of the overlying layer above drain level. The layer below 1.5 m can therefore be considered impervious for flow towards drains, thereby confirming the conclusions of the study of groundwater flow.

TABLE 8.6 K-values of the less pervious layer

Period	$h_{3.5}^1$ m	$h_{1.5}^1$ m	Δh m	D' m	s mm/day	c days	K' m/day
9-11 Dec. '75	2.68	2.38	0.30	2	0.40	750	0.003
23-24 Feb. '76	2.61	2.40	0.21	2	0.45	467	0.004
4-5 Mar. '76	2.59	2.38	0.21	2	0.20	1 050	0.002
24-27 Mar. '76	2.57	2.30	0.27	2	0.17	1 588	0.001

¹ Reference level = depth of the impervious mudstone (3.5 m)

To summarize, a value of 0.6 m/day can be used for the hydraulic conductivity of the soil profile between a depth of 0.5 m and drain level. Below drain level the soil is considered impervious. The permeability of the upper layer (0-50 cm) is about 1.5 m/day. Hence, if the water table is shallow after heavy rainfall or irrigation, a value of 1 m/day can be used for the hydraulic conductivity of the soil profile.

8.4.4 Comparison of the results obtained

During the experimental period the hydraulic conductivity for different depths of the groundwater table was measured by the auger hole method. The hydraulic conductivity above the water table was estimated by the inversed auger hole method. In addition, undisturbed soil cores were taken in horizontal and vertical directions to measure the hydraulic conductivity in the laboratory.

The object of these direct measurements of hydraulic conductivity was to compare field and laboratory methods in which only a small body of soil is measured, with large-scale field determinations that use the hydraulic head/discharge analysis. This comparison could be useful in drainage projects for which only direct measurements are available.

The average result obtained by the auger hole method (Table 8.7) was lower than that derived from the hydraulic head discharge analysis: 0.2 m/day versus 0.6 m/day.

TABLE 8.7 Hydraulic conductivity measured by the auger hole method

No. of drain group	Date	Water table depth	Depth of the hole	K
		m	m	m/day
1 clay	October '76	1.15 - 1.30	1.4	0.21
	February '77	0.80 - 1.10	1.4	0.13
	February '77	1.30 - 1.40	1.7	0.00
2 clay/gravel	October '76	1.30 - 1.50	1.7	0.12
	February '77	1.15 - 1.35	1.6	0.21
3 PVC/gravel	October '76	1.10 - 1.20	1.4	0.29
	February '77	0.90 - 1.30	1.5	0.20
4 PVC	October '76	0.95 - 1.15	1.5	0.11
	February '77	0.40 - 0.80	1.2	0.05
	February '77	0.80 - 1.20	1.5	0.03
5 PVC/straw	October '76	0.65 - 0.80	1.3	0.15
	October '76	1.20 - 1.35	1.5	0.05
	February '77	0.20 - 0.40	1.0	0.11
	February '77	0.55 - 1.05	1.4	0.16
6 PVC/esp.	February '77	0.45 - 0.80	1.1	0.07
	February '77	0.70 - 1.15	1.4	0.07
7 PVC/coco	October '76	0.60 - 0.90	1.1	0.09
	February '77	0.50 - 0.75	1.2	0.11
	February '77	0.80 - 1.10	1.4	0.04
8 clay/gravel	February '77	0.80 - 1.00	1.5	0.18

Table 8.7 shows that the K-values measured in fields where the drains function properly, are generally higher than those measured in fields whose drains have a high entrance resistance and where the water table seldom drops below 1 m.

No satisfactory results were obtained with the inversed auger hole method used above the water table, since hardly any fall of water level was observed in the "pour-in holes". Augering in these silty clay soils may have sealed the soil pores.

The results obtained by laboratory measurements in undisturbed soil cores (Table 8.8) show a greater variability and are even lower than those measured by the auger hole method. Nevertheless, they reveal that the soil is anisotropic, since the hydraulic conductivity in vertical direction is always higher than that in horizontal direction, probably due to the presence of root-holes and cracks. They also confirmed the decrease of hydraulic conductivity with depth.

TABLE 8.8 Laboratory determinations of the hydraulic conductivity in undisturbed soil cores

Depth m	Direction	K m/day
0 - 0.50	horizontal	0.004
	vertical	0.970
0 - 0.30	horizontal	0.040 ¹
	vertical	0.690
0.50 - 0.85	horizontal	0.015
	vertical	0.730
0.85 - 1.00	horizontal	0.001
	vertical	0.180
1.00 - 1.50	horizontal	0.001
	vertical	0.010
1.50 - 2.00	horizontal	0.001
	vertical	0.020

¹ after subsoiling

The conclusion could thus be drawn that once the order of hydraulic conductivity has been calculated from the experimental fields, the auger hole method can be used to estimate the hydraulic conductivity at a large number of sites for use in a later phase of large-scale drainage projects.

8.5 Determination of the entrance resistance

In the proximity of the drain the groundwater flow has to overcome an extra resistance because the drain pipes are not pervious over their entire surface; water enters only through the joints of the clay tile drains or through the perforations of the plastic pipes.

The entrance resistance can be expressed by the following equation (Engelund 1957, Cavelaars 1967):

$$W_e = \frac{h_i}{q} = \frac{h_i}{sL} \quad (18)$$

where

- q = discharge per unit length of drain (m^2/day)
- s = discharge per unit area (m/day)
- L = drain spacing (m)
- h_i = difference in hydraulic head between the drain trench and the tile (m)
- W_e = entrance resistance (day/m)

The entrance resistance is inversely proportional to the hydraulic conductivity of the soil in the proximity of the drain, or

$$W_e = \frac{a}{K} \quad (19)$$

where

- K = hydraulic conductivity of the medium (m/day)
a = factor depending on the type of drain pipe

Equation (18) can be used to calculate the entrance resistance if the head loss between the edge of the drain trench and the drain pipe, and its corresponding discharge, are known. The difference in hydraulic head was determined by two methods. The first consisted of a direct reading of the piezometers installed in the drain trench and on the drain itself; the second (indirect) method was by calculation once the position of the groundwater table was known.

8.5.1 Direct method of determining the W_e value

The direct method is based on the correlation between the discharge per unit length (sL) and the head loss between the edge of the drain trench and the drain (h_i).

The W_e -value must be equal to the slope of the straight line expressed by:

$$h_i = W_e (sL) \quad (20)$$

The values of h_i were plotted against the corresponding values of sL and the line through the points was calculated by linear regression. The slope of this straight line equals the entrance resistance W_e (Fig.8.21).

For each combination of drainage and filter materials, calculations were made seasonally. The observation period commenced in October 1974.

For each period analysed at least 20 pairs of observations were compared. These observations pertain to periods with a falling water table. A few determinations in which the correlation coefficient was less than 0.9 were ignored.

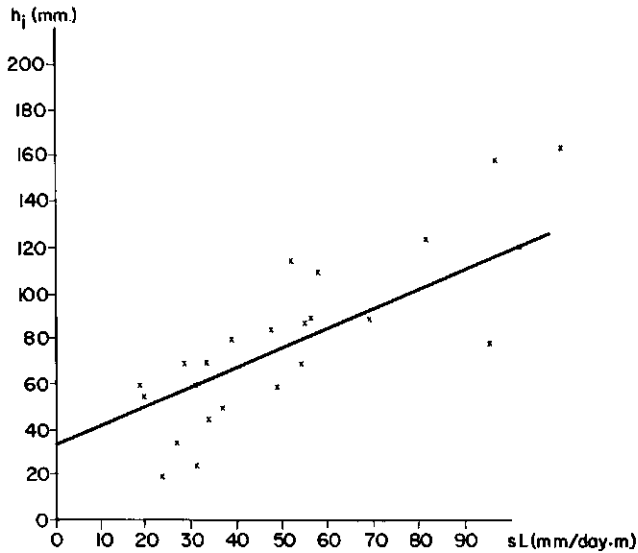


Fig.8.21: Calculation of the W_e -value with the direct method.

The head loss near the drain (h_i) was obtained from the difference between the readings in the piezometer installed 0.20 m from the drain and that on the drain itself (Fig.7.16).

An average value was taken for h_i from two observations made in piezometers placed at both sides of the drain. For drains with a length of 250 m an average value was adopted from readings in their two piezometer lines.

The expression for the regression lines obtained reads as follows:

$$h_i = W_e sL + a_0 \quad (21)$$

From a theoretical point of view, a_0 should equal zero because the hydraulic head should be zero when there is no discharge. Figure 8.21, however, shows that, when the drain discharge becomes zero, there is still a difference in hydraulic head between the piezometer 0.20 m from the drain and the piezometer on the drain.

The existence of this residual value a_0 may be due to two factors. One is that the drain is located in a less pervious layer, and the other is that the piezometer 0.20 m from the drain was not placed inside the trench but slightly outside it, thereby yielding a higher value for h_i (Fig.8.22).

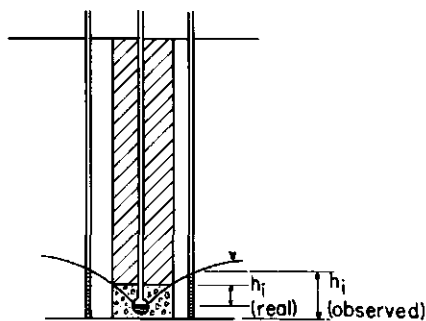


Fig.8.22: Difference between observed h_i and real h_i .

The W_e -values for successive periods are presented in Table 8.9 and concern all the combinations of drainage and filter materials except PVC pipes with straw cover (Drain Group 5), which did not function properly because the water flow inside the pipe was impeded.

Table 8.9 allows the conclusion that the entrance resistance remained fairly constant during the period under analysis. Nevertheless, the increase in entrance resistance (Fig.8.23) for the combination PVC/esparto shows that the esparto filter gradually becomes less pervious. The data from the PVC/cocos were somewhat irregular but show a similar tendency towards increasing W_e -values.

These results indicate that the best combination for the soils of the Alera field is clay pipes with gravel cover. These materials have the lowest entrance resistance ($W_e \approx 2$ day/m) and the highest durability.

Corrugated PVC pipes with gravel cover can also be used although their entrance resistance is more than twice that of the clay pipes with gravel cover ($W_e \approx 4.6$ days/m). It must be taken into account that the exterior

diameter of the plastic pipes is 5 cm, whereas the diameter of the clay tiles is 8 cm. It may well be that the entrance resistance of greater diameter PVC-pipe is lower.

Table 8.9 Entrance resistance values (W_e , days/m)

Year	Season	No. of drain Group						
		1 clay	2 clay/gravel	3 PVC/gravel	4 PVC	6 PVC/esparto	7 PVC/cocos	8 clay/gravel
1974	Autumn	8.4	1.2	6.9	13.4	-	-	-
1975	Winter	9.0	1.2	10.4	11.0	-	-	-
	Spring	3.6	3.7	2.3	12.2	-	-	-
	Summer	5.0	0.8	6.7	12.8	-	-	-
	Autumn	-	1.2	3.9 ¹	8.1 ¹	3.8	12.1	2.2
1976	Winter	-	0.7 ¹	6.2	12.2	6.5	23.7	2.7
	Spring	-	1.2	-	-	9.5	21.0	1.5
	Summer	3.6	0.8	5.3 ¹	7.9	6.7	22.3	2.0
	Autumn	-	1.7	2.8 ¹	15.1	12.3	19.7	4.6
1977	Winter	6.9	3.2	9.9 ¹	-	24.4	35.3	6.6
	Spring	6.8	0.6 ¹	3.1 ¹	-	34.6	35.3	3.3
	Summer	-	1.4 ¹	-	-	15.5	15.7	2.6
Mean entrance resistance (\bar{x})		5.2	1.5	4.6	12.8	- ²	21.7	2.7
Standard deviation (s)		1.6	1.0	1.8	1.4	- ²	1.7	1.0
Number of periods (n)		5	12	8	6	- ²	4	7

¹ less than 20 pairs of observations

² no average has been calculated since W_e increases with time (Fig.8.23)

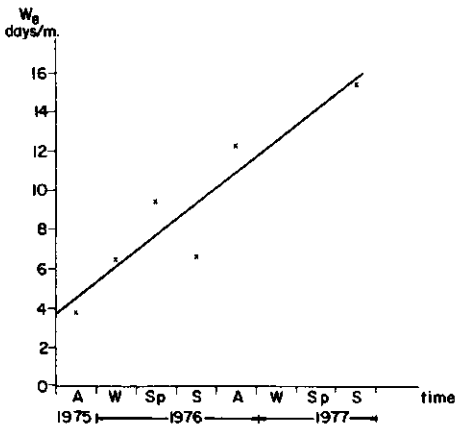


Fig.8.23: Increase of the W_e -value with time (PVC/esparto drains).

Clay pipes without gravel have almost the same entrance resistance as PVC pipes with gravel ($W_e \approx 5.2$ days/m).

Corrugated PVC pipes without a filter show a high entrance resistance ($W_e \approx 13$ days/m).

Plastic pipes with cocos and esparto filters show an even higher entrance resistance than pipes without filters. The PVC/esparto drains initially had a lower entrance resistance than the filterless plastic drains, but the W_e -value gradually increased (Fig.8.23). Obviously there is no advantage to be gained in using this envelope. Although the increase in the W_e -value of PVC/cocos drains is not so clearly manifest, a similar tendency exists.

Barley straw is not suitable as cover material since it rots easily and clogs the pipe. These drains show very small but long-lasting discharges and consequently the fall of the water table is slow. The drainage water smells of H_2S and forms a precipitate of sulphur at the drain outlets. Obviously, microbiological processes cause a rapid decomposition of the straw envelope, at the same time reducing sulphates (abundantly present in the groundwater) to H_2S . At the outlets, sulphur bacteria oxidize H_2S to H_2O and S, forming whitish and sticky precipitates in the outlet pipes (Fig.8.24).

The a_o -value of Eq.(21) was not constant for every drain group. Its variation during the observation period is shown in Table 8.10. A decrease in the a_o -value can be observed for those combinations that had the lowest entrance resistance and showed a deeper and more frequent fall of the water table, which can probably be explained by an improved permeability in the drain trench.



Fig.8.24: Whitish sulphur precipitates in the outlet pipes of PVC/straw drains.

TABLE 8.10 Residual values obtained in the calculation of W_e (a_0 in cm)

Year	Season	No. of drain group						
		1 clay	2 clay/gravel	3 PVC/gravel	4 PVC	6 PVC/esparto	7 PVC/cocos	8 clay/gravel
1974	Autumn	36.6	20.8	30.8	20.6	-	-	-
1975	Winter	32.4	21.7	25.5	26.9	-	-	-
	Spring	34.6	14.5	26.2	26.8	-	-	-
	Summer	30.0	18.3	24.7	30.9	-	-	-
	Autumn	-	14.0	18.8 ¹	40.7 ¹	50.0	42.3	27.3
1976	Winter	-	3.6 ¹	6.0	27.5	35.2	32.1	23.1
	Spring	-	6.9	-	-	34.8	34.8	20.5
	Summer	23.8	3.6	28.3 ¹	23.0 ¹	32.4	33.1	19.6
	Autumn	-	4.5	10.5 ¹	27.7	33.5	48.4	22.1
1977	Winter	19.8	0.0	1.8 ¹	24.2 ¹	24.7	39.7	18.2
	Spring	18.9	6.1 ¹	16.9 ¹	-	10.8	28.5	19.2
	Summer	-	9.4 ¹	-	-	22.1	36.4	22.3

¹ less than 20 pairs of observations

8.5.2 Indirect method of determining the W_e value

The values of the entrance resistance obtained in the previous section were checked by a second, indirect, method. The reason for doing so was that errors may have been introduced into the calculations because of the piezometers not being placed exactly at the edge of the drain trench. The indirect method is based on the shape of the water table measured in the piezometers installed midway between drains (10 m), at 5 m, and at 1 m from the drain (Fig.7.16). This analysis was originally developed by van Hoorn (1960).

The discharge per unit length can be calculated by applying Darcy's law:

$$q = -K \frac{dy}{dx} y \quad (22)$$

The flow rate through a section of the region of flow at a distance x from the drain is

$$-q = s (0.5 L - x) \quad (23)$$

where

- q = discharge per unit length at one side (m^2/day)
- s = discharge per unit area (m/day)
- K = hydraulic conductivity (m/day)
- y = hydraulic head at distance x from the drain (m)
- x = distance variable (m)
- L = drain spacing (m)

From Eqs. (22) and (23) the following differential equation is obtained:

$$K y \frac{dy}{dx} = s (0.5 L - x) \quad (24)$$

Integration of Eq. (24) leads to

$$K \frac{y^2}{2} = s \left(0.5 L x - \frac{x^2}{2} \right) + C \quad (25)$$

For the boundary conditions $x = 0.5L$, $y = h$ = hydraulic head midway between the drains (Fig.8.25), the integration constant is:

$$C = \frac{1}{2} (K h^2 - s (0.5 L)^2)$$

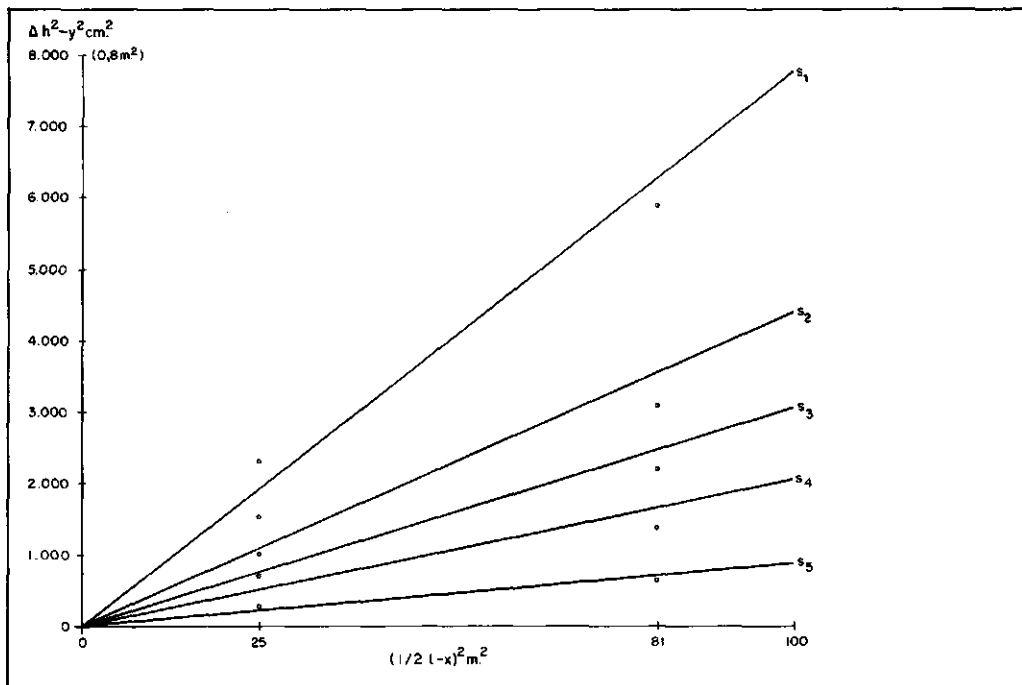


Fig.8.25: Calculation of the hydraulic head loss due to the entrance resistance by extrapolation of the groundwater table position.

Substituting into Eq.(25) gives:

$$K (y^2 - h^2) = -s \{x^2 + (0.5 L)^2 - 2(0.5 L) x\}$$

Solving for the discharge yields:

$$\frac{s}{K} = \frac{h^2 - y^2}{(0.5 L - x)^2} \quad (26)$$

Putting $(0.5 L - x)$ equal to ϵ and rearranging gives:

$$\frac{\epsilon^2}{\frac{Kh^2}{s}} + \frac{y^2}{h^2} = 1 \quad (27)$$

which is the equation for an ellipse.

The semi-minor axis is h and the semi-major axis is $h\sqrt{K/s}$. If the entrance resistance $W_e = 0$, the semi-major axis is $0.5 L$. Then

$$\frac{L}{2} = h\sqrt{\frac{K}{s}} \quad \text{or } L^2 = \frac{4 K h^2}{s} \quad (28)$$

Equation (28) is the Hooghoudt formula for steady flow above drain level. If $W_e > 0$ the semi-major axis is longer and only part of an ellipse appears between the drains ($h\sqrt{K/s} > 0.5 L$).

For unsteady flow the Boussinesq equation also shows an almost elliptic shape of the water table. This allows Eq.(26) to be used for unsteady flow.

From piezometer readings the y -values for distance $x = 1$ m and $x = 5$ m are known. Likewise the h -value is known for $x = 10$ m.

By plotting values of $(h^2 - y^2)$ against those of $(0.5 L - x)^2$ for different s -values a set of straight lines can be drawn (Fig.8.25), each having a slope of

$$\tan \alpha = \frac{s}{K} \quad (29)$$

From these straight lines the hydraulic head in the proximity of the drain can be derived by extrapolation, since for $x = 0$, $(0.5 L - x)^2 = 100$ and $y = h_i$.

For several values of h_i and sL the regression line can be drawn, the slope of which equals the entrance resistance (Eq.20).

With this indirect method the W_e -values for different combinations of drain and filter materials were calculated from the winter data of 1975 to 1977.

The results obtained are listed in Table 8.11, and can be compared with the values derived by the direct method for the same period in which h_i was measured instead of calculated. The mean values already presented in Table 8.9 are shown again in Table 8.11.

TABLE 8.11 Values of entrance resistance W_e in day/m obtained by two methods

No. of Drain group	For winter period according to		Mean value according to h_i measured (Tab.8.9)
	h_i calculated (Eq.26)	h_i measured (Eq.20)	
2 clay/gravel	2.7	2.2	1.5
8 clay/gravel	4.5	4.7	2.7
3 PVC/gravel	5.3	10.4	4.6
4 PVC	15.7	12.2	12.8
6 PVC/esparto	13.4	15.3	-
7 PVC/coco	23.1	29.5	21.7

Table 8.11 shows that both methods give similar results, though deviations occur in some periods, due possibly to errors in the observations.

The hydraulic conductivity can be derived from Eq.(29). Table 8.12 shows the K-values thus obtained for the periods in which W_e was calculated.

TABLE 8.12 Calculated K-values

Period	No. of drain group	Water table below surface level m	K m/day
Winter '75	2 (clay/gravel)	> 0.4	0.61
Winter '77		> 0.8	1.70
Winter '76	8 (clay/gravel)	> 0.4	0.67
Winter '77		> 0.5	0.80
Winter '75	3 (PVC/gravel)	> 0.4	0.61
Winter '75	4 (PVC)	> 0.2	0.36
Winter '76		> 0.5	0.36
Winter '77		> 0.4	0.67
Winter '76	6 (PVC/esparto)	> 0.2	0.58
Winter '77		> 0.2	0.52
Winter '76	7 (PVC/coco)	> 0.4	0.55
Winter '77		> 0.4	1.46

If those K-values that deviate from the general tendency shown in Table 8.12 are ignored, an average hydraulic conductivity of 0.6 m/day is found (standard deviation $s \approx 0.1$). This value agrees fairly well with that derived earlier for the clay tile drains with gravel cover.

From the analysis of those cases in which the hydraulic conductivity differs greatly from the average value, the following conclusions can be drawn:

1. When the groundwater table is deep (Drain Group 2 - winter 1977), the calculated hydraulic conductivity is higher than the actual one because some flow occurs below drain level.
2. When the entrance resistance is high (Drain Group 7 - winter 1977) and the slope of the groundwater table is small (Fig.8.26), errors of a few centimetres in the piezometer readings result in great differences in the value of $\tan \alpha$ and consequently in the value of the hydraulic conductivity.

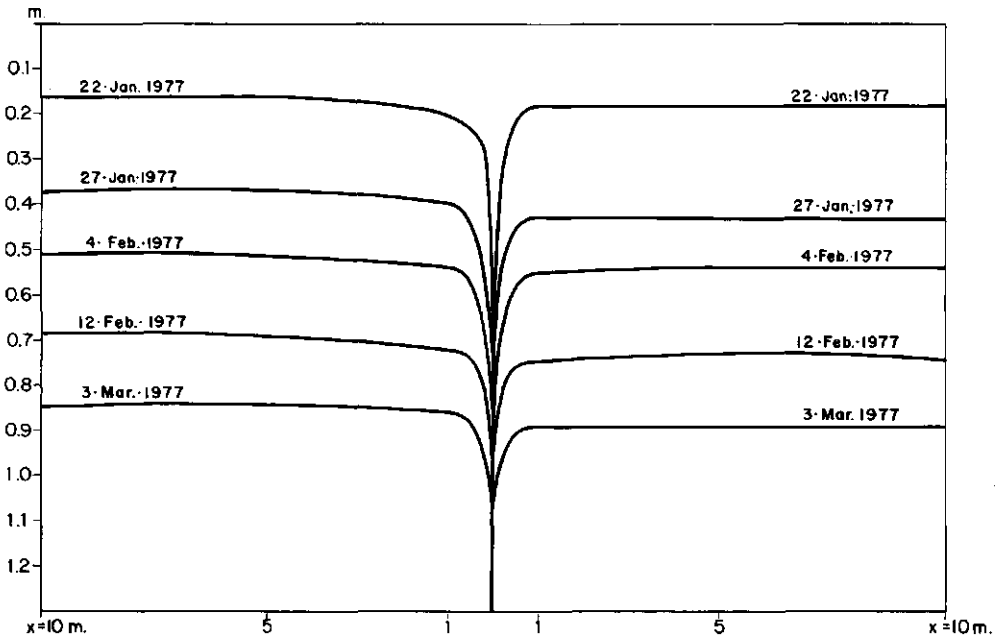


Fig.8.26: Shape of the water table where laterals have a high entrance resistance (Drain Group 7, PVC/cocos, winter 1977).

Nevertheless this method has its uses in determining the hydraulic conductivity, especially in cases where the Boussinesq theory cannot be applied because the drains have a considerable entrance resistance (Drain Groups 3, 4, and 6).

9. Desalinization process

9.1 Stages of the process

The desalinization of the soils of the Alera experimental unit consisted of two stages: an initial leaching period without crops, with intermittent irrigation and drainage of the leaching water, followed by a second phase in which moderately resistant to salt-tolerant crops were grown under irrigation. During the second stage the percolation losses completed the desalinization process.

The object of research in the first phase was to determine the leaching efficiency coefficients by comparing the actual desalinization process with theoretical models. This would make it possible to predict the amount of irrigation water required for the desalinization of soils with differing initial salt contents and the duration of their leaching processes.

In the second phase the relation between crops and groundwater table depth was studied for its use in assessing the drainage criteria to be applied in further land reclamation projects. In addition some water management factors, e.g. field application efficiency, were derived.

The initial leaching of the area drained by Drain Groups 1 to 5 started in September 1974 and continued until August 1975, after which the cropping programme began. The leaching period of the area drained by Drain Groups 6 to 8 extended from autumn 1975 to summer 1976.

9.2 Water balance of the initial leaching phase

The water balance assessed during the first stage of the desalinization process was made to determine experimentally the evaporation amount, and to compare this value with those calculated by conventional methods. If they agreed reasonably well, one could conclude that seepage and capillary rise, which are other unknown components of the water balance, had been correctly estimated.

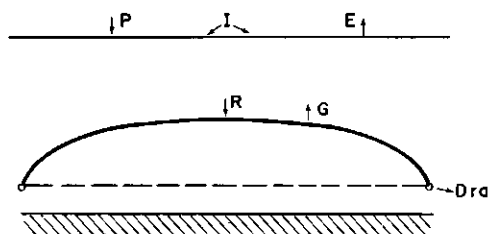


Fig.9.1: Water balance of the initial leaching phase.

The water balance equation for the unsaturated zone reads:

$$I + P + G = E + R + \Delta W \quad (1)$$

where

- I = effective amount of irrigation water (mm)
- P = effective amount of precipitation (mm)
- G = amount of capillary rise from the groundwater table (mm)
- E = amount of evaporation (mm)
- R = amount of deep percolation ("recharge"; mm)
- ΔW = change in amount of moisture stored (mm)

If R^* is the net percolation ($R^* = R - G$) Eq.(1) can be simplified to:

$$I + P = E + R^* + \Delta W \quad (2)$$

As the soil lacked natural drainage the water balance of the saturated zone could be expressed by the following equation:

$$R^* + S = Dr_a + \mu \Delta h \quad (3)$$

where

- R^* = net downward percolation (mm)
- S = amount of seepage (mm)
- Dr_a = amount of artificial drainage (mm)
- μ = drainable pore space
- Δh = change in water table height averaged over the entire drain spacing L (mm).

The water balance of the entire soil profile down to the impervious layer, which coincides with the drain level, was obtained by Eqs.(2) and (3).

$$I + P = E + (Dr_a + \mu \Delta h - S) + \Delta W \quad (4)$$

During the initial leaching both precipitation and irrigation were effective amounts because surface runoff did not occur.

According to the discharge hydrographs (Chap.8) both lateral seepage and upward flow through the less pervious layer were negligible, thus S equalled zero. Equation (4) then reduced to:

$$I + P = E + Dr_a + \mu \Delta h + \Delta W \quad (5)$$

While the water table was falling, evaporation caused no significant capillary rise. If it had, the hydraulic head hydrographs (Chap.8) would have shown a steeper decline and greater differences would have been observed between the falls in winter and summer. Hence, the capillary rise was negligible ($G \approx 0$) and deep percolation equalled net percolation ($R^* = R$).

If in the collector discharge hydrographs (Fig.9.2) periods of time are chosen in which the discharge rate at the beginning and end of the periods is equal, i.e. four or five days after an irrigation or heavy rainfall, the depth of the water table should also be approximately equal.

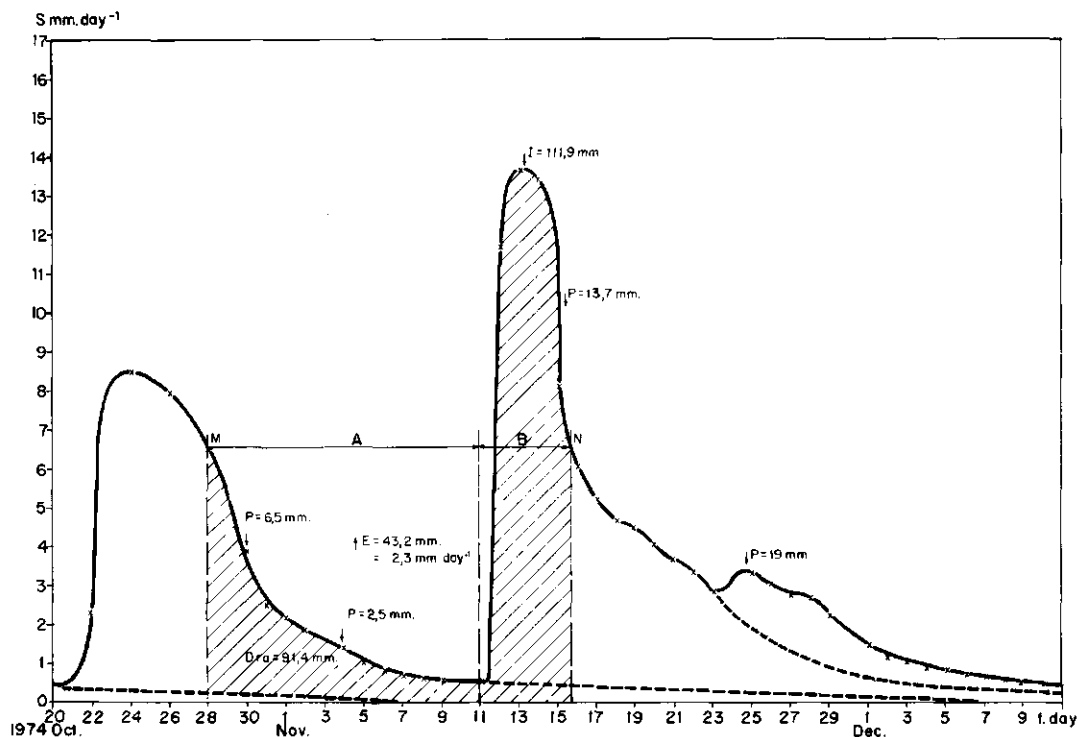


Fig.9.2: Collector discharge hydrograph (irrigation).

Likewise, when the infiltration process is over, four or five days after an irrigation the moisture content in the unsaturated zone should correspond approximately to field capacity.

TABLES 9.1 and 9.2: Water balance of the initial leaching phase without crops (1974-1975; 1975-1976).

Period	Irrigation	Rainfall	Drainage	Actual evaporation	Mean actual evaporation
	mm	mm	mm	mm	mm/day
1 9 7 4 - 1 9 7 5					
Sept.8 - Oct. 8	412.2	87.2	-	-	-
Oct. 8 - Oct.28	120.0	7.7	69.7	58.0	2.9
Oct.28 - Nov.30	119.9	45.1	107.8	49.2	1.5
Nov.30 - Jan.19	128.2	14.7	75.6	67.3	1.3
Jan.19 - Feb. 8	-	26.6	17.5	9.1	0.5
Feb. 8 - Feb.15	-	21.9	12.9	9.0	1.3
Feb.15 - Mar.12	126.1	10.6	84.1	52.6	2.1
Mar.12 - Mar.22	-	24.5	2.0	22.5	2.3
Mar.22 - Apr.25	127.4	135.5	142.1	120.8	3.2
Apr.25 - May 12	-	38.1	8.9	29.2	2.3
May 12 - May 30	-	69.1	11.6	57.5	3.2
May 30 - Jun.19	130.7	2.3	92.9	40.1	2.0
Jun.19 - Jul.17	145.7	1.6	91.3	56.0	2.0
Jul.17 - Aug.15	-	55.4	4.8	50.6	1.7
Aug.15 - Aug.26	110.2	11.5	50.0	71.7	6.5
1 9 7 5 - 1 9 7 6					
Nov.19 - Dec.17	-	70.3	45.0	25.3	0.9
Dec.17 - Feb. 1	87.2	8.5	38.1	57.6	1.3
Feb. 1 - Feb.12	-	55.0	33.8	21.2	1.9
Feb.12 - Apr. 8	90.5	81.1	60.2	111.4	2.0
Apr. 8 - May 12	85.6	42.7	65.6	62.7	1.8
May 12 - June 2	81.0	22.0	45.5	57.5	2.7
June 2 - Jul.10	121.4	77.0	39.1	159.3	4.2
Jul.10 - Jul.13	-	30.0	16.0	14.0	4.7
Jul.13 - Jul.31	119.6	2.7	45.0	77.3	4.3
Jul.31 - Sept28	110.3	104.8	44.4	170.7	2.9
Sept28 - Oct.12	-	58.0	15.2	42.8	2.9
Oct.12 - Oct.24	-	33.0	9.7	23.3	1.9

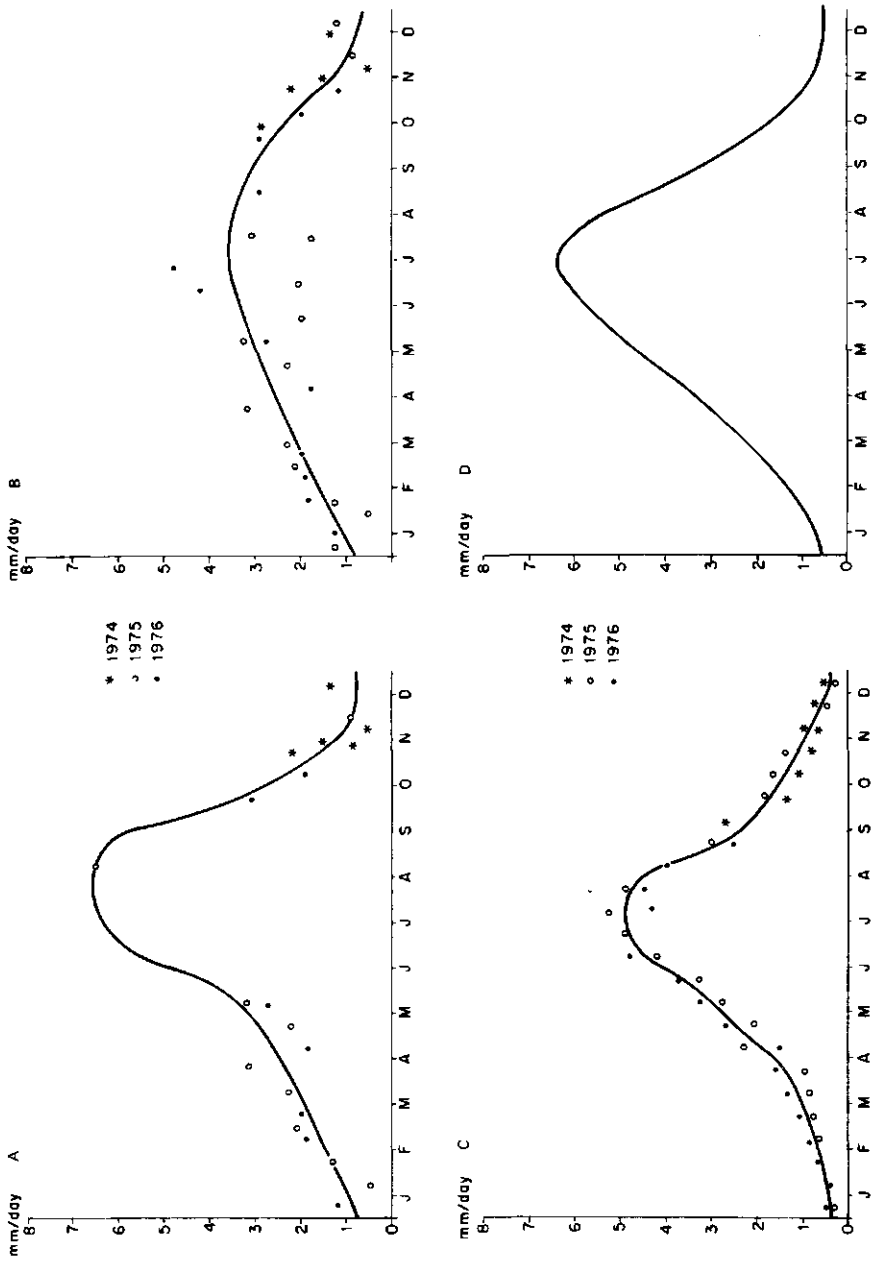


Fig. 9.4: a) Potential evaporation (from the water balance). b) Actual evaporation (from the water balance). c) Potential evaporation (Thornthwaite). d) Evaporation from a free water surface (Penman).

Some conclusions can be derived from a comparison of the curves of Figs.9.4a and 9.4b. During the initial leaching, a precipitation deficit occurred from June to September, due to the long intervals between consecutive waterings and the lack of rainfall. In this arid period there was no capillary flow that could compensate the precipitation deficit. In fact, once the surface soil became dry, evaporation ceased. Consequently, the fall of the water table was scarcely influenced by evaporation.

Figure 9.4c shows the potential evaporation calculated by the Thornthwaite method for the same period. The shape of the curve is similar to that derived from the water balance (Fig.9.4a), but the calculated values are lower than those determined experimentally, the difference being greater in the cold months. The explanation for this difference is that the Thornthwaite formula is based on mean temperature and heat index. It does not take into account, as an evaporation factor, the dry winds which occur frequently in the area during the cold months.

Figure 9.4d shows the evaporation from a free water surface calculated by the Penman method and based on data from the Zaragoza observation station. This station is representative of a climate similar to that of the Alera field, but with a greater aridity (Chap.2). In addition, the value calculated with the Penman method (E_0) refers to a free water surface which has a different roughness height and albedo than a moist soil.

To summarize, the evaporation values obtained from the water balance agreed fairly well with those calculated by conventional methods, thereby confirming that seepage and capillary rise were negligible.

9.3 Theoretical leaching approach

9.3.1 Series of reservoirs

The theoretical series-of-reservoirs model developed by van der Molen (1973) divides the rootzone into four layers, each 25 cm thick, and regards each layer as representing a reservoir.

Irrigation water supplied to the first reservoir percolates to the second, from the second to the third, and from the third to the fourth (Fig.9.5).

The volume of water in each reservoir corresponds with the moisture content of each soil layer, and can be considered constant because the water and salt movement occur at a moisture content near field capacity.

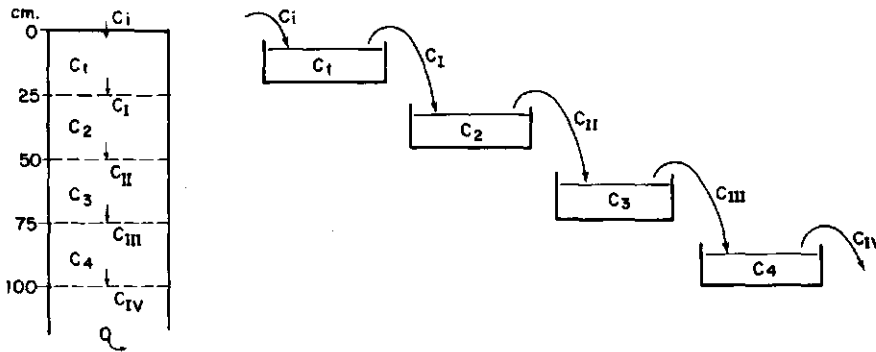


Fig.9.5: Series-of-reservoirs model.

The salt balance in the first reservoir is expressed by the following differential equation:

$$V \frac{dc_{fc}}{dt} = (c_i - c_r) Q \quad (7)$$

where

- V = volume of the reservoir filled with water (l)
- $\frac{dc_{fc}}{dt}$ = change in salt concentration of the soil solution at field capacity (meq/l)
- c_i = concentration of the influent (irrigation water; meq/l)
- c_r = concentration of the effluent (meq/l)
- Q = rate of flow through the system (l/s)
- dt = differential interval (s)
- $T = V/Q =$ time of residence (s)

For the first reservoir the concentration of the effluent is

$$c_r = f c_{fc} + (1 - f) c_i \quad (8)$$

where

- f = leaching efficiency coefficient representing the percentage of irrigation water mixing with the soil solution

From Eqs.(7) and (8) the following differential equation is derived:

$$\frac{dc_{fc}}{c_{fc} - c_i} = -f \frac{Q}{V} dt \quad (9)$$

Integration of Eq.(9) for the boundary conditions $t = 0, c_{fc} = c_i$ and $t = t, c_{fc} = c_r$ yields

$$c_r = c_i + (c_i - c_r) e^{-ft/T} \quad (10)$$

where

c_I = concentration of the effluent percolating from the first reservoir into the second (meq/l)

In a similar way the concentration of the effluents from the second, third, and fourth reservoirs are obtained:

$$c_{II} = c_i + (c_1 - c_i) \frac{ft}{T} e^{-ft/T} + (c_2 - c_i) e^{-ft/T} \quad (11)$$

$$c_{III} = c_i + (c_1 - c_i) \frac{f^2 t^2}{2T^2} e^{-ft/T} + (c_2 - c_i) \frac{ft}{T} e^{-ft/T} + (c_3 - c_i) e^{-ft/T} \quad (12)$$

$$c_{IV} = c_i + (c_1 - c_i) \frac{f^3 t^3}{6T^3} e^{-ft/T} + (c_2 - c_i) \frac{f^2 t^2}{2T^2} e^{-ft/T} + (c_3 - c_i) \frac{ft}{T} e^{-ft/T} + (c_4 - c_i) e^{-ft/T} \quad (13)$$

The concentration values of Eqs. (10), (11), (12), and (13) can be expressed either in meq/l of soluble salts or in terms of electrical conductivity, the latter being proportional to the former (Fig.9.6).

As the moisture content at field capacity is 40 per cent by volume, a layer 25 cm thick will have a volume of water equivalent to 100 mm at field capacity. If units of percolation flow of 100 mm are chosen, the value of ft/T will be numerically equal to f .

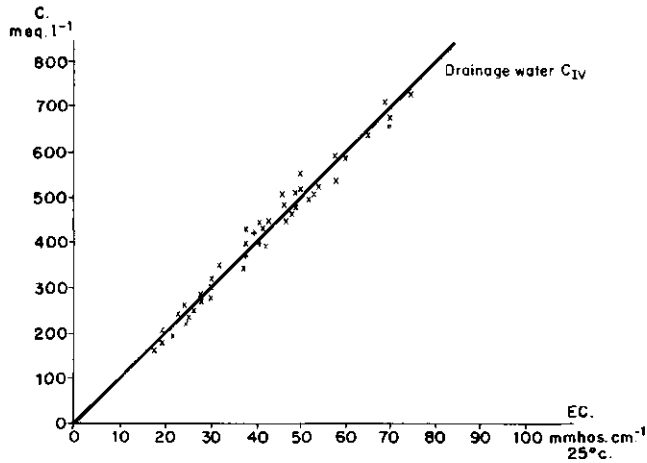


Fig.9.6: Correlation between c (meq/l) and EC (mmhos/cm) in drainage water.

Using Eqs.(10), (11), (12), and (13) and taking the average electrical conductivity of the irrigation water constant at 0.4 mmhos/cm, theoretical desalinization curves were obtained for different initial salt contents and distinct leaching efficiency coefficients (Fig.9.7).

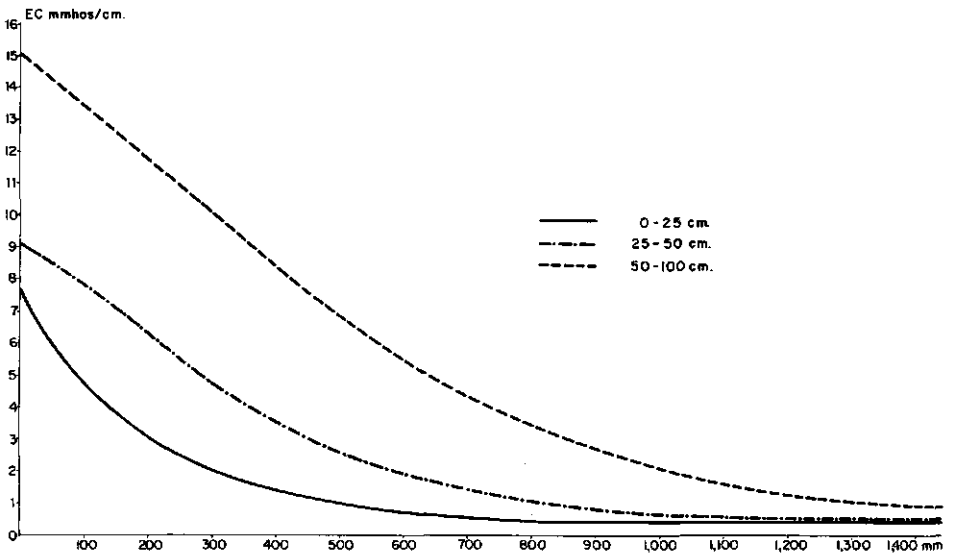


Fig.9.7a: Theoretical desalinization curves (Soil Site 2, $f = 0.5$).

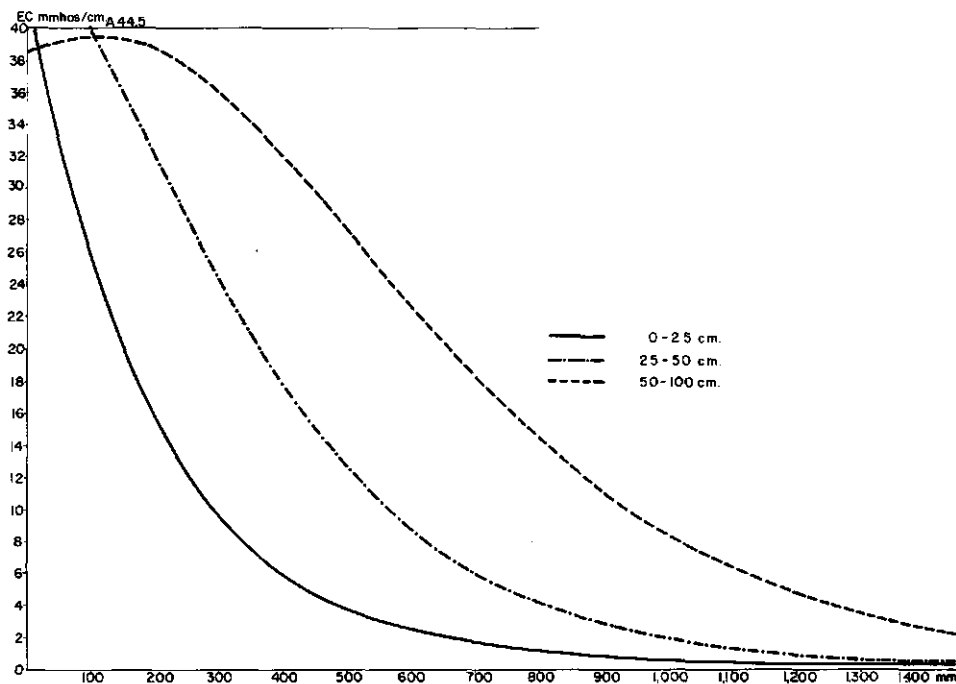


Fig. 9.7b: Theoretical desalinization curves (Soil Site 3, $f = 0.5$).

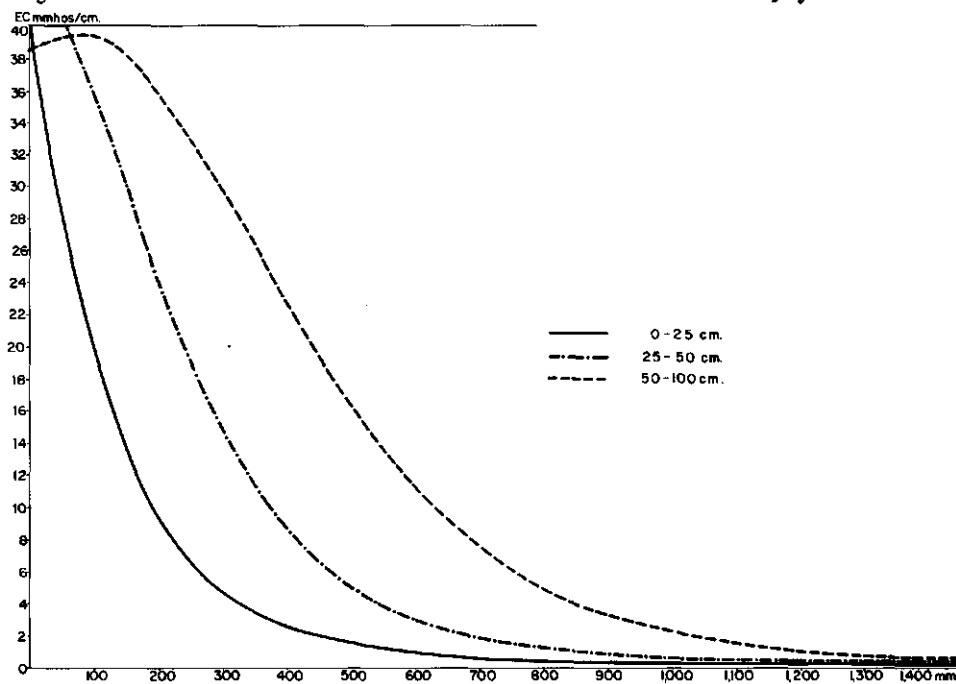


Fig. 9.7c: Theoretical desalinization curves (Soil Site 3, $f = 0.75$).

9.3.2 Numerical method

If a constant leaching efficiency coefficient is taken, the series-of-reservoirs model provides a semi-analytical solution to the leaching problem. For soils such as those of the Alera field, however, where the degree of cracking decreases with depth, a variable leaching efficiency coefficient increasing with depth can be expected.

Introducing variable f -values leads to very complicated equations. For this reason a simpler, numerical method is used.

If in the first layer a net amount (a) of irrigation water of concentration (c_i) is mixed with an amount (b) of the soil solution that has an initial concentration of (c_1), the concentration of the percolation water from the first layer (c_I) to the second can be expressed as follows:

$$c_I = \frac{ac_i + bc_1}{a + b} \quad (14)$$

The concentration of the water from the second layer (c_{II}) can be calculated in the same manner. If the amount of net percolation (a) is constant throughout the soil profile, i.e. no moisture is retained, the expression reads:

$$c_{II} = \frac{ac_I + dc_2}{a + d} \quad (15)$$

For layers of the same thickness and same moisture-holding capacity, the amounts of moisture are the same and are equal to the moisture content at field capacity ($b = d = W_{fc}$).

Expressions similar to Eqs.(14) and (15) can be derived for the third and fourth layers.

In Eqs. (14) and (15) a leaching efficiency coefficient equal to 1 is assumed. In practice the net amount of percolation water can be adapted to suit the possibly varying leaching efficiency coefficient of each soil layer.

9.4 Actual desalination process

To monitor the desalination process, five soil sampling sites were chosen in the area drained by Drain Groups 1 to 5 (Chap.7). One site was a soil patch of high initial salinity (Site 3, $EC_e = 45$ mmhos/cm) and two others had moderate salinity (Sites 2 and 5, $EC_e = 10$ mmhos/cm) and were located in areas with different drainage conditions (Drain Group 2 clay/gravel and Drain Group 5 PVC/straw). In the undrained control area Site 1 was chosen for a study of the salinity evolution under natural conditions. Site 4 was located in a drained basin but leaching was caused only by rainfall. In the area drained by Drain Groups 6 to 8 two extra monitoring sites were selected, one of high initial salinity (Site 6, $EC_e = 27$ mmhos/cm) and the other of moderate salinity (Site 7, $EC_e = 7$ mmhos/cm).

The leaching curve shows the relation between the decrease of the salinity, expressed in terms of electrical conductivity, and the average amount of water drained by the laterals between which the monitoring site was located (Fig.9.8).

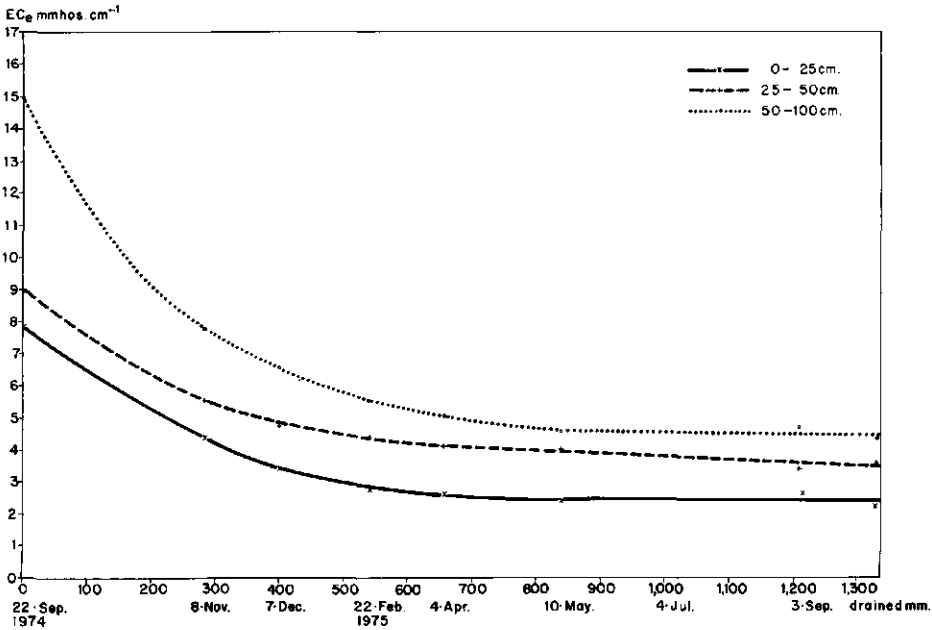


Fig.9.8: Actual desalination curve (Soil Site 2, moderate salinity).

Three desalination curves were selected to show the leaching achieved at three sites with differing initial salt content and drainage conditions.

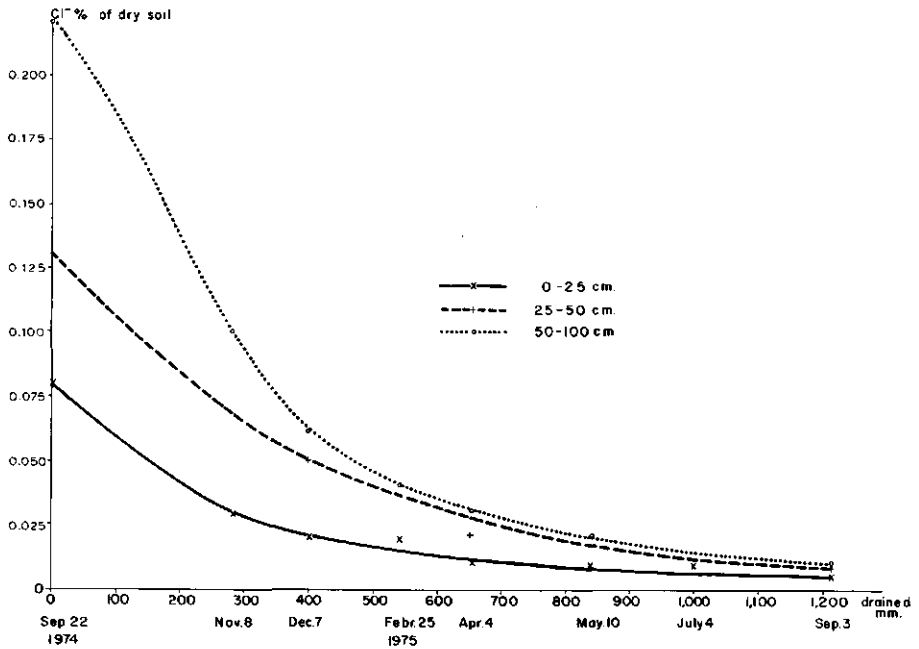


Fig. 9.11: Actual leaching curve of a soil with moderate initial salinity (Soil Site 2) and good drainage conditions (Drain Group 1, clay/gravel).

Figure 9.11 shows the desalination of a moderately saline soil (average value of three layers: $Cl^- = 0.16\%$, $EC_e = 11$ mmhos/cm), in which the drainage system (clay tiles) functioned properly. After 850 mm of water had been drained a soil profile of 100 cm was virtually desalinated ($Cl^- = 0.02\%$, $EC_e < 4$ mmhos/cm). During the desalination process no alkalinization was observed since at the end of the leaching period (1,200 mm of drainage water) soil pH remained around 8 and the SAR was equal to 6.

Figure 9.12 shows the leaching of a soil whose initial salinity was high ($Cl^- = 0.80\%$, $EC_e = 43$ mmhos/cm), and whose drainage system had a low entrance

resistance (PVC/gravel). Reliable results were only obtained for the top two layers, so no desalinization curve has been drawn for the deeper layer. In the upper 50 cm rapid desalinization was observed, 600 mm of leaching water being sufficient to reduce the salinity level to below half of the initial value ($Cl^- = 0.3\%$, $EC_e = 18$ mmhos/cm). After that, slower desalinization was observed and at the end of the initial leaching period (1200 mm of drainage water) moderate salinity remained ($Cl^- = 0.20\%$, $EC_e = 13$ mmhos/cm), or four times less than the initial value. No alkalization symptoms were observed during the leaching process and the pH-value remained near 8.

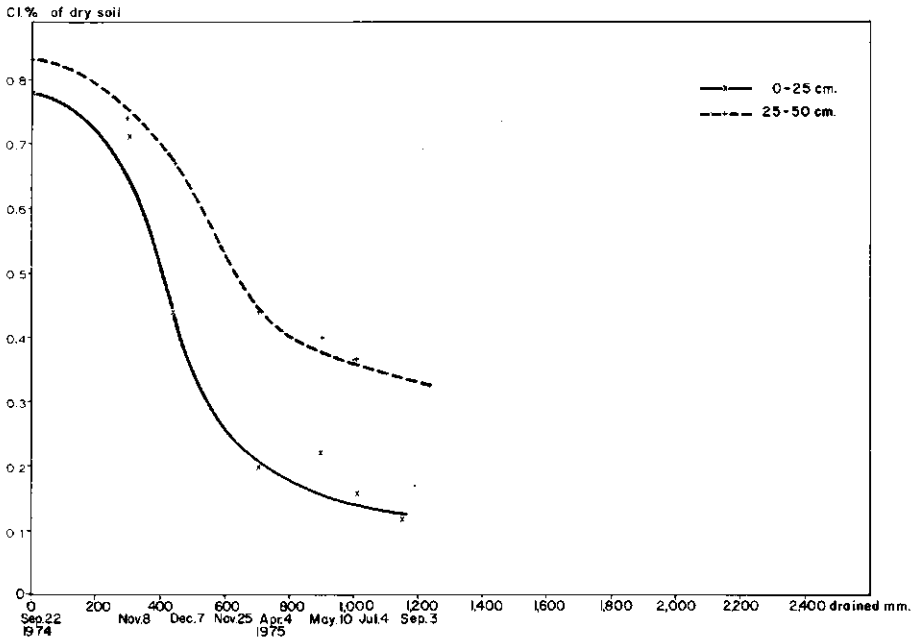


Fig.9.12: Actual leaching curve of a soil with high initial salinity (Soil Site 3) and good drainage conditions (PVC/gravel).

Figure 9.13 shows the leaching of a moderately saline soil ($Cl^- = 0.18\%$, $EC_e = 12$ mmhos/cm), with poor drainage conditions caused by high entrance resistance (PVC and PVC/straw). Here, the water table was rarely below 80 cm.

and causes scarcely any percolation to the water table.

Nevertheless, desalinization of the upper 50 cm was achieved and at the end of the leaching period the soil was almost salt free ($Cl^- = 0.02\%$, $EC_e = 4$ mmhos/cm). No reliable data were obtained for the layer below 50 cm.

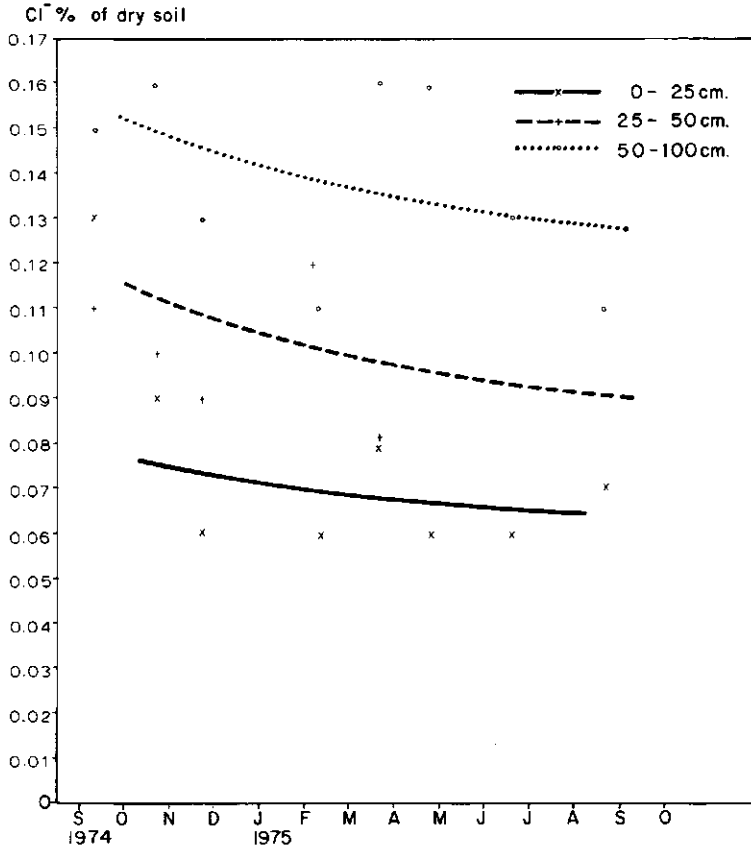


Fig.9.15: Actual leaching curve in a drained soil leached only with rain water.

No soil samples were taken to study the desalinization of soil layers between a depth of 1 m and drain level, but to ascertain the variation of the salt content in this deep soil layer, the drainage water was analysed when the groundwater table was below 1 m.

For different initial salt contents and drainage conditions, the Schoeller diagrams of Figs.9.16 and 9.17 show the decrease in salinity of the drainage water during the leaching period. In the graph of Fig.9.18 the desalinization is expressed in terms of electrical conductivity.

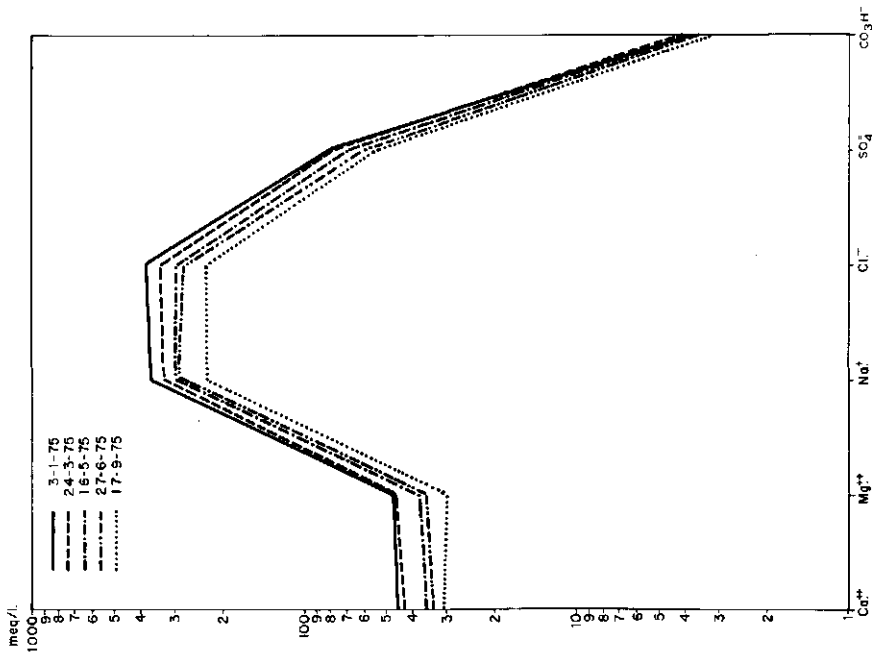


Fig. 9.17: Schoeller diagram (Drain Group 3, PVC/gravel).

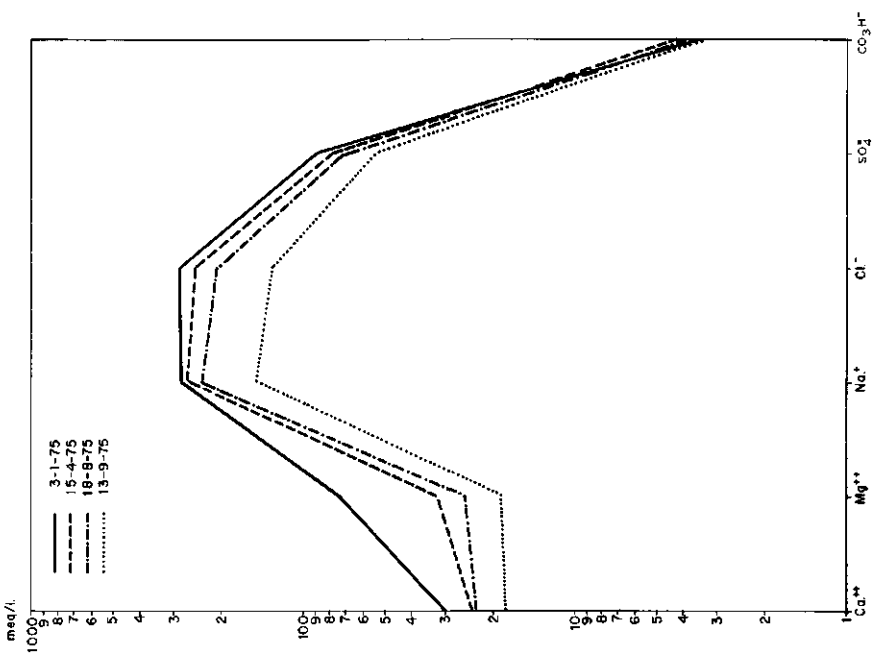


Fig. 9.16: Schoeller diagram showing the decrease of the salt content of the groundwater (Drain Group 2, clay/gravel).

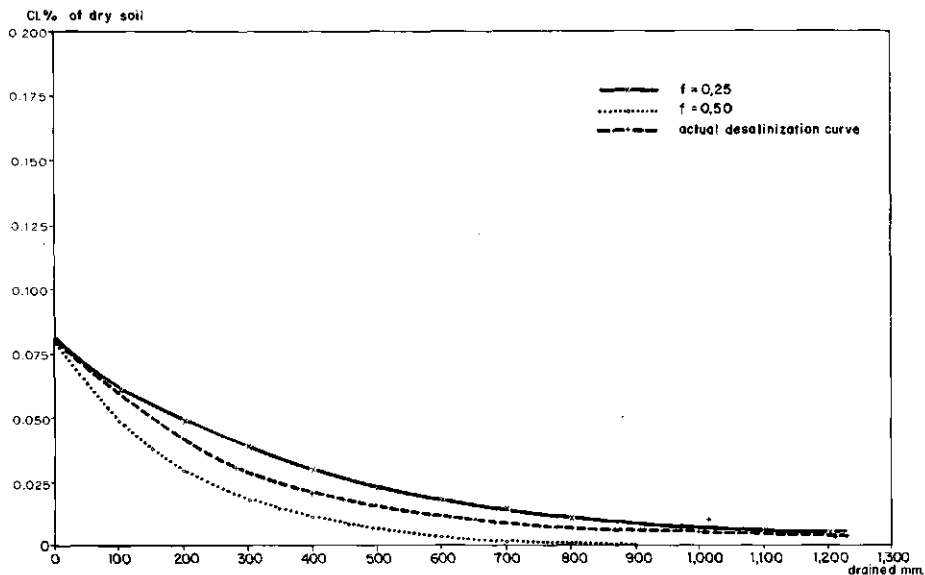


Fig.9.19: Determination of the leaching efficiency coefficient (Soil Site 2, layer 0 - 25 cm).

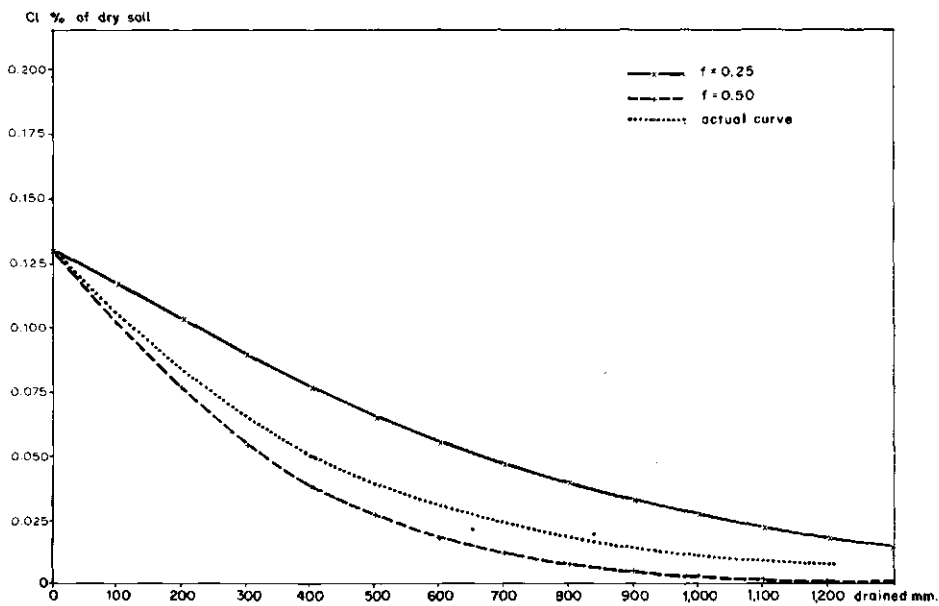


Fig.9.20: Determination of the leaching efficiency coefficient (Soil Site 2, layer 25 - 50 cm).

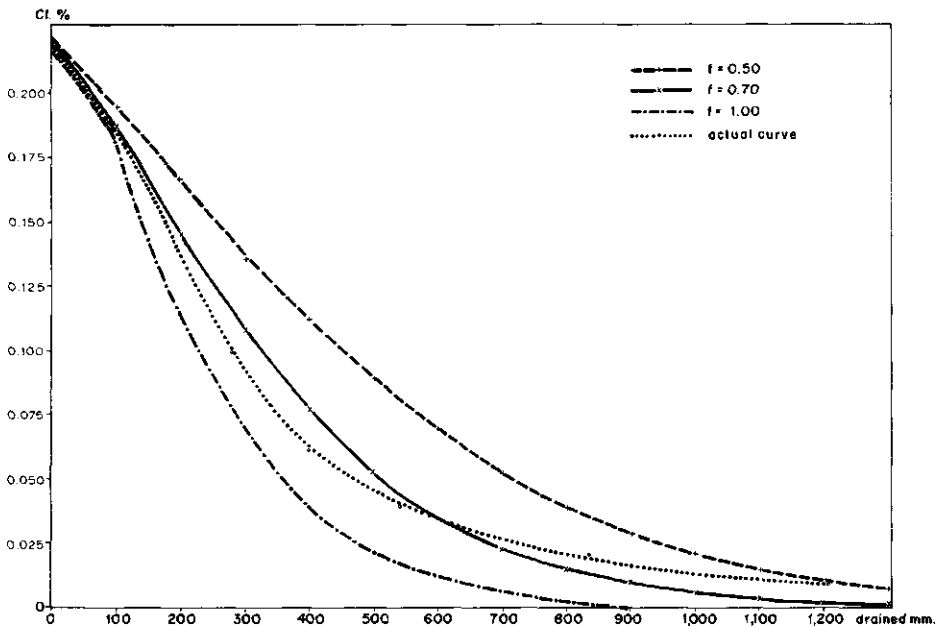


Fig.9.21: Determination of the leaching efficiency coefficient (Soil Site 2, layer 50 - 100 cm).

Two important conclusions emerged from the comparative study of the leaching of a moderately saline soil (Soil Site 2). The first is that the leaching efficiency coefficient is not constant but increases with depth. The second is that the leaching efficiency coefficient is higher in the first stage of desalinization and decreases gradually as the soil becomes less saline.

The explanation for the first conclusion is that even though the soil texture remains almost the same, cracks are less developed in the deeper layers.

The second conclusion also has a logical explanation. At the beginning of leaching the salts are accumulated at the aggregate surfaces, and are easily washed out. At a later stage when the soil becomes less saline, some salts remain in the interior of less pervious aggregates and the diffusion of salts into the percolation water slows down.

The difference between the f-values obtained from Sites 3 and 2 may be explained by Site 3 having a high initial salinity and being located in a patch of rather compact soil with a lower infiltration rate than the rest of the area. The amount of drainage water calculated previously corresponds to the average amount of water percolating through the whole drainable area, whereas the amount of water actually percolating at Site 3 was probably less. Therefore, in reality, the leaching efficiency coefficient could be somewhat higher than the calculated value.

At sites where the drains have a high entrance resistance, the actual amount of leaching water may be greater than that measured in the drain outlets, because some of the water may flow to adjacent areas drained by laterals with a lower entrance resistance. If the real amount of leaching water is greater than that used for the calculation, the leaching efficiency coefficient should in reality be lower than the value calculated.

Notwithstanding these sources of error, the leaching efficiency coefficients reflect the differences in soil structure being higher in well-structured soil patches like Sites 2 and 5. The values also reflect the initial salt content since Sites 2 and 5, having a better soil structure, had a lower initial salt content because of better natural leaching in the past.

9.6 Prediction of the initial leaching requirements

To predict the initial leaching requirement, the numerical method was used. For soils like those of the experimental field, an average leaching efficiency coefficient of 0.5 for the upper soil layer (0 to 50 cm) was assumed. For the deeper layer (> 50 cm) a value of 1.0 was used, provided that drainage conditions were adequate.

Assuming a salinity corresponding to an EC_e of 15 mmhos/cm as being representative of the saline soils of the fluvio-colluvial valleys, approximately 1 000 mm of percolation water must be drained by the field laterals to leach the soil profile to a depth of 1 m (Fig.9.11).

If the desalinization is done by intermittent leaching (i.e. irrigation water is applied when the water table is near drain level and the discharge is approximately 0.5 mm/day), the average discharge during the leaching period is 6 mm/day provided the entrance resistance of the laterals is low.

With intermittent leaching and an average irrigation cycle of 25 days, about 6 months are required for the initial leaching. Taking into account that heavy rainfall can occur during the leaching period and that the discharge will then be lower than with irrigation, the total duration of the initial leaching period can be up to 8 months. Leaching should therefore start in early autumn and continue to late May.

Although the initial leaching is performed during the months of low evaporation, approximately 450 mm of evaporation must be added to the amount of percolation water. The water supplied by rainfall varies considerably from one year to another. Even so, the total irrigation requirement can be estimated to vary between 1100 and 1400 mm, i.e. 8 to 10 applications of 140 mm each.

From the study of the initial salinity conditions and the behaviour of the soils under leaching, it can be concluded that the initial salinity correlates with soil physical properties that influence drainage conditions. Important properties such as infiltration rate and permeability depend on the compactness of the soil, irrespective of texture. The highest initial salinities found in the experimental field corresponded to two soil patches whose surface layers were compact. The amount of percolation water needed to reclaim their upper layers (0 to 50 cm) is approximately 1300 mm (Fig. 9.27).

The main restraint to the reclamation of the severely saline soils is the poor downward water movement through the soil profile. This, however, can be improved by deep subsoiling and by local applications of gypsum.

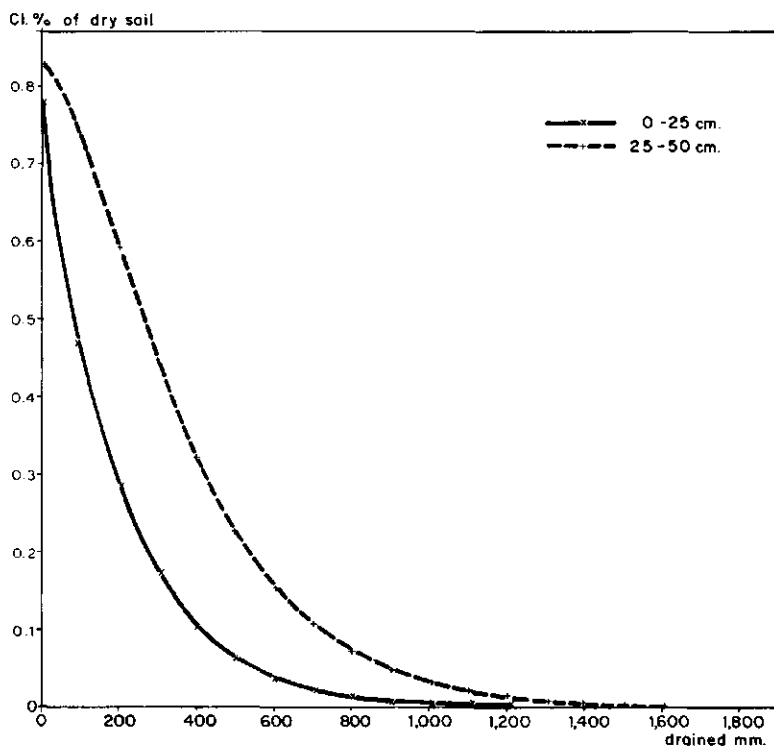


Fig.9.27: Prediction of Leaching requirements to reclaim the surface layer (0-50 cm) of a highly saline soil (Soil Site 3).

9.7 Leaching requirement during the cropping stage

Once the initial leaching stage is over, the salinity level in the root-zone corresponds to an EC_e of 3 mmhos/cm ($Cl^- < 0.02\%$), due to the presence of slightly soluble salts. There is always a possibility, however, that the soils may be resalinated by salts contained in the irrigation water and salts transported by capillary rise from the groundwater.

To evaluate this hazard of secondary salinization the salt balance of irrigated crops was obtained from the water balance for sugar beet, which had been cultivated during the 1976 irrigation season and whose water balance had been assessed to determine the irrigation efficiency and the percolation losses (Table 9.3).

TABLE 9.3: Water balance for irrigated sugar beet
(April - December 1976)

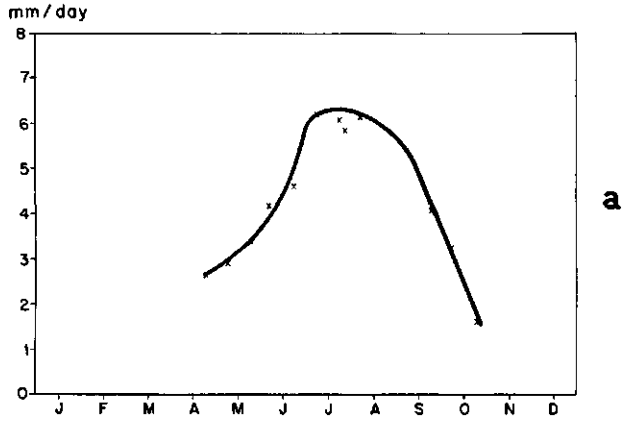
Period	Irrigation mm	Rainfall mm	D r a i n a g e		Consumptive use		e _a
			subsurface mm	surface mm	mm	mm/day	
Apr. 7 - Apr. 18	95.8	0	46.3	7.0	42.5	0	0.51
Apr. 18 - Apr. 30	41.1	21.7	28.5	2.0	32.3	2.7	0.26
Apr. 30 - May 9	62.1	0	34.5	1.8	25.8	2.9	0.42
May 9 - May 26	72.4	14.0	26.9	1.8	57.7	3.4	0.60
May 26 - June 14	79.4	61.1	60.3	0	80.2	4.2	0.24
June 14 - July 2	89.1	21.9	27.9	0	83.1	4.6	0.69
July 2 - July 13	76.0	40.1	45.2	1.5	69.4	6.3	0.39
July 13 - July 24	85.4	2.7	20.0	1.6	66.5	6.1	0.75
July 24 - Aug. 2	83.7	0	31.9	0	51.8	5.8	0.62
Aug. 2 - Aug. 13	97.9	0	30.0	0	67.9	6.2	0.69
Aug. 13 - Aug. 31	105.7	45.8	36.4	0	115.1	6.4	0.66
Aug. 31 - Sept.11	83.5	11.0	34.7	0	59.8	5.5	0.58
Sept.11 - Sept.29	90.2	28.0	45.2	0	73.0	4.1	0.50
Sept.29 - Oct. 14	0	62.0	13.2	0	48.8	3.3	-
Oct. 14 - Oct. 29	0	29.0	8.9	0	20.1	1.6	-

This water balance was assessed by means of the equations and methodology described in Section 2 of this chapter. When data on discharge were not available, percolation losses were calculated with the following equation:

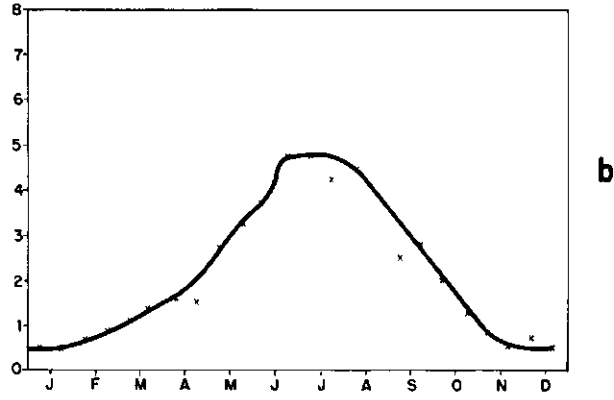
$$R = \mu \Delta h$$

An average value of Δh was determined from the readings of five piezometer lines placed in the irrigated basin.

Figure 9.28a shows the variation in the consumptive use of sugar beet throughout the irrigation season. The consumptive use was 894 mm, made up of the net irrigation requirement, 557 mm, plus effective rainfall, 337 mm. For an average field irrigation efficiency of approximately 0.53, the total irrigation requirement was 1050 mm. In practice 1062 mm of water was applied.



a



b

Fig.9.28a: Consumptive use for sugar-beet derived from the water balance.

Fig.9.28b: Potential evapotranspiration (Thorntwaite) for the same period as Fig.9.28a.

Assuming capillary rise to be negligible, the leaching requirement to prevent secondary salinization by salts in the irrigation water could be calculated with the salt equilibrium equation (van der Molen and van Hoorn, 1976).

$$R^* = (E - P) \frac{(1 - f) EC_{fc} + f EC_i}{f (EC_{fc} - EC_i)} \quad (24)$$

where

- R^* = net leaching requirement (mm)
- $E - P$ = precipitation deficit (mm)
- f = leaching efficiency coefficient
- EC_i = electrical conductivity of irrigation water (mmhos/cm)
- EC_{fc} = electrical conductivity of the soil solution at field capacity (mmhos/cm)

The following assumptions were made: average value of f is 0.75 for a depth to 1 m, $EC_i = 0.4$ mmhos/cm, $EC_{fc} = 6$ mmhos/cm, and the precipitation deficit $E - P = 557$ mm. Substituting these values into Eq.(24) yielded the leaching requirement: $R = 239$ mm.

Hence, there is no risk of secondary salinization by the irrigation water if conditions of good drainage are maintained, because the measured percolation losses (490 mm) are twice the leaching requirement. In fact, during the irrigation season the salt content of Soil Site 4, expressed in terms of chloride percentage, remained below 0.02 (equivalent $EC_e = 3$ to 3.5 mmhos/cm).

Capillary rise from the water table is indeed negligible because seepage from adjacent slopes is caught by interceptor drains. Some capillary rise may occur in the fallow period after winter cereal growing if seepage from adjacent irrigated summer crops recharges the groundwater. Even so, any salts accumulated in the rootzone during the fallow period can be leached by one or two irrigations applied after the cereal harvest and just before the seed bed is prepared for the next crop.

To summarize, secondary salinization after reclamation can be prevented if two aspects of water management are borne in mind: i.e. good drainage conditions should be maintained by keeping the field laterals and collector drains clean, and irrigated crop rotation of lucerne, maize, and sugar beet should be practised.

10. Subsurface drainage system

10.1 Drainage criteria for unsteady-state conditions

One of the objectives of the research undertaken in the experimental fields was to assess drainage criteria that could be used in large-scale drainage and reclamation projects. To meet this objective, the following steps were taken:

- Study of the relation between crop yields and water table depth for irrigated summer crops and for winter cereal crops irrigated only in spring.
- Study of the relation, especially in winter, between water table depth and the mobility of agricultural machinery on the land.
- Study of the relation between heavy precipitation and the corresponding rise in water table.
- Study of the relation between percolation losses from irrigation and water table rise.

After these studies had been completed, drainage criteria for unsteady flow were derived to meet both the requirements of crops and the mobility of agricultural machinery.

The next step was to convert the unsteady-state criteria to steady-state criteria, these being easier to use in drainage projects.

Finally these criteria were compared with those assessed for the ini-

tial leaching requirements (Chap.9). This allowed the duration of the desal-
inization period to be predicted because the drainage system was designed
only to meet the requirements of irrigated agriculture.

10.1.1 Relation between crop yields and water table depth

To study the relation between crop yields and water table depth, data
from the Alera experimental field were used. The data covered the yields of
cereals and vetch grown during two consecutive winters (Figs.10.1, 10.2 and
10.3) and the yields of irrigated sugar beet, maize, and lucerne grown
during two consecutive summers.



Fig.10.1: View of wheat just before the heavy rainfalls of winter 1977.

TABLE 10.2: Crop yields in kg/ha and relative yield

	N o . o f D r a i n g r o u p				
	1	2	3	4	5
	clay	clay/gravel	PVC/gravel	PVC	PVC/straw
Wheat	5,250	5,250	5,600	4,570	4,570
	0.95	0.95	1.00	0.82	0.82
Barley	5,500	5,500	★	★	4,430
	1.00	1.00			0.81

★Crop yield affected by soil salinity

A comparison of Tables 10.1 and 10.2 shows that if the water table remained within the upper 50 cm for 3 consecutive days, no obvious harm was done to winter cereals. This was even true if the 3-day period coincides with the time of the crop's maximum development (i.e. tillering and ear formation stages). This conclusion could be drawn because the 5 per cent difference in yield between Drain Group 3 and Drain Groups 1 and 2 is not significant. There is, however, some evidence that if the water table remained within a depth of 50 cm for 9 or more consecutive days, the yield for both wheat and barley decreased from 15 to 20 per cent. These reductions were observed in the 1977 winter season notwithstanding a late-winter nitrogen application. Ammonium nitrate (33.5% N) at 200 kg/ha was applied when crops in areas with shallow water tables showed nitrogen deficiency symptoms. The yield reductions agree with the results obtained by SIEBEN (1974) in the IJssel Lake Polders. Sieben observed a reduced supply of nitrogen from the soil due to a slowing down of mineralization as a result of shallow winter water tables. In his experimental plots he observed that this reduction in the nitrogen supply could be compensated by an extra dressing of nitrogen.

An estimate of the relation between sugar beet yields and water table depth could be made by comparing the data of Tables 10.3 and 10.4. It seems that a period with a water table within a depth of 50 cm, for 3 consecutive days is not critical. This water table proved to be critical at the seedling stage in poorly drained plots (PVC/straw drains) making transplantation necessary at the singling stage.

TABLE 10.3: Number of consecutive days in which the water table was within the depth indicated in cm (irrigation season 1976)

	No. of Drain group											
	2			3			4			5		
	clay/gravel			PVC/gravel			PVC			PVC/straw		
	25	50	100	25	50	100	25	50	100	25	50	100
cm depth			cm depth			cm depth			cm depth			
April	-	3	15	1	6	15	-	8	15	1	9	30
May	-	-	8	-	-	21	-	3	31	-	5	31
June	-	3	17	1	3	21	-	-	27	-	-	30
July	1	6	10	1	3	20	-	-	31	-	1	31
August	-	-	12	-	4	19	-	1	29	-	3	31
September	-	7	10	-	9	15	-	8	30	-	8	30

TABLE 10.4: Sugar beet yield (in kg/ha) and relative yield (1976)

	No. of Drain group			
	2	3	4	5
	clay/gravel	PVC/gravel	PVC	PVC/straw
Yield* (kg/ha)	45,500	50,500	40,400	45,500
Relative yield	0.90	1.00	0.80	0.90

* Yields were only estimated because of difficulties in harvesting

These conclusions were confirmed during the 1977 irrigation season. A comparison of the data of Tables 10.5 and 10.6 shows that sugar beet grows well (Fig.10.4) if the water table is kept between 75 and 100 cm and, if it rises above this level, does not remain within the upper 50 cm of the soil for longer than 3 to 4 days.

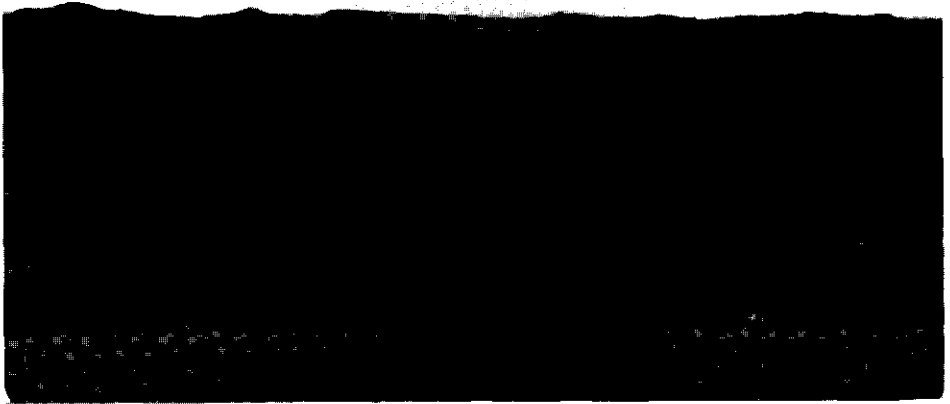


Fig.10.4: View of sugar-beet grown during the first irrigation season after the desalinization period.

TABLE 10.5: Number of consecutive days in which the water table was within the depth indicated (irrigation season 1977)

	No. of Drain group											
	6				7				8			
	PVC/esparto				PVC/coco				clay/gravel			
	25	50	75	100	25	50	75	100	25	50	75	100
cm depth												
June	1	6	20	50	-	4	20	30	-	3	6	24
July	1	2	11	31	-	2	11	31	-	2	3	31
August	1	2	8	31	-	1	4	30	1	2	4	22
September	1	2	5	30	-	1	3	19	-	1	2	18

TABLE 10.6: Crop yields and relative yields (1977)

	No. of Drain group		
	6	7	8
	PVC/esparto	PVC/coco	clay/gravel
Lucerne* (kg/ha)	1,235	1,685	2,160
	0.57	0.78	1.00
Sugar beet (kg/ha)	42,500	42,500	42,500
	1.00	1.00	1.00

*Two cuts of lucerne sown in spring 1977

Lucerne is more sensitive to high water tables (Table 10.6, Fig.10.5). Table 10.8 gives the hay yields obtained from lucerne sown the previous autumn in plots with different drainage conditions (Table 10.7).



Fig.10.5: Differences in drainage conditions after the heavy rainfalls of winter 1977 are obvious in a first year lucerne.

TABLE 10.7: Number of consecutive days in which the water table was within the depth indicated (irrigation season 1977)

	N o . o f D r a i n g r o u p															
	2				3				4				5			
	clay/gravel				PVC/gravel				PVC				PVC/straw			
	25	50	75	100	25	50	75	100	25	50	75	100	25	50	75	100
cm depth				cm depth				cm depth				cm depth				
June	4	5	6	20	5	6	10	30	5	9	22	30	5	20	30	30
July	2	3	4	10	2	3	10	31	1	10	25	31	1	19	31	31
August	2	4	5	16	3	6	10	31	2	14	28	31	3	24	30	31
September	2	4	5	7	3	4	8	23	3	8	17	30	3	8	14	30

TABLE 10.8: Lucerne yield* and relative yield (1977)

	N o . o f D r a i n g r o u p							
	2		3		4		5	
	clay/gravel		PVC/gravel		PVC		PVC/straw	
Yield (kg/ha)	12,195		7,600		5,780		5,415	
Relative yield	1.00		0.62		0.47		0.44	

*Five cuts of first year Lucerne, sown in autumn 1976

A good yield was obtained where the water table remained within the surface 25 cm for less than 3 days, within 50 cm for 4 to 5 days, and within 75 cm for 5 to 6 days (Fig.10.6). A significant yield decrease of 40 per cent occurred where the water table remained for 10 consecutive days within a depth of 75 cm and continuously within 100 cm. These results were confirmed by the yields of lucerne sown in spring 1977 (Table 10.6). The results obtained for maize in 1977 (Tab.10.9) are similar to those for lucerne (Tab. 10.8).

TABLE 10.9: Maize yield and relative yield (1977)

	N o . o f D r a i n g r o u p							
	2		3		4		5	
	clay/gravel		PVC/gravel		PVC		PVC/straw	
Yield (kg/ha)	5,800		4,000		1,730		1,180	
Relative yield	1.00		0.69		0.30		0.20	



Fig.10.6: Detail of the growth of the lucerne of Fig.10.5 in well-drained areas.

10.1.2 Relation between water table depth and mobility of agricultural machinery

The winter of 1976-1977 being wetter than usual, the water table remained near the soil surface in the worst drained areas. These conditions affected the seedbed operations for winter wheat.

Table 10.10 shows water table depths in three areas with different drainage conditions and their effect on the mobility of agricultural machinery for seedbed preparation (Fig.10.7).

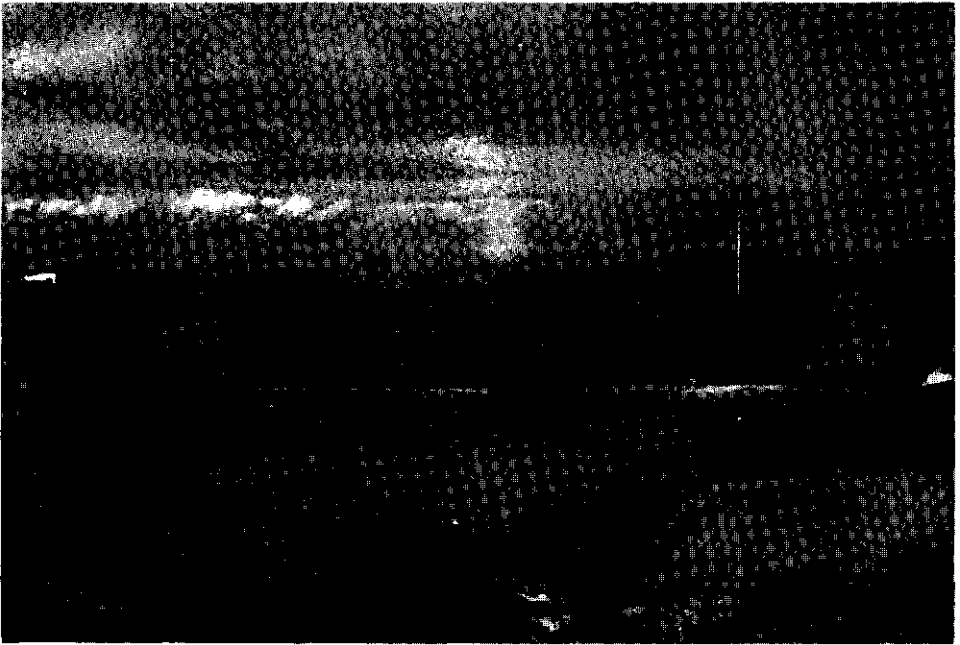


Fig.10.7: Differences in soil colour show distinct drainage conditions affecting mobility of agricultural machinery.

TABLE 10.10: Relation between water table depth and mobility of agricultural machinery (winter 1976-1977)

	No . of Drain group											
	6				7				8			
	PVC/esparto				PVC/coco				clay/gravel			
	25	50	75	100	25	50	75	100	25	50	75	100
cm depth				cm/depth				cm depth				
No. of days with water table within the indicated depth	3	16	29	31	3	13	25	31	-	1	8	18
Possibility of seed-bed preparation	negative				negative				positive			

From Table 10.10 it can be concluded that if the water table remains almost continuously within 75 cm, the mobility of agricultural machinery is impeded.

10.1.3 Rainfall distribution and water table rise

Data on maximum rainfall during 1 to 6 consecutive days expected for different return periods are shown in Table 10.11. These figures were derived from the depth duration frequency curves discussed in Chap.2.

TABLE 10.11: Maximum rainfall (in mm) distribution
(Gumbel analysis)

Return period (years)	C o n s e c u t i v e d a y s					
	1	2	3	4	5	6
1	14.5	24.5	29.0	33.0	36.0	38.0
2	40.0	54.0	58.5	62.5	65.5	67.5
5	55.0	72.0	76.5	79.0	82.5	85.5
10	67.5	82.0	88.0	92.0	95.0	98.0
20	79.0	97.0	100.0	103.0	106.5	109.5
100	101.0	121.0	124.5	127.0	131.5	135.0

The probability of long duration maximum rainfall is low since the precipitation to be expected in 4 to 6 consecutive days is scarcely more than that expected in 3 days, as shown in Table 10.11.

The Gumbel probability analysis was applied separately for the irrigation season from March to October. Table 10.12 gives the results obtained.

TABLE 10.12: Rainfall in mm during 3
consecutive days expected
in the irrigation season

Return period (years)	Rainfall (mm)
1	11.0
2	50.0
5	68.5
10	81.5
20	93.0
100	120.0

A comparison of Tables 10.11 and 10.12 shows that there is no marked seasonal distribution of heavy rainfall, although the rainfall of the autumn-winter season is slightly higher than that of spring-summer. Hence the annual values shown in Table 10.11 could be used to assess the winter drainage criteria.

Assuming that the water table is near drain level and that the moisture content of the unsaturated zone corresponds approximately to field capacity, it can be expected that the water table will rise to the soil surface at least once every 2 years. In fact, if the effective porosity is 4 per cent, the storage capacity of the soil profile above the average drain level (1.20 m) is approximately 50 mm. Although it is difficult to assess the soil moisture content before rainfall, it can be expected that irrigated soils will have a moisture content near field capacity during the autumn-winter season.

10.1.4 Relation between percolation losses from irrigation and water table rise

Observations made during two irrigation seasons (1976 and 1977) showed that water applications varied from 80 to 90 mm in the larger basins (300 × 50 m) where the slope is almost zero, while in smaller basins (180 × 50 m) where the slope of the furrows is 0.1 per cent the water application was about 60 mm.

The interval between two consecutive applications varied from 12 to 14 days during the summer season. In the smaller basins it was generally 1 or 2 days shorter.

The irrigation practice was similar for sugar beet, lucerne, and maize, except that sugar beet received one or two water applications more than lucerne in April, and maize was not irrigated in May.

Water losses were almost solely due to percolation, since little "tail water" (no more than a few mm) was left after an irrigation.

The application efficiency was lower in the larger irrigation basins ($e_a = 0.55$ to 0.60) than in the smaller ones ($e_a = 0.70$ to 0.75).

During the period of maximum water requirement, i.e. from mid-July to mid-August, the amount of water applied was about 90 mm every 11 days. The irrigation efficiency, however, was greater because the high evapo-transpiration (5 to 6 mm/day) increased the soil moisture deficit.

The water lost by percolation varied from 30 to 35 mm in the larger basins and from 15 to 20 mm in the smaller ones. If the entrance resistance of the drainage material was low, part of this water flowed directly into the drain trench. The amount of water recharging the groundwater was thus estimated at 25 to 30 mm for the larger basins. It caused the water table to rise by about 0.7 m (Fig.8.4).

10.1.5 Assessment of drainage criteria for unsteady-state conditions

Two periods were distinguished: the summer irrigation season and the winter season with spring irrigation.

Winter season

In the previous sections it was established that in winter the water table can remain within 50 cm for about 3 days without any appreciable reduction in the yield of cereals. However, if the water-logging lasted 9 days the yield was reduced by 15 to 20 per cent, which is a considerable loss. No harm was done if the water table remained within 25 cm for 1 or 2 days.

Soil conditions at the start of seed-bed preparation must be such that the movement of agricultural machinery is not impeded. Assuming that the critical water table depth to ensure such conditions is 65 cm and that seed-bed preparation should not be delayed longer than one week, the winter drainage criteria for unsteady flow as given in Table 10.13 could be applied.

TABLE 10.13: Winter drainage criteria for unsteady flow*

Drawdown of water table (from - to) (m)	h_o (m)	h_t (m)	t (days)
0.00 - 0.25	1.20	0.95	2
0.25 - 0.50	0.95	0.70	2
0.50 - 0.65	0.70	0.55	4

*Average drain depth = 1.20 m; $\mu = 0.04$

Summer season

If irrigation water is applied every 12 days and each time causes the water table to rise an average of 0.7 m, a gradual rise of the water table will occur unless the drainage system is capable of lowering the water table by 0.7 m during each irrigation interval.

To maintain an optimum moisture content of the rootzone during the irrigation season, the depth to the (fresh) groundwater should not be more than 1 m.

If the water table is approximately 0.8 m deep at the start of an irrigation, the maximum hydraulic head at the start of water table draw-down is:

$$h_o = h_t + \frac{R}{\mu} = 0.4 + 0.7 = 1.1 \text{ m} \quad (1)$$

As irrigated crops seem to tolerate a water table within a depth of 0.5 m for at least 3 days, the drainage criteria applicable during the irrigation season for unsteady flow were tentatively assessed as shown in Table 10.14.

TABLE 10.14: Unsteady-state drainage criteria for the summer season*

Drawdown of water table (from - to) (m)	h_o (m)	h_t (m)	t (days)
0.10 - 0.25	1.10	0.95	1
0.25 - 0.50	0.95	0.70	2
0.50 - 0.70	0.70	0.50	4
0.70 - 0.80	0.50	0.40	5

*Average drain depth is 1.20; $\mu = 0.04$

10.2 Drain spacing

With the use of the unsteady-state drainage criteria and the hydrological factors experimentally derived in Chap.8, the drain spacing was calculated with the Boussinesq equation:

$$L^2 = \frac{4.46 K h_o h_t t}{\mu(h_o - h_t)} \quad (2)$$

where

- L = drain spacing (m)
- K = hydraulic conductivity (m/day)
- h_o = hydraulic head midway between drains immediately after instantaneous recharge (m)
- h_t = hydraulic head midway between drains after t days (m)
- t = time (days)
- μ = drainable pore space (dimensionless)

Table 10.15 shows the drain spacings calculated with Eq.(2), using the criteria for both the winter and the summer season.

TABLE 10.15: Drain spacing computed by Eq.(2)*

Period	Drainage criteria			Hydrological factors		Drain spacing m
	h_o (m)	h_c (m)	t (day)	K (m/day)	μ	
Winter	1.20	0.95	2	1.0	0.04	32
	0.95	0.70	2	1.0	0.04	24
	0.70	0.55	4	0.6	0.04	26
Summer	1.10	0.95	1	1.0	0.04	28
	0.95	0.70	2	1.0	0.04	24
	0.70	0.50	4	0.6	0.04	22
	0.50	0.40	5	0.6	0.04	26

*Average drain depth = 1.20 m

An average drain depth of 1.20 m was assumed. This means that for laterals with a length of 200 m and a slope of 0.1 per cent, the initial drain depth is 1.1 m and the outlet to the collector drains is at 1.3 m. For the lateral drains to meet the drainage requirements of both the summer and winter season, they must be installed at a depth of 1.20 m and spaced at 25 m.

10.3 Drainage criteria for steady-state conditions

In the above calculation of drain spacing with unsteady-state criteria, the entrance resistance was not taken into account. In Chap.8, however, it was shown that the entrance resistance of some drainage and filter materials is high. Hence it was necessary to take the entrance resistance into account in calculating drain spacings. For this purpose, steady-state drainage equations with criteria corresponding to those defined earlier for unsteady-state conditions were used.

The steady-state criteria were derived from the Hooghoudt equation for drains located on an impervious layer:

$$s = \frac{4 K h^2}{L^2} \quad (3)$$

Introducing into Eq.(3) the mean h-values and their corresponding drain spacings and hydraulic conductivity values taken from Table 10.15 yielded the corresponding values of s. In this way the steady-state criteria equivalent to those for the actual unsteady-state conditions were derived (Table 10.16).

TABLE 10.16: Conversion of drainage criteria*

Period	Unsteady-state conditions			Steady-state conditions		
	h_o (m)	h_t (m)	t (days)	average water table depth (m)	h (m)	s (mm/day)
Winter	1.20	0.95	2	0.1	1.1	4.7
	0.95	0.70	2	0.4	0.8	4.4
	0.70	0.55	4	0.6	0.6	1.3
Summer	1.10	0.95	1	0.2	1.0	5.1
	0.95	0.70	2	0.4	0.8	4.4
	0.70	0.50	4	0.6	0.6	1.8
	0.50	0.40	5	0.7	0.5	0.9

*Average drain depth = 1.2 m; $\mu = 0.04$

From Table 10.16 an average s/h relation for steady-state conditions of 3.9×10^{-3} was obtained. Table 10.17 gives values of s, h, and water table depth corresponding to this s/h relation.

TABLE 10.17: Drainage criteria for steady-state conditions*

Water table depth (m)	h (m)	s (mm/day)
0.25	0.95	3.7
0.50	0.70	2.7
0.75	0.45	1.8
1.00	0.20	0.8

*Average drain depth = 1.2 m; $\mu = 0.04$

A water table depth of 0.5 m under steady-state conditions means that the hydraulic head midway between drains is 0.7 m and the discharge 2.7 mm/day, or 33 mm in 12 days, which agrees with the drainage requirements in the summer season.

If in the initial leaching period the average drain discharge is 3 mm/day, approximately 11 months would be required to drain 1 000 mm of leaching water, which seems reasonable in view of the leaching requirements calculated in Chap.9. Hence, the criteria developed for the cropping period also yield satisfactory drainage conditions for the desalinization process.

10.4 Drain spacings required for different combinations of drainage and filter materials

10.4.1 Steady flow

Since the entrance resistance must be taken into account, the Ernst equation (Ernst, 1962) could be used to calculate drain spacings. According to the Ernst theory for steady flow, the hydraulic head can be divided into three components corresponding to vertical, horizontal, and radial flow. To these a fourth component, corresponding to the entrance flow, was added:

$$h = h_v + h_h + h_r + h_i \quad (4)$$

The general expression of the Ernst equation is:

$$h = s \frac{D_v}{K_v} + s \frac{L^2}{8 KD} + s L W_r + s L W_e \quad (5)$$

where

h = hydraulic head midway between drains (m)

s = discharge (m/day)

- D_v = average thickness with regard to vertical flow (m)
 K_v = hydraulic conductivity for vertical flow (m/day)
 L = drain spacing (m)
 KD = transmissivity (m^2/day)
 W_r = radial resistance (day/m)
 W_e = entrance resistance (day/m)

In the soils of the Alera experimental field the vertical and radial flow components are negligible, the flow being restricted to the profile above drain level. Equation (5) thus reads:

$$h = h_h + h_i = s \frac{L^2}{8 KD} + s L W_e \quad (6)$$

For drains located on an impervious layer, D equals $h/2$ and Eq.(6) changes to

$$h = s \frac{L^2}{4 Kh} + s L W_e \quad (7)$$

Equation (7) was used to calculate drain spacings for different combinations of drainage and filter materials. For this calculation the drainage criteria for steady flow assessed in the previous section and the entrance resistances calculated in Chap.8 were used. Table 10.18 shows the results.

TABLE 10.18: Relation between entrance resistance and drain spacing according to Eq.(7)

	No. of Drain group					
	1 clay	2,8 clay/gravel	3 PVC/gravel	4 PVC	6 PVC/esparto	7 PVC/cocos
W_e (day/m)	5.2	2.1	4.6	12.8	16.0	21.7
L (m)	16.0	18.0	16.5	12.0	10.5	8.5
Drain density (m/ha)	625.0	555.5	606.0	833.0	952.5	1176.5

$$\ln \frac{h_t}{h_o} = - \frac{t}{\mu L W_e} = - \alpha t \quad (13)$$

with $\alpha = 1/\mu L W_e$, known as the reaction factor.

Then again it holds that

$$h_t = h_o e^{-\alpha t} \quad (14)$$

Solving Eq.(13) for L yields a formula that enables drain spacings to be calculated for unsteady flow through a high resistance:

$$L = \frac{t}{\mu W_e \ln(h_o/h_t)} \quad (15)$$

Table 10.20 shows the results obtained with Eq.(15).

TABLE 10.20: Relation between entrance resistance and drain spacing according to Eq.(15)

Type of drains	W_e (day/m)	Drainage criteria			L (m)	Remarks
		h_o (m)	h_t (m)	t (day)		
PVC	12.8	1.20	0.95	2	16.7	
		0.95	0.70	2	12.8	critical
PVC/ esparto	16.0	1.20	0.95	2	13.4	
		0.95	0.70	2	10.2	critical
		0.70	0.55	4	25.9	
PVC/coco	21.7	1.20	0.95	2	9.9	
		0.95	0.70	2	7.6	critical
		0.70	0.55	4	19.1	

The results obtained from the different calculation methods (Tables 10.18 to 10.20) show a good agreement. They all reveal that if drainage and filter materials of high entrance resistance are used, the drain density (m/ha) is twice that needed with drains of low entrance resistance. Moreover, materials with a high entrance resistance involve more risk of failure than good materials that allow a wider spacing. If the entrance resistance of some drains is double the average amount, such drains would be a practical failure. If there were a tendency for W_e to increase with time, as is probably so with PVC/esparto drains, the situation would be even worse.

In choosing drainage and filter materials a decision in favour of low entrance resistance drains is the obvious one, even if the costs are higher, since these will be offset by a lower drain density.

List of symbols

SYMBOL	DESCRIPTION	DIMENSION
A	cross-sectional area (m ²)	L ²
a	geometric factor, constant	dimensionless
B	drain length (m)	L
b	bottom width of channel (m) constant	L dimensionless
C	salt concentration (meq/litre) correction for drain spacing (m)	L
c	hydraulic resistance of semipervious layer for vertical flow (day)	T
D	thickness of aquifer or saturated layer (m) thickness of layer below drain level (m)	L L
d	thickness of equivalent depth in Hooghoudt equation; inside diameter of pipe drain (m)	L
D'	thickness of layer through which vertical flow occurs (m)	L
Dr _a	amount of artificial drainage (mm) rate of artificial drainage (mm/day)	L LT ⁻¹
E	amount of evapotranspiration (mm) rate of evapotranspiration (mm/day)	L LT ⁻¹
EC	electrical conductivity (mmhos/cm)	ohm ⁻¹ cm ⁻¹
ESP	exchangeable sodium percentage	dimensionless
e	base of natural (Napierian) logarithm	dimensionless
e _a	field irrigation efficiency	dimensionless
f	leaching efficiency coefficient in regard to irrigation water	dimensionless
G	amount of capillary rise of groundwater (m) rate of capillary rise (mm/day)	L LT ⁻¹
h	hydraulic head; height of water table above drain level midway between drains (m)	L
h _h	component of the hydraulic head due to horizontal flow (m)	L

SYMBOL	DESCRIPTION	DIMENSION
h_i	component of the hydraulic head due to entrance flow (m)	L
h_o	height of water table above drain level midway between drains after instantaneous recharge (m)	L
h_r	component of the hydraulic head due to radial flow (m)	L
h_t	height of water table above drain level midway between drains at any time t (m)	L
h_v	component of the hydraulic head due to vertical flow (m)	L
$\overline{\Delta h}$	average fall of water table between drains (m)	L
I	effective amount of irrigation water (mm)	L
I_{bas}	basic infiltration rate (mm/day)	LT^{-1}
i	hydraulic gradient	dimensionless
j	reservoir coefficient (day)	T
K	hydraulic conductivity (m/day)	LT^{-1}
K'	hydraulic conductivity for vertical flow (m/day)	LT^{-1}
K_a	hydraulic conductivity of the layer above drain level (m/day)	LT^{-1}
K_b	hydraulic conductivity of the layer below drain level (m/day)	LT^{-1}
KD	transmissivity of water-bearing layer (m^2/day)	L^2T^{-1}
L	drain spacing (m)	L
L_o	drain spacing for horizontal flow (m)	L
n	number; Manning roughness coefficient	dimensionless
P	effective amount of precipitation (mm) precipitation (mm/day)	L LT^{-1}
pF	logarithm of the water tension in cm water column	dimensionless
Q	discharge (m^3/s) rate of flow through a system (l/s)	L^3T^{-1} L^3T^{-1}
q	discharge per unit length (m^2/day)	L^2T^{-1}
R	amount of deep percolation (mm) percolation rate (mm/day) hydraulic radius (m)	L LT^{-1} L
R^*	amount of net downward percolation leaching requirement (mm) net percolation rate (mm/day)	L LT^{-1}

SYMBOL	DESCRIPTION	DIMENSION
r	radius (m)	L
	correlation coefficient	dimensionless
RSC	residual sodium carbonate value (meq/l)	
S	amount of seepage (mm)	L
	seepage (mm/day)	LT ⁻¹
SAR	sodium adsorption ratio	dimensionless
s	specific discharge; drain discharge per unit area (mm/day)	LT ⁻¹
s _t	ordinate of s-hydrograph (mm/day)	LT ⁻¹
T	time of residence (s;day)	T
	return period (year)	T
t	time, period (s;day)	T
u	wetted perimeter of drain (m)	L
V	volume of reservoir (m ³)	L ³
v	flow velocity (m/day)	LT ⁻¹
v _z	flow density (m/day)	LT ⁻¹
W _{fc}	soil moisture content at field capacity (mm)	L
W _e	entrance resistance (day/m)	L ⁻¹ T
W _r	radial resistance (day/m)	L ⁻¹ T
x, y, z	cartesian coordinates (m)	L
x	distance variable (m)	L
y	hydraulic head function at a distance x from the drain; water depth in channel (m)	L
α	angle	degree
δ	partial derivative sign	dimensionless
Δ	small increment of	dimensionless
μ	effective porosity; drainable pore space	dimensionless

Literature

- BERNSTEIN, L. 1974. Crop growth and salinity. Drainage for Agriculture, Agronomy 17. Madison.
- BOUSSINESQ, M.J. 1904. Recherches théoriques sur l'écoulement des nappes d'eau infiltrées dans le sol et sur le débit des sources. Journal des Mathématiques Pures et Appliquées, 10, 1-78.
- BOUWER, H. 1974. Developing drainage design criteria. Drainage for Agriculture. Agronomy 17. Madison.
- BRAUN-BLANQUET and O.DE BOLOS. 1957. Les groupements végétaux du Bassin Moyen de l'Ebro et leur dynamisme. Anales de la Estación Experimental de Aula Dei. Zaragoza.
- BURINGH, P. 1960. Soils and soil conditions in Iraq. Wageningen.
- . 1970. Halomorphic soils. Introduction to the study of soils in tropical and subtropical regions. PUDOC. Wageningen.
- CAVELAARS, J.C. 1974. Subsurface field drainage systems. Drainage Principles and Applications. Publ.16, Vol.IV. ILRI, Wageningen.
- DE LOS RIOS, F. 1966. Colonización de las Bardenas, Cinco Villas, Somontano y Monegros. Institución Fernando El Católico, Zaragoza.
- DE MEESTER, T. 1970. Soils of the Great Konya Basin, Turkey. PUDOC, Wageningen.
- DE RIDDER, N.A. 1974. Groundwater survey. Drainage Principles and Applications. Publ.16, Vol.III. ILRI, Wageningen.
- DIELEMAN, P.J. (Ed.) 1963. Reclamation of salt affected soils in Iraq. Soil hydrological and agricultural studies. ILRI, Publ.11. Wageningen.
- . 1974. Deriving soil hydrological constants from field drainage tests. Drainage Principles and Applications. Publ.16, Vol.III. ILRI, Wageningen.

- DRIESSEN, P.M. 1970. Soil salinity and alkalinity in the Great Konya Basin, Turkey. PUDOC, Wageningen.
- ELIAS CASTILLO, F., JIMENEZ ORTIZ, R. 1965. Evapotranspiraciones potenciales y balances de agua en España. Mapa Agronómico Nacional. Madrid.
- FAO/UNESCO. 1973. Irrigation, Drainage and Salinity. An International source book. London.
- GOUSEN. 1967. Aerial photo-interpretation in soil survey. Soils Bulletin No.6. FAO, Rome.
- HERNANDEZ PACHECO, E. 1949. Las Bardenas Reales. Rasgos fisiográficos y geológicos. Institución Príncipe de Viana No.XXXVII. Pamplona.
- IGME. Mapa Geológico de España 1:1 000 000. Síntesis geológica 1:200 000. Hojas y Memorias del Mapa Geológico de España 1:50 000: Ejea, Sádaba, Sos y Tauste. Instituto Geológico y Minero de España. Madrid.
- ILRI. 1964. Code of practice for the design of open water courses and ancillary structures. Bulletin 7. International Institute for Land Reclamation and Improvement. Wageningen.
- . 1972. Veldboek. Fieldbook for land and water management experts. Wageningen.
- IRYDA. 1973/1975. Reconocimiento detallado de los suelos de la Zona Regable de las Bardenas. Zaragoza y Navarra. Sección de Suelos del Instituto Nacional de Reforma y Desarrollo Agrario. Madrid.
- KESSLER, J. 1973. Field drainage criteria. Drainage Principles and Applications. Publ.16, Vol.II. ILRI, Wageningen.
- , DE RAAD, S.J. 1974. Analyzing rainfall data. Drainage Principles and Applications. Publ.16, Vol.III. ILRI, Wageningen.
- OOSTERBAAN, R.J., KESSLER, J. 1974. Determining hydraulic conductivity of soils. Drainage Principles and Applications. Publ.16, Vol.III. ILRI, Wageningen.
- RHOADES, J.D. 1974. Drainage for salinity control. Drainage for Agriculture. Agronomy 17. Madison.

- RICHARDS, L.A. (Ed.) 1954. Diagnosis and improvement of saline and alkaline soils. Agr.Handbook 60. USDA, Washington D.C.
- SAENZ GARCIA, C. 1942. Estructura general de la Cuenca del Ebro. Estudios Geográficos. Año III. Tomo 7. Madrid.
- SIEBEN, W.H. 1974. Effect of drainage conditions on nitrogen supply and yield of young loamy soils in the IJsselmeerpolders. Den Haag.
- SOIL SURVEY STAFF. 1951. Soil Survey Manual. Agr.Handbook 18. USDA, Washington D.C.
- . 1975. Soil Taxonomy. Agr.Handbook 936. Washington D.C.
- SOLE SABARIS. 1954. Sobre la estratigrafía de las Bardenas y los límites del Oligoceno y Mioceno en el Sector Occidental de la depresión del Ebro. Real Sociedad Esp. de Historia Natural. Madrid.
- TALSMA, T. 1963. The control of saline groundwater. Mededelingen van de Landbouwhogeschool. Wageningen.
- VAN DER MEER, K., MESSEMAECKERS VAN DE GRAAFF. 1974. Hydropedological Survey. Drainage Principles and Applications. Publ.16, Vol.III. ILRI, Wageningen.
- VAN DER MOLEN, W.H. 1972. Water management (drainage). Syllabus M.Sc. Course on Soil Science and Water Management. Agric.University, Wageningen.
- . 1972. Non-steady groundwater flow. Syllabus M.Sc.Course on Soil Science and Water Management. Agric.University, Wageningen.
- and J.W.van HOORN. 1976. Salt balance and leaching requirement. Syllabus of the 15th International Course on Land Drainage. ILRI, Wageningen.
- VAN HOORN, J.W. 1960. Groundwater flow in basin clay soil and the determination of some hydrological factors in relation with the drainage system. PUDOC, Wageningen.
- . 1974. Drainage of heavy clay soils. Drainage Principles and Applications. Publ.16, Vol.IV. ILRI, Wageningen.
- VEENENBOS, J.S. 1972. Soil Maps and Soil Survey Interpretation. Syllabus of the M.Sc.Course on Soil Science and Water Management. Agric.University, Wageningen.

WESSELING, J. 1973. Subsurface flow into drains. Drainage Principles and Applications. Publ.16, Vol.II. ILRI, Wageningen.

WITHERS, B., and VIPONS, S. 1954. Irrigation design and practice. Batsford. London.

Summary

Chapter 1

The Ebro basin is situated in north-eastern Spain and forms a geographic unit bounded by high mountains. The Bardenas area lies in the Ebro basin and forms part of the Bardenas Alto - Aragón irrigation scheme, which was designed to make use of the surface water resources from the Pyrenees.

Chapter 2

The Ebro basin is a tertiary sedimentation basin in which the Ebro river and its main tributaries have incised alluvial valleys. The tertiary sediments consist mainly of mudstone, locally with interbedded gypsum layers, and very fine siltstone. Both sedimentary rocks are fine textured and, because they were deposited in a brackish lacustrine environment, contain harmful soluble salts.

The main landscape-forming processes were erosion, transport, and deposition under semi-arid climatic conditions. The highest parts of the landscape consist of old tertiary formations which form the uplands of a dissected plain. At a lower level mesas occur, which consist of coarse alluvium covering the underlying tertiary sediments. Most of the eroded sediments were removed from the area but local sedimentation also occurred. Owing to the semi-arid conditions, both sediments and salts were deposited. The highest salt concentrations are found in the lowest parts of the alluvial formations, especially where the alluvium was derived from the eroded mudstone and siltstone. Between the residual uplands and the low-lying alluvial formations, piedmont and colluvial slopes occur.

Within the Bardenas area ten major physiographic units were defined, each of them subdivided into minor components and indicated on the soil map.

The Ebro basin is the driest part of northern Spain. The climate is semi-arid and becomes drier from the borders to the centre of the depression.

The seasonal variation in temperature is great. Potential evapotranspiration exceeds total precipitation, which is extremely variable and is not concentrated in distinct rainy seasons. Wind velocity is high and both cold and warm dry winds are common. Evaporation thus occurs even in winter when temperatures are low.

A great part of the area is cultivated, so that natural vegetation is restricted to residual and eroded soils not used for agriculture and to salt-affected soils where halophytes grow.

Irrigated farming is influenced by soil conditions. Salt-free soils are under full irrigation, the main crops being maize, lucerne, sugar beet, and some horticultural crops.

The cropping pattern on the saline soils depends on the degree of salinity. Barley and sugar beet are grown on moderately saline soils and lucerne on successfully leached soils. On the higher lands, not under the command of the irrigation scheme, barley is grown.

Chapter 3

The study area comprises two drainage basins. The northern part drains to the Aragón river, the southern part to the Riguel river, which is a tributary of the Arba river.

Drainage and salinity of the groundwater depend on the situation of each geomorphological unit and its relation to adjacent units. The groundwater in the fluvio-colluvial formations of the northern basin is shallow and highly saline. An ephemeral perched water table is found in the mesas,

where the groundwater is non-saline. No shallow water table was found in other physiographic units.

The irrigation water is of good quality as its EC is at the lower end of the C_2 -range. The SAR is also in the lowest range S_1 and the RSC is zero, so there is no danger of alkalinization.

Chapter 4

The physiographic approach was used to prepare the soil map. Each mapping unit is a broad association of soils having similar salinity hazards and possibilities of reclamation.

Five main soil associations were distinguished:

a) The residual soils of the siltstone outcrops, which have only a thin surface horizon overlying the hard siltstone.

b) The soils of the mesas, which consist of a reddish loamy surface horizon overlying semi-consolidated coarse alluvium rich in calcium-carbonate but free of other salts. This in turn overlies the impervious mudstone. Texture and depth of the soil profile vary. Where moderately deep soils occur, a prosperous irrigated agriculture flourishes.

c) The soils of the piedmont and colluvial slopes were developed from a mixture of fine colluvium and material from the underlying tertiary sediments. They are generally deep and fine textured and have an intrinsic, though variable, salinity, increasing with depth. Because of the low permeability and the salinity of the subsoil, the most suitable irrigation method is sprinkling.

d) The non-saline soils of the alluvial valleys of the main rivers. Soil conditions vary greatly, but the older terrace soils are usually shallower and less suitable for irrigation than the youngest deeper (alluvial) soils. In general, prosperous irrigated agriculture exists on these soils.

e) The saline alluvial and fluvio-colluvial soils of valleys and fans, whose parent material was derived from denudation of the tertiary sediments. Soil conditions and the degree of salinity vary in each mapping unit, and consequently the possibilities of reclamation vary as well.

Piezometers were installed to monitor the water table. Precipitation was measured, as were the amounts of irrigation and drainage water. Soil samples were taken at fixed sites to determine the salinity during the leaching process.

Chapter 8

At the Valareña field, water flowed directly into the drain trench through the upper layer of soil, in which the stratification had been disrupted by levelling and subsoiling. Below this layer, there was no percolation of water and therefore no desalinization. These soils cannot be leached merely by the provision of a drainage system but also require deep subsoiling.

At the Alera field, unsteady groundwater flow prevailed. At the end of tail recession, flow conditions approached those of steady flow. The discharge/hydraulic head relation had a parabolic shape showing that flow was restricted to the soil above drain level because the drains had been placed just above the impervious layer.

The Boussinesq theory was very suitable to study the drainage of the Alera field. At the end of tail recession, if the term for flow below drain level was disregarded, the Hooghoudt equation could be applied.

Drainable pore space was determined from the fall of the water table and the amount of drainage water during periods of low evapotranspiration. An average value of 4 per cent was found.

The hydraulic conductivity was calculated from the discharge/hydraulic head relation using the Boussinesq and Hooghoudt equations for periods of low evapotranspiration. In general good agreement was found among the values obtained. It could thus be concluded that:

- Hydraulic conductivity decreases with depth, becoming negligible below drain level.
- The hydraulic conductivity between a depth of 0.5 m and drain level equals about 0.6 m/day, and is about 1.5 m/day in the upper layer.

- For high water table conditions, the average hydraulic conductivity of the soil profile is 1 m/day.

A comparison of hydraulic conductivity values obtained with field and laboratory methods and those obtained from the discharge/hydraulic head relation showed that:

- The results obtained with the auger hole method ($K \approx 0.2$ m/day) were lower than those derived from the discharge/hydraulic head relation.

- No satisfactory results were obtained from the inversed auger hole measurements above the water table.

- The results obtained from laboratory measurements in undisturbed soil cores showed the anisotropy of the soil.

The entrance resistance (W_e) of different combinations of drainage and filter materials was calculated from the drain discharge and the head loss of the water table measured in the drain trench (h_1). Another method, by which the head loss in the trench was calculated from the shape of the water table was also applied. Both methods gave similar results, yielding the following conclusions:

- The W_e -values remained fairly constant with time, except for plastic pipes with an envelope of esparto or coconut fibre for which an increase in W_e was observed.

- The best combination was clay pipes with a gravel cover ($W_e = 2$ day/m).

- Corrugated PVC-pipes with gravel covering and clay pipes without gravel may be used also ($W_e = 5$ day/m).

- Corrugated plastic pipes without a filter gave less satisfactory results ($W_e = 13$ day/m).

- Plastic pipes with coconut fibre and esparto filters showed an even higher W_e than plastic pipes without a filter.

- Barley straw is an unsuitable cover material since it rots easily and clogs the pipe.

Chapter 9

The desalinization of the Alera field started with an initial leaching, followed by the irrigated cultivation of moderately salt-resistant crops.

The leaching efficiency coefficient was determined by comparing the actual desalinization process with theoretical models. Thus the leaching requirement could be predicted for different initial salt contents.

To exclude the influence of slightly soluble salts, the desalinization curves were drawn in terms of chloride content. The correlation between chloride percentage and electrical conductivity was high.

The following conclusions emerged from the study of the leaching process:

- The leaching efficiency coefficient was not constant but increased with depth.
- The leaching efficiency coefficient was higher at the beginning of the desalinization process and decreased gradually as the soil became less saline.
- The calculated values reflected the differences in soil structure.
- An average value of 0.5 was determined for the upper layer (0-50 cm), and a value of 1.0 for the deeper layer (50-100 cm).
- The initial salinity was related to soil physical properties (infiltration rate and permeability) which, in turn, were dependent on the compactness of the soil.
- For an initial EC_e of 15 mmhos/cm, approximately 1000 mm of percolation water are required, which meant 1100 to 1400 mm of irrigation water. The leaching period could last up to 8 months, from early autumn to late May.
- Deep subsoiling and local gypsum applications improved the structure of the upper soil layer.
- The leaching of saline soils could be split into two phases: an initial leaching of the upper layer, followed by the irrigated cultivation

of a moderately salt-resistant crop (sugar beet), during which percolation losses leached the deeper layers.

- There was no risk of alkalization during the leaching period.
- To prevent secondary salinization after reclamation, good drainage conditions must be maintained and an irrigated crop rotation practised.

Chapter 10

From the relation between the depth of the water table, crop growth, and the mobility of agricultural machinery on the soil, and from a study of the groundwater regime in winter and during the irrigation season drainage criteria for unsteady-state conditions were derived. These criteria were converted to steady-state criteria for easier use in drainage projects.

The following conclusions could be drawn from the study:

- Little harm is done to winter cereals if a water table remains within a depth of 50 cm for no more than 3 consecutive days.
- With a water table between 75 and 100 cm, sugar beet grows well and is not harmed if a water table is within the top 50 cm for 3 to 4 consecutive days.
- Lucerne is more sensitive than sugar beet to high water tables. For good yields, a water table must not remain longer than 3 days within the top 25 cm of soil, 4 or 5 days within the top 50 cm, and 5 or 6 days within the top 75 cm.
- A water table depth shallower than 65 cm prevents the movement of machinery and hampers seed-bed preparation in winter.

The following drainage criteria were assessed:

- a) In winter, a water table drawdown from the soil surface to a depth of 0.65 m in 8 days.
- b) In the irrigation season, a water table rise of 0.7 m caused by irrigation losses must be lowered in the 12 days between two consecutive irrigations, and must be deeper than 0.7 m after 7 days.

Applying these criteria in the Boussinesq equation for unsteady flow and using the values for hydraulic conductivity and drainable pore space determined at the experimental field, a spacing of 25 m for drains installed at a depth of 1.2 m was obtained.

Equivalent drainage criteria for steady flow are a minimum depth of 0.5 m for the unsaturated zone, with a corresponding hydraulic head midway between drains of 0.7 m and a drain discharge of 3 mm/day.

If the entrance resistance was taken into account, the Ernst equation for steady flow and the Hellinga/de Zeeuw equation for unsteady flow could be used in calculating the drain spacing. The results obtained by both approaches agree well and allowed the following conclusions:

- For drainage and filter materials with a high entrance resistance, the drain density (m/ha) required becomes twice that needed for materials with low entrance resistance.

- Material with high entrance resistance involves much more risk of failure than a wider spacing with good material.

Resumen

Capítulo 1

La cuenca del Ebro está situada en el nordeste de España y forma una unidad geográfica rodeada por altas montañas. La zona de las Bardenas está situada en la cuenca del Ebro y forma parte del plan de riegos Bardenas-Alto Aragón, proyectado para el aprovechamiento de los recursos hidráulicos procedentes de los Pirineos.

Capítulo 2

La depresión del Ebro es una cuenca de sedimentación terciaria en la que el río Ebro y sus afluentes principales han formado valles aluviales. Los sedimentos terciarios consisten en margas limosas, a veces con capas de yeso intercaladas y areniscas de grano muy fino. Las dos rocas sedimentarias son de textura fina y contienen sales solubles debido a que fueron depositadas en un medio lacustre salobre.

El principal proceso remodelador del paisaje ha sido la erosión seguida de transporte y deposición bajo condiciones climáticas semiáridas. Las formaciones terciarias más antiguas ocupan las posiciones más altas del paisaje, formando las tierras altas de una llanura diseccionada. A un nivel más bajo existen mesas formadas por un aluvio grueso que descansa sobre sedimentos terciarios subyacentes. La mayor parte de los sedimentos erosionados fueron transportados fuera del área, pero también ha habido sedimentación local. Debido a las condiciones semiáridas, tanto los sedimentos como las sales transportadas fueron depositadas juntas. Por tanto las mayores concentraciones de sales se encuentran en las partes más bajas de las formaciones aluviales, especialmente en las que el aluvio procede de las margas y areniscas erosionadas. Entre las tierras altas residuales y las formaciones aluviales más bajas existen laderas de piedemonte y laderas coluviales.

e) Los suelos salinos aluviales y fluvio-coluviales de los valles y abanicos, en los que el material parental procede de la denudación de los sedimentos terciarios. Las condiciones de los suelos y el grado de salinidad varían en cada unidad cartográfica y consecuentemente las posibilidades de recuperación varían también.

Capítulo 5

El origen de las sales es por tanto la salinidad intrínseca de estos materiales parentales y la salinización secundaria en zonas que reciben agua y que carecen de drenaje natural. Bajo riego la movilización y redistribución de sales continúa y ciertamente aumenta.

Los suelos salinos de la zona están afectados principalmente por cloruro sódico, componente dominante en todas las muestras. Además en la cuenca norte existen sulfato de calcio y magnesio, mientras que en la sur, los cloruros de calcio y magnesio predominan sobre los sulfatos.

El SAR aumenta a medida que la EC lo hace. La alcalinidad del suelo puede considerarse como un reflejo de la salinidad, ya que los suelos muy salinos son sódicos también. Suelos alcalinos no-salinos no han sido encontrados y valores de pH mayores de 8.5 no existen.

Los resultados sobre la tolerancia de los cultivos a la salinidad, obtenidos en pruebas de campo corresponden bien con los niveles de tolerancia generalmente aceptados.

La utilización permanente de los suelos ligeramente salinos puede asegurarse manteniendo el sistema de drenaje actual de zanjas abiertas y drenes interceptores, y manteniendo los suelos bajo riego total. Las pérdidas por percolación inherentes al riego de gravedad son suficientes para lavar las sales depositadas en la zona radicular.

El riego por aspersion es una solución apropiada para los suelos de las laderas, ya que no requiere nivelación y las pequeñas cantidades de agua de riego que se aplican reducen las filtraciones de agua salina. El sistema de drenaje requerido se reduce a un dren interceptor entre la ladera y el valle adyacente.

Capítulo 6

Los suelos aluviales salinos requieren recuperación. Para ello debe instalarse un sistema de drenaje, y a continuación practicar un lavado inicial para reducir el contenido de sales.

Como no había experiencia local sobre los procesos de drenaje y desalinización, se llevó a cabo un proceso experimental de recuperación. En consecuencia se seleccionaron dos fincas experimentales.

La finca de Alera representa los suelos mal drenados de las formaciones fluvio-columviales de la cuenca norte. Son suelos arcillo-limosos cuya porosidad y permeabilidad decrece con la profundidad. Por debajo de una profundidad media de 1,5 m el suelo llega a ser casi impermeable. La salinidad aumenta con la profundidad, llegando a ser de 20 a 35 mmhos/cm en la capa menos permeable. En la capa superficial la variación es mayor.

La finca de Valareña representa los suelos salinos de los valles y abanicos aluviales de la cuenca de drenaje sur. Son suelos franco-arcillo-limosos con una marcada estratificación muy fina. A una profundidad media de 2,5 m existe un aluvio grueso saturado de agua muy salina, que descansa sobre una marga impermeable. Debido a la estratificación la conductividad hidráulica es anisotrópica. La salinidad del suelo está distribuida más uniformemente que en los suelos de Alera.

El proceso de recuperación consistió en las fases siguientes:

- a) Diseño teórico del sistema de drenaje, basado en las propiedades hidrológicas del suelo medidas por métodos de campo convencionales y en criterios de drenaje supuestos.
- b) Realización del sistema diseñado en las parcelas experimentales.
- c) Recopilación de los datos de campo y determinación de las propiedades hidrológicas del suelo y de los criterios de drenaje reales.
- d) Diseño del sistema de drenaje definitivo que pueda ser la base de las recomendaciones para la recuperación de suelos salinos con condiciones similares.

lares, deduciéndose las siguientes conclusiones:

- Los valores de W_e permanecieron constantes, excepto en la tubería de plástico con envolvente de fibra de coco y esparto en los que se observó un incremento de W_e .
- La mejor combinación consiste en tubería de cerámica con filtro de grava ($W_e = 2$ días/m).
- También pueden utilizarse tuberías de PVC corrugado con filtro de grava y tuberías de cerámica sin grava ($W_e = 5$ días/m).
- La tubería de PVC corrugado sin filtro ha mostrado resultados menos satisfactorios ($W_e = 13$ días/m).
- Las tuberías de plástico con filtros de esparto y coco han mostrado una resistencia aún más alta que las tuberías sin filtro.
- La paja de cebada no es adecuada como material envolvente ya que se descompone fácilmente y obtura la tubería.

Capítulo 9

El proceso de desalinización de los suelos de la finca de Alera comenzó con un lavado inicial seguido de riego de cultivos resistentes a la salinidad.

El coeficiente de eficacia de lavado fué determinado por comparación del proceso de desalinización real con modelos teóricos. De este modo pueden hacerse predicciones de las necesidades de lavado para diferentes contenidos salinos iniciales.

Para evitar la influencia de sales ligeramente solubles las curvas de desalinización fueron dibujadas en términos de contenido de cloruros. La correlación entre el porcentaje de cloruros y la conductividad eléctrica es alta.

Del estudio del proceso de lavado se dedujeron las siguientes conclusiones:

- El coeficiente de lavado no fué constante, sino que aumentaba con la profundidad.
- El coeficiente de lavado fué mayor al comienzo del proceso de desalinización y decreció gradualmente a medida que el suelo era menos salino.
- Los valores calculados reflejaron las diferencias en estructura del suelo.
- En la capa superficial (0 - 50 cm) se determinó un valor medio de 0.5, y para la capa muy profunda (50 - 100 cm) un valor de 1.0.
- El nivel de salinidad inicial estaba relacionado a propiedades físicas del suelo (velocidad de infiltración y permeabilidad), que dependen a su vez de la compacidad del suelo.
- Para una EC_e inicial de 15 mmhos/cm se necesitan unos 1.000 mm de agua de percolación, lo que significa de 1.100 a 1.400 mm de agua de riego. El periodo de lavado puede durar unos 8 meses, desde el comienzo del otoño hasta finales de Mayo.
- Un subsolado profundo en unión de aplicaciones locales de yeso, mejoraron la estructura de la capa superior del suelo.
- El lavado de suelos altamente salinos podrá dividirse en dos fases: un lavado inicial de la capa superficial, seguido de cultivo de plantas moderadamente resistentes a la salinidad (remolacha azucarera), durante el cual las pérdidas por percolación continúan el lavado de las capas más profundas.
- No hubo riesgo de alcalinización durante el período de lavado.
- Para impedir la salinización secundaria después de la recuperación, deben mantenerse condiciones de drenaje libre y debe practicarse una rotación de cultivos bajo riego.

Capítulo 10

Los criterios de drenaje para régimen variable se han deducido del estudio de la relación entre la profundidad de la capa de agua, el crecimiento de los cultivos y la movilidad de maquinaria agrícola sobre el suelo y del estudio del régimen del agua freática en invierno y durante la estación de riego. Estos criterios fueron reducidos a criterios de régimen permanente, para una utilización más sencilla en proyectos de drenaje. Del estudio pueden deducirse las conclusiones siguientes:

- Los cereales de invierno no presentan daños considerables si la capa freática permanece a menos de 50 cm de la superficie durante 3 días consecutivos.
- La remolacha azucarera se desarrolla bien con una capa de agua permanente entre 75 y 100 cm, siempre que la capa de agua no permanezca en los 50 cm más superficiales durante más de 3 ó 4 días consecutivos.
- La alfalfa es con mucho más sensible a capas freáticas altas. Se obtuvo una buena producción cuando la capa freática permaneció menos de 3 días en los 25 cm superficiales, durante 4 ó 5 días por encima de 50 cm y de 5 a 6 días por encima de 75 cm.
- La existencia de una capa de agua por encima de 65 cm impide el movimiento de maquinaria y por tanto la preparación de la siembra en invierno.

Los criterios de drenaje fueron definidos de la siguiente forma:

- a) En invierno, debe conseguirse un descenso de la capa de agua desde la misma superficie hasta una profundidad de 0.65 m en 8 días.
- b) En la estación de riego debe controlarse una elevación de la capa de agua de 0.7 m, debida a pérdidas de riego, en un período de 12 días entre dos riegos consecutivos, y debe estar por debajo de una profundidad de 0.7 m después de 7 días.

Aplicando estos criterios a la ecuación de Boussinesq para flujo variable y utilizando los valores de la conductividad hidráulica y del espacio poroso drenable determinados en la finca experimental, se obtuvo un espaciamiento de 25 m para drenes instalados a una profundidad de 1.2 m.

Los criterios de drenaje equivalentes para régimen permanente son: una profundidad mínima de la zona radicular no saturada de 0.5 m, con una correspondiente carga hidráulica en el punto medio entre dos drenes de 0.7 m y una descarga de 3 mm/día.

Si se tuviera en cuenta la resistencia de entrada podrían utilizarse la ecuación de Ernst para régimen permanente y la ecuación de Hellinga-de Zeeuw para régimen variable para el cálculo del espaciamiento entre drenes. Los resultados obtenidos con ambas aproximaciones mostraron una buena concordancia y permitieron deducir las siguientes conclusiones:

- Con materiales de drenaje y filtros que presentan altas resistencias de entrada, la densidad de drenes (m/ha) requerida llega a ser doble que la requerida con drenes de baja resistencia de entrada.
- Un material con alta resistencia de entrada lleva consigo mucho más riesgo de fracaso, que un mayor espaciamiento con un buen material.

Samenvatting

Hoofdstuk 1

Het stroomgebied van de Ebro ligt in het noordoosten van Spanje en vormt een geografische eenheid die door hoge bergen wordt begrensd. Het Bardenas gebied ligt binnen het stroomgebied van de Ebro en maakt deel uit van het Bardenas-Alto Aragón irrigatieproject dat zijn oppervlaktewater uit de Pyreneeën betreft.

Hoofdstuk 2

Het Ebro stroomgebied is een tertiair sedimentatiebekken waarin de Ebro en zijn zijrivieren alluviale dalen hebben gevormd. De tertiaire afzettingen bestaan hoofdzakelijk uit moddersteen, waarin plaatselijk lagen van gips en zeer fijne siltsteen zijn ingeschakeld. Beide afzettingsgesteenten bezitten een fijnkorrelige textuur en bevatten schadelijke oplosbare zouten, omdat zij werden afgezet in een lacustrisch brakwater milieu.

Het belangrijkste landschapsvormende processen waren erosie, transport en afzetting onder semi-aride klimaatsomstandigheden. De hoogste delen van het landschap bestaan uit oud-tertiaire formaties, die plateaus vormen in een door rivieren doorsneden vlakte. Op een lager niveau komen mesas voor, die bestaan uit grof alluviaal materiaal dat de onderliggende tertiaire afzettingen bedekt. Het meeste geërodeerde materiaal werd uit het gebied afgevoerd, maar plaatselijk vond ook sedimentatie plaats. Tengevolge van de semi-aride omstandigheden kwamen eerder genoemde sedimenten en zouten tot afzetting. De hoogste zoutgehalten worden dan ook aangetroffen in de laagstgelegene delen van de alluviale afzettingen, in het bijzonder daar waar het alluviale materiaal afkomstig is van de geërodeerde moddersteen en siltsteen. Tussen de voor erosie gespaard gebleven plateaus en de laaggelegen alluviale

afzettingen komen piedmont-vlakten en colluviale hellingen voor.

In het Bardenasgebied werden tien grote fysiografische eenheden onderscheiden, die in kleinere eenheden werden onderverdeeld en op een bodemkaart aangegeven.

Het Ebrobekken is het droogste gebied van Noord-Spanje. Het klimaat is semi-aride en wordt naar het centrum van het bekken droger. De temperatuur vertoont een grote seizoensschommeling. De potentiële verdamping overtreft de neerslag die van jaar tot jaar grote verschillen te zien geeft en niet geconcentreerd is in duidelijke regenseizoenen. De windsnelheid is hoog en zowel warme als koude droge winden komen voor. De verdamping is daarom ook in de winter, wanneer de temperatuur laag is, niet te verwaarlozen.

In een groot gedeelte van het gebied wordt landbouw uitgeoefend, zodat de natuurlijke begroeiing beperkt is tot de geërodeerde plateaus die niet voor de landbouw worden gebruikt en tot de zoute gronden die een vegetatie van halofyten bezitten.

Bodemomstandigheden zijn bepalend voor de vorm van geïrrigeerde landbouw. Volledige irrigatie wordt toegepast op niet-zoute gronden, met mais, luzerne, suikerbieten en enige tuinbouwgewassen als de voornaamste gewassen. Het gewassenpatroon op de zoute gronden hangt af van het zoutgehalte van de grond. Gerst en suikerbieten worden op matig zoute gronden verbouwd, luzerne op gronden die met goed resultaat zijn ontzout. Op de hoger gelegen gronden, die buiten het irrigatiegebied vallen, wordt gerst verbouwd.

Hoofdstuk 3

Het bestudeerde gebied watert naar twee zijden af, het noordelijke gedeelte naar de Aragon en het zuidelijke naar de Riguel, een zijrivier van de Arba.

De afwatering en het zoutgehalte van het grondwater zijn afhankelijk van de ligging van de verschillende geomorfologische eenheden ten opzichte van aangrenzende eenheden. In de noordelijk gelegen fluvio-colluviale afzettingen komt ondiep, zeer zout grondwater voor. Een tijdelijke grondwater-

spiegel op geringe diepte wordt aangetroffen in de mesas, waar het grondwater zoet is. In de andere fysiografische eenheden komen geen ondiepe grondwaterspiegels voor.

Het irrigatiewater is van goede kwaliteit: de EC-waarde bedraagt ongeveer 0,3 mmhos/cm. Er bestaat geen gevaar voor alkalinisatie, want de SAR-waarde varieert van 0,2 tot 1,3 en de RSC-waarde is nul.

Hoofdstuk 4

Volgens de fysiografische benaderingswijze werd een bodemkaart van het onderzoeksgebied samengesteld. Iedere kaarteenheden bestaat uit een groepering van bodemsoorten met overeenkomstige verzoutingsgevaaren en mogelijkheden tot ontginning. De volgende vijf hoofdbodemgroepen werden onderscheiden:

a) De residuaire gronden van de dagzomende siltsteenafzettingen, die gekenmerkt worden door een dunne oppervlaktelaag gelegen op harde siltsteen.

b) De mesa-gronden die bestaan uit een roodachtige, lemige bovenlaag gelegen op ten dele verkit, grof alluviaal materiaal dat rijk is aan calciumcarbonaat, maar waarin andere zouten ontbreken. Aan de onderzijde wordt dit materiaal begrensd door ondoorlatende moddersteen. De textuur en de diepte van het bodemprofiel variëren. Op de matig diepe gronden komt een welvarende, geïrrigeerde landbouw voor.

c) De gronden van de piedmont-vlakten en colluviale hellingen ontwikkelden zich uit een mengsel van fijn colluvium en materiaal van de onderliggende tertiaire afzettingen. Deze, doorgaans diepe, gronden hebben een fijne textuur en bevatten zout waarvan de concentratie van plaats tot plaats wisselt maar met de diepte toeneemt. In verband met de geringe doorlatendheid en het zoutgehalte van de ondergrond, is berekening de meest geschikte irrigatiemethode.

d) De niet-zoute gronden van de alluviale dalen der hoofd rivieren. De bodemomstandigheden wisselen sterk, maar gewoonlijk zijn de oudere terrasgronden ondieper en minder geschikt voor irrigatie dan de jongere, diepere,

alluviale gronden. In het algemeen is op deze gronden welvarende geïrrigeerde landbouw.

e) De zoute, alluviale en fluvio-colluviale gronden van dalen en puinkegels waarvan het moedermateriaal afkomstig is van geërodeerde tertiaire afzettingen. De bodemomstandigheden en het zoutgehalte verschillen binnen elke kaarteenheden en derhalve ook de mogelijkheden tot ontginning.

Hoofdstuk 5

De herkomst van het zout moet gezocht worden in het zoute moedergesteente. Secundaire verzouting treedt op in gebieden die water ontvangen, maar geen natuurlijke drainage bezitten. Wanneer in deze gebieden wordt geïrrigeerd, gaan oplossing, transport en herverdeling van zouten door en neemt de verzouting toe.

Natriumchloride is het meest voorkomende zout in de bodem. Bovendien zijn in het noordelijke gedeelte van het gebied calcium- en magnesiumsulfaat aanwezig, terwijl in het zuidelijke deel meer calcium- en magnesiumchloride voorkomen.

De SAR-waarde neemt toe met de EC-waarde. Alkaliniteit kan derhalve beschouwd worden het zoutgehalte van de grond te weerspiegelen daar zeer zoute gronden ook een hoog gehalte aan natrium bezitten. Niet-zoute alkali-gronden komen niet voor, evenmin als pH-waarden die hoger zijn dan 8,5.

De resultaten van veldproeven betreffende de zouttolerantie van gewassen komen goed overeen met de algemeen aanvaarde normen voor zout-tolerantie.

Het blijvend in gebruik houden van de zwak-zoute gronden (EC = 4 tot 8 mmhos/cm) kan verzekerd worden door het huidige drainage stelsel van open sloten en interceptor drains te handhaven en de gronden regelmatig te irrigeren. De normale percolatieverliezen die bij basisirrigatie optreden, zijn voldoende om de zouten uit de wortelzone te spoelen.

Berekening is geschikt voor de gronden op de hellingen, omdat in dat geval geen egalisatie nodig is en de kleine watergiften de stroming van zout water naar aangrenzende gebieden beperken. Slechts een interceptor drain tussen de helling en het dal is nodig.

Hoofdstuk 6

Voor de ontginning van de zoute gronden moet een drainagestelsel worden aangelegd waarna doorspoeling moet plaats vinden om het zoutgehalte te verlagen. Plaatselijke ervaring met drainage en ontzilting ontbrak, reden waarom werd besloten tot het nemen van proeven. Voor dit doel werden twee proefvelden uitgekozen.

Het *Alera proefveld*, gelegen op de fluvio-colluviale afzettingen van het noordelijke gedeelte van het gebied, werd representatief geacht voor de slecht ontwaterde gronden in dit gebied. Deze gronden bestaan uit zware klei waarvan het poriënvolume en de doorlatendheid met de diepte afnemen. Beneden een diepte van 1,5 m is de grond vrijwel ondoorlatend. Het zoutgehalte neemt met de diepte toe en bereikt in de vrijwel ondoorlatende laag waarden overeenkomende met 20 tot 35 mmhos/cm in elektrische geleidbaarheid. Het zoutgehalte in de bovenlaag varieert sterk.

Het *Valareña proefveld* ligt op de zoute gronden van de alluviale dalen en puinkegels in het zuidelijke deel van het gebied. Deze gronden bestaan uit lichte klei met een uitgesproken laagsgewijze opbouw. Op een diepte van 2,5 m ligt de overgang naar grofkorrelig alluviaal materiaal, dat met zeer zout grondwater verzadigd is en dat rust op de ondoorlatende moddersteen. Als gevolg van de sterke gelaagdheid vertoont de doorlatendheid een duidelijke anisotropie. De bodemverzouting komt veel regelmatig verdeeld voor dan in het Alera proefgebied.

Het onderzoek bestond uit de volgende stappen:

- a) Theoretisch ontwerp van het drainagestelsel, waarbij gebruik gemaakt werd van de hydrologische bodemeigenschappen die werden bepaald volgens conventionele veldmethoden, en van aangenomen drainage criteria.
- b) Aanleg van de drainagestelsels in de beide proefvelden.
- c) Verzamelen van veldgegevens gevolgd door bepaling van de werkelijke hydrologische bodemeigenschappen en drainage criteria uit deze gegevens.
- d) Ontwerp van het definitieve drainagestelsel dat als uitgangspunt zal dienen voor het doen van aanbevelingen voor de ontginning van zoute gronden onder soortgelijke omstandigheden.

Hoofdstuk 7

Na een gedetailleerde hydrologische en bodemkundige kartering werd voor beide proefvelden een drainafstand van 20 m bij een draandiepte van 1,5 m berekend. Om de geringe infiltratiesnelheid te verbeteren, werden beide velden gewoeld tot een diepte van 0,5 m. Piezometers werden geplaatst om de veranderingen in de grondwaterstand te kunnen waarnemen. De hoeveelheden irrigatie- en drainagewater werden gemeten, evenals de neerslag. Op vaste plekken werden bodemonsters genomen ter bepaling van het zoutgehalte tijdens de doorspoeling.

Hoofdstuk 8

Op het Valareña proefveld stroomde het water direct door de bovenlaag naar de drainsleuf, omdat de gelaagdheid door woelen en egaliseren van deze laag verbroken was. Beneden deze laag vond geen percolatie van water plaats en derhalve geen ontzilting. Voor het doorspoelen van deze gronden is niet alleen een drainagestelsel nodig, maar zij moeten ook tot grotere diepte gewoeld worden.

Op het Alera proefveld verliep de grondwaterstroming niet-stationair. Tegen het einde van het staartverloop werd een stationaire stroming benaderd. Uit het verband tussen afvoer en potentiaal, dat een parabolische vorm had, bleek dat de stroming beperkt bleef tot het profiel boven drainniveau en dat de drains op een slecht doorlatende laag gelegen waren.

De Boussinesq theorie bleek zeer geschikt voor de bestudering van de drainage in het Alera proefgebied. Aan het eind van het staartverloop kon de formule van Hooghoudt worden toegepast, onder weglating van de term voor de stroming beneden drainniveau.

De bergingscoëfficiënt werd bepaald uit de daling van de grondwaterstand en de hoeveelheid drainagewater gedurende perioden met lage verdamping. De gemiddelde waarde bedroeg 4%.

De doorlatendheid werd berekend uit het verband tussen afvoer en potentiaal met behulp van de formules van Boussinesq en Hooghoudt voor perioden

met lage verdamping. In het algemeen bleken de berekende waarden onderling goed overeen te stemmen. Uit de resultaten van dit onderzoek konden de volgende conclusies worden getrokken:

- De doorlatendheid neemt af met de diepte en is verwaarloosbaar klein beneden drainniveau.
- De doorlatendheid bedraagt 0,6 m/dag tussen een diepte van 0,5 m en drainniveau en ongeveer 1,5 m/dag in de bovenlaag.
- De gemiddelde doorlatendheid is 1 m/dag wanneer hoge grondwaterstanden voorkomen.

Uit een vergelijking van doorlatendheidswaarden verkregen met veld- en laboratoriummethoden enerzijds en uit het verband tussen afvoer en potentiaal anderzijds is gebleken dat:

- de waarden gemeten met de boorgatenmethode (0,2 m/dag) lager waren dan die berekend uit het verband tussen afvoer en potentiaal;
- geen bevredigende resultaten werden verkregen met de omgekeerde boorgatenmethode toegepast op de onverzadigde zone;
- de metingen aan ongeroerde grondmonsters in het laboratorium op een anisotropie van de grond wezen.

De intreeweerstand (W_e) van verschillende combinaties van drain- en filtermaterialen werd berekend uit de drainafvoer en het potentiaalverschil (h_i) gemeten tussen de rand van de drainsleuf en de drainbuis. Een andere methode, waarbij dit potentiaalverschil berekend wordt uit de vorm van de grondwaterspiegel, werd eveneens toegepast. Beide methoden leverden vrijwel dezelfde uitkomsten op, waaruit de volgende conclusies konden worden getrokken:

- De W_e -waarden blijven vrijwel constant, uitgezonderd bij plastic buizen omhuld met esparto- of cocosvezel die een toeneming van de intreeweerstand met de tijd vertonen.

- De beste combinatie bestaat uit gebakken drainbuizen met grind ($W_e = 2$ dagen/m).
- Plastic ribbelbuizen met grind of gebakken buizen zonder grind kunnen ook worden gebruikt ($W_e = 5$ dagen/m).
- Plastic ribbelbuizen zonder omhulling geven weinig bevredigende resultaten ($W_e = 13$ dagen/m).
- Plastic ribbelbuizen met een omhulling van esparto- of cocosvezel bezitten zelfs een nog hogere intreeweerstand dan zonder omhulling.
- Gerststro is onbruikbaar als omhullingsmateriaal omdat het gemakkelijk rot en de buis verstopt.

Hoofdstuk 9

De ontzilting van het Alera proefveld begon met een periode van doorspoeling, gevolgd door de verbouw van geïrrigeerde, matig zoutresistente gewassen.

De coëfficiënt die het nuttig effect van de doorspoeling uitdrukt, werd bepaald door een vergelijking van de werkelijke ontzilting met de, volgens een theoretisch model, berekende ontzilting. Aldus was het mogelijk de doorspoelingsbehoefte te voorspellen voor verschillende initiële zoutgehalten.

Het zoutgehalte werd uitgedrukt in het chloridegehalte om de invloed van slecht oplosbare zouten uit te schakelen. De correlatie tussen het chloridegehalte en de elektrische geleidbaarheid was hoog. De uitkomsten van het onderzoek leidden tot de volgende conclusies:

- De coëfficiënt die het nuttig effect van de doorspoeling uitdrukt was niet constant, maar nam met de diepte toe.
- De coëfficiënt was hoger aan het begin van de ontzilting en nam geleidelijk af naarmate de grond minder zout werd.

- De berekende waarden van de coëfficiënt weerspiegelden de verschillen in bodemstructuur.
- Voor de bovenlaag (0 - 50 cm) werd een gemiddelde waarde van 0,5 bepaald en voor de volgende laag (50 - 100 cm) een waarde van 1.
- Het zoutgehalte bij het begin hing af van bodemfysische eigenschappen, zoals infiltratiesnelheid en doorlatendheid die op hun beurt weer afhankelijk waren van de verdichting van de grond.
- Bij een beginwaarde van 15 mmhos/cm voor de elektrische geleidbaarheid van de grond zijn ongeveer 1000 mm water voor doorspoeling nodig, hetgeen betekende een hoeveelheid irrigatiewater van 1100 tot 1400 mm. De doorspoelingsperiode kon 8 maanden duren, vanaf het begin van de herfst tot eind mei.
- Diepwoelen en plaatselijke gipsbemesting verbeterden de structuur van de bovenlaag.
- De doorspoeling van zoute gronden vond in twee fasen plaats, namelijk een eerste fase met alleen doorspoeling, gevolgd door een tweede fase met de verbouw van een geïrrigeerd, matig zoutresistent gewas (suikerbieten), waarbij de percolatieverliezen de diepere lagen doorspoelen.
- Gedurende de doorspoelingsperiode bestond er geen gevaar voor alkalinisatie van de grond.
- Om secundaire verzouting na ontginning te voorkomen, moesten de voorwaarden voor een goede drainage gehandhaafd worden en dienen geïrrigeerde gewassen verbouwd te worden.

Hoofdstuk 10

De drainage criteria voor niet-stationaire omstandigheden werden afgeleid uit het verband tussen grondwaterstand, gewasopbrengst en bewerkbaarheid van de grond, en uit het grondwaterstandsverloop in de winter en tijdens de irrigatieperiode. Deze criteria werden vervolgens herleid tot criteria

voor stationaire omstandigheden die handiger zijn voor gebruik in drainage projecten. Uit dit onderzoek werden de volgende conclusies getrokken:

- Wintergranen ondervinden weinig schade wanneer de grondwaterspiegel zich niet langer dan drie opeenvolgende dagen op minder dan 50 cm beneden maaiveld bevindt.
- Bij grondwaterstanden tussen 75 en 100 cm beneden maaiveld vertonen suikerbieten een goede groei en zij ondervinden geen schade indien de waterstand tijdelijk, gedurende 3 tot 4 dagen, hoger komt dan 50 cm beneden maaiveld.
- Luzerne is gevoeliger voor hoge grondwaterstanden dan suikerbieten. Voor goede opbrengsten dient de grondwaterstand niet langer dan 3 dagen op minder dan 25 cm beneden maaiveld, 4 tot 5 dagen op minder dan 50 cm, en 5 tot 6 dagen op minder dan 75 cm beneden maaiveld te staan.
- Grondwaterstanden minder dan 65 cm beneden maaiveld verhinderen het gebruik van machines en belemmeren het bewerken van de grond, zoals het gereedmaken van het zaaibed.

De volgende drainage criteria werden vastgesteld:

- a) Wanneer in de winter de grondwaterspiegel tot aan maaiveld stijgt moet deze in 8 dagen tot een diepte van 65 cm verlaagd worden.
- b) Tijdens de irrigatieperiode moet de grondwaterstand, na een stijging van 70 cm veroorzaakt door irrigatieverliezen, in de 12 dagen tussen twee opeenvolgende irrigaties tot het oorspronkelijke niveau verlaagd worden en na 7 dagen dieper dan 70 cm beneden maaiveld zijn.

Bij toepassing van deze criteria in de Boussinesq vergelijking voor niet-stationaire stroming en door gebruik te maken van de doorlatendheid en bergingscoëfficiënt die op het proefveld waren bepaald, werd een afstand

van 25 m berekend voor drains op een diepte van 1,20 m. De hiermee overeenkomende drainage criteria voor stationaire stroming waren een minimum diepte van 0,5 m voor de onverzadigde zone, hetgeen leidt tot een potentiaal van 0,7 m en een drainafvoer van 3 mm/dag.

Wanneer rekening wordt gehouden met de intreeweerstand, konden de vergelijking van Ernst voor stationaire stroming en die van Hellinga en de Zeeuw voor niet-stationaire stroming worden gebruikt voor de berekening van de drainafstand. Beide methoden leverden overeenkomstige resultaten op waaruit de volgende conclusies konden worden getrokken:

- Wanneer drainage- en filtermaterialen met een hoge intreeweerstand worden gebruikt zal de dichtheid van het netwerk van drains (in m/ha) tweemaal zo groot zijn als bij materialen met een lage intree weerstand.

- Het gebruik van materialen met een hoge intreeweerstand houdt een veel groter risico van mislukking in dan een wijde drainafstand met goed materiaal.

Curriculum vitae

Julian Martinez Beltrán was born in Soria (Spain) on September 19th 1947. In 1964, after completing secondary school at the Instituto "Antonio Machado" in Soria, he studied at the Polytechnical University of Madrid, graduating as Agricultural Engineer on December 9th 1969. From January to June 1970 and from October 1972 to June 1973, he attended postgraduate courses on Soil Science at the Madrid University.

In October 1970, he worked with the Ebro branch of the Instituto Nacional de Colonización in soil surveys for irrigation projects. In June 1972 he joined the Soils Department of the Instituto Nacional de Reforma y Desarrollo Agrario (IRYDA) in Madrid.

From August to December 1973 he attended the 12th International Course on Land Drainage, held in Wageningen and organized by the International Institute for Land Reclamation and Improvement (ILRI). After returning to Spain, he began the research work for this thesis under the supervision of Prof.Dr.W.H.van der Molen and Prof.Dr.P.Buringh of the University of Agriculture, Wageningen. Field work was done at the Alera and Valareña experimental fields in the Bardenas area and research work at the Department of Land and Water Use and the Department of Tropical Soil Science of the Wageningen University. The project was financed by IRYDA.

His present address is: *Soils Department of IRYDA, Velázquez 147, Madrid 2, Spain.*